PRIORITIZATION OF SITE-SUITABLE WATERSHED-SCALE LOW IMPACT DEVELOPMENT PRACTICES

by

Thomas C. Walsh

A dissertation submitted to the faculty of
The University of Utah
in partial fulfillment of the requirements for the degree of

Doctor of Philosophy

Department of Civil and Environmental Engineering

The University of Utah

May 2015

The University of Utah Graduate School

STATEMENT OF DISSERTATION APPROVAL

The dissertation of **Thomas C. Walsh**
has been approved by the following supervisory committee members:

Christine A. Pomeroy	, Chair	**May 5, 2014** Date Approved
Simon Brewer	, Member	**May 5, 2014** Date Approved
Steven J. Burian	, Member	**May 5, 2014** Date Approved
Philip E. Dennison	, Member	**May 5, 2014** Date Approved
James Ehleringer	, Member	**May 5, 2014** Date Approved
Brian McPherson	, Member	**May 9, 2014** Date Approved

and by **Michael Barber** , Chair/Dean of

the Department/College/School of **Civil and Environmental Engineering**

and by David B. Kieda, Dean of The Graduate School.

ABSTRACT

There is a need to improve the methods involved with targeted implementation and design of distributed, watershed-scale low impact development (LID) practices. The goal of this dissertation was to improve the targeted implementation and design of distributed, watershed-scale low impact development (LID) practices, focusing on rainwater harvesting (RWH). This research resulted in protocols and customized geospatial analysis toolsets that filter local LID constraint datasets. These products were then applied to the 31 square kilometer case study location, Chollas Creek, San Diego, CA, USA, to determine their accuracy and reproducibility in targeting cost-effectiveness (e.g., best hydrologic reduction per dollar invested).

The baseline for improvement was established with the analysis of a passive watershed RWH program using traditional, uniform applications of design parameters. To remedy uniformity assumptions, a suitability-based protocol was developed and tested. This protocol incorporated object-based image analysis (OBIA) classification techniques, via eCognition, to improve the identification and quantification of individual, parcel-level rooftops. OBIA was 92% accurate for overall classification of residential rooftops, using area-based quality assessment guidelines. A customized geospatial analysis toolset aided the filtering of extensive datasets, which were established as RWH constraints,

for watershed-scale design and implementation. Compared with the uniform results, the Suitability Protocol quantified an average rooftop area of 227 square meters, with 11% less households (by number) and 51% greater cumulative rooftop area. Long-term hydrologic simulations found 51% and 44% greater reductions in average annual watershed peak outflow rates and volumes, respectively, with the Suitability Protocol. The Suitability Protocol included the LID Site Suitability (*LIDSS*) and Quality Assessment (*QA*) toolsets.

The targeting of intrawatershed locations, via the Suitability Protocol, was improved with the Prioritization Protocol and the Rainwater Harvesting Analyzer (*RWHA*) and Prioritization LID (*PriorLID*) toolsets. Prioritization was driven by user-defined hydrologic and economic thresholds to yield the most cost-effective spatial configuration for watershed-scale RWH. The Prioritization Protocol resulted in refined intrawatershed priority locations with increasing iterations of the protocol/toolsets. Monte Carlo Uncertainty Estimation (MCM) yielded an insensitive watershed hydrologic response to changes in subcatchment imperviousness (n=100). Extended to RWH effectiveness, uncertainty results highlighted a watershed buffering capacity (18%) for increases in imperviousness.

I am honored to dedicate this dissertation to those who made me the person I am today. For Julie Haeger and Edward Smithback, who knew this day would come long before I did.

TABLE OF CONTENTS

LIST OF TABLES

LIST OF ABBREVIATIONS AND ACRONYMS

BMP	Best Management Practice
DEM	Digital Elevation Model
DSM	Digital Surface Model
DTM	Digital Terrain Model
EAC	Equivalent Annual Cost
ENVI	Environment for Visualizing Images
GI	Green Infrastructure
GIS	Geographic Information Systems
LC/LU	Land Cover/Land Use
LID	Low Impact Development
LIDSS	Low Impact Development Site Suitability
Lidar	Light Detection and Ranging
nDSM	Normalized Digital Surface Model
NAIP	National Agricultural Imagery Program
NDVI	Normalized Difference Vegetation Index
NIR	Near Infrared
OBIA	Object-Based Image Analysis
PBIA	Pixel-Based Image Analysis
PriorLID	Prioritization of LID Toolset
QA	Quality Assessment Toolset
RWH	Rainwater Harvesting
RWHA	Rainwater Harvesting Analyzer
SWMM	Storm Water Management Model

ACKNOWLEDGEMENTS

I am grateful to my advisor, Dr. Christine Pomeroy, for the support and trust throughout the pursuit of my passions and research. I am also indebted to my committee, including Dr. Simon Brewer, Dr. Steve Burian, Dr. Philip Dennison, Dr. Jim Ehleringer, and Dr. Brian McPherson. Because of this amazing core of individuals, I was able to refine and strengthen the research presented herein. Specifically, the improved classification techniques, uncertainty analysis with Monte Carlo Methods, and climatic analysis were the direct result of the hands-on and constructive aid my committee afforded me. I eagerly await the day to pay this forward in the pursuit of my future professional and personal endeavors.

I would also like to also recognize the support I received from the Department of Civil and Environmental Engineering, the Office of Sustainability, the Margaret S. Borg Graduate Scholarship, the Global Change and Sustainability Center (GCSC), and the NSF EPSCoR iUTAH project. In particular, the latter two organizations contributed greatly to the success I feel with respect to education, outreach, and interdisciplinary research. Because of these avenues, I look forward to many successful future collaborations in the pursuit of sustainability, vulnerability, and adaptation research related to the complexities of urban watersheds.

Dr. Dasch Houdeshel, Dr. Alfred Kalyanapu, Zach Magdol, Shannon Reynolds, Kristianne Sandoval, Dan Stout, and Megan Walsh were all pivotal to my success. Thank you for the hours of edits, discussions of harebrained ideas, and honest support. I also acknowledge Scott Morrison and the work he completed on the Rainwater Harvesting Analyzer (RWHA), which I could not have done on my own. I recognize the support of the Urban Water Research Group and its members, past and present, who are a strong group of collaborators. I am grateful for the wonderful friends I have made while here in Salt Lake City. Countless miles, laughs, and cold beers have been shared with you all.

Last, the love and support of my family is the means for my success. I have made it here with and for you. Especially, my mother and father, Amy and Mike, who sacrificed and gave so that I could achieve. To my siblings, Signe, Keifer, and Chad, who love me despite my shortcomings and are always in my corner. Thank you for every sacrifice and for giving me perspective on the important pieces of life. You all are the world to me and this is as much yours as it is my own. I also thank my new family, Nguon, Leang, and Jessica, who treat me as one of their own. Finally, I cannot overstate the love, support, and strength of my partner, Christina. Your unending positivity, perseverance, and tough love enrich my life tenfold.

CHAPTER 1

INTRODUCTION

The goal of this research is to develop and apply a reproducible methodology combining image analysis classification, geospatial analysis, hydrologic model simulations, and cost-effectiveness to inform the planning, design, operation and maintenance of watershed-scale low impact development (LID) practices. This research improves current methods that uniformly apply LID principles to sustainable urban watershed stormwater management due to dataset and processing limitations requiring time and resources on the part of modelers and analysts. The Chollas Creek watershed, in San Diego, CA, USA, serves as the case study location for which the protocols and toolsets were applied and assessed. The targeted audience of this work includes engineers, geoscientists, and urban planners.

1.1 Study Background

1.1.1 Urban Stormwater Management

Urbanization has negatively impacted the resources and processes of the natural environment. Specifically, the conversion from natural to impervious land cover has affected stormwater quantity and quality, including increased flood risk

and pollution of receiving water bodies (Schueler, 1994; Lee & Heaney, 2003). To mitigate these consequences, traditional stormwater management focused on improving conveyance with centralized mitigation (Roy et al., 2008; Debo & Reese, 2010). This resulted in watershed management plans that often span multiple municipalities and governing bodies (Brown et al., 2007). Such plans enforced the construction of large capacity, end-of-pipe practices located at downstream termination points within large drainage areas. These practices, and other urban infrastructure, may be increasingly vulnerable to changes in climatic and anthropogenic conditions (Bates et al., 2008; Dorfman & Mehta, 2011). This is compounded by the fact that some traditional designs were based on parameter stationarity, which assumed that the runoff load would remain constant within an expected window of variability over time (Denault et al., 2006). As such, historic designs may become over- or under-utilized as a function of increasingly variable future storm events. In response, stormwater management practices (e.g., low impact development, LID) have evolved to mimic natural, pre-developed conditions by focusing on annual rainfall distribution patterns rather than a single return event.

LID represents decentralized practices, providing source control with smaller capacity units. Mitigation is accomplished via the capture, storage, infiltration, and treatment of stormwater runoff (Prince George's County, 1999; USEPA, 2007a). In 1999, Prince George's County released a seminal document detailing integrated design strategies for sustainable management of stormwater runoff. This guide highlighted the importance of site planning, hydrologic

principles, and hydrologic analysis tools (Prince George's County, 1999), all of which necessitate site-specific knowledge on the part of the designer. Research repeatedly cites local conditions' applicability and effectiveness of the stormwater control measure (SCM) as the most important component of data analysis (Marsalek & Chocat, 2002; NRC, 2008). In addition, nontechnical obstacles to LID success include property owner motivation and education, such that sustainable modifications to land cover and policies result (Braden & Johnston, 2004; Chocat et al., 2007). By targeting these individuals, who manage the largest proportion of developed land (e.g., residential), the likelihood of achieving significant improvements in stormwater runoff mitigation increases (Lee & Heaney, 2003). Supporting research found that LID practices provide quantifiable reductions in annual average runoff volumes, peak discharge rates, and pollutant loading (Dietz, 2007; Han et al., 2008; Roy et al., 2008; Lim et al., 2010; Spatari et al., 2011; Jia et al., 2012). An empirical study by Burns et al. (2014) monitored demand supplementation and runoff management impacts from RWH (capacity range of 3,000 to 28,000 liters per household). Results stressed the importance of regular, large domestic demands to yield substantial stormwater runoff reductions in addition to larger unit capacities (Burns et al., 2014).

The majority of this research has focused on smaller spatial scales, including households, parcels, and the neighborhood (Sample & Heaney, 2006; Gilroy & McCuen, 2009). Consequently, a knowledge gap exists that limits the extension of these results to expanded scales of planning, design and hydrologic analysis (Bedan & Clausen, 2009; Lee et al., 2012). When empirical data at the

watershed-scale are available, as in the research by Yang and Li (2013), results reinforce the effectiveness of integrated suites of LID in improving stormwater runoff reductions and water quality enhancements. However, due to the depth and complexity of data required for such analyses, duplication of similar efforts is difficult (Thomas et al., 2003; Jensen et al., 2010). Beyond data needs, accurate representation of LID at the necessary local and regional scales is a challenge due to the exhaustive methods and user-knowledge required to characterize and quantify impacts (Burian & Pomeroy, 2010).

This approach of targeting site-specific stormwater management with decentralized source controls in pursuit of wider goals (e.g., watershed health) has been termed 'flow-regime management' by Burns et al. (2012) and remains in its infancy. Despite the aforementioned limitations, researchers increasingly extrapolate and apply LID principles either uniformly or as over-simplified, disconnected measures to address broader issues. This generalization reduces the accuracy of model representation (i.e., input parameter values) and has the potential to skew simulated hydrologic results. For instance, a study of urban rooftop runoff control practices in Brussels found that a 2.7% reduction in overall watershed runoff could be achieved by targeting a uniform 10% of rooftop infrastructure (Mentens et al., 2006). Similarly, despite designing RWH units that fill to 35% of capacity with the 90^{th} percentile storm event, Basinger et al. (2010) indicate only 28% annual reduction in stormwater runoff volume. For larger areas comprised of heterogeneous land covers and land uses, site-specific planning and design require intensive analysis capable of discerning between datasets

and underlying variability. Thus, it is imperative that methods be developed to efficiently assess and characterize large, urban datasets for direct application in hydrologic models and subsequent simulations (Pataki et al., 2011).

1.1.2 Watershed Modeling

Traditional hydrologic modeling of urban watersheds is dependent upon the modeler's judgment of parameters and methods, such that realistic conditions were recreated within the model framework. This involves time-intensive manual delineation and digitizing of vector data layers from aerial imagery or in-field observations (Thomas et al., 2003; Sterr & Yui Lau, 2012). The time and resources required to do this accurately increase with scale, with greater focus on replicating existing conditions. Improvements in remote sensing data, such as Light Detection and Ranging (lidar), and image analysis have increased precision in identifying and visualizing land cover types and objects (Wechsler, 2007; Amatya et al., 2013). Compared with manual delineation, this has resulted in finer resolutions of hydrologic model inputs, including basin area, slopes, flow paths, connectivity, and channel lengths (Rumman et al., 2005; Kunapo et al., 2009; Amatya et al., 2013). Finer dataset resolutions are also pivotal to identifying, classifying, and modeling watershed boundaries, surface classes, and characteristics that impact hydrology (Luzio et al., 2005; Rumman et al., 2005; Kunapo et al., 2009; Cao et al., 2012). As a result, this has improved the ability of water resources engineers and urban planners to model and analyze the structure and functionality of stormwater management plans.

Of particular importance to these improvements are publicly-available

remotely-sensed datasets, which have expanded the ability to assess both local and regional scales (James et al., 2007; Kunapo et al., 2009). In particular, lidar (light detection and ranging) is increasingly employed in the visualization, characterization, and delineation of both surface and hydrologic models regardless of obstructions (e.g., tree canopy and buildings) and surface types (Frazier & Page, 2000; James et al., 2007; Im et al., 2008; Jensen et al., 2010; Zhu et al., 2012). These datasets have also contributed to the improvement of three-dimensional visualization and classification methodologies (Zhu et al., 2012). For instance, classifications based solely on spectral signatures are improved by including other datasets, such as elevation and textural information. Lidar, in this case, minimizes uncertainty, or lack of precision, by incorporating both elevation and textural data (Lu & Weng, 2007; Peteri & Ranchin, 2007; Yu et al., 2010; Weng, 2012).

Incorporation of elevation and textural data reduces misclassification due to shadows and improves extraction of specific land uses (e.g., rooftops versus paved areas). This differentiation was exhibited for a small catchment (e.g., 550 hectares) with unusually rich resources (e.g., GIS, lidar, and aerial imagery) to test the siting of bioretention and green rooftops (Jensen et al., 2010). While researchers were able to extract sites suitable for these practices, the universal difficulty in duplication resulting from the limited availability of pertinent resources was acknowledged (Jensen et al., 2010). As such, the means to reliably and accurately extract and filter these resources for large areas must be made available for the range of backgrounds and skillsets of multiple users.

A potential solution to these issues resides in the improvement of methodologies, protocols and toolsets that employ the ever-increasing public repository of fine resolution, spatially diverse datasets, including spectral datasets and lidar point clouds. Alternatively, dataset complexity and heterogeneity must be accounted for with these improvements, since classification of land cover and land use are based on statistical pattern recognition (Jensen, 2005). As classification methods attempt to represent reality, modeled physical conditions will inherently contain degrees of error (Di Gregorio & Jansen, 2000). This error can be increased by heterogeneity in data, especially when employing pixel-based image analysis, or PBIA (Myint et al., 2011). PBIA algorithms are based solely on pixels' spectral values, thereby increasing the potential for confusion between different objects or surfaces with similar spectral signatures (Hsieh et al., 2001; Zhu & Blumberg, 2002; Yang et al., 2010a). Thus, the ability to consider entire features, or a collection of pixels that represents a discrete unit, becomes preferable over PBIA.

This ability to target features is satisfied with the object-based image analysis (OBIA) methodology. Typically, OBIA is a function of the spatial, contextual, and thematic elements within a scene containing spectral, elevation and textural datasets. The incorporation of scale, context, geometry, and color improves classification by OBIA to excel over PBIA when targeting specific objects (Yang et al., 2010b; Wu & Yuan, 2011). OBIA applications and methodologies research have continually addressed issues related to land cover/land use mapping. For instance, in extracting impervious surfaces, greater

accuracy was achieved with OBIA by Hu and Weng (2011). The focus of this research targeted residential areas versus a complex, central business district (CBD), which registered 95% and 92% accuracy, respectively. This combination of fine-scale lidar and spectral datasets has resulted in the continual improvement of OBIA.

Dataset processing has been used to improve classification results. For instance, the processing of elevation datasets to represent standardized heights of elevated structures has been shown to improve identification of targeted objects in urban areas (Lee et al., 2007; Yu et al., 2010; Solyman, 2012). One example of elevation standardization is the normalized Digital Surface Model (nDSM), which results from filtering the digital terrain model (DTM) from the digital surface model (DSM). The nDSM has been shown to be the most important feature in the classification improvement (Blaschke, 2010; Aguilar et al., 2012). The addition of texture analysis can also improve detection of objects based on variations in brightness values for pixel groups (Ferro & Warner, 2002; Mumby & Edwards, 2002). Spectral processing, such as the Normalized Difference Vegetation Index (NDVI) has been repeatedly shown to distinguish green, or vegetated, areas from urban impervious surfaces (Carlson & Ripley, 1997; Gillies et al., 1997; Wang et al., 2010). Together, these methods can provide accurate thematic map layers that reframe the traditional goal of watershed stormwater planning and management as using this information to identify and design LID practices for suitable locations.

1.1.3 Geospatial Analysis

Determination of locations meeting user-defined objectives can be achieved with GIS-based postprocessing, which improves the model analyst's ability to weigh and filter multiple datasets (Malczewski, 2004; Wang et al., 2010). Specifically, Wang et al. (2010) highlight the link between remote sensing and GIS, with thematic layer development driving planning and site search analysis measures that, in turn, inform future conditions (Fig. 1.1).

With site search analysis, the spatial characteristics of targeted areas can be explicitly extracted as a function of user-defined suitability criteria (Malczewski, 2004). Specific search methods include multiple criteria decision analysis (MCDA) and spatial clustering analysis, which weigh complex factors and present recommendations based upon input criteria (Malczewski, 2004). Jacquez (2008) used spatial clustering to recognize patterns with visualization, spatial statistics, and geostatistics such that locations, magnitudes, and shapes of statistically significant pattern descriptors were identified. Hotspot identification has also been applied for targeting resources and minimizing risk within a larger system (Anderson, 2009). Translation of geospatially distributed point data into representative surfaces is another method of geospatial analysis. Surface models are generated with individual point values (e.g., cost, elevation, or population) serving as the basis for surface interpolation. Methods for translating data to surfaces include inverse distance weighting (IDW), kriging, natural neighbors, and spline, which can be separated as either deterministic or geostatistical methods.

Deterministic interpolation assigns values to cells based on surrounding measured values, via specific mathematical formulas that smooth the resultant surface. Geostatistical methods provide a measure of certainty or accuracy for results as a function of autocorrelation, which measures the statistical relationship among the targeted points. Deterministic methods include IDW, natural neighbor, and spline, while kriging is an example of a geostatistical method (ESRI, 2013). IDW estimates raster cell values based on distance from a set of sample points that have been assigned weights, such that cells further from the sample set receive less weight when calculating the cell's value (ESRI, 2013). Kriging, similar to IDW with its weighting of surrounding values to derive a prediction for an unmeasured location, interpolates with a weighted sum of the data and accounts for the overall spatial arrangement of the measured points. This is accomplished with variography, in which points that are closer are more alike than those farther apart (Fig. 1.2). With kriging, outputs include both the predicted surface and the accuracy of those predictions (ESRI, 2013).

Despite these advances in geospatial site search analysis of local and regional watershed conditions, much of the research targeting LID as a watershed-scale stormwater management option has been applied with over-simplified, uniformity assumptions. Additionally, incorporation of economics is largely missing from expanded scales, due to an undervalued national stormwater utility fee structure (NRC, 2008; Campbell, 2012). However, the economic analysis of distributed LID practices is a growing field of research, combining cost-effectiveness with stormwater management benefits, such as

flood risk mitigation (Kousky et al., 2013). Improvements to targeting resources within a watershed, which account for subcatchment-scale impacts from site-specific LID, can be obtained with geospatial analysis of remotely sensed datasets, hydrologic simulations, and cost estimations. This approach, termed 'flow-regime management,' by Burns et al. (2012), requires further development of methodologies and toolsets that employ publicly-available datasets and industry-standard software programs. As such, with LID practices as components of a watershed stormwater management plan, research that improves the suitability and prioritization of locations and designs based on user-defined values is essential.

1.2 Problem Statement and Research Hypotheses

Traditional watershed stormwater management is comprised of large, centralized practices, which traditionally focus on mitigating runoff quantity and flooding (Prince George's County, 1999; Lee & Heaney, 2003). Such designs are capable of managing urban area runoff resulting from larger events; however, negative water quality impacts have occurred (e.g., erosion and sedimentation) due to extended release rates and poor peak control for more frequent, smaller events (Shaver et al., 2007; NRC, 2008; Roy et al., 2008). In response, LID shifts management objectives away from quantity to quality by providing control of smaller events (Lee & Heaney, 2003). As such, research and design methodologies have focused primarily at individual scales. Integrating LID practices and principles as components of a broader system's stormwater management plan has been recommended and studied, though gaps exist

regarding design methods and anticipated impacts to the hydrologic cycle (Marsalek & Chocat, 2002; Berke et al., 2003; Thurston et al., 2003; Roy et al., 2008; Shuster et al., 2008). When watershed LID frameworks are designed, it is typically completed on a case-by-case, or pilot project, basis (Damodaram et al., 2010; Mandarano, 2011). Thus, the ability to assess large areas and their current parameters is required to successfully advance the ability of users to model and analyze the hydrologic implications of watershed-scale LID.

Another critical gap is the lack of examples providing technical guidance, insight, or empirical data for reproducibility in other watersheds (Northeast Ohio Regional Sewer District, 2011; Central New York Regional Planning & Development Board, 2012; Yang & Li, 2013). A study by Yang and Li (2013) highlights empirically-derived water quality benefits of green infrastructure by comparing monitored results from two case study watersheds. However, it is widely acknowledged that the depth of required data and analyses for such scales proves challenging (Jensen et al., 2010). This results in a greater requirement of time, expertise and resources on the part of designers (Burian & Pomeroy, 2010). More often, LID research at this scale relies on oversimplification of methods and modeling processes applied to dynamic underlying watershed parameters. Economically, insufficient evidence hampers public support of investment in watershed-scale LID networks (Godchalk et al., 2009). Thus, there exists the need to improve the planning, design, and management methodologies accounting for LID constraints and toolsets that facilitate prioritization. Doing so would improve the targeted identification of urban

stormwater management frameworks as a function of user-defined criteria rather than lumping, or uniformly distributing, LID practices. Further, the need for accurate protocols and parameters addresses the design and modeling requirements for individual, distributed LID practices, which would improve hydrologic modeling scenarios and, when combined with cost analysis, indicate the spatially explicit cost-effectiveness for variations in both user-defined constraints and goals.

This dissertation addressed the following hypotheses:

Hypothesis I: The identification of site-suitable LID locations in urban watershed that meet user-defined criteria is improved by combining remote sensing and geospatial analysis. Accuracy of the methodology was established as a minimum 85% overall accuracy for Object-Based Image Analysis (OBIA) classification results. Confirmation of this hypothesis validated the use of the proposed Suitability Protocol and related toolsets, including the LID Site Suitability (*LIDSS*) and Quality Assessment (*QA*) tools. More importantly, it indicated that OBIA of publicly-available datasets can improve the accuracy of both identifying suitable RWH locations and designing RWH practices specific to the parcel scale of analysis.

Hypothesis II: The targeting, or prioritization, of intrawatershed suitable LID locations is informed by geospatial analysis and visualization of long-term hydrologic simulations and life cycle economic datasets. Since the accuracy of suitable locations was determined through work completed addressing Hypothesis I, the accuracy of prioritized locations was assessed through user-

defined economic and hydrologic threshold scenarios. These scenarios, representative of the subcatchment classes containing homogenous cost-effectiveness values, were ranked according to meeting the economic threshold established by the user. Hydrologic analysis of the targeted classes then provided an estimate of whether hydrologic thresholds could be met. This hypothesis was further assessed with Monte Carlo Methods (MCM) of uncertainty analysis for the subcatchment percent imperviousness' impact on the simulated long-term hydrologic model rainfall-runoff response.

1.3 Study Objectives

The goal of the proposed research is to improve the ability of users to prioritize the implementation of LID, using RWH as the targeted practice, through improved local design constraint analysis. This is accomplished by (1) establishing the requirements and extent of results provided following traditional hydrologic analysis methods with the application of a passive watershed RWH management plan, (2) developing a Suitability Protocol, with geospatial analysis toolsets, that identifies, quantifies, and collates suitable locations for implementation of LID at the watershed-scale, and (3) Developing a Prioritization Protocol, with RWH design and site search toolsets, that filter and target suitable LID practices as a function of top-down economic and hydrologic reduction thresholds. Finally, the impact of subcatchment percent imperviousness on watershed hydrologic response was assessed with Monte Carlo Methods (MCM) of uncertainty estimation, with results extended to the effectiveness of LID.

1.4 Uniqueness of Research

As previously outlined, traditional stormwater management planning relies on large, centralized practices designed to mitigate urban runoff volumes. These inadequate designs have led to negative impacts to the receiving environment for smaller, more frequent events. In response, LID has arisen as an alternative to provide quality improvements. LID design is focused on smaller, more frequent events; however, distributing these small, site-focused practices throughout the greater watershed is often done on a site-by-site basis and without regard to a wider stormwater management framework. Therefore, the need exists to develop protocols that address the combination of urban land cover characterization and remote sensing analysis with urban hydrologic simulations. Reproducibility and accuracy of the protocol and related toolsets is a priority of the research; therefore, publicly-available datasets and widely used software programs are incorporated. The adaptability is also a concern, since users will opt for incorporation of expanded datasets and analysis methods to adequately plan, design, and manage watershed-scale stormwater plan scenarios. The research proposed herein serves as the initial basis for contributing to the ultimate goal of improving the suitability and priority of watershed-scale stormwater management frameworks based on distributed LID principles.

The Suitability Protocol improves visualization and understanding of the multiple factors influencing the placement of LID at the watershed level. The Prioritization Protocol aids in the targeting of locations as a function of cost and hydrologic benefit relative to top-down thresholds (e.g., budget, hydrologic

reduction goals). This study is novel in that it builds upon remote sensing methods of land cover/land use characterization, with customized OBIA methods, and spatial targeting of resources throughout heterogeneous, urbanized watersheds. These identified locations and their characteristics are used to size LID practices, amend validated hydrologic models, and provide long-term simulation results. Incorporation of equivalent annual costs (EAC) with hydrologic results for individual subcatchments can be analyzed to prioritize suitable locations as a function of existing watershed constraints and municipal economic and hydrologic thresholds.

1.5 Overview of Methodology

In contributing to the field of flow regime management, this dissertation addressed existing gaps by accomplishing the following tasks. First, a watershed-scale management plan incorporating passive rainwater harvesting was tested and analyzed for the Chollas Creek watershed, San Diego, CA, USA (Walsh et al., 2014). This research followed traditional methods of LID implementation and provided the basis upon which suitability and prioritization protocols would be developed and assessed. Next, land cover/land use classification was carried out with customized process rule sets within an OBIA framework. Pertinent to this analysis were processed lidar, thematic (e.g., parcel, subcatchment), and aerial imagery datasets. OBIA was carried out with eCognition. Resultant classifications representing existing building rooftops were exported for quality assessment and further geospatial analysis. Quality assessment of OBIA results was based on random sample sites (n=50, 3.14

hectares) targeting areal- and location-based metrics (e.g., Root Mean Square Error) for households. Classifications served as a driving component within the LID Site Suitability (*LIDSS*) toolset. *LIDSS* was developed to provide geospatial analysis of the constraining physical datasets throughout the watershed. It was driven by user-defined parameters for maximum allowable slopes, the land cover/land use types, the soils, the depth to groundwater (when available), the presence of flood risk or floodway zones, and the proximity to existing infrastructure.

Running *LIDSS*, which filtered through the datasets, resulted in the extraction of suitable locations for the implementation of the targeted LID. The objective of *LIDSS* was not on individual LID practices, rather to allow the broader ability of users to guide extraction and identification by more general design parameters. The attribute table for this layer, containing parcel- and subcatchment-specific values for drainage areas, was used to quantify the number and design parameters of LID practices required to meet hydrologic goals. The resultant Suitability Protocol and toolsets were applied, In this case, for RWH. The results were then imported using the Rainwater Harvesting Analyzer (*RWHA*), which was a VBA-enabled toolset that sized parcel-scale practices based on user guidance. This included the specific design event depth (e.g., Water Quality Control Volume, or WQCV) and nominal RWH unit capacity. Results automatically amended a validated SWMM *.inp* model for simulation of the rainfall-runoff response for the user-designed watershed RWH scenario (*LID227)*. Hydrologic simulations were facilitated using the EPA Storm Water

Management Model (SWMM), version 5.0.022, and the validated model from previous work (Walsh et al., 2014). This work was presented as a case study paper, to be submitted Summer 2014 (Walsh et al., in review) to the *Journal of Water Resources Planning and Management*.

Based on the results of the Suitability Protocol (Walsh et al., in review), prioritization was geospatially assessed by combining long-term hydrologic simulations with long-term costs. Hydrologic simulations targeted the overall watershed and subcatchment-scales, with outflow volumes and peak flow rates highlighted. Time scales of analysis include cumulative, long-term (1948-2012), annual, and monthly. For cost estimation, the WERF BMP and LID Whole Life Cost Model, version 2.0, was used to calculate a total cost for the options. The equivalent annual cost (EAC) was then calculated, accounting for capital, operation and maintenance, and replacement of all units (at 50 years) throughout the entire 62-year lifetime. These values were then joined to a spatially-explicit map for analysis at the subcatchment scale. Long-term hydrologic results were joined to the subcatchments, as well, providing spatial distribution of both volume and rate data. With these data, surfaces were interpolated with the Inverse Distance Weighted (IDW) method. These surfaces provided the basis for cost-effectiveness derivation, by dividing the benefit by the cost and applying the zonal statistics to the individual subcatchments.

Assessment of priority was driven by the prioritization toolset, referred to as *PriorLID*, which was created to iterate classifications of the rasterized cost-effectiveness surface to provide groupings, or classes, of homogenous values.

Values represented the cost-effectiveness, or volumetric reduction per dollar invested. Top-down economic thresholds were established relative to the maximum EAC for the watershed and based on realistic budgets, which drove postprocessing selection of classes. These classes, then, represented the most cost-effective locations meeting both user-defined suitability criteria and economic thresholds. The suitability hydrologic model (*LID227*) was then adapted to represent the classes meeting the economic threshold (*LID227p*). Comparisons were made with both the *BASE* and *LID227* model results. Simulations were driven by long-term, hourly precipitation data (1948-2012). Results determined the locations that provided not only the most cost-effective choices based on economic thresholds but also an acceptable overall watershed reduction based on hydrologic thresholds.

The addition of seven climatic regimes' continuous, hourly precipitation (1960-1991) provided an analysis of the impacts of precipitation characteristics on watershed RWH reductions. Event-specific results were binned by depth and compared against those obtained with San Diego data. The change in watershed-scale reductions was analyzed with respect to the change in precipitation characteristics (e.g., interevent time, duration, intensity, and depth). Uncertainty analysis was applied to quantify the impact of variability in subcatchment percent imperviousness on hydrologic model simulations. A Monte Carlo Method (MCM) of uncertainty estimation was employed for 100 randomized models that simulated runoff response with continuous, hourly precipitation from 1999-2007. Targeted results included the exceedance

probabilities of monthly peak flow rates and monthly total outflow volumes. Randomized models were further extended to assess the independent variable's impact on the suitably-extracted RWH scenarios (which were held constant while percent imperviousness varied). This research was presented as an application paper, to be submitted Summer 2014 (Walsh & Pomeroy, in review) to the *Journal of Urban Planning and Development*.

Ultimately, this dissertation improves the extraction of distributed locations meeting user-defined constraints and goals for site-specific LID practices, primarily RWH. The resultant thematic maps and data attribute tables are not only representative of the underlying parameters but are also prioritized to yield a cost-effective stormwater management solution meeting users' objectives. The Suitability Protocol was found to provide acceptable approximations of rooftop areas and filter locations for further implementation and design at both the parcel and subcatchment-scales. The Prioritization Protocol improved the ability to account for both economic and hydrologic thresholds, as determined by the user. Uncertainty analysis found negligible impact of subcatchment imperviousness on overall watershed hydrologic response. Together, these protocols and toolsets are available to several disciplines, from urban planning to civil and environmental engineering, and employ publicly-available datasets and widespread software. Together, the work in this dissertation improves upon the conventional methods of LID design and distribution at the watershed-scale.

1.6 Organization of Dissertation

The details for the research methodologies and results obtained are presented in the following chapters. Beginning with Chapter 2, the development and application of a hydrologic model targeting the implementation of a passive RWH program for an urbanized, semi-arid watershed is presented and discussed. This research followed traditional methods of RWH implementation and assessed the impacts of variations in storage capacity, watershed percent of implementation, and management parameters (e.g., drain delay, drain duration). This chapter was published, with co-authors Dr. Christine Pomeroy and Dr. Steve Burian, in the *Journal of Hydrology* in January 2014. Next, Chapter 3 presents the development and application of an LID Site Suitability Protocol, with associated toolsets. This research incorporates remote sensing image-based analysis methods in conjunction with geospatial analysis toolsets to characterize, identify, and quantify locations meeting user-defined suitability criteria. This chapter is currently under review by co-authors, Dr. Christine Pomeroy and Dr. Philip Dennison. It will be submitted Summer 2014 to the *Journal of Water Resources Planning and Management*.

Chapter 4 presents the development and application of an LID Prioritization Protocol, with associated toolsets. This section builds on the needs and base models established in Chapter 2 and the results and toolsets from Chapter 3. This research provides geospatial analysis of both cost and hydrologic estimations for suitably extracted RWH frameworks. Monte Carlo Methods (MCM) of uncertainty estimation were applied to the independent

parameter, subcatchment percent of imperviousness, with watershed and subcatchment outflow hydrologic responses targeted for assessment of impacts. To date, this journal article has not been submitted, though a Summer 2014 submission to the *Journal of Landscape Planning and Management* is projected. Chapter 5 provides a summary of the conclusions from each of the research sections, a description of future research topics, and recommendations for improvements to the development and application of suitability and priority driven protocols. Finally, four appendices are included, highlighting Software and Data Sources (Appendix A), Hydrologic Model Development, Calibration, and Validation (Appendix B), RWH Design Guidance and Resources (Appendix C), and Protocol Application Guidelines (Appendix D).

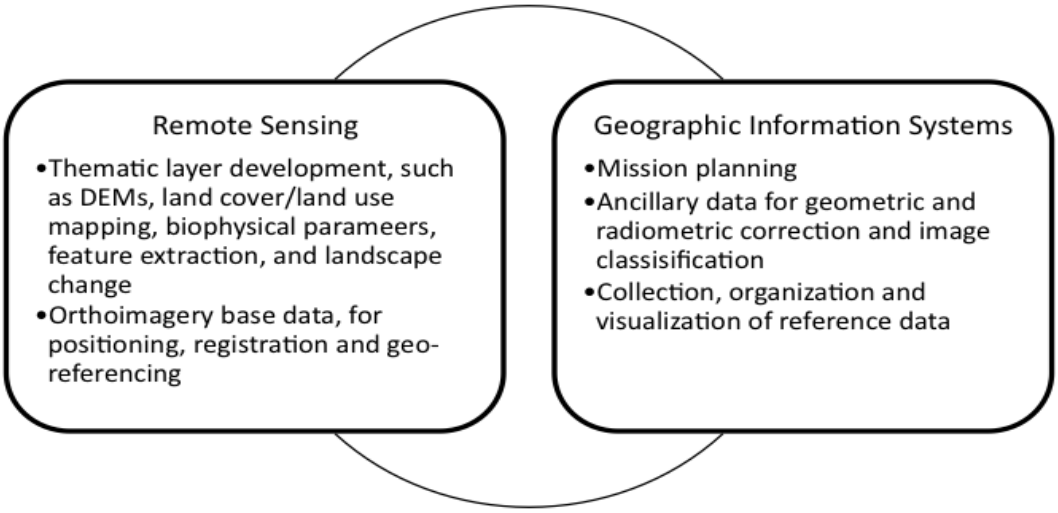

Figure 1.1: Integrated contributions of remote sensing and GIS applications (adapted from Wang et al., 2010).

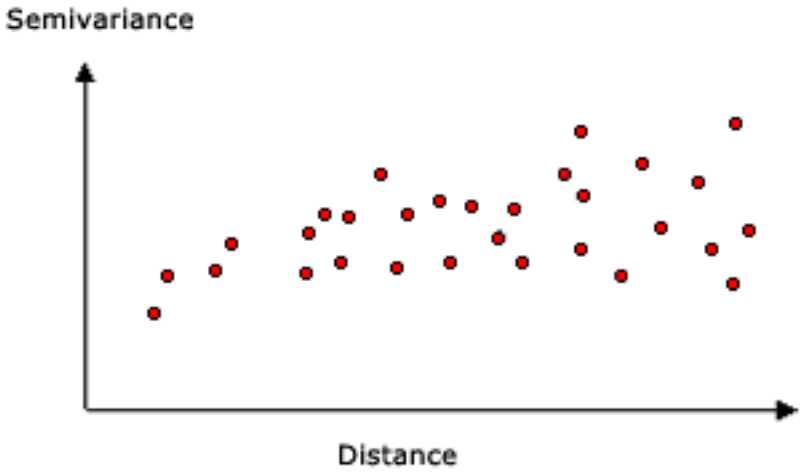

Figure 1.2: Generalization of an empirical semivariogram plot, in which points that are spatially closer together are more alike than those further apart (ESRI, 2013).

1.7 References

Aguilar, M. A., Vicente R., Aguilar F. J., Fernandez A., & Saldana, M. M. (2012). Optimizing object-based classification in urban environments using very high resolution Geoeye-1 imagery. Proceedings from: *ISPRS Annals of the Photogrammetry, Remote Sensing and Spatial Information Sciences, Volume 1-7. XXII ISPRS Congress.* Melbourne, AU: ISPRS.

Amatya, D., Trettin, C., Panda, S., & Ssegane, H. (2013). Application of LiDAR data for hydrologic assessments of low-gradient coastal watershed drainage characteristics. *Journal of Geographic Information System*, *5*, 175-191.

Anderson, T. K. (2009). Kernel density estimation and k-means clustering to profile road accident hot spots. *Accident Analysis & Prevention*, *41*(3), 359-364.

Basinger, M., Montalto, F., & Lall, U. (2010). A rainwater harvesting system reliability model based on nonparametric stochastic rainfall generator. *Journal of Hydrology, 392*, 105-118.

Bates, B. C., Kundzewicz Z. W., Wu, S., & Palutikof, J. P. (Eds.). (2008). *Climate change and water: Technical paper of the intergovernmental panel on climate change.* Geneva: IPCC Secretariat.

Bedan, E. S., & Clausen, J. C. (2009). Stormwater runoff quality and quantity from traditional and low impact development watersheds. *Journal of the American Water Resources Association*, *45*(4), 998-1008.

Berke, P. R., Macdonald, J., White, N., Holmes, M., Line, D., Oury, K., & Ryznar, R. (2003). Greening development to protect watersheds: Does new urbanism make a difference? *Journal of the American Planning Association, 69*(4), 397-413.

Blaschke, T. (2010). Object based image analysis for remote sensing. *ISPRS Journal of Photogrammetry and Remote Sensing*, *58*, 239-258.

Braden, J. B., & Johnston, D. M. (2004). Downstream economic benefits from storm-water management. *Journal of Water Resources Planning and Management*, *130*(6), 498-505.

Brown, K., Claytor, R., Holland, H., Kwon, H. Y., Winer, R., & Zielinski, J. (2007). *Better site design: An assessment of the better site design principles for communities implementing Virginia's Chesapeake Bay Preservation Act.* Ellicott City, MD: Center for Watershed Protection.

Burian, S. J., & Pomeroy, C. A. (2010). Urban impacts on the water cycle and potential green infrastructure implications. In J. Aitkenhead-Peterson & A. Volder (Eds.), *Urban ecosystem ecology* (pp. 277-296). Madison, WI: American Society of Agronomy, Crop Science Society of America, Soil Science Society of America.

Burns, M. J., Fletcher, T. D., Walsh, C. J., Ladson, A. R., & Hatt, B. E. (2012). Hydrologic shortcomings of conventional urban stormwater management and opportunities for reform. *Landscape and Urban Planning*, *105*(3), 230-240.

Burns, M. J., Fletcher, T. D., Duncan, H. P., Hatt, B. E., Ladson, A. R., & Walsh, C. J. (2014). The performance of rainwater tanks for stormwater retention and water supply at the household scale: An empirical study. *Hydrological Processes*, in press. doi 10.1002/hyp.10142.

Campbell, C. W. (2012). Western Kentucky University stormwater utility survey 2012. Retrieved from http://wku.edu/engineering/documents/swusurveys/swusurvey-2012.pdf

Cao, Y., Wei, H., Zhao, H., & Li, N. (2012). An effective approach for land-cover classification from airborne lidar data fused with co-registered data. *International Journal of Remote Sensing*, *33*(18), 5927-5953.

Carlson, T. N., & Ripley, D. A. (1997). On the relation between NDVI, fractional vegetation cover, and leaf area index. *Remote Sensing of Environment*, *62*, 241-252.

Central New York Regional Planning & Development Board. (2012). Green infrastructure planning for improved stormwater management in central New

York. Retrieved from http://www.dec.ny.gov/docs/water_pdf/arrafnlrptcny265.pdf

Chocat, B., Ashley, R., Marsalek, J., Matos, M. R., Rauch, W., Schilling, W., & Urbonas, B. (2007). Toward the sustainable management of urban storm-water. *Indoor and Built Environment, 16*(3), 273-285.

Damodaram, C., Giacomoni, M. H., Khedun, C. P., Holmes, H., Ryan, A., Saour, W., & Zechman, E. M. (2010). Simulation of combined best management practices and low impact development for sustainable stormwater management. *Journal of the American Water Resources Association, 46*(5), 907-918.

Debo, T. N., & Reese, A. (2010). *Municipal stormwater management* (2nd ed.). Boca Raton, FL: CRC Press.

Denault, C., Miller, R. G., & Lence, B. J. (2006). Assessment of possible impacts of climate change in an urban catchment. *Journal of the American Water Resources Association*, *45*(2), 512-533.

Di Gregorio, A., & Jansen, L. J. M. (2000). Land Cover Classification System (LCCS): Classification concepts and user manual. Retrieved from http://www.fao.org/docrep/003/X0596E/X0596e00.htm

Dietz, M. E. (2007). Low impact development practices: A review of current research and recommendations for future directions. *Water, Air & Soil Pollution*, *186*, 351-363.

Dorfman, M., & Mehta, M. (2011). *Thirsty for answers: Preparing for the water-related impacts of climate change in American cities*. New York, NY: Natural Resources Defense Council.

ESRI (Environmental Systems Resource Institute). (2013). ESRI ArcMap Software (Version 10.1) [ArcMap 10.1]. Redlands, California.

Ferro, C. J. S., & Warner, T. A. (2002). Scale and texture digital image classification. *Photogrammetric Engineering & Remote Sensing, 68*(1), 51-63.

Frazier, P. S., & Page, K. J. (2000). Water body detection and delineation with landsat TM data. *Photogrammetric Engineering and Remote Sensing*, *66*(12), 1461-1467.

Gillies, R. R., Carlson, T. N., Cui, J., Kusta, W. P., & Humes, K. S. (1997). A verification of the 'triangle' method for obtaining surface soil water content and energy fluxes from remote measurements of the Normalized Difference

Vegetation Index (NDVI) and surface radiant temperature. *International Journal of Remote Sensing*, *18*, 3145-3166.

Gilroy, K. L., & McCuen, R. H. (2009). Spatio-temporal effects of low impact development practices. *Journal of Hydrology, 367*, 228-236.

Godschalk, D. R., Rose, A., Mittler, E., Porter, K., & West, C. T. (2009). Estimating the value of foresight: Aggregate analysis of natural hazard mitigation benefits and costs. *Journal of Environmental Planning and Management*, *52*(6), 739-756.

Han, M. Y., Mun, J. S., & Kim, H. J. (2008). An example of climate change adaptation by rainwater management at the Star City rainwater project. Proceedings from: *3rd Rainwater Harvesting and Management Workshop*. Sydney, AU: IWA.

Hsieh, P. F., Lee, L. C., & Chen, N. Y. (2001). Effect of spatial resolution in classification errors of pure and mixed pixels in remote sensing. *IEEE Transactions on Geoscience and Remote Sensing*, *39*, 2657-2663.

Hu, X., & Weng, Q. (2011). Impervious surface area extraction from IKONOS imagery using an object-based fuzzy method. *Geocarto International*, *26*(1), 3-20.

Im, J., Jensen, J. R., & Hodgson, M. E. (2008). Object-based land cover classification using high-posting-density LiDAR data. *GIScience & Remote Sensing*, *45*(2), 209-228.

Jacquez, G. M. (2008). Spatial cluster analysis. In J. P. Wilson & A. S. Fotheringham (Eds.), *The handbook of geographic information science* (1st ed., pp. 395-416). Victoria, AU: Blackwell Publishing.

James, L. A., Watson, D. G., & Hansen, W. F. (2007). Using lidar data to map gullies and headwater streams under forest canopy: South Carolina, USA. *CATENA*, *71*(1), 132-144.

Jensen, J. R. (2005). *Introductory digital image processing* (3rd ed.). Upper Saddle River, NJ: Prentice Hall.

Jensen, C. A., Quinn, R. J., & Davis, T. H. (2010). Urban watershed management: Using remote sensing to implement low impact development. Proceedings from: *2010 Third International Conference on Infrastructure Systems and Services: Next Generation Infrastructure Systems for Eco-Cities.* Shenzhen, China: IEEE.

Jia, H., Lu, Y., Yu, S. L., & Chen, Y. (2012). Planning of LID-BMPs for urban

runoff control: The case of Beijing Olympic Village. *Separation and Purification Technology*, *84*, 112-119.

Kousky, C., Olmstead, S. M., Walls, M. A., & Macauley, M. (2013). Strategically placing green infrastructure: Cost-effective land conservation in the floodplain. *Environmental Science & Technology*, *43*, 3563-3570.

Kunapo, J., Chandra, S., & Peterson, J. (2009). Drainage network modelling for water-sensitive urban design. *Transactions in GIS*, *13*(2), 167-178.

Lee, J. G., & Heaney, J. P. (2003). Estimation of urban imperviousness and its impacts on storm water systems. *Journal of Water Resources Planning and Management*, *129*, 419-426.

Lee, J. G., Selvakumar, A., Alvi, K., Riverson, J., Zhen, J. X., Shoemaker, L., & Lai, F. (2012). A watershed-scale design optimization model for stormwater best management practices. *Environmental Modelling and Software*, *37*, 6-18.

Lim, S-R, Suh, S., Kim, J-H, & Park, H. S. (2010). Urban water infrastructure optimization to reduce environmental impacts and costs. *Journal of Environmental Management*, *91*, 630-637.

Lu, D., & Weng, Q. (2007). A survey of image classification methods and techniques for improving classification performance. *International Journal of Remote Sensing*, *28*(5), 823-870.

Luzio, M. D., Arnold, J. G., & Srinivasan, R. (2005). Effect of GIS data quality on small watershed stream flow and sediment simulations. *Hydrological Processes*, *19*, 629-650.

Malczewski, J. (2004). GIS-based land-use suitability analysis: A critical overview. *Progress in Planning*, *62*(1), 3-65.

Mandarano, L. (2011). Clean waters, clean city: Sustainable storm water management in Philadelphia. In M. I. Slavin (Ed.), *Sustainability in america's cities: Greening the metropolis* (pp. 157-179). Washington, DC: Island Press.

Marsalek, J., & Chocat, B. (2002). International report: Stormwater management. 2nd World Water Congress: Integrated water resources management. *Water Science and Technology, 46*(6-7), 1-17.

Mentens, J., Raes, D., & Hermy, M. (2006). Green roofs as a tool for solving the rainwater runoff problem in the urbanized 21st century? *Landscape and Urban Planning, 77*(3), 217-226.

Mumby, P. J., & Edwards, A. J. (2002). Mapping marine environments with IKONOS imagery: Enhanced spatial resolution can deliver greater thematic accuracy. *Remote Sensing of Environment*, *82*, 258-257.

Myint, S. W., Gober, P., Brazel, A., Grossman-Clarke, S., & Weng, Q. (2011). Per-pixel vs. object-based classification of urban land cover extraction using high spatial resolution imagery. *Remote Sensing of Environment*, *115*(5), 1145-1161.

Northeast Ohio Regional Sewer District. (2011). Walworth run green infrastructure feasibility study. Retrieved from https://www.neorsd.org/I_Library.php?a=download_file&LIBRARY_RECORD_ID=5344

National Research Council of the National Academies (NRC). (2008). *Urban stormwater management in the United States.* Washington, DC: The National Academies Press.

Pataki, D. E., Carreiro, M. M., Cherrier, J., Grulke, N. A., Jennings, V., Pincetl, S., Pouyat, R. V., Whitlow, T. H., & Zipperer, W. C. (2011). Coupling biogeochemical cycles in urban environments: Ecosystem services, green solutions, and misconceptions. *Frontiers in Ecology and the Environment, 9*(1), 27-36.

Peteri, R., & Ranchin, T. (2007). Road networks derived from high spatial resolution satellite remote sensing data. In Q. Weng (Ed.), *Remote sensing of impervious surfaces* (pp. 215-236). Boca Raton, FL: CRC Press.

Prince George's County, Maryland (June 1999). Low-impact development design strategies: An integrated design approach. Retrieved from http://water.epa.gov/polwaste/green/upload/lidnatl.pdf.

Roy, A. H., Wenger, S. J., Fletcher, T. D., Walsh, C. J., Ladson, A. R., Shuster, W. D., Thurston, H. W., & Brown, R. R. (2008). Impediments and solutions to sustainable, watershed-scale urban stormwater management: Lessons from Australia and the United States. *Environmental Management*, *42*, 344-359.

Rumman, N., Lin, G., & Li, J. (2005). Investigation of GIS-based surface hydrological modelling for identifying infiltration zones in an urban watershed. *Environmental Informatics Archives*, *3*, 315-322.

Sample, D., & Heaney, J. (2006). Integrated management of irrigation and urban storm-water infiltration. *Journal of Water Resources Planning and Management*, *132*(5), 362-373.

Schueler, T. (1994). The importance of imperviousness. *Watershed Protection*

Techniques, *1*(3), 100-111.

Shaver, E., Horner, R., Skupien, J., May, C., & Ridley, G. (2007). *Fundamentals of urban runoff management: Technical and institutional issues* (2nd ed.). Madison, WI: North American Lake Management Society.

Shuster, W. D., Morrison, M. A., & Webb, R. (2008). Front-loading urban stormwater management for success – a perspective incorporating current studies on the implementation of retrofit low-impact development. *Cities and the Environment (CATE), 1*(2), Art. 8.

Solyman, L. G. E - D. T (2012). Improving automatic feature detection from LIDAR intensity by integration of LIDAR height data and true orthoimage from digital camera. *International Journal of Circuits, Systems and Signal Processing*, *3*(6), 221-230.

Spatari, S., Zu, Y, & Montalto, F. A. (2011). Life cycle implications of urban green infrastructure. *Environmental Pollution*, *159*, 2174-2179.

Sterr, N., & Yui Lau, M. (2012). Impervious surfaces in WRIA 9-Green-Duwamish watershed. Report created for King County Department of Natural Resources and Parks Water and Land Resources Division as part of the course requirements for Geography 469, Spring 2012.

Thomas, N., Hendrix, C., & Congalton, R. G. (2003). A comparison of urban mapping methods using high-resolution digital imagery. *Photogrammetric Engineering & Remote Sensing, 69*(9), 963-972.

Thurston, H., Goddard, H., Szlag, D., & Lemberg, B. (2003). Controlling storm-water runoff with tradable allowances for impervious surfaces. *Journal of Water Resources Planning and Management*, *129*(5), 409-418.

USEPA. (December, 2007a). Reducing stormwater costs through low impact development (LID) strategies and practices. EPA 841-F-07-006. Retrieved from http://water.epa.gov/polwaste/green/costs07_index.cfm

Walsh, T. C., Pomeroy, C. A., & Burian, S. J. (2014). Hydrologic modeling analysis of a passive, residential rainwater harvesting program in an urbanized, semi-arid watershed. *Journal of Hydrology*, *508*, 240-253.

Wang, K., Franklin, S. E., Guo, X., & Cattet, M. (2010). Remote sensing of ecology, biodiversity and conservation: A review from the perspective of remote sensing specialists. *Sensors*, *10*, 9647-9667.

Wechsler, S. P. (2007). Uncertainties associated with digital elevation models for hydrologic applications: A review. *Hydrology and Earth System Sciences, 11*,

1481-1500.

Weng, Q. (2012). Remote sensing of impervious surfaces in the urban areas: Requirements, methods, and trends. *Remote Sensing of Environment*, *117*, 34-49.

Wu, C., & Yuan, F. (2011). Remote sensing of high resolution urban impervious surfaces. In X. Yang (Ed.) *Urban remote sensing: Monitoring, synthesis and modeling in the urban environment* (1st ed., pp. 239-252). Oxford, UK: John Wiley & Sons.

Yang, B., & Li, S. (2013). Green infrastructure design for stormwater runoff and water quality: Empirical evidence from large watershed-scale community developments. *Water*, *5*, 2038-2057.

Yang, H., Ma, B., Du, Q., & Yang, C. (2010a). Improving urban land use and land cover classification from high-spatial-resolution hyperspectral imagery using contextual information. *Journal of Applied Remote Sensing 4*, 041890, 1-13.

Yang, Y., Zhou, Q., Gong, J., & YingYing, W. (2010b). Gradient analysis of landscape spatial and temporal pattern changes in Beijing metropolitan area. *Science China, Technological Sciences*, *53*(1), 91-98.

Yu, B., Liu, H., Wu, J., Hu, Y., & Zhang, L. (2010). Automated derivation of urban building density information using airborne LIDAR data and object-based method. *Landscape and Urban Planning*, *98*, 210-219.

Zhu, G., & Blumberg, D. G. (2002). Classification using ASTER data and SVM algorithms; the case study of Beer Sheva, Israel. *Remote Sensing of Environment*, *80*(2), 233-240.

Zhu, L., Shortridge, A. M., & Lusch, D. (2012). Conflating LiDAR data and multispectral imagery for efficient building detection. *Journal of Applied Remote Sensing*, *6*, 1-17.

CHAPTER 2

HYDROLOGIC MODELING ANALYSIS OF A PASSIVE, RESIDENTIAL RAINWATER HARVESTING PROGRAM IN AN URBANIZED, SEMI-ARID WATERSHED[1]

This research study was published in the *Journal of Hydrology* in January 2014 with my co-authors, Dr. Christine Pomeroy and Dr. Steve Burian.

2.1 Abstract

This paper presents the results of a long-term, continuous hydrologic simulation analysis of a watershed-scale residential rainwater harvesting (RWH) program in the Chollas Creek watershed, San Diego, California, USA. The U.S. Environmental Protection Agency's Storm Water Management Model (SWMM) simulated rainfall-runoff responses for variations in a RWH network, including the RWH unit storage size, the number of implementing households, the amount of time before a unit is allowed to release captured runoff (i.e., drain delay), and the time it takes for the unit to drain (i.e., coefficient of discharge). Comparison of

1 Reprinted with permission from Elsevier, *Journal of Hydrology*.

results found reductions to increase linearly with capacity and implementation. Maximum long-term watershed volumetric reductions between 10.1% - 12.4% were observed for the period of analysis (1948-2011) with a range of RWH storage sizes (227 liter barrels to 7,571 liter cisterns). The ratio of overflow to underdrain flow, ranging from 5.17 - 0.014 (227 - 7,571 liters), exhibits the ability of cisterns to fully capture the majority of annual and long-term events. Sensitivity analysis found regional precipitation characteristics and disconnection of rooftop runoff to impact long-term watershed reduction potential more so than available RWH capacity. Drain delay control and dry duration time increased reduction variability with cisterns, though long-term reductions were not significantly impacted. Normalization of net present value (NPV) to volumetric reductions yielded a RWH unit cost of $0.20-$1.71 per 1,000 liters of watershed runoff reduced on average per year. Minor variations in cost based on the extent of watershed implementation highlight the potential to incrementally institute RWH programs. For the case study location, the 227-liter rain barrel provided the greatest cost-effectiveness, reducing an average 6,500 liters of runoff per dollar invested for the analysis period.

2.2 Introduction

The impervious characteristics and interconnectivity of built-up urban areas contribute negatively to stormwater quantity and quality (Alley & Veenhuis, 1983; Schueler, 1994; Lee & Heaney, 2003). In response, low impact development (LID) practices have been designed to mimic natural, pre-developed conditions through the capture, infiltration, and treatment of

stormwater runoff at its source (Prince George's County, 1999; USEPA, 2000; USEPA, 2007a). This reduces annual average runoff volumes (De Graaf & Der Brugge, 2010; Foraste & Hirschman, 2010; Jia et al., 2012), peak discharge rates (Mitchell et al., 2007; Dietz, 2007; Han et al., 2008), and pollutant loading (Roy et al., 2008; Lim et al., 2010; Spatari et al., 2011). One such LID practice is rainwater harvesting (RWH), which intercepts rooftop runoff to meet end uses (Prince George's County, 1999; USEPA, 2000), including subsurface infiltration, landscape irrigation, nonpotable indoor uses, and potable consumption (County of San Diego, 2012). RWH is unique in its ability to supplement water demands with captured runoff, thereby reducing water bills, and to provide stormwater storage in space-limited areas, resulting in a higher retrofit-ability.

Against other storage-based LID practices, studies found comparable stormwater runoff reductions from RWH (Benedict & McMahon, 2002; Shuster et al., 2008; Endreny & Collins, 2009; Young et al., 2009); however, knowledge gaps exist with respect to design procedures, effectiveness, and application (Schneider & McCuen, 2006; Ahiablame et al., 2012), specifically, expansion of study scales from lot to watershed, assessing cumulative impacts to watershed-scale stormwater runoff (Bedan & Clausen, 2009; Lee et al., 2012), and movement towards simulations driven by long-term, continuous precipitation (McClintock et al., 1995; Roesner, 1999; Grimaldi et al., 2012). Improving on this knowledge informs spatio-temporal considerations, designs, and implementation extents prior to inclusion in local stormwater management plans (Gilroy & McCuen, 2009; Shen et al., 2013).

For instance, design storm simulations fail to account for long-term antecedent conditions, which influence catchment hydrologic response (Bhaduri et al., 2000). This is important when simulating RWH's impact on water balance (Baek & Coles, 2011). For RWH at single-family residential lots, Gilroy and McCuen (2009) simulated 1- and 2-year design storms, and found significant reductions in runoff volumes (e.g., 32%, 30%) and peak rates (e.g., 10%, 6%) at the lot scale without regard for long-term viability. Despite finding similar results, Damodaram et al. (2010) recommended both application of RWH with other LID practices and increasing the range of storm events when determining efficiency. Such volume-centric results appear promising despite neglecting a continuous range of events, which can lead to misrepresentations of LID effectiveness (Pitt, 1999). For example, in a study to improve reliability of RWH capture estimates for demand supplementation, Basinger et al. (2010) did not pay similar attention to stormwater runoff, highlighting a mere 28% annual reduction for units that would theoretically fill to 35% of capacity with the 90^{th} percentile storm event.

These studies highlight the need for long-term simulations (Pitt, 1999), watershed-scale LID implementation (Rosemarin, 2005), and targeted hydrologic metrics that replace single, flow-based standards and inform urban water management (Olden & Poff, 2003, Petrucci et al., 2012). Expanded metrics include the magnitude, frequency, and duration of long-term events, emphasizing conservation and rehabilitation (Olden & Poff, 2003; Booth et al., 2004; Kennard et al., 2010**;** Petrucci et al., 2012). Normalizing reductions to long-term costs yields feasibility of implementation relative to the bottom line (Herrmann & Hasse

1997; Damodaram et al., 2010). Together, these allow comparisons of program variations and, ultimately, a recommendation for the most feasible option as a watershed-scale stormwater management practice.

This paper presents a quantification of the stormwater management benefits associated with watershed-scale implementation of a storage-based RWH program for a densely urbanized, semi-arid region. Determination of reduction significance and benefit normalization to the net present value (NPV) of implementation was completed at the watershed outlet and subcatchment-scales. This provided a measure of cost-effectiveness for comparison with other storage-based stormwater management practices. A linear relationship is theorized to exist between RWH capacity and reductions in watershed stormwater runoff. Given the precipitation characteristics of the study location, the high urban density, and the routing of LID mediated flow to pervious areas, the smaller RWH configuration (e.g., 227 liter barrels) is expected to provide the most cost-effective long-term option for the watershed.

2.3 Materials and Methods

The following sections outline and discuss the study area, study design, hydrologic analysis and municipal RWH scenarios employed in this study.

2.3.1 Study Area

The South Fork of Chollas Creek, part of the greater Pueblo Watershed, is located southeast of downtown San Diego, California, USA within the San Diego-Carlsbad-San Marcos metropolitan area (Fig. 2.1). It has a drainage area of 30.7

square kilometers (km^2) (Weston Solutions, Inc., 2010a; 2010b) and was selected due to interest by City of San Diego stormwater officials in implementing a rain barrel downspout disconnect (RBDD) program (City of San Diego, 2010). The headwaters are located in Lemon Grove, ultimately discharging into the San Diego Bay and Pacific Ocean. Soils are predominantly Hydrologic Soils Group D, with low infiltration rates (SanGIS, 2012). The total impervious area (TIA) is 50%, while directly connected impervious area (DCIA) is between 38% and 46%, calculated using the methods of Wenger et al. (2008) and Alley and Veenhuis (1983), respectively. The DCIA parameter was approximated using land use estimates based on parcel data. Impervious areas were digitized for four random subcatchments, quantifying the subcatchment-specific TIA.

Population density is roughly 5,400 people per km^2 (City Data, 2011), representative of a high-density residential area (City of San Diego, 2002) and comprised of typical urban land uses (Fig. 2.2). Chollas Creek is not tidally influenced in the study reach, but does experience intermittent flow (City of San Diego, 2002; Weston Solutions, Inc., 2006). Since rainfall patterns are spatially consistent, streamflow can be attributed to urban rainfall runoff (City of San Diego, 2002; Weston Solutions, Inc. 2006; 2010a; 2010b). On average, precipitation ranges from 0.05 – 51.6 mm per month (i.e., 0.2% of annual rainfall in July and 20% in January) and 259 mm annually. The 85^{th} percentile 24-hour duration storm event depth is approximately 16.5-mm. Average monthly potential evaporation ranges from a high (6.3 mm/day) in July to a low (2.3 mm/day) in December.

2.3.2 Study Design

Discussions with San Diego Coastkeeper and City of San Diego stormwater management staff aided in the development of RWH scenarios, with the greatest potential at single-family residential lots. Commercial and industrial rooftops were excluded from this study. The first step to identify single-family residential lots was to cross-reference GIS-based residential parcels with local business addresses (SanGIS, 2012). Validation was completed by combining extracted residential parcels with aerial imagery for visual verification, yielding 20,787 single-family residential lots. Next, calculation of the average rooftop area was completed with a random sample of 150 parcels identified as residential, providing an average of 186 square meters (m^2). A conservative 50% capture efficiency was then applied to account for losses including evaporation, the inability to detain all rooftop runoff, and the assumption that RWH units would only be placed at one corner of the household, with additional units connected in series. The adjusted area (93 m^2) was multiplied by the validated number of single-family residential lots to obtain the subcatchment-specific percent of impervious area treated by RWH.

In this study, the researchers quantified the watershed impacts of RWH by assessing changes in the cumulative, annual, and daily stormwater runoff volumes, flow rates (i.e., peak and average), and event exceedance frequency for long-term (water years 1949-2011) hydrologic simulations. Design storms (up to the 24-hour, 0.01 probability event) provided watershed reduction comparisons with continuous, long-term simulations, in which antecedent conditions are

considered. Sensitivity analysis was performed by varying one independent variable at a time. Independent variables included: the capacity of the units (a total of five volumes), the percent of maximum watershed households targeted (a total of four allocations), the coefficient of discharge, and the drain delay parameter. For each individual variation, both overall and hourly time series long-term simulation results were collated for analysis. Differences in annual performance, in terms of precipitation depth, average event intensity, and seasonal variation, were targeted. Comparison of RWH scenario results with a base case (no RWH) provided quantification. Last, normalization of runoff results to the total NPV per permutation gave a cost-based metric for relating multiple LID practices (Foraste et al., 2012; McGarity, 2012), with insight to option feasibility. Sensitivity analysis of storage capacity, RWH discharge-governing parameters (e.g., drain delay and drain duration), and modeling methods (e.g., LID Editor versus LID storage conversion to impervious area depression storage) extended the interpretation of results.

2.3.3 Hydrologic Analysis

Hydrologic modeling was performed using the U.S. Environmental Protection Agency's (USEPA) Storm Water Management Model (SWMM), Version 5.0.022 (Rossman, 2010), a dynamic stormwater runoff and hydraulic routing software that simulates water quantity, quality, and LID controls (USEPA, 2012). SWMM is a widely used framework suited to development of sizing guidelines for devices and programs, such as municipal RWH, across the catchment, subdivision, and site scales (Elliott & Trowsdale, 2007). Multiple

sources of data were used to build the Chollas Creek model. Subcatchments were delineated via discussions with the City of San Diego and validated with digital elevation model (DEM) and land use data, resulting in 78 subcatchments ranging in size from 0.02 - 3.06 km^2. Land surface slopes were estimated using 0.61-m contours acquired from SanGIS (2012), ranging between 0.5% - 10.9%. Manning's roughness values of 0.20 (e.g., dense grass) and 0.009 were assigned to pervious and impervious surfaces, respectively. Pervious depression storage was representative of lawns (e.g., 3.81 mm) and impervious depression storage was set as 0.635 mm (ASCE, 1992). Conduit slope and lengths were determined with node elevations provided by SanGIS (2012) storm drain network data. Average slope along the 10-km main branch of Chollas Creek was found to be 1.33%.

The storm drainage network is comprised of 151 open (e.g., natural channel) and closed (e.g., drain pipe) segments. Characterization of the channel geometry and lengths was obtained from storm sewer GIS shapefiles (e.g., point and polyline) and confirmed with aerial imagery (SanGIS, 2012). Conduit roughness (Manning's n coefficient) was set as 0.013 for circular, concrete pipes and 0.02 for trapezoidal concrete-lined channels (USDOT, 1986; ASCE, 1992). The Green-Ampt method was chosen to govern soil infiltration, with the following parameters: suction head of 239 mm (i.e., sandy clay), conductivity of 1.27 mm/hour (i.e., sandy clay), and initial deficit of 0.25 (Rossman, 2010; County of San Diego, 2012). Long-term hourly precipitation data, acquired for San Diego Lindbergh Field airport (COOP ID 047740, 32°44'N/117°11'W, period of record

1948-2011), and SCS Type I design storms were created, with Chollas Reservoir station data (ID 92-0510, 32°43'N/117°4'W, period of record 1926-2003), following a 24-hour cumulative pattern (NOAA, 2012). The 1.0, 0.5, 0.2, 0.1, 0.04, and 0.01 probability events register total depths of 34.8-, 47-, 62.7-, 74.9-, 91.2-, and 115.6-mm, respectively.

As continuous streamflow data were unavailable, model calibration was performed using an iterative method of extracting individual storm event results from the long-term simulations and comparing them to individual measured events provided by annual water quality and urban runoff monitoring reports (Weston Solutions, Inc., 2007; 2010a; 2010c). Calibration was performed by iteratively adjusting subcatchments' overland flow path width, surface roughness coefficient, depression storage, and percent impervious area parameters. To minimize flooding and system losses, surcharge and ponding depths were established at the nodes of the largest subcatchments. After calibration, simulated peak flow rates matched the seven monitored events to within an average of 3.1%. Validation was accomplished by the same method but for a different set of measured events, provided by Schiff and Carter (2007). Differences in volume and outflow rate ranged from 5% - 20% for seven monitored events from 2006 (Schiff & Carter, 2007), representative of a range of storm event sizes and durations.

Fig. 2.3 shows a comparison of modeled and monitored flow rates to precipitation depths for the storm events used for validation. The precipitation events measured in the watershed during the calibration and validation differed

from those used for the continuous simulations, with the differences in watershed discharge response linearly related. A final check involved the simulation of the 0.01 probability, 24-hour event used by the Federal Emergency Management Agency (FEMA) for floodplain mapping. This simulated a 5.8% difference in the peak flow rate upstream of the confluence of the two reaches, known as the Encanto Branch (City of San Diego, n.d.).

Discrepancies between the modeled and measured values are attributed to differences in contributing watershed area and variation in the temporal pattern of rainfall associated with each runoff producing event. Since continuously monitored streamflow data do not exist for the watershed, the resulting calibration and validation was deemed acceptable in meeting the quantification and scenario comparison goals of the researchers.

2.3.4 Municipal RWH Scenarios

Two nominal RWH capacities were evaluated in this study: 227 and 7,571 liters, with footprints of 0.23 m^2 and 22.3 m^2, respectively. The 227-liter barrel has a maximum height of 914 mm and the 7,571-liter cistern height is 3,568 mm. The primary benefits of the 227-liter configuration are a smaller barrel footprint and a shorter duration of retention time (i.e., mitigating potential water quality and/or vector concerns). Alternatively, larger cisterns capture a wider range of storm events, with the potential for extended temporal storage and longer periods of use. RWH drain time is important since vector potential (e.g., mosquitoes) may increase with storage times exceeding 48 hours (County of San Diego, 2012). Household RWH configurations were chosen to represent variations of nominal

unit sizes, with variations in capacity and drain-governing parameters investigated. For 227-liter barrels, households were outfitted with one, two, four, or eight units, for maximum storage capacities of 227, 454, 908, and 1,817 liters, respectively. Only one 7,571-liter cistern per household was considered due to its footprint to typical lot area ratio. To account for uncertainty of public adaptation, the maximum number of households was downscaled by increments of 25%, with details for the total of 21 RWH model permutations (including the base model) provided in Table 2.1.

Cost and volume are typically linear for nominally sized units. A conservative price is $100 for a 227-liter barrel, whereas a 7,571-liter cistern can be upwards of $1,000 (Tank Depot, 2012). Several Do It Yourself packages exist for smaller units, while larger cisterns require professional guidance for construction and stabilization (Smith, 2012). Operation and maintenance (O&M) is assumed to be undertaken by homeowners, which was found by Coombes (2002) to be negligible. As a result, the cost analysis from the perspective of the local government did not consider O&M. Additionally, with proper care, the expected life of RWH units can exceed 50 years (Coombes et al., 2000). Thus, replacement of all units was provided at 50 years of service. Future values of replacement costs were accounted for by applying an inflation rate of 1.5% (as of April 2013) in the calculation of the NPV. This provides the current total cost for each scenario with a 3.0% discount rate, including one-time cash outflows in years zero and 50 for purchasing and replacing RWH units, respectively. Thus, costs incurred for this study included the one-time purchasing costs at times zero

and 50.

Within SWMM, RWH discharge (i.e., both overflow and underdrain flow) was directed to the pervious portion of the subcatchment to represent the routing of residential rooftop runoff to lawns (e.g., downspout disconnection). In SWMM, flow through the underdrain (*q*, unit depth per time) is governed by Eq. (1) and was modeled as a submerged orifice. *C* represents the drain coefficient, *n* is the drain exponent, *h* is the unit height, and H_d is the drain offset.

$$q = C\left(h - H_d\right)^n \quad \text{.....(1)}$$

Duration of outflow is controlled by the drain coefficient, *C*, and Eq. (1). The *C* parameter can be estimated using Eq. (2), which accounts for the required time (*T*) to drain a depth, in inches, of stored water (*D*). The exponent value represents flow through an orifice and the drain offset was established at the bottom of each unit (e.g., zero). RWH outflow is driven by storage head, representing passive outflow control. A simplified diagram illustrating RWH flow routing with the SWMM LID Editor is provided in Fig. 2.4.

$$C = {2\left(D^{0.5}\right)}/{T} \quad \text{.....(2)}$$

To drain barrels (e.g., 227 liters) over a 24-hour period and cisterns (e.g., 7,571 liters) within 48 hours, *C* values of 0.5 were obtained with Eq. (2). These were then applied to Eq. (1) to simulate underdrain outflow. These

aforementioned drain durations were established to adhere to recommended lawn watering quantities for Southern California Coast climates (Hartin et al., 2001). For instance, a typical South Coast lot (e.g., 843 m^2, including an average building footprint of 186 m^2) requires a monthly 22,220-63,141 liters of irrigation (Hanak & Neumark, 2006). This range represents December minimums and July maximums, translating to an application rate of 30-85 liters/hour, respectively. In addition, RWH drain durations fell within the prescribed drawdown time range for other storage-based LID practices (e.g., 24-48 hours) (USEPA, 2000).

RWH distinguishes itself from other LID practices by offering monetary savings to homeowners (e.g., supplementing potable water demands); however, the goal of this study was to quantify watershed reductions resulting from distributed site-specific storage and assess cost-effectiveness from the local government's perspective. Therefore, RWH captured runoff was not subject to household demand patterns. Instead, a time release dependent, storage-discharge function controlled the drainage to pervious receiving areas. These details were modeled with the SWMM LID Editor. To account for no irrigation during or directly after precipitation events, a 24-hour drain delay was established for all models. This requires 24 consecutive hours of no precipitation to elapse before the underdrain (e.g., outlet orifice) is allowed to open. This, in effect, simulates a passive release method that reduces vector potential and assumes reliable homeowner control (e.g., opening and closing the RWH units). Variations in drain delay and outflow duration parameters determined the impact of temporal fluctuations (i.e., homeowner neglect, malfunctioning RWH units, and

climatic conditions).

After adapting the base model to account for each RWH scenario, long-term, continuous (1948-2011) and design storm simulations were carried out for a total of 21 models. To capture the dynamic response typical of urbanized catchments, a 30-second routing time step, with 5-minute wet and dry weather runoff time steps, was applied (Fletcher et al., 2013). Finally, hourly results were adjusted to provide a water year (10/1 - 9/30) analysis, as opposed to a Julian date (1/1 - 12/31) reducing the full record to 62 years. The frequency of daily peak flow events (years), *T*, was calculated using the Cunnane (1978) method (Eq. 3), where *N* represents the number of years of record, *M* is the rank of the event magnitude (after being arranged in descending order), and *a* is the plotting position parameter (i.e., a value of 0.4 was used).

$$T = \left[N + 1 - (2a)\right] / (M - a) \quad \text{.....(3)}$$

With Eq. (3) results, the number of exceedances per year, *E*, was calculated via Eq. (4).

$$E = 1/T \quad \text{.....(4)}$$

A one-way between subjects analysis of variance (ANOVA) was conducted to compare the effects RWH unit volume had on annual runoff volumes among the six scenarios tested, including the base. It was also applied

to long-term subcatchment reductions for the 20 model scenario results. ANOVA assumes independent, normally distributed datasets, with equal variances amongst the populations. The null hypothesis states there is no difference between the means of the data sets compared. The Tukey HSD post hoc test was applied to ANOVA results in which the null hypothesis was rejected. This determined the specific groups in the sample population that differed significantly.

2.4 Results

Analysis of long-term precipitation finds 66% of total depths and 58% of events to occur in the wet months of January to April, with an average depth per event of 8 mm (range 5.2 - 9.2 mm). Remaining months average 4.3 mm per event (range 1.1 - 8.2 mm). These periods established the two seasons analyzed for this study. Analysis of annual precipitation illuminates the region's small storm hydrology (Fig. 2.5). Total annual precipitation depths in exceedance of the long-term average (259 mm) were denoted as wet years, while dry years' cumulative precipitation fell below this depth.

2.4.1 Results of RWH Storage Capacity on Discharge

2.4.1.1 Watershed Outlet

Variations in RWH storage capacity resulted in linearly increasing volumetric runoff reductions for the long-term simulation totals (Fig. 2.6). For watershed coverage extents ranging from 25% to 100%, 227-liter barrels provided reductions in runoff volume (2.5% - 10.4%), peak flow rate (0.4% -

1.4%), and average flow rate (2.7% - 10.5%). For the 7,571-liter cisterns, the same watershed configurations yielded reductions in volume (3.1% - 12.4%), peak flow rate (0.5% - 1.9%), and average flow rate (3.2% - 13.7%). In general, reductions were found to increase with watershed allocation, maximizing at 100% of households targeted. There was a significant effect of RWH storage capacity on annual average runoff volumes at the $p<0.05$ level for the six model conditions [$F(5,366)=11.61$, $p=1.98E-10$]. Post hoc comparisons using the Tukey HSD test indicated that the mean score for the Base condition ($M=0.384$, $SD=0.0018$) was significantly different from all other conditions. There was a significant effect of RWH storage capacity on annual average volumetric reductions at the $p<0.05$ level for the five RWH conditions [$F(4,305)=23.09$, $p=1E-16$]. Post hoc comparisons using the Tukey HSD test indicated that the mean score for the 7,571-liter scenario ($M=0.049$, $SD=2E-5$) was significantly different from all other conditions and the mean score for the 1,817-liter scenario ($M=0.046$, $SD=1E-5$) was significantly different than the 227- and 456-liter scenarios. Average annual reductions in volumes and peak discharge rates were greater during dry years than wet years (Table 2.2).

Long-term simulation flow rate exceedance frequency curves (Fig. 2.7) demonstrated differences between pre- and post-LID application results (Table 2.3). Design storm runoff reductions ranged from 13.1% - 9.3% (7,571-liter scenario) and 13.1% - 4.4% (227-liter scenario). For the range of storage sizes, the highest reductions were achieved for the 2.0 probability event. Differences in runoff reductions were shown to increase with precipitation depth (Fig. 2.8).

Overflow of individual RWH units occurs, with the ratio of overflow to underdrain-mediated flow ranging on average from 5.17 – 0.014 for the smallest to largest storage sizes. Compared with continuous simulations, individual storm events simulations demonstrated a greater magnitude of watershed runoff reductions for the range of RWH scenarios, indicating the impacts of antecedent conditions. Differences between RWH reductions increase with the combination of available RWH capacity and precipitation depth (Fig. 2.8). This highlights the ability of cisterns to completely capture greater event depths, while barrels overflow with relatively small storms (e.g., approximately 2.4 mm for the adjusted rooftop area fills the 227-liter unit).

2.4.1.2 Subcatchment

Plotting the percent of impervious area controlled by RWH versus stormwater runoff reductions at the subcatchment level yields a linear trend similar to that of the overall watershed (Fig. 2.9). Average long-term subcatchment volumetric reductions per dollar invested range from 8,410 – 1,046 liters/$. There was a significant effect of RWH storage capacity on long-term subcatchment runoff reductions at the $p<0.05$ level for the 20 RWH conditions [$F(19,1520)=10.65$, $p=2E-30$]. Post hoc comparisons using the Tukey HSD test (Table 2.4) indicates scenario comparisons with significant differences (e.g., <>).

2.4.1.3 Modeling Methods

To assess the LID Editor for RWH, comparisons were made with a traditional modeling alternative of converting cumulative storage volume into

impervious area depression storage. Simulations for the range of RWH permutations found watershed volumetric reduction overestimation to increase with storage size while smaller capacities yielded underestimations (Fig. 2.10). Differences in reductions provided by the range of RWH capacities increase when precipitation exceeds the 0.1 probability event (e.g., 74 mm).

2.4.2 Impact of Drain Delay and Duration on Discharge

2.4.2.1 Watershed Outlet

Lengthening RWH drain duration resulted in increased RWH unit overflow. Ultimately, higher runoff volumes were simulated at the watershed outlet, with increases in flooding in conduits. As expected, volumetric sensitivity analysis demonstrated that the RWH barrels (e.g., 227 liters) reach capacity with smaller precipitation events, relative to the larger cisterns (e.g., 7,571 liters). Therefore, increases in drain duration limit the unit's ability to capture subsequent runoff. Similarly, increasing drain delay yielded increases in the ratio of overflow to underdrain flow for RWH units. Reductions in annual outflow volumes highlight the variability introduced by altering the drain delay for RWH. Compared with a responsible 24-hour drain delay, severe homeowner neglect (504 hours) resulted in annual reduction differences between -46% to 13% and -26% to 47% for 227- and 7,571-liter scenarios, respectively. Overall watershed runoff coefficients experienced less than 1% deviations from the 24-hour drain delay results. Fig. 2.11 exhibits improvements in long-term volumetric reductions at the watershed outlet with smaller barrels, while cistern removal was slightly impeded. Variation in outflow duration did not impact the long-term watershed outflow reductions for

the Chollas Creek watershed. There was not a significant effect of varying drain delay times on RWH storage capacities' annual average runoff volumes at the $p<0.05$ level for the 227-liter [$F(2,183)=0.69$, $p=0.51$] and 7,571-liter [$F(2,183)=0.73$, $p=0.48$] conditions.

2.4.2.2 Subcatchment

Extending drain duration resulted in increased subcatchment runoff coefficients, indicating a higher ratio of outflow to precipitation. Flooding in conduits was also increased. Prolonged drain delay times had different impacts on subcatchment runoff reductions for the RWH scenarios. For 7,571-liter cisterns, 504-hour drain delays simulated less reduction relative to the 24-hour delay results. Alternatively, 227-liter barrels provided greater reductions in runoff for 504 hours, versus a 24-hour drain delay. Quantification of reduction differences for the range of drain delay times exhibited a linearly decreasing effectiveness with the percent of impervious area targeted for cisterns. Rain barrels difference quantifications found a linearly increasing effectiveness (Fig. 2.12).

2.4.3 Cost-Effectiveness

2.4.3.1 Watershed Outlet

Total program NPVs ranged from $0.52 - $30.8 million US dollars (USD) for all of the RWH permutations (Fig. 2.13). Normalization of overall watershed volumetric reductions to the NPV provided an economic analysis weighing implementation extent and cost with stormwater benefits. Regardless of the

extent of implementation, the greatest reductions per dollar were derived from the single 227-liter barrel. On average, this scenario provided a long-term removal of 6,481 liters per dollar (liters/$).

Cisterns removed 757 liters/$ (Fig. 2.14). The range for overall watershed long-term RWH cost-effectiveness is $0.15 - $1.35 per 1,000 liters. Analysis of annual cost-effectiveness highlights greater benefit in wet years than dry, with an average NPV per 1,000 liter reductions ranging between $0.12 - $0.97 and $0.25 - $2.20, respectively. Long-term annual averages ranged from $0.13 - $1.15 per 1,000 liters.

2.4.3.2 Subcatchment

Subcatchment total NPVs follow a linearly increasing trend, similar to the overall watershed results. Normalization of NPV to reductions finds greater cost-effectiveness with rain barrels, versus cisterns. The relationship between percent of impervious area targeted and costs normalized to reductions exhibited a point of diminishing returns for both rain barrels and cisterns (Fig. 2.15). Cost-effectiveness decreases as the percent of targeted impervious area is expanded. Baseline cost-effectiveness (e.g., minimums) of $0.10 and $0.81 per 1,000 liter reductions in volume were established for the 227- and 7,571-liter scenarios, respectively. Long-term average subcatchment cost-effectiveness is $0.12 and $0.98 for 227- and 7,571-liter configurations.

2.5 Discussion and Conclusions

It should be noted that the results presented are specific to the case study, though these general conclusions provide guidance for implementation in other watersheds.

2.5.1 Watershed

Results of this study indicated a linear relationship between runoff reductions and available capacity, maximizing with the largest RWH scenarios (e.g., 100% of the watershed households supplied with 7,571 liter cisterns). However, since a primary goal of municipal stormwater management is maximizing volumetric runoff reductions and minimizing flooding, a decentralized residential RWH program cannot be expected to provide such quantities by itself. Alternatively, if a local government requires supplemental reductions to increase the effectiveness of existing centralized stormwater controls, then consideration of RWH as a network component may be prudent. This study found that a watershed-scale RWH program, when operated as a passive storage-based practice, can provide significant annual average watershed runoff volume reductions, though only to an annual maximum of 14% for all scenarios. With respect to existing infrastructure, such reductions in long-term loads can complement a watershed's stormwater management goals.

Comparison of long-term continuous and design storm simulation results demonstrates the importance of capturing regional precipitation characteristics and antecedent conditions when watershed-scale impacts of distributed RWH are warranted. Precipitation characteristics include interevent dry time, variation

in event depth, wet versus dry year conditions, and seasonality. For the case study watershed, investigation of variations in annual seasonal precipitation found increased reductions in dry years, stemming from greater overall capture of annual events. For all climatic regions, it is important that simulations capture the full range of the watershed's precipitation and flow-routing characteristics, as these were found to influence watershed outlet reductions more so than varying RWH storage size. Due to overland flow routing, conversion to impervious area depression storage results in over-estimation of captured runoff when input precipitation volume is less than the available storage. This is evident in the 41% runoff reduction with the 7,571-liter scenario despite a maximum volume available to input precipitation volume of 36% (Fig. 2.10). The LID Editor method is preferred since pervious area routing (i.e., downspout disconnection) is accounted for and reduction errors due to overland flow removal with depression storage are mitigated.

While variation in drain delay and outflow duration were not significant, the elongation of drain delay time (i.e., homeowner negligence and malfunctioning units) resulted in a greater range of annual average volumetric reductions. This variability stems from the drain delay either syncing with or exceeding the dry duration. Dry duration, in this case, is the consecutive time period in which no precipitation event occurs. When drain delay exceeds the dry duration, the RWH unit is not allowed to empty and, instead, is more likely to overflow to the pervious discharge location. When drain delay is less than the dry duration, the units are allowed to empty unimpeded by precipitation events, leaving greater

capacity for future events. However, as drain delay approaches the dry duration, captured water will be directed to the pervious discharge location, resulting in soil saturation and, thereby, less infiltration of approaching precipitation events. Thus, drain delay may have a greater impact on long-term reductions for watersheds with different climates (i.e., wetter, less dry durations). Similarly, outflow duration did not have a significant impact on average annual runoff reductions for RWH scenarios. This demonstrates the double-edged implication of transferring RWH O&M responsibilities to the homeowner collective, highlighting greater annual variability with larger units, a dampening of long-term reduction variability with downspout disconnection, and importance of drain delay relative to dry duration (Maher & Lustig, 2003).

Individually, rain barrels are not only less likely to reduce overall volumes and rates but are also more likely to be capacity-limited and, therefore, overflow. For example, while the 227-liter rain barrel had the highest ratio of overflow to underdrain-mediated flow (e.g., 5.17), compared with the cistern, the difference in long-term watershed reductions were found to be statistically similar. For individual events, sensitivity analysis of RWH storage size found a 72% greater runoff reduction for the 0.01 probability event with the 7,571-liter cistern, versus the 227-liter rain barrel (Fig. 2.8). Both of these examples highlight the dampening of storage size impacts by regional precipitation characteristics and flow routing of rooftop runoff to pervious areas (e.g., downspout disconnection). Studies by Steffen et al. (2013) and Dixon et al. (1999) drew similar conclusions regarding decreased stormwater reductions with increasing precipitation and the

driving factors of RWH storage size and climatic patterns.

Normalization of the NPV to the respective scenario reductions determined economic feasibility from the standpoint of the municipality. The greatest watershed benefits were derived from the 227-liter barrel scenario, with an average reduction of 6,500 liters per dollar invested (range 6,322 – 6,703 liters/$). The least economic scenario is the 7,571-liter cistern, resulting in a long-term average reduction of 750 liters per dollar invested (range 743 – 763 liters/$). Minor variations in cost-effectiveness result for the range of implementation permutations. This indicates that incremental implementation would likely be the method of choice by local jurisdictions. Annual analysis finds increased cost-effectiveness in wet years, due to the greater overall volumes removed by downspout disconnection.

In addition to its cost-effectiveness, the single 227-liter barrel provides the fastest drain times (i.e., within recommendations for monthly South Coast irrigation rates), the smallest footprint, and the greatest ease when it comes to implementation and O&M by homeowners. Minimal differences for the range of RWH sizes and relatively constant volumetric reductions for scenarios the range of RWH sizes over the 50-year life span (e.g., less than 2%) further reinforce the recommendation of employing rain barrels over cisterns.

2.5.2 Subcatchment

Results of this study reinforced the linearly increasing trend of subcatchment reductions with the percent of impervious area targeted by RWH. Greater reductions in outflow volumes and rates were simulated as RWH storage

capacity and targeted rooftop area increased. ANOVA and Tukey HSD post hoc investigations (Table 2.4) guide planning level scenario implementation to achieve statistically significant reductions, again finding greater benefit with greater capacity. Variations in drain delay and duration parameters resulted in trends similar to those at the watershed-scale. However, when plotted against the percent of impervious area targeted by RWH, the difference between reductions resulting from 24- and 504-hour drain delays linearly increased for 227-liter barrels and linearly decreased for 7,571-liter cisterns (Fig. 2.12). While this reinforced the conclusion of the previously emphasized drivers (e.g., precipitation and pervious area routing), it also indicated that negligence was dampened in smaller units due to the ability to quickly empty. Alternatively, cistern effectiveness was hampered due to longer temporal drain periods.

Quantification of subcatchment cost-effectiveness provided a finer analysis compared to the overall watershed. Logarithmic relationships were found to exist between the percent of impervious area targeted and the normalized costs to reductions (Fig. 2.15), indicating that negligible changes in cost-effectiveness resulted from increasing the impervious area routed to the RWH units. These baseline values (e.g., approximately $0.83 and $0.10 per 1,000 liter reduction for cisterns and barrels, respectively) aid in establishing a watershed's maximum expected cost-effectiveness for the RWH program configuration applied. Thus, in combination with climate and pervious area routing, these conclusions further reinforce the choice of rain barrels over cisterns, both at the watershed and subcatchment-scales.

2.5.3 Future

As SWMM5.0.022 does not allow for placement of a household demand to dictate RWH outflow, the results of this study provide a baseline for not only potential stormwater runoff reductions but also cost-effectiveness of a RWH program from the perspective of a municipality. Future work will expand this study to include additional LID practices to determine a logical combination, or framework, such that watershed benefits are maximized with cost-effectiveness. This work is currently underway for the options provided in SWMM5.0.022. The geographic placement and sizing of these networks and LID practices will be based on land cover classification and geospatial analysis of the watershed governing parameters of LID implementation and design. The results of this LID feasibility study lend further insight to not only the cost-effectiveness of reductions from a range of RWH storage sizes but also the potential impacts of transferring a portion of stormwater management responsibilities from the local government to the citizen.

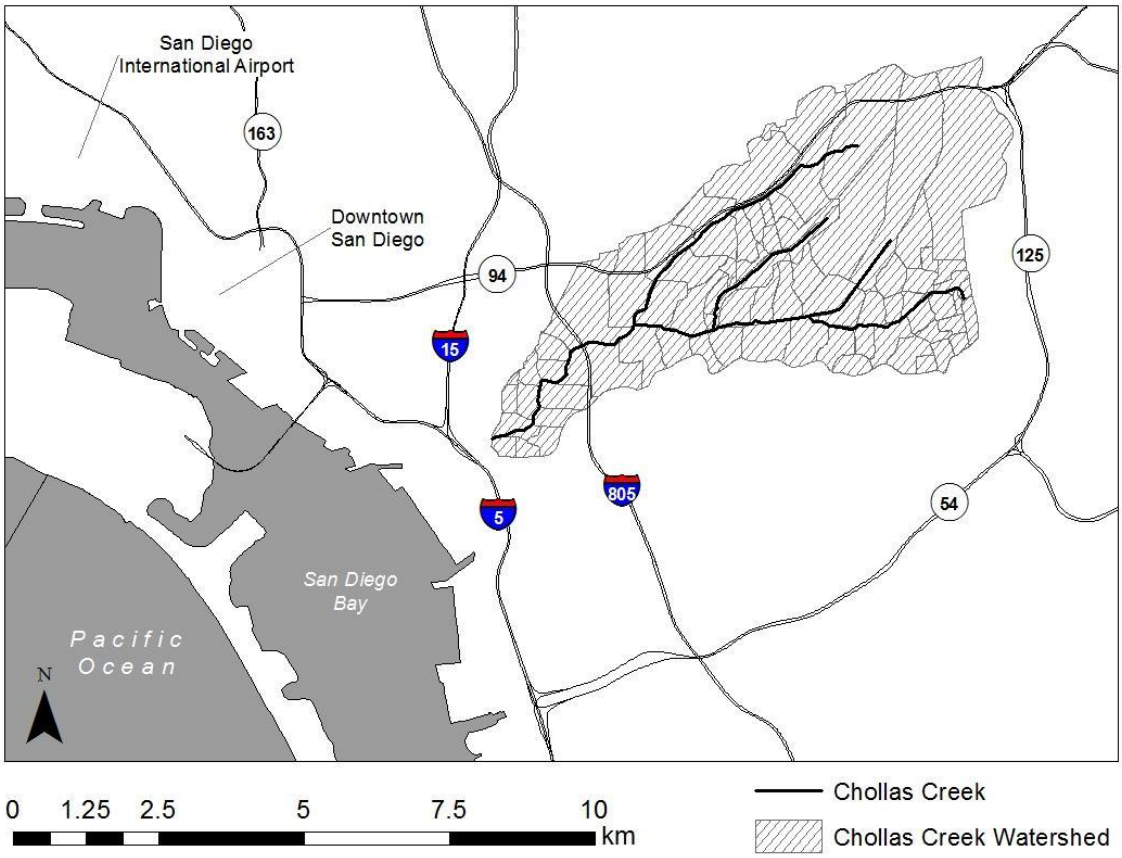

Figure 2.1: Geographical location of the study area.

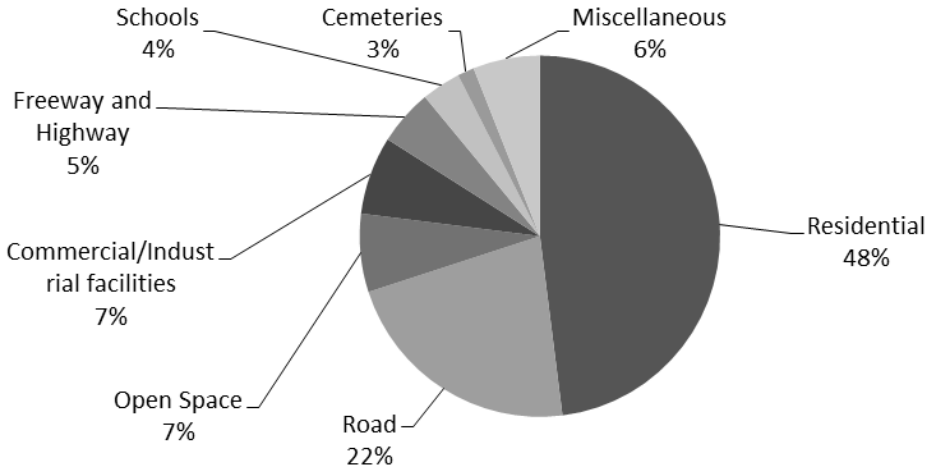

Figure 2.2: Land use composition of Chollas Creek watershed.

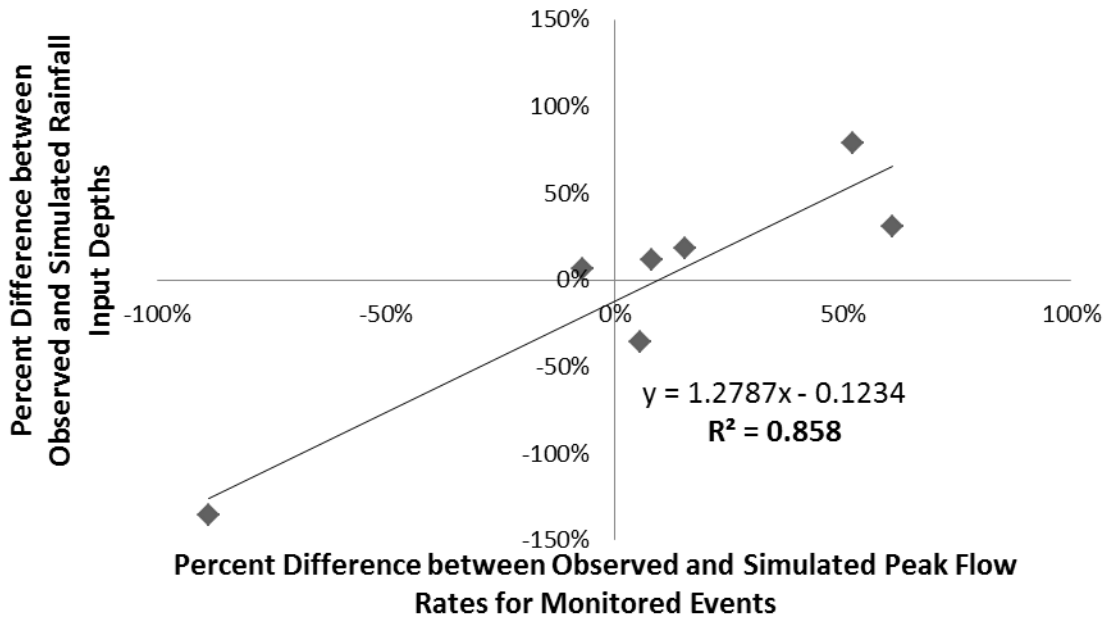

Figure 2.3: Percent difference between observed and simulated storm events' input precipitation depths versus peak flow rates.

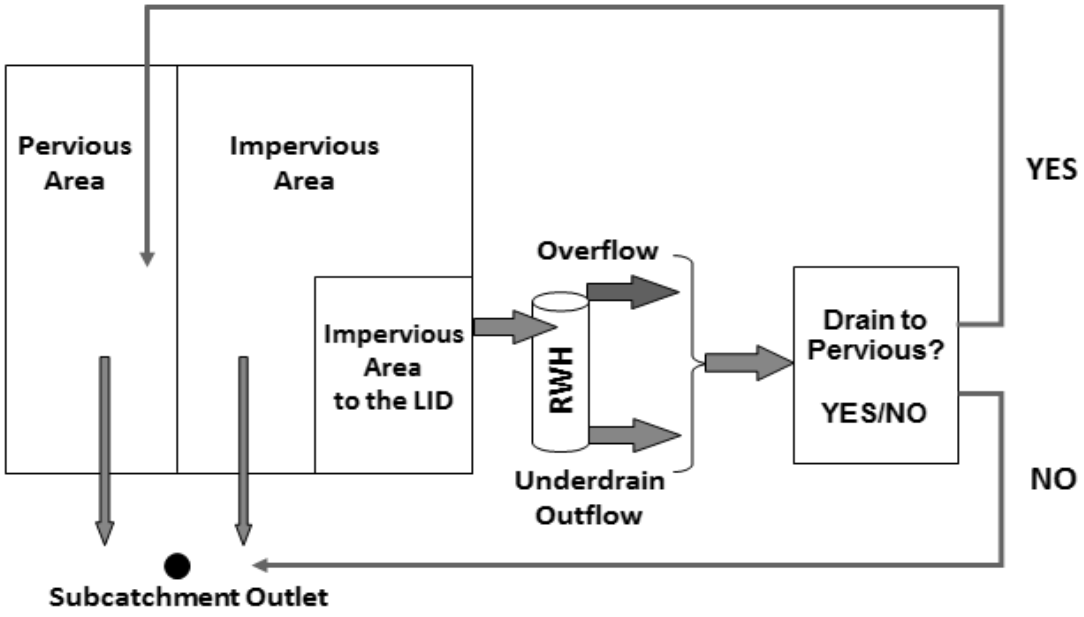

Figure 2.4: SWMM5.0.022 flow routing, with RWH chosen as the LID. Underdrain outflow is established with the drain delay and Eq. (1) functions, with drain outflow driven by head.

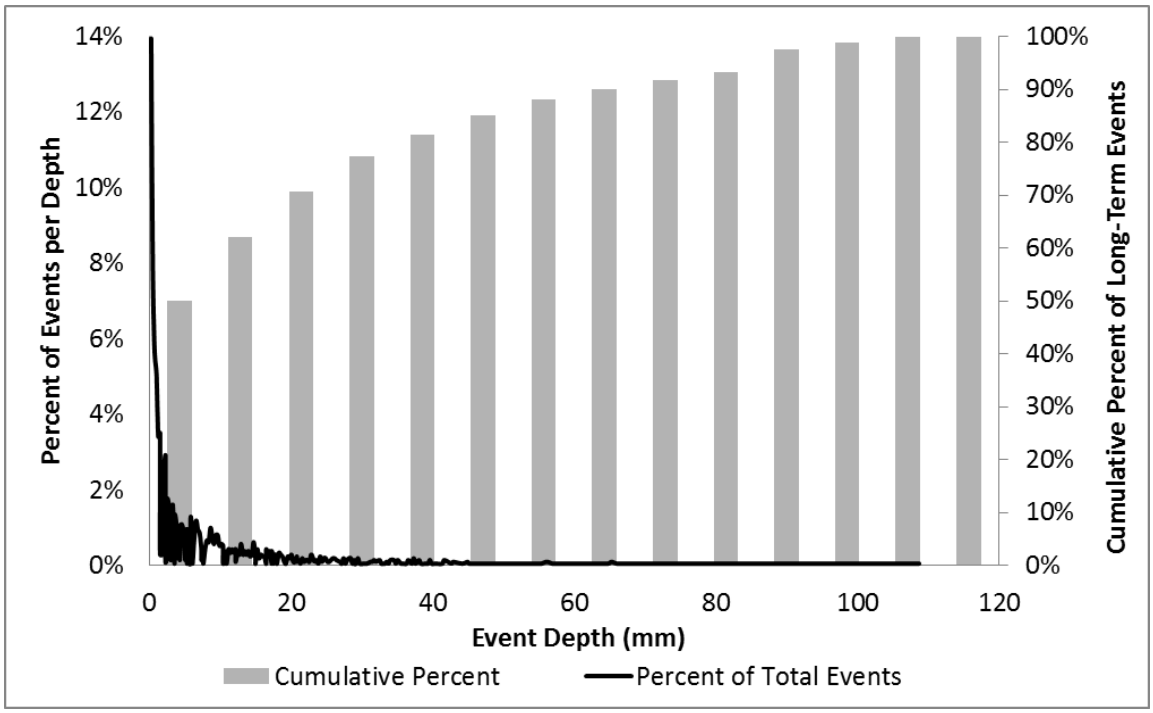

Figure 2.5: Long-term precipitation analysis, with event depth as a percent of the total rainfall record storm events (primary axis) and the cumulative percent of events (secondary axis) for each depth.

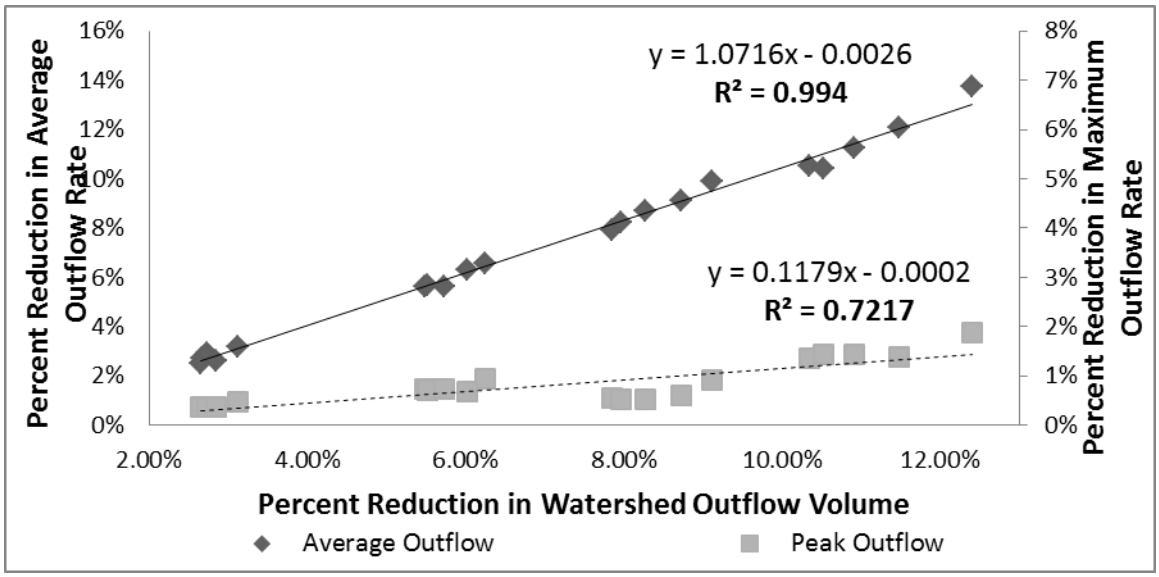

Figure 2.6: Presentation of long-term watershed reductions in average (primary axis) and peak (secondary axis) flow rates for RWH scenarios' reductions in watershed stormwater runoff. Note: clusters represent the impact of varied watershed RWH implementation rate, with less variation at lower watershed allocations.

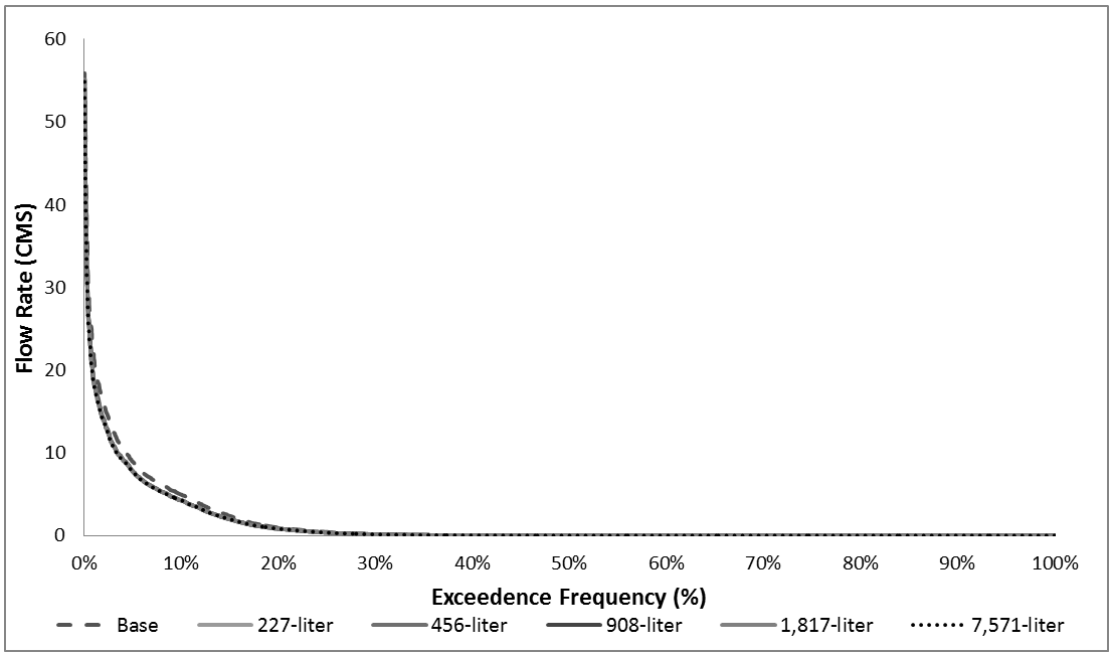

Figure 2.7: Flow duration curve, highlighting the negligible differences between RWH scenarios at maximum (e.g., 100%) watershed implementation. Inset exhibits the difference for event exceedance probabilities less than 0.01. Flow rates are exhibited in cubic meters per second (CMS).

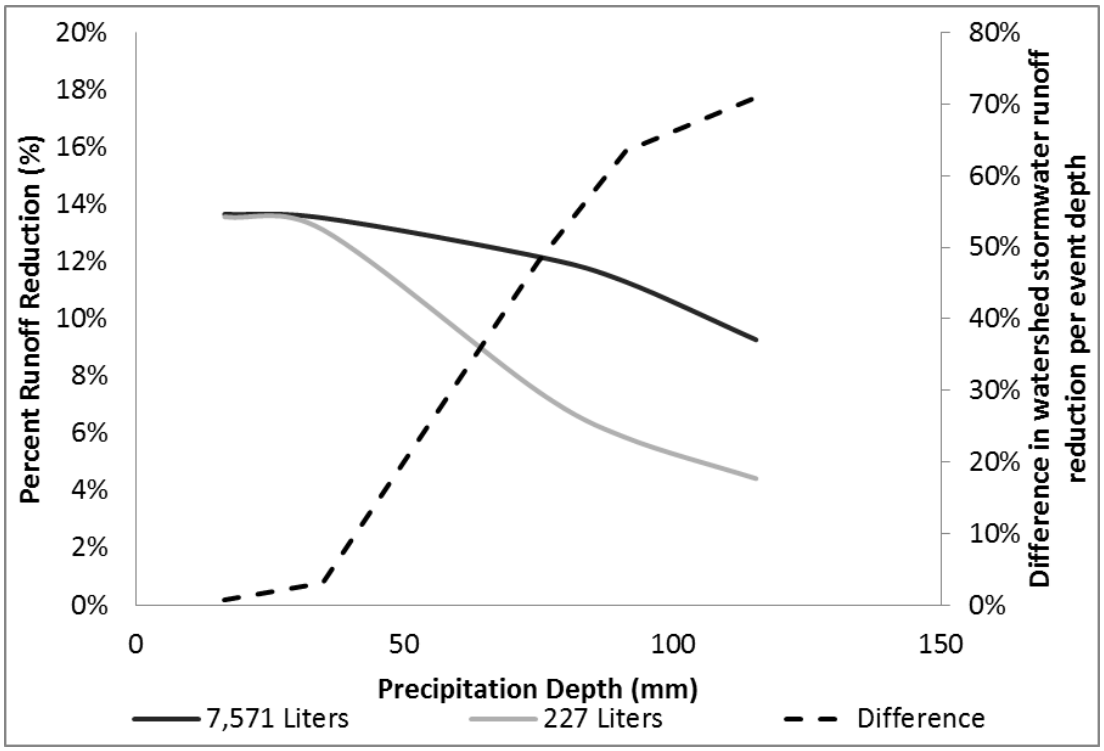

Figure 2.8: Individual precipitation event results, highlighting the difference in watershed stormwater runoff reduction for the RWH capacity range. Simulations include the 2.0, 1.0, 0.1, 0.04, and 0.01 probability events.

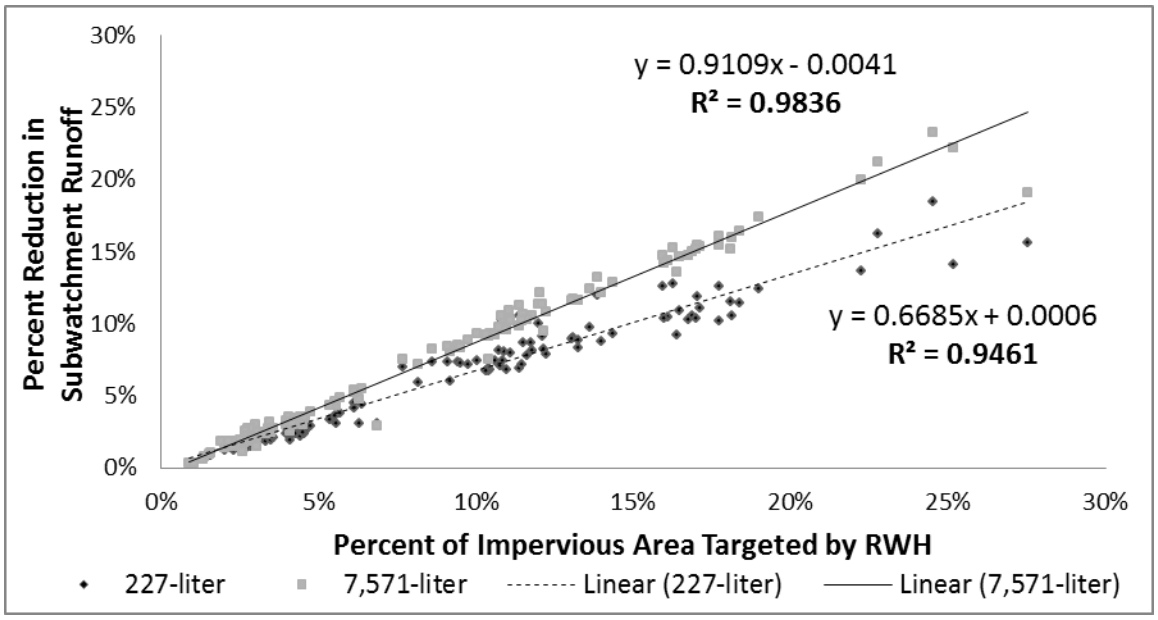

Figure 2.9: Long-term subcatchment stormwater runoff reductions versus the percent of subcatchment impervious area targeted by RWH.

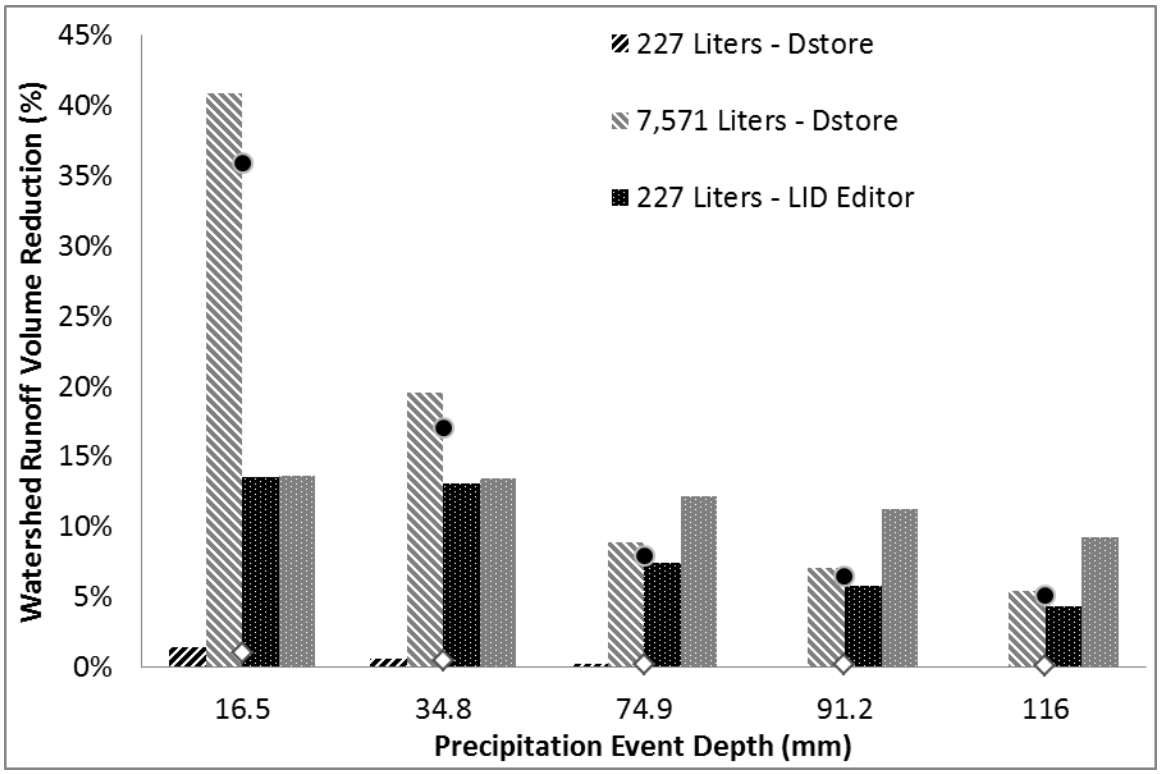

Figure 2.10: Comparison of watershed runoff volume reductions for the range of capacities, when RWH is modeled either as Impervious Area Depression Storage or with the LID Editor. The addition of maximum RWH capacity to input precipitation volume indicates the maximum volumetric removal achievable for each scenario.

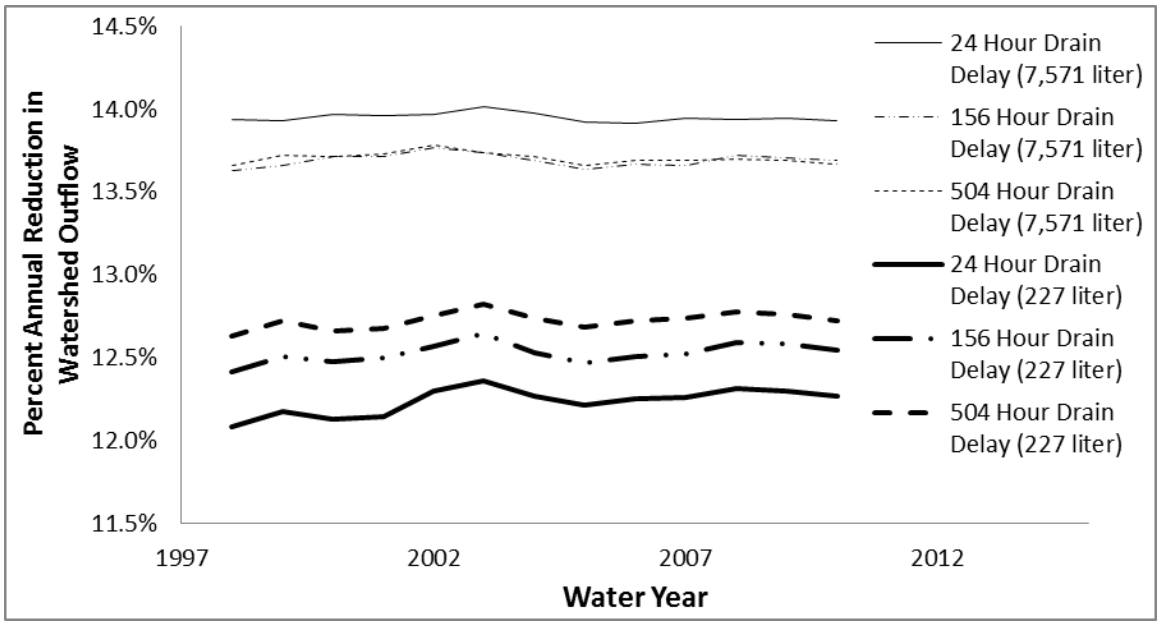

Figure 2.11: Comparison of 50-year moving averages for annual watershed runoff reductions provided by 227-liter and 7,571-liter units when drain delay is varied to represent homeowner neglect.

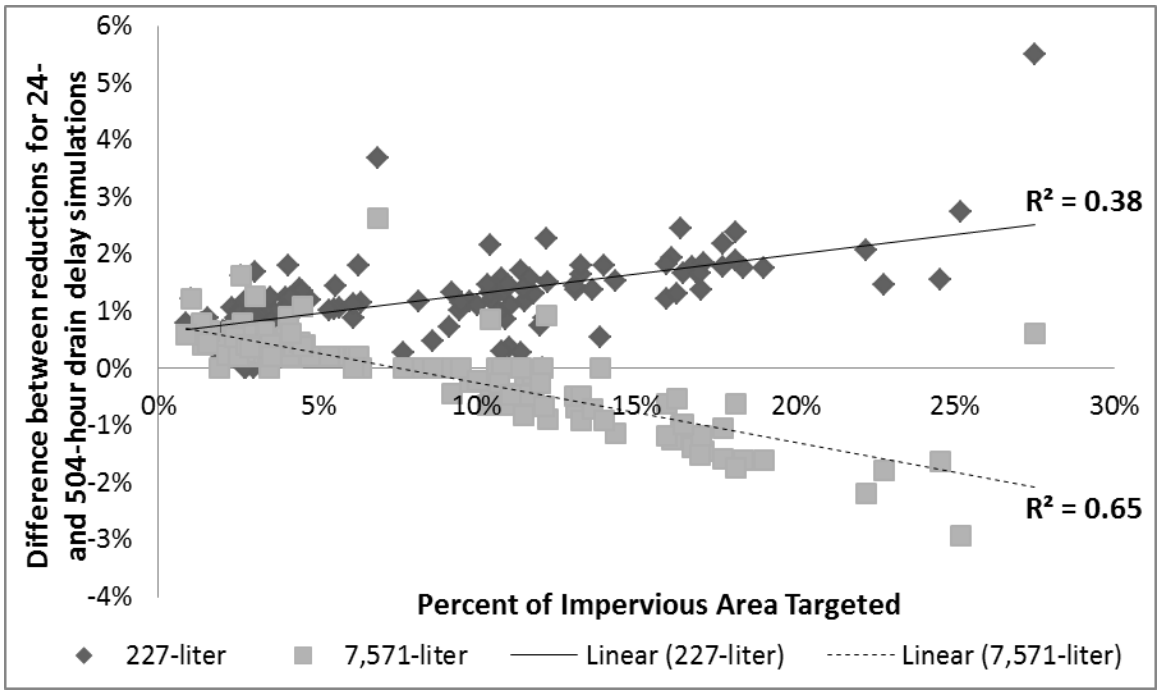

Figure 2.12: Difference between runoff reductions simulated for the range of RWH storage sizes when drain delays of 24 and 504 hours were selected.

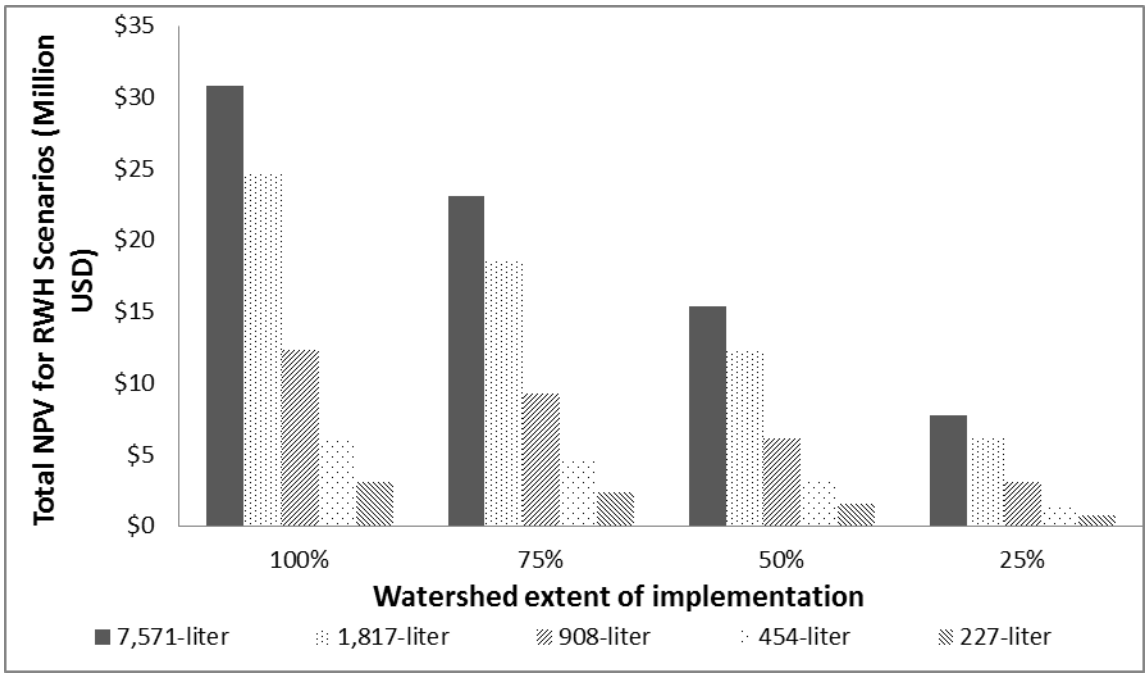

Figure 2.13: NPV for each RWH scenario permutation.

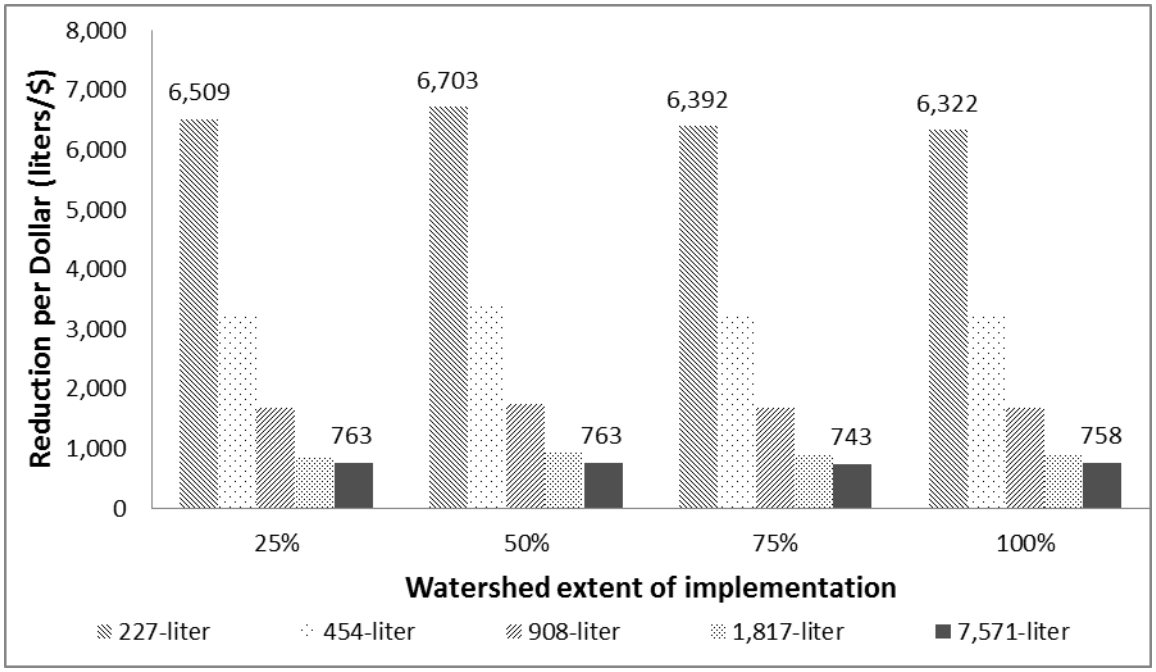

Figure 2.14: Volumetric reduction (liters) per dollar invested for each permutation of RWH with increasing extent of watershed implementation.

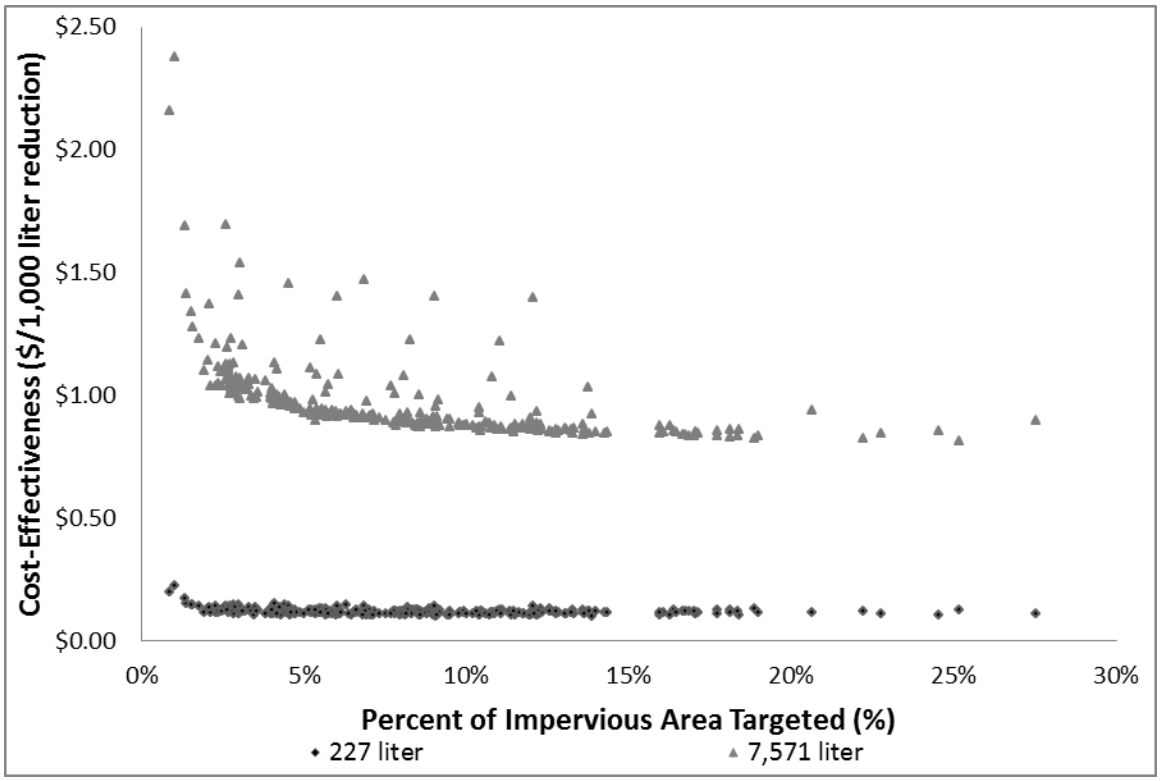

Figure 2.15: Subcatchment cost-effectiveness (NPV per 1,000 liters volumetric reduction) versus the percent of impervious area targeted by RWH.

Table 2.1: Estimates for total RWH capacity per household with variations in the extent of watershed implementation.

Implementation	Units	227-liter	454-liter	908-liter	1,817-liter	7,571-liter
%	#	Million liters	Million liters	Million liters	Million liters	Million liters
25	5,197	27	54	216	864	216
50	10,394	108	216	864	3,457	864
75	15,590	243	486	1,944	7,778	1,944
100	20,787	432	864	3,457	13,827	3,457

Table 2.2: Reductions in average annual outflow volumes and peak outflow rates for the total record simulated, the wet years (i.e., annual precipitation exceeding 24.6 cm), the dry years (i.e., annual precipitation less than 24.6 cm), and the difference between annual reductions for wet and dry years.

Target Variable	Annual Average	227-liter	454-liter	908-liter	1,817-liter	7,571-liter
Volume	Total Record	11.00%	11.20%	11.60%	12.10%	12.80%
	Wet Years	10.10%	10.30%	10.70%	11.20%	12.20%
	Dry Years	11.60%	11.80%	12.20%	12.70%	13.20%
	Difference between Wet and Dry Years	-13.80%	-13.60%	-13.10%	-12.60%	-7.90%
Q_{peak}	Total Record	10.90%	11.20%	11.80%	12.50%	13.90%
	Wet Years	8.60%	8.80%	9.30%	10.10%	12.30%
	Dry Years	12.50%	12.80%	13.40%	14.20%	15.00%
	Difference between Wet and Dry Years	-37.00%	-37.00%	-36.10%	-33.70%	-19.80%

2.3: Recurrence event flow rate results (cubic meters per second, CMS) for all model scenarios with 100% implementation, as extracted from the flow duration curves for the long-term, continuous simulations (Fig. 2.7). Reductions are calculated with the base scenario results (no RWH provided). Note: Q_n represents the flow rate for the n-probability event, as extracted from the long-term simulation results transformed by the Cunnane Method.

Scenario	$Q_{2.0}$	Reduction	$Q_{1.0}$	Reduction	$Q_{0.5}$	Reduction	$Q_{0.2}$	Reduction	$Q_{0.1}$	Reduction
Liters	CMS	%	CMS	%	CMS	%	CMS	%	CMS	%
0	*16.8*	*N/A*	*22.3*	*N/A*	*29.1*	*N/A*	*42.7*	*N/A*	*48.8*	*N/A*
227	14.7	13.00%	19.1	14.50%	26	10.50%	37.5	12.20%	42.8	12.40%
454	14.6	13.40%	19.1	14.70%	26.1	10.20%	37.3	12.60%	42.7	12.50%
908	14.5	13.90%	19	14.80%	25.9	11.00%	36.9	13.70%	42.6	12.80%
1,817	14.4	14.30%	18.9	15.20%	25.4	12.40%	36.6	14.30%	42.1	13.70%
7,571	14.4	14.40%	18.7	16.40%	25.1	13.70%	36	15.60%	41.4	15.10%

Table 2.4: ANOVA and Tukey HSD post hoc results for subcatchment long-term volumetric reductions. Columns and rows are listed in order of greatest to least mean reduction for the full range of scenarios (n=20). Cells present statistical significance of combined RWH capacity and percent of implementation. Acceptance of the null (=) indicates statistically similar means while a rejection of the null (<>) designates statistical difference. Shading by percent of implementation indicates scenario extent of significance with respect to volumetric reductions for the case study watershed. Scenarios listed as (A) 7,571 L, (B) 1,817 L, (C) 908 L, (D) 456 L, and (E) 227 L.

Scenario/Percent Implementation		A	B	C	D	E	A	B	C	D	E	A	B	C	D	E	A	B	C	E	D
		100					75					50					25				
A	100	=	=	=	=	=	=	=	=	=	=	=	=	=	=	=	=	=	=	=	=
B		=	=	=	=	=	=	=	=	=	=	=	=	=	=	=	=	=	=	=	=
C		=	=	=	=	=	=	=	=	=	=	=	=	=	=	=	=	=	=	=	=
D		=	=	=	=	=	=	=	=	=	=	=	=	=	=	=	=	=	=	=	=
E		=	=	=	=	=	=	=	=	=	=	=	=	=	=	=	=	=	=	=	=
A	75	=	=	=	=	=	=	=	=	=	=	=	=	=	=	=	=	=	=	=	=
B		=	=	=	=	=	=	=	=	=	=	=	=	=	=	=	=	=	=	=	=
C		=	=	=	=	=	=	=	=	=	=	=	=	=	=	=	=	=	=	=	=
D		<>	=	=	=	=	=	=	=	=	=	=	=	=	=	=	=	=	=	=	=
E		<>	=	=	=	=	=	=	=	=	=	=	=	=	=	=	=	=	=	=	=
A	50	<>	<>	=	=	=	=	=	=	=	=	=	=	=	=	=	=	=	=	=	=
B		<>	<>	=	=	=	=	=	=	=	=	=	=	=	=	=	=	=	=	=	=
C		<>	<>	<>	=	=	=	=	=	=	=	=	=	=	=	=	=	=	=	=	=
D		<>	<>	<>	=	=	=	=	=	=	=	=	=	=	=	=	=	=	=	=	=
E		<>	<>	<>	=	=	=	=	=	=	=	=	=	=	=	=	=	=	=	=	=
A	25	<>	<>	<>	<>	<>	<>	<>	=	=	=	=	=	=	=	=	=	=	=	=	=
B		<>	<>	<>	<>	<>	<>	<>	<>	=	=	=	=	=	=	=	=	=	=	=	=
C		<>	<>	<>	<>	<>	<>	<>	<>	=	=	=	=	=	=	=	=	=	=	=	=
E		<>	<>	<>	<>	<>	<>	<>	<>	<>	=	=	=	=	=	=	=	=	=	=	=
D		<>	<>	<>	<>	<>	<>	<>	<>	<>	=	=	=	=	=	=	=	=	=	=	=

2.6 References

Ahiablame, L. M., Engel, B. E., & Chaubey, I. (2012). Effectiveness of low impact development practices: Literature review and suggestions for future research. *Water, Air, & Soil Pollution*, *223*, 4253-4273.

Akan, A. O., & Houghtalen, R. J. (2003). *Urban hydrology, hydraulics, and stormwater quality: Engineering applications and computer modeling* (1st ed.). Hoboken, NJ: John Wiley & Sons.

Alley, W. M., & Veenhuis, J. E. (1983). Effective impervious area in urban runoff modeling. *Journal of Hydraulic Engineering, 109*(2), 313-319.

ASCE (American Society of Civil Engineers). (1992). *Design and construction of urban stormwater management systems*. New York, NY: ASCE.

Bhaduri, B., Harbor, J., Engel, B., & Grove, M. (2000). Assessing watershed-scale, long-term hydrologic impacts of land-use change using a GIS-NPS model. *Environmental Management, 26*(6), 643-658.

Baek, C. W., & Coles, N. A. (2011). Defining reliability for rainwater harvesting systems. Proceedings from: *19th International Congress on Modelling and Simulation*. Perth, AU: MODSIM.

Basinger, M., Montalto, F., & Lall, U. (2010). A rainwater harvesting system reliability model based on nonparametric stochastic rainfall generator. *Journal of Hydrology, 392*, 105-118.

Bedan, E. S., & Clausen, J. C. (2009). Stormwater runoff quality and quantity from traditional and low impact development watersheds. *Journal of the American Water Resources Association*, *45*(4), 998-1008.

Benedict, M. A., & McMahon, E. T. (2002). Green infrastructure: Smart conservation for the 21st century. *Renewable Resources Journal, 20*(3), 12-17.

Booth, D. B., Karr, J. R., Schauman, S., Konrad, C. P., Morley, S. A., Larson, M. G., & Burger, S. J. (2004). Reviving urban streams: Land use, hydrology, biology, and human behavior. *Journal of the American Water Resources Association*, *40*(5), 1351-1364.

City Data. (2011). Chollas Creek neighborhood in San Diego, California (CA), 92105 detailed profile. Retrieved from http://www.city-data.com/neighborhood/Chollas-Creek-San-Diego-CA.html

City of San Diego. (2002). Chollas Creek enhancement program. Retrieved from http://www.sandiego.gov/planning/community/pdf/chollasmaster.pdf

City of San Diego. (2010). Rain barrel/downspout disconnect best management practice effectiveness monitoring and operations program. Prepared by: Weston Solutions, Inc. Retrieved from http://www.sandiego.gov/thinkblue/pdf/rainbarrelfinalreport.pdf

City of San Diego. (n.d.) Chollas Creek south branch implementation program. Retrieved from http://www.sandiego.gov/planning/community/pdf/chollassouthmaster.pdf

Coombes, P. J., Argue, J. R., & Kuczera, G. (2000). Figtree Place: A case study in water sensitive urban development (WSUD). *Urban Water*, *1*(4), 335-343.

Coombes, P. J. (2002). Rainwater tanks revisited: New opportunities for urban water cycle management. Unpublished Ph.D. Thesis. University of Newcastle, Callaghan, NSW, Australia.

County of San Diego. (2012). Standard urban stormwater mitigation plan for land development and public improvement projects. Retrieved from http://www.sdcounty.ca.gov/dpw/watersheds/susmp/susmppdf/susmp_manual_2012.pdf

Cunnane, C. (1978). Unbiased plotting positions – A review. *Journal of Hydrology*, *37*, 205-222.

Damodaram, C., Giacomoni, M. H., Khedun, C. P., Holmes, H., Ryan, A., Saour, W., & Zechman, E. M. (2010). Simulation of combined best management practices and low impact development for sustainable stormwater management. *Journal of the American Water Resources Association, 46*(5), 907-918.

De Graaf, R., & Der Brugge, R. (2010). Transforming water infrastructure by linking water management and urban renewal in Rotterdam. *Technological Forecasting and Social Change, 77*, 1282-1291.

Dietz, M. E. (2007). Low impact development practices: A review of current research and recommendations for future directions. *Water, Air & Soil Pollution*, *186*, 351-363.

Dixon, A., Butler, D., & Fewkes, A. (1999). Water saving potential of domestic water reuse systems using greywater and rainwater in combination. *Water Science and Technology*, *39*(5), 25-32.

Elliott, A. H., & Trowsdale, S. (2007). A review of models for low impact urban stormwater drainage. *Environmental Modelling & Software, 22*(3), 394-405.

Endreny, T., & Collins, V. (2009). Implications of bioretention basin spatial arrangements on stormwater recharge and groundwater mounding.

Ecological Engineering, *35*, 670-677.

Fletcher, T. D., Andrieu, H., & Hamel, P. (2013). Understanding, management and modelling of urban hydrology and its consequences for receiving waters: A state of the art. *Advances in Water Resources*, *51*(0), 261-279.

Foraste, J. A. & Hirschman, D. (2010). A methodology for using rainwater harvesting as a stormwater management BMP. Proceedings from: *ASCE International Low Impact Development Conference, Redefining Water in the City*. San Francisco, CA: ASCE.

Foraste, J. A., Goo, R., Thrash, J., & Hair, L. (2012). Measuring the cost-effectiveness of LID and conventional stormwater management plans using life cycle costs and performance metrics. Proceedings from: *Ohio Stormwater Conference*. Toledo, OH.

Gilroy, K. L., & McCuen, R. H. (2009). Spatio-temporal effects of low impact development practices. *Journal of Hydrology, 367*, 228-236.

Grimaldi, S., Petroselli, A., & Serinaldi, F. (2012). Design hydrograph estimation in small and ungauged watersheds: Continuous simulation method versus event-based approach. *Hydrological Processes, 26*, 3124-3134.

Han, M. Y., Mun, J. S., & Kim, H. J. (2008). An example of climate change adaptation by rainwater management at the Star City rainwater project. Proceedings from: *3rd Rainwater Harvesting and Management Workshop*. Sydney, AU: IWA.

Hanak, E., & Davis, M. (2006). Lawns and water demand in California. Retrieved from http://www.ppic.org/content/pubs/cep/EP_706EHEP.pdf

Hartin J., Geisel, P. M., & Unruh, C. L. (2001). Lawn watering guide for California. publication 8044. Retrieved from http://anrcatalog.ucdavis.edu/pdf/8044.pdf

Hartsig, T., & Rodie, S. (2009). Bioretention garden: A manual for contractors in the Omaha region to design and install bioretention gardens. Retrieved from http://www.omahastormwater.org

Herrmann, T., & Hasse, K. (1997). Ways to get water: Rainwater utilization or long distance water supply. *Water Science Technology*, *36*(8-9), 313-318.

Jia, H., Lu, Y., Yu, S. L., & Chen, Y. (2012). Planning of LID-BMPs for urban runoff control: The case of Beijing Olympic Village. *Separation and Purification Technology, 84*, 112-119.

Kennard, M. J., Mackay, S. J., Pusey, B. J., Olden, J. D., & Marsh, N. (2010).

Quantifying uncertainty in estimation of hydrologic metrics for ecohydrological studies. *River Research and Applications, 26*, 137-156.

Lee, J. G., & Heaney, J. P. (2003). Estimation of urban imperviousness and its impacts on storm water systems. *Journal of Water Resources Planning and Management*, *129*(5), 419-426.

Lee, J. G., Selvakumar, A., Alvi, K., Riverson, J., Zhen, J. X., Shoemaker, L., & Lai, F. (2012). A watershed-scale design optimization model for stormwater best management practices. *Environmental Modeling & Software, 37*, 6-18.

Lim, S-R, Suh, S., Kim, J-H, & Park, H.S. (2010). Urban water infrastructure optimization to reduce environmental impacts and costs. *Journal of Environmental Management, 91*, 630-637.

Maher, M., & Lustig, T. (2003). Sustainable water cycle design for urban areas. *Water Science and Technology, 47*(7-8), 25-31.

McClintock, K. A., Harbor, J. M., & Wilson, T. P. (1995). Assessing the hydrological impact of land use change in wetland watersheds: A case study from northern Ohio, USA. In D. F. M. McGregor & D. A. Thompson (Eds.), *Geomorphology and land management in a changing environment* (pp. 107-119). New York, NY: John Wiley & Sons.

McGarity, A. E. (2012). Storm-water investment strategy evaluation model for impaired urban watersheds. *Journal of Water Resources Planning and Management, 138*, 111-124.

Mitchell, V. G., Deletic, A., Fletcher, T. D., Hatt, B. E., & McCarthy, D. T. (2007). Achieving multiple benefits from stormwater harvesting. *Water Science and Technology, 55*(4), 135-144.

NOAA (National Oceanic and Atmospheric Administration). (2012). NOAA atlas 14 point precipitation frequency estimates: CA. Retrieved from http://hdsc.nws.noaa.gov/hdsc/pfds/pfds_map_cont.html?bkmrk=pa .

Olden, J. D., & Poff, N. L. (2003). Redundancy and the choice of hydrologic indices for characterizing streamflow regimes. *River Research and Applications, 19*(2), 101-121.

Petrucci, G., Deroubaix, J., De Gouvello, B., Deutsch, J. C., Bompard, P., & Tassin, B. (2012). Rainwater harvesting to control stormwater runoff in suburban areas. An experimental case-study. *Urban Water Journal, 9*(1), 45-55.

Pitt, R. (1999). Small storm hydrology and why it is important for the design of stormwater control practices. In W. James (Ed.), *Advances in modeling the*

management of stormwater impacts (Vol. 7, pp. 1-30). Boca Raton, FL: Lewis Publishers/CRC Press.

Prince George's County, Maryland. (June 1999). Low-impact development design strategies: An integrated design approach. Retrieved from http://water.epa.gov/polwaste/green/upload/lidnatl.pdf.

Roesner, L. A. (1999). Urban runoff pollution – summary thoughts – the state-of-practice today and for the 21st century. *Water Science and Technology, 39*(12), 353-360.

Rosemarin, A. (2005). Sustainable sanitation and water in small urban centres. *Water Science and Technology, 51*(8), 108-118.

Rossman, L. A. (2010). Storm water management model user's manual, version 5.0.

Roy, A. H., Wenger, S. J., Fletcher, T. D., Walsh, C. J., Ladson, A. R., Shuster, W. D., Thurston, H. W., & Brown, R. R. (2008). Impediments and solutions to sustainable, watershed-scale urban stormwater management: Lessons from Australia and the United States. *Environmental Management, 42*, 344-359.

SanGIS. (2012). GIS data warehouse. Retrieved from http://www.sangis.org/download/index.html

Scheuler, T. (1994). The importance of imperviousness. *Watershed Protection Techniques, 1*(3), 100-111.

Schiff, K., & Carter, S. (2007). Monitoring and modeling of Chollas, Paleta, and Switzer creeks, technical report 513. Retrieved from http://www.waterboards.ca.gov/rwqcb9/water_issues/programs/tmdls/docs/sediment_toxicity/SCCWRP_Final_C_P_S_Monitoring_ModelingReport.pdf

Schneider, L., & McCuen, R. (2006). Assessing the hydrologic performance of best management practices. *Journal of Hydrologic Engineering, 11*(3), 278-281.

Shen Z., Chen, L., & Xu, L. (2013). A topography analysis incorporated optimization method for the selection and placement of best management practices. *PLoS ONE* 8(1), e54520. doi:10.1371/journal.pone.0054520

Shuster, W. D., Morrison, M. A., & Webb, R. (2008). Front-loading urban stormwater management for success – a perspective incorporating current studies on the implementation of retrofit low-impact development. *Cities and the Environment (CATE), 1*(2), Art. 8.

Smith, P. (2012). Rainwater harvesting: Recycling a precious resource.

Coastwatch winter 2012. Retrieved from http://www.ncseagrant.org/home/coastwatch?task=showArticleandview=listarticlesandid=725

Spatari, S., Yu, Z., & Montalto, F. A. (2011). Life cycle implications of urban green infrastructure. *Environmental Pollution, 159*, 2174-2179.

Steffen, J., Jensen, M., Pomeroy, C. A., & Burian, S. J. (2013). Water supply and stormwater management benefits of residential rainwater harvesting in U.S. cities. *Journal of the American Water Resources Association*, *49*(4), 810-849.

Tank Depot. (2012). 2000 gallon vertical fresh water tank (CRMI-2000vtfwg). Retrieved from http://www.tank-depot.com/productdetails.aspx?part=CRMI-2000VTFWGandref=base

USDOT (United States Department of Transportation). (1986). *Design of roadside channels with flexible linings, hydraulic engineering circular #15*. Washington, DC: USDOT.

USEPA (United States Environmental Protection Agency). (2000). Low impact development (LID), a literature review. Washington, DC: Office of Water.

USEPA. (2007). Reducing stormwater costs through low impact development (LID) strategies and practices. Washington, DC: Office of Water.

USEPA. (2012). Storm water management model (SWMM), version 5.0.022 with low impact development (LID) controls. Retrieved from http://www.epa.gov/nrmrl/wswrd/wq/models/swmm/

Weston Solutions, Inc. (2006). Chollas Creek TMDL source loading, best management practices, and monitoring strategy assessment: Final report. Final Report prepared for City of San Diego.

Weston Solutions, Inc. (2007). San Diego County municipal committees 2005-2006 urban runoff monitoring: Volume i – final report. Final Report prepared for County of San Diego.

Weston Solutions, Inc. (2010a). Chollas Creek total maximum daily load (TMDL) 2009-2010 water quality compliance monitoring. Final Report submitted to San Diego Regional Water Quality Control Board.

Weston Solutions, Inc. (2010b). Rain barrel/downspout disconnect best management practice effectiveness monitoring and operations program. Final Report submitted to City of San Diego, Storm Water Department, Pollution Prevention Division.

Weston Solutions, Inc. (2010c). Chollas Creek total maximum daily load compliance monitoring investigation order no. r9-2004-0277: 2008-2009 water quality monitoring final report. Final Report prepared for San Diego Regional Water Quality Control Board.

Young, K. D., Younos, T. Dymond, R. L., & Kibler, D. F. (2009). Virginia's stormwater impact evaluation. VWRRC Special Report No. SR44-2009. Retrieved from http://www.harvesth2o.com/adobe_files/VI_Stormwater_BMP.pdf

CHAPTER 3

GREEN INFRASTRUCTURE SUITABILITY PROTOCOL

This journal article is entitled, Application of Object-Based Image Analysis with Geospatial Analysis to Quantify Suitable Sites for Watershed-Scale Low Impact Development. My co-authors include Dr. Christine Pomeroy and Dr. Philip Dennison, who are currently reviewing a draft of this work. Expected submission is Summer 2014, to the *Journal of Water Resources Planning and Management*.

3.1 Abstract

Low impact development (LID) practices are traditionally site-specific, requiring assessment of local constraints for proper planning and design; however, they are increasingly applied to solve watershed-scale stormwater management issues. This necessitates accurate representation of watershed parameters, over the conventional uniform design and distribution of LID resulting from the complexity of required LID analysis methods and lack of pertinent datasets (e.g., extent, resolution). Researchers created the LID Site Suitability (*LIDSS*) toolset to filter layers necessary for proper hydrologic

modeling, simulation, and analysis. These datasets included land cover/land use from object-based classification, slopes, soils, and flood zones. This paper presents the results of a study combining object-based image classification methods (91.3% overall classification accuracy of buildings) with geospatial analysis to identify suitable locations for rainwater harvesting (RWH) throughout the Chollas Creek watershed, San Diego, CA, USA. Quality assessment (n=50 sites, 3.14 hectares) of the protocol indicated over-classification of building areas by an average 23%. This resulted from discrepancy between the spatial resolutions of the elevation and spectral datasets. Comparison with a uniformly distributed RWH scenario (*UNI227*) found rooftop area to be 51% greater with *LIDSS*. A 44% long-term (1948-2011) average annual volumetric reduction difference (range 34%-51%) with *LID227* was achieved versus *UNI227*, relating to a 16% long-term watershed outflow reduction. Changes in average peak flow rate reductions (51%) followed changes in rooftop area, whereas a smaller difference (44%) was simulated for watershed outflow volumes. This study finds the suitability protocol and toolsets provide adequate estimates for LID siting and design for hydrologic modeling, though finer resolution elevation data are expected to improve estimates and final results.

3.2 Introduction

Urbanization has negatively impacted the resources and processes of the natural environment. Specifically, the conversion from natural to impervious land cover affects stormwater quantity and quality, including increased flood risk and pollution of receiving water bodies (Schueler, 1994; Lee & Heaney, 2003). To

mitigate these consequences, traditional stormwater management focused on improving conveyance with centralized mitigation (Roy et al., 2008; Debo & Reese, 2010). This resulted in watershed management plans that often span multiple municipalities and governing bodies (Brown et al., 2007). Such plans enforced the construction of large capacity, end-of-pipe practices located at downstream termination points within large drainage areas. Recent emphasis has been increasingly placed on site-specific practices, known as low impact development (LID), incorporating water quality management of smaller, more frequent events (Prince George's County, 1999). However, the majority of research assessing the quantity and quality benefits of LID has focused on smaller scales, such as the parcel or neighborhood, at the expense of the expanded watershed (Bedan & Clausen, 2009; Lee et al., 2012). Studies at the watershed-scale, including those that are empirically-based, are difficult to duplicate, requiring time and money (Jensen et al., 2010; Yang & Li, 2013). Regardless, a gap exists with regard to users' abilities to characterize and quantify the impacts of LID distributed at the local and regional scales (Burian & Pomeroy, 2010).

The fields of remote sensing and geospatial analysis, in tandem with publicly-available, high-resolution datasets, have expanded the abilities of modelers to assess fine-scale watershed conditions (Kunapo et al., 2009). In addition, classification of input datasets (e.g., elevation, spectral, and thematic) has expanded from pixel-by-pixel algorithms (Yang et al., 2010b) to object-based rule sets, which allows for consideration of individual features (i.e., collection of

homogeneous pixels representing an object) (Yang et al., 2010a; Wu & Yuan, 2011). Combining these classifications with other LID implementation and design constraint layers, such as slopes, floodplain zones, soils, can satisfy watershed-scale user-defined objectives via GIS-based postprocessing (Malczewski, 2004). For instance, conditional filtering based on targeted, user-defined values (Malczewski, 2004), spatial clustering (Jacquez, 2008), and hotspot analysis (Anderson, 2009) can improve the identification of locations, magnitudes, and shapes of statistically-significant clusters. In this case, clusters are represented by the design, implementation, benefits, and costs of individual LID practices throughout the watershed.

The goal of our work is to present an applied methodology combining OBIA with geospatial analysis to identify locations for LID implementation meeting both the user's requirements and the physical constraints of the watershed. For this application, the LID practice known as rainwater harvesting (RWH) was targeted. We highlight the application and quality assessment (*QA*) of OBIA classification of watershed land cover/land use (e.g., rooftops). We then address the geospatial analysis components required to filter, quantify, and design RWH units meeting user requirements and watershed constraints aided by customized toolsets. Finally, accuracy estimation of the suitability methodology was applied to the case study watershed, Chollas Creek, Sand Diego, CA, USA. Specific objectives included the creation of a reliable process rule set for OBIA, testing performance for varying spatial scales of implementation, and assessing the resultant RWH framework relative to a

traditional, uniformly applied scenario. This work ultimately provides a novel methodology for assessing a watershed's current conditions, via publicly-available elevation, spectral, and thematic datasets, to design and assess the potential long-term stormwater management benefits from LID at the watershed-scale.

3.3 Background

Urban infrastructure, stormwater management in particular, may be increasingly vulnerable to changes in climatic and anthropogenic conditions (Bates et al., 2008; Dorfman & Mehta, 2011), given the assumption of parameter stationarity in their design (Denault et al., 2006). Input stationarity implies that the runoff load used for sizing is assumed to remain constant within an expected window of variability over time (Denault et al., 2006). As such, historic designs may become over- or under-utilized as a function of future storm events. In response, stormwater management practices (e.g., low impact development, LID) have evolved to mimic natural, predeveloped conditions by focusing on annual rainfall distribution patterns rather than single return events (e.g., 10-year, 24-hour).

LID consist of decentralized practices, providing source control with smaller capacity units. Mitigation is accomplished via the capture, storage, infiltration, and treatment of stormwater runoff (Prince George's County, 1999; USEPA, 2007a). In 1999, Prince George's County released a seminal document detailing integrated design strategies for sustainable management of stormwater runoff. This guide highlighted the importance of site planning, hydrologic

principles and hydrologic analysis tools (Prince George's County, 1999), all of which necessitate site-specific knowledge on the part of the designer. Research repeatedly cites local conditions' applicability and effectiveness of the stormwater control measure (SCM) as the most important component of data analysis (Marsalek & Chocat, 2002; NRC, 2008). In addition, nontechnical obstacles to LID success include property owner motivation and education, such that sustainable modifications to land cover and policies result (Braden & Johnston, 2004; Chocat et al., 2007). By targeting these individuals, who manage the largest proportion of developed land (e.g., residential), the likelihood of achieving significant improvements in stormwater runoff mitigation increases (Lee & Heaney, 2003). Supporting research found that LID practices provide quantifiable reductions in annual average runoff volumes, peak discharge rates, and pollutant loading (Dietz, 2007; Han et al., 2008; Roy et al., 2008; Lim et al., 2010; Spatari et al., 2011; Jia et al., 2012). An empirical study by Burns et al. (2014) monitored demand supplementation and runoff management impacts from RWH (capacity range of 3,000 to 28,000 liters per household). Findings stress the importance of regular, large domestic demands to yield substantial stormwater runoff reductions in addition to larger unit capacities (Burns et al., 2014).

It should be noted that the majority of this research has focused on smaller spatial scales (e.g., household, parcel, and neighborhood). Consequently, a knowledge gap results that limits their extension to expanded scales of planning, design and hydrologic analysis (Bedan & Clausen, 2009; Lee et al., 2012). When empirical data at the watershed-scale are available, as in the

research by Yang and Li (2013), results reinforce the effectiveness of integrated suites of LID in improving stormwater runoff reductions and water quality enhancements. However, due to the depth and complexity of data required for such analyses, duplication of similar efforts is recognized as difficult (Thomas et al., 2003; Jensen et al., 2010). Beyond data needs, accurate representation of LID at the necessary local and regional scales is a challenge due to the exhaustive methods and knowledge required on the part of the user to characterize and quantify impacts (Burian & Pomeroy, 2010).

This approach of targeting site-specific stormwater management with decentralized source controls in pursuit of wider goals (e.g., watershed health) has been termed ‘flow-regime management’ by Burns et al. (2012) and is still in its infancy. Despite the aforementioned limitations, researchers increasingly extrapolate and apply LID principles either uniformly or as over-simplified, disconnected measures to address broader issues. This generalization coarsens the resolution of both model representation and simulation results. For instance, a study of urban rooftop runoff control practices related a 10% conversion of rooftop infrastructure in the city of Brussels to a watershed runoff reduction of 2.7%, with single buildings capable of reducing 54% of annual runoff (Mentens et al., 2006). For larger areas comprised of heterogeneous land covers and land uses, site-specific planning and design requires intensive analysis capable of discerning between datasets and underlying variability. Thus, it is imperative that methods be developed that efficiently assess and characterize large, urban datasets for direct application to hydrologic models and subsequent simulations

(Pataki et al., 2011).

Traditionally, hydrologic modeling of urban watersheds was dependent upon the modeler's judgment of parameters and methods, such that realistic conditions were recreated within the model framework. This involved time-intensive manual delineation and digitizing of vector data layers from aerial imagery or in-field observations (Thomas et al., 2003; Sterr & Yui Lau, 2012). Improvements in remote sensing (e.g., Light Detection and Ranging, or lidar) and image analysis have increased precision in identifying and visualizing land cover types and objects (Wechsler, 2007; Amatya et al., 2013). Compared with manual delineation, this has resulted in finer resolutions of hydrologic model inputs, including basin area, slopes, flow paths, connectivity, and channel lengths (Rumman et al., 2005; Kunapo et al., 2009; Amatya et al., 2013). Finer dataset resolutions are also pivotal to identifying, classifying, and modeling watershed boundaries, surface classes, and characteristics that impact hydrology (Luzio et al., 2005; Rumman et al., 2005; Kunapo et al., 2009; Cao et al., 2012). As a result, this has improved the ability of water resources engineers and urban planners to model and analyze the structure and functionality of stormwater management plans.

Of particular importance to these improvements are remotely sensed datasets, which have expanded the abilities of modelers to assess both local and regional areas (James et al., 2007; Kunapo et al., 2009). In particular, lidar has been increasingly employed in the visualization, characterization, and delineation of both surface and hydrologic models regardless of obstructions (e.g., tree

canopy and buildings) and surface types (Frazier & Page, 2000; James et al., 2007; Im et al., 2008; Jensen et al., 2010; Zhu et al., 2012). Lidar complements traditional high-resolution color imagery by providing elevation and structural information. This reduces misclassification due to shadows and improves extraction of specific land uses separated by relative elevation (e.g., rooftops versus paved areas). For example, a small catchment (e.g., 550 hectares) with unusually rich resources (e.g., GIS, lidar, and orthoimagery) was used to test the siting of bioretention and green rooftops (Jensen et al., 2010). While researchers were able to extract suitable sites, they acknowledged difficulty in duplication stemming from the limited availability of pertinent resources (Jensen et al., 2010). As such, the means to reliably and accurately extract and filter these resources for large(r) areas must be made available for multiple users' skillets.

A potential solution to this resides in the ever-increasing resolution and spatial extent of publicly-available datasets, including NAIP aerial imagery and lidar point cloud data. However, these improvements are also the source for increased complexity and heterogeneity inherent in the data. As such, there exists greater potential to complicate classification methods and reduce overall accuracy, especially when employing pixel-based image analysis, or PBIA (Myint et al., 2011). Since PBIA classification algorithms are based solely on pixels' spectral values, the potential for confusion between different objects or surfaces with similar spectral signatures is more likely (Hsieh et al., 2001; Zhu & Blumberg, 2002; Yang et al., 2010a). Alternatively, object-based image analysis (OBIA) is applied to both spatial and thematic elements within the scene. OBIA

excels over PBIA in that it incorporates scale, context, geometry, and color (Yang et al., 2010b; Wu & Yuan, 2011). Research on OBIA applications and methodologies continually address land cover and land use mapping. For instance, in extracting impervious surface areas, Hu and Weng (2011) achieved greater accuracy in residential areas over the more complex, central business district (CBD), registering 95% and 92%, respectively. The combination of lidar datasets with spectral imagery is increasingly shown to improve OBIA classification results, with the normalized Digital Surface Model (nDSM) proving to be the most important feature for improvement (Blaschke, 2010; Aguilar et al., 2012). Using these methods to provide accurate thematic map layers, the goal of watershed stormwater planning and management then becomes finding and designing LID practices for suitable locations.

Determination of locations meeting user-defined objectives can be achieved with GIS-based postprocessing, which improves the model analyst's ability to weigh and filter multiple datasets (Malczewski, 2004). Site search analysis explicitly extracts areas, along with spatial characteristics, meeting suitability criteria (Malczewski, 2004). Specific search methods include multiple criteria decision analysis (MCDA) and spatial clustering analysis, which weigh complex factors and present recommendations based upon input criteria (Malczewski, 2004). Jacquez (2008) used spatial clustering to recognize patterns with visualization, spatial statistics, and geostatistics such that locations, magnitudes, and shapes of statistically significant pattern descriptors were identified. Hotspot identification has also been applied for targeting resources

and minimizing risk within a larger system (Anderson, 2009). The economic analysis of distributed LID practices is a growing field of research, combining cost-effectiveness with stormwater management benefits, such as flood risk mitigation (Kousky et al., 2013).

3.4 Materials and Methods

3.4.1 Case Study and Hydrologic Model

The 3,110-hectare south branch of the Chollas Creek watershed, San Diego, California was chosen as the case study location. The heterogeneity and complexity of the existing land cover and land use provided adequate conditions for which the study's objectives could be tested and improved. With PBIA, the watershed was found to consist of 52.7% impervious surface, a combined 43.9% pervious surface (e.g., grasses and tree canopy), and 3.4% water surface. An analysis of parcel level owner data found the total number of residential, single-family households to be 20,787. Quantification of rooftop areas for a random sampling of 150 households yielded an average area of 186 square meters, which was multiplied by a conservative factor of 0.5 to account for losses resulting in an adjusted average rooftop area of 93 m^2 (Walsh et al., 2014). The work completed by Walsh et al. (2014) focused on synthesizing a hydrologic model and assessing the impact of variations in a passive RWH program, comparing reductions in watershed and subcatchment runoff volumes and rates. Results found greater cost-effectiveness with smaller barrels (227 liters) versus larger cisterns (7,571 liters) for the specific catchment, with overall reductions ranging from 10.1% to 12.4% for the range of RWH unit sizes (assuming 100

percent of households were fitted with units). Further details of the watershed, the hydrologic parameters and models, and results can be found in Walsh et al. (2014).

As a comparison for the application of the OBIA classification and LID Site Suitability methodology, rainwater harvesting was chosen as the targeted LID. The hydrologic models that were calibrated and validated through previous work (Walsh et al., 2014) served as the basis for applying and comparing the results of the proposed methodology. The original hydrologic models involved in this study included the base model, representing current conditions without additional LID practices implemented, and the 227-liter scenario model, representing an adapted base model in which all households implemented a single 227-liter rainwater harvesting barrel. These models are hereby referred to as *BASE* and *UNI227*, respectively. To model the results from the suitability methodology, the BASE model was adapted. For RWH, 227-liter barrels were implemented at all extracted households meeting the suitability criteria. This model is hereby referred to as *LID227*. As this research was focused on the application of the synthesized protocols to improve the siting and hydrologic modeling of LID practices, namely RWH, variations in the hydrologic model parameters were not considered. For instance, drain delay, drain coefficients, and unit sizing remained constant for both *UNI227* and *LID227*.

3.4.2 Classification

An object-based approach was used to classify building rooftops within the study watershed, which required elevation (via lidar), orthoimagery, and thematic

parcel datasets for classification. Fig. 3.1 presents the workflow for the OBIA classification processes, with the following comments provided as guidance.

(A) Lidar point cloud datasets were obtained for the watershed (approximately two-meter point spacing); however, the spatial extent of these datasets was limited, representing 75% of the total watershed. Datasets were then merged using BCAL Tools (BCAL LiDAR Tools ver. 1.5.3, 2013) and LAStools (Isenburg, 2013). These toolsets offer a suite of open-source options to process, analyze, and visualize lidar datasets, with LAStools providing additional ArcGIS plug-ins (Isenburg, 2013). For processing the lidar point cloud, a methodology similar to Shiravi et al. (2012) was adapted, including filtering points to extract rasterized surfaces representing the minimum (i.e., last), maximum (i.e., first), and bare earth returns. Erroneous, or No Data, values were replaced using ENVI's replace values tool. As a check, a finer resolution bare earth raster was created from the 0.5-meter elevation contours (SanGIS, 2012) using ArcGIS (ESRI, 2013). Band math, which is the process of applying an operator to one or several bands (e.g., raster surface or aerial red band) to create a new band that is a function of the inputs, was then performed. One example of band math is the creation of the normalized Digital Surface Model (nDSM), which normalizes all objects of height from the minimum raster to the bare earth raster layer, or band. For this research, the nDSM was extracted with a method similar to Zhu et al. (2012), resulting in a raster, or band, featuring only objects of height, such as buildings and trees. To remove low ground objects (e.g., cars), a height filter of 2.6-meters was instituted, leaving only objects with targeted heights. The filtered

nDSM was then used for classification.

(B) Orthoimagery was obtained from the National Agricultural Imagery Program (NAIP) at one-meter resolution (USGS). Imagery dated from 2010, with a total of four bands (Red, Green, Blue and Near Infrared). To ensure the datasets were aligned, image-to-image spatial registration was used. To differentiate vegetation from other land surfaces, band math using the Near Infrared (NIR) and Red bands was completed, yielding the Normalized Difference Vegetation Index (NDVI) raster. In combination, the NDVI and lidar datasets have been found to improve distinction between natural and manmade structures, with greater NDVI and height values for trees, respectively (Zhu et al., 2012). The original and NDVI imagery datasets were then used for classification. (C) The thematic layer representing parcel boundaries was obtained for the study area to improve the classification for the scale required. All input dataset coordinates were converted to UTM, NAD83, Zone 11, California State Quarter Quadrangle (meters). The elevation, spectral, and thematic datasets were used for OBIA with eCognition.

(D) The first step in OBIA undertaken was image segmentation, which split the input datasets into separate regions, or objects, as a function of the user-defined parameters: shape, compactness, and scale. The shape factor adjusts for homogeneity relative to the object's shape while compactness determines how smooth and compact the boundaries are for the object's shape. The scale parameter determines the size of homogeneous objects, or the maximum change in heterogeneity that may occur in merged objects (Wu & Yuan, 2011). To

finalize segmentation weights and components, variations in scale parameters (5-50) and shape factors (0.1-0.9) were evaluated with respect to their impacts on classification, similar to Wu and Yuan (2011). Weights applied to the shape, compactness, and scale parameters for image segmentation were 0.1, 0.1 and 15, respectively. For spectral input, weights were applied uniformly to the Red, Green, Blue, and NIR bands. Due to spatial discrepancy with the spectral inputs (one meter), the elevation dataset (two meter) was not included for image segmentation. Image segmentation was then carried out for the prior weights and components, resulting in object-based classes throughout the study area. (E) Next, qualitative and quantitative assessments of the resultant segmentations were provided with trial and error, assuring that the segmentation components were adequate.

The process-based rule set for refinement of the segmented image was synthesized as a function of the elevation, spectral, and contextual input data. Since rainwater harvesting was the LID method chosen for the application, only two land cover classes were targeted for delineation: buildings and unclassified (e.g., everything except rooftops). The latter was disregarded in the geospatial analysis since rooftop runoff was the primary focus of the suitability analysis. (F) The first step in the rule set involved classification by elevation with the standard deviation filter, which is a relational function that calculates the standard deviation of an image object to its neighbors. Neighbors are defined as the relation image object at the same level, or elevation in this case. When the standard deviation is high, this indicates greater variation in height values within

a given area and, thus, can be classified as trees, whereas buildings will have low standard deviation values since they are relatively constant within a given area. (G) Refinement based on spectral information targeted the band indices NDVI and Ratio Vegetation Index (RVI). RVI is a band math procedure that relates NIR to Red. These steps further distinguished objects representing vegetation (H) Final refinement was based on contextual information, employing the mean difference to neighbors and number of brighter objects for elevation. The mean distance to neighbors assesses the difference between objects within a given distance (e.g., 50, based on the objects' center of gravity) that fall within that mean area. This helped relate targeted groups of similar land cover types. With the number of brighter objects, refinement was based on normalized objects of height, with brighter cells indicating higher elevations and darker cells indicating lower elevations. In sequence, the process rule set functions were carried out, resulting in all classified objects representing rooftop areas. (I) Finally, these regions were merged and exported as a vector layer (polygon shapefile) for accuracy assessment and geospatial analysis in ArcGIS. It is important to note that, due to the limitation on the spatial extent of lidar data, only the fully classified subcatchments were used in the overall comparison of the classifications.

To assess the accuracy of OBIA classification results, methods must go beyond simple pixel- and block-based approaches to determine whether the object is represented accurately (Whiteside et al., 2014). Geometric accuracy of shape and location is important when resultant images are required to drive

further analysis, such as in GIS or decision-making (Foody, 2002; Schopfer et al., 2008; Whiteside et al., 2014). Heavily used in PBIA validation are confusion matrices, which are not able to provide the level of detail required for OBIA assessment (Whiteside et al., 2014). Therefore, an appropriate sampling design must be employed in assessing the accuracy of the OBIA classification (Foody, 2002). For this study, we chose a simple random sampling method for accuracy assessment of thematic errors (errors of commission and omission). A similar approach was completed by Whiteside et al. (2014) to assess area-based validation of OBIA classifications. This method used random sampling accuracy assessment, which addresses the lack of observed rooftop area data for the entire watershed.

Random distribution of sample points (n = 50) throughout the Chollas Creek watershed was provided via ArcGIS and in accordance with recommendations by Congalton (1991). A 100-m buffer was then applied to all random points, resulting in individual sample areas of 3.14 hectares. This established a total validation area of 157 hectares, representing 5% of the overall watershed area. A qualitative assessment of the randomly generated sample sites found them to be fully representative of the land use and land cover conditions found throughout the watershed (Foody, 2002). Manual delineation of building footprints within each sample site was completed using the NAIP aerial imagery. These validated polygons were used in the thematic and geometric accuracy assessments of the classification results for each area and throughout the watershed. Within ArcGIS, a Quality Assessment (*QA*) toolset was created to

determine the accuracy of land cover/land use classifications. The input layers to *QA* included the validated building polygons, classified building polygons, and sample site area polygons. The *QA* workflow consisted of quantifying the true positive, false positive, and false negative areas relative to the sample sites. These values were then used to construct the confusion matrix and assess the overall, user's, and producer's accuracies for the resultant classification. Assessment of nonthematic errors (e.g., misregistration) was completed with the RMSE for the location of centroids (Eq. 1) for spatial registration (Zhan et al., 2005; Congalton & Green, 2009). *QA* completed this by converting the classified and validated polygons to points (i.e., centroids) and calculating the near distances between the two (e.g., within a 10-m radius).

$$RMSE_{centroid} = \sqrt{\sum_{i=1}^{n}\left[\left(x_{ci} - x_{Ri}\right)^2 + \left(y_{ci} - y_{Ri}\right)^2\right] / n} \quad \text{.....(1)}$$

For Eq. (1), x_{ci} and y_{ci} represent the classified coordinates while x_{Ri} and y_{Ri} represent the validated coordinates for the sample population, n. Assessment of the RMSE for the individual areas per sample sites was also provided (Eq. 2), where y_i is the classified building area and represents the validated building area for the sample population, n.

$$RMSE_{area} = \sqrt{\sum_{i=1}^{n}\left(y_i - \hat{y}_i\right)^2 / n} \quad \text{.....(2)}$$

3.4.3 Geospatial Analysis

The first step in LID design and planning is to acquire the necessary datasets beyond the contributing drainage area, including the digital elevation model (DEM), elevation contours, land use, land cover, parcel boundaries, flood zones, soils, and stormwater infrastructure (SanGIS, 2012). Since rainwater harvesting was chosen as the applied LID practice, the rooftop classifications from eCognition represented the impervious area to be targeted by the stormwater management framework. Using the previously mentioned datasets, the hydrologic model was created via the delineation and quantification of catchment areas, land surface slopes, surface roughness estimates, depression storage estimations, and channel geometry and roughness characteristics. For hydrologic analysis of the suitable locations and designs, the model simulations were driven by long-term hourly precipitation data. Precipitation was obtained for the nearby San Diego Lindbergh Field airport (COOP ID 047740, 32°44'N/117°11'W) (NOAA 2012), which is located approximately seven kilometers (km) from the watershed outlet. The precipitation record was determined to be uniformly representative of the local climatic conditions throughout the watershed.

3.4.3.1 LID Site Suitability Toolset

The LID Site Suitability (*LIDSS*) toolset was created to facilitate the identification and quantification of areas meeting user-defined criteria for stormwater management practices. The workflow for *LIDSS*, including the inputs, methods, commentary and outputs, is visualized with Fig. 3.2.

To filter the design constraint layers, the LID Site Suitability (*LIDSS*) tool was created. The goal of *LIDSS* was to identify specific locations throughout the expansive case study area as a function of user constraints, given the multiple datasets, for the LID practice chosen. To begin, *LIDSS* requires input be in raster format; thus, dataset manipulation was applied to create a slope raster from elevation contours. The resultant raster was validated with DEM data acquired for the same location. To determine locations meeting the ideal soil, slope, land use, and land cover conditions, *LIDSS* relies on conditional if-then statements to filter through datasets on a cell-by-cell basis. Resulting filtered areas are presented as both raster and vector layers, as determined by the analyst. Either format allows for further analysis or quantification of identified locations' design parameters. Pertinent parameters include area, perimeter, slope, soil, and unique identifier for each site. With this information, users are prompted to establish a sub-area upon which to integrate the extracted locations layer, such as the parcel or subcatchment. Next, the tool recalculates the design parameters for the sub-area discretized layer and exports the results as a geodatabase. This data attributes table can then be opened with any application for further analysis and design (e.g., Microsoft Excel). *LIDSS'* framework ensures that selected locations are not only a function of user-specific, local criteria but also spatially accurate representations of existing conditions. This toolset and research improves upon the traditional, uniform application of LID principles to the watershed-scale of planning, design, and analysis.

In applying *LIDSS*, users were capable of establishing a maximum slope,

for which values in exceedance would be removed from the resulting thematic map. Next, the soils and land use datasets were manually simplified to represent infiltration rates and general uses. Land use was grouped into one of five classes: residential, road/paved, pervious/vegetated, building (not residential), and water surface. Users were then able to further filter based on infiltration and land use requirements, yielding locations satisfying the three former design constraints. *LIDSS* was shown to be capable of filtering through these datasets, guided by user-defined constraints, to yield locations either meeting or exceeding the required range of parameters. For users not familiar with design constraints of LID, these can be found in numerous documents, such as the Prince George's County LID Manual (1999), which has been adapted and summarized for this research (Table 3.1).

For this application of *LIDSS*, specifically targeting the planning and design of rainwater harvesting, the only applicable layer became the OBIA classified dataset (e.g., Land Use Raster). For this study, both the parcel and subcatchment thematic layers were joined as the subarea analysis layers, such that the hydrologic model (*LID227*) accurately represented RWH for the pertinent scales. Running *LIDSS* resulted in the aforementioned geodatabase file, containing the subcatchment identifier, parcel identifier, area of rooftop (m^2), and perimeter of rooftop (m^2) for all of the classified rooftop areas within the watershed.

3.5 Results

3.5.1 Classification and Suitability Analysis

OBIA classification resulted in the quantification of 273 hectares of total rooftop area throughout the Chollas Creek watershed (negating those subcatchments not fully classified). This translated to an average rooftop area of 213 m^2 (102 – 517 m^2) per subcatchment, while the total rooftop area per subcatchment averaged 4.0 hectares (0.3 – 22.5 hectares). The total number of households meeting the classification and analysis methodology was 14,263. Excluding the subcatchments that were not completely classified, the total number of rooftops was reduced by 10.2% to 12,813.

The rooftop analysis completed by Walsh et al. (2014) was adjusted for the same subset of catchments, resulting in a total of 14,412 households. This represented a 30.7% reduction in the potential number of RWH locations from the original *UNI227* model. In their work, Walsh et al. (2014) quantified the average rooftop area to be 186 m^2, which was adjusted by 50% to 93 m^2 to account for losses. Combined with the subset of households per subcatchment, this resulted in 268 and 134 hectares, respectively, for total rooftop area. Since only the adjusted rooftop area was employed by Walsh et al. (2014) for scenario comparison, the same conditions were used for this study. This equated to nearly 51% less impervious area managed by RWH for *UNI227* compared with *LID227*.

The *LIDSS* toolset was found capable of identifying and quantifying the criteria-specific locations for the range of user requirements, including residential rooftop land use and land cover, no slope or soil restrictions, and not to be

implemented within the 100-year flood zone. An example of the classified rooftop areas meeting the *LIDSS* constraints (e.g., Buildings) is presented, with validated areas presented with solid black boundaries within sample sites (Fig. 3.3). Results from the centroid RMSE are visualized in Fig. 3.4.

3.5.2 Accuracy Assessment

The resulting OBIA rooftop area classification was found to have an overall feature classification accuracy, measured by total positive classified pixels to validated pixels, of 91.3%. An accuracy of 75.2% was achieved for the Buildings feature class producer's and user's accuracy throughout the 50 sample sites, as indicated by the confusion matrix (Table 3.2). Calculation of the average $RMSE_{Area}$ resulted in 0.7% (208 m^2), which represents the ratio of the RMSE area to the total sample site area.

There appeared to be confusion between some rooftop areas with similar spectral reflectance values to that of pavement and red soil, as indicated in Fig. 3.3. This supported the accuracies achieved with the confusion matrix. The results of the OBIA classification accuracy assessment for sample sites' versus validated datasets are presented in Fig. 3.5. This plot also shows that the classification protocol resulted in slightly greater overall sample site areas delineated versus those validated (average of 5% greater). The extracted R-squared value of 0.74 was deemed acceptable for this application. Relative to the location of the centroids, a 3.3 m $RMSE_{centroid}$ was calculated. This indicated that a classified centroid would be within +/- 3.3 m of the actual, or validated, centroid.

3.5.3 Hydrologic Model Alteration

With the suitability results from *LIDSS*, the BASE model was altered to represent the new parameters associated with the residential households targeted for RWH. Hydrologic simulations were carried out for all of the models with the long-term hourly precipitation record driving simulations. Results were recorded at hourly time steps and collated for both the watershed outlet and subcatchment-scales. Results were then broken down annually for further analysis. At the watershed-scale, with results assessed at the watershed outlet node, reductions resulting from the uniform (*UNI227*) and suitability (*LID227*) methodologies are presented in Table 3.2. Using Analysis of Variance (ANOVA) for annual results found watershed outlet volumetric reductions to be significantly different [$F(1,124)=190.7$, $p=0$] between the *UNI227* and *LID227* model simulations. All watershed-scale reductions followed a normal distribution. For the fully classified subcatchments, results followed the trend of increasing reduction with increasing LID-targeted area. However, the application of RWH did not produce reductions for all subcatchments. For instance, subcatchments D49 and D69 simulated a 5% and 10% increase for the long-term record, respectively. For the range of all other subcatchments, reductions can be found in Table 3.4.

3.6 Discussion

The combination of the accuracy of the OBIA classification targeting rooftop areas with the increased efficiency via the related toolsets (e.g., *LIDSS*, *QA*) reveals the novelty of this methodology to urban water resources

engineering. This research improves upon the approaches of past works that employed the assumption of uniformity due to either limited data availability or lack of analyst time and resources. The suitability methodology and toolsets stem from a discipline with a long history of applying similar methods to quantify land cover and land use for numerous other assessments. The ability to more efficiently characterize and quantify the land cover and land use components of urbanized watersheds allows designers and planners to focus their attention on enhancing the sustainability of the water infrastructure with finer resolution results. With reference to Fig. 3.5, it appears the OBIA methodology overclassified the rooftop areas for the sample site locations. It is expected that this overclassification results from coarseness of elevation data. As a comparison, classification accuracy (92%) was similar to that targeting impervious areas for residential and densely urbanized (e.g., CBD) locations, 95% and 92%, respectively (Hu & Weng, 2011). In terms of time required, the manual delineation of the 1,500 building areas for the 50 sample sites was just over 14 hours. As previously stated, these sample sites totaled only 5% of the entire watershed, which has an average population density of 5,400 persons per km^2 (City Data, 2011). Thus, for the majority of stakeholders and regions without vast resources, such as existing thematic maps representing building footprints, the proposed suitability methodology and toolsets can improve not only outcomes but also monetary savings otherwise spent on labor intensive duties, such as digitizing land use/land cover.

Beyond accuracy and efficiency, *LIDSS* improves the ability of the user to

both vary the constraining parameters to meet local conditions and thresholds and visualize these variations for the locations extracted. The ability to manipulate constraints as a function of watershed conditions, based on site-specific criteria, provides a powerful stand-alone tool that is capable of functioning with many common, stand-alone software programs, such as Microsoft Excel and ArcGIS. Specific to the application of RWH, *LIDSS* not only identified household areas for both parcel- and subcatchment-scales but also allowed the analysts to design a RWH framework mitigating all suitable contributing drainage areas. This application could have been further refined to include commercial and industrial buildings by expanding the conditional statement pertaining to land use or cadastre datasets. Similarly, if an infiltration-based practice was the focus of the study, *LIDSS* users have the potential to establish constraints on soils (i.e., infiltration) and groundwater data.

Finally, the suitability methodology provides users the ability to manipulate the output geodatabase file as a function of local or individual design requirements, such as the Water Quality Control Volume (WQCV) depth. This control more accurately translates and projects realistic conditions into the hydrologic modeling space. This is important for locations where parcels are less dictated by the lack of available area and, therefore, possess greater potential for cistern implementation. As robust models, such as SWMM, continue to make improvements with subarea routing, LID representation, and computational time, the methods and toolsets presented in this research can only further reinforce their importance for the average analyst, designer, and planner.

Extending results from OBIA classification and geospatial analysis to the hydrologic models and, by extension, to hydrologic simulations resulted in major differences between the *UNI227* and *LID227* scenarios. Compared with the method of uniform subcatchment application, based on a random sampling of the average rooftop area (n=150 households), *LID227* simulated greater reductions in the overall watershed volumes and rates. For instance, the *LIDSS* method produced in an increase in both the long-term and annual average reductions ranging from 44% to 51%. At the subcatchment-scale, this range was slightly higher (46% – 55%), with a 22% average long-term volumetric reduction and a 22% peak rate dampening. Focusing on individual subcatchments, annual reductions followed a similar trend to that of the overall watershed.

3.7 Conclusions

The proposed protocol and associated toolsets allow users to establish local requirements and to account for local constraints when searching for suitable locations specific to the LID practice(s) chosen. As with a site-specific LID design, the local guidelines should be observed in selecting parameters (Table 3.1). Application of the proposed methodology exhibited the ability to accurately account for the multiple datasets required when designing site-specific practices for expanded scales of implementation. Additionally, the time required to classify contributing drainage areas (e.g., individual rooftops) was greatly reduced with OBIA classification. Due to the open-source nature of *LIDSS*, user manipulation of inputs to account for variability in future climate and watershed development is a potential avenue for investigation. For instance, users can

employ resampling of land use datasets to represent alterations to or future projections in the existing conditions. Since precipitation datasets are also external of the toolset, yet pivotal to the hydrologic model simulations, users have the opportunity to further analyze vulnerabilities and the adaptive capacity of green and grey infrastructure into the future.

With respect to the OBIA classification component, the process rule set provided accurate areal approximations for household rooftops within the heterogeneous landscapes employing publicly-available datasets, with an overall accuracy of 92%. Producer's and user's accuracies for buildings were 72% and 74%, respectively (see Table 3.2). These values indicate the probabilities that a building on the ground will be classified correctly and that a building classified as such will actually be a building, respectively. For the random sample sites assessed, a RMSE of 0.7% (218 m^2) for the OBIA methodology was found to adequately extract and quantify rooftop areas throughout the heterogeneous landscape assessed. Limitations related to the classification included the discrepancy in spatial resolution between the elevation and spectral datasets. Choice of a different surface interpolation algorithm and improved orthorectification of datasets is anticipated to improve classifications. In applying the results to amend the base input file (*BASE*) for SWMM, results found the suitability protocol (*LID227*) to result in stronger positive correlations between stormwater runoff reduction and watershed area targeted, as compared with the uniform method (*UNI227*). Researchers determined this to further reinforce the accuracy of the classification method and *LIDSS*, since building

misclassifications (e.g., over- and under-simplifications) with *UNI227* resulted in skewed hydrologic reductions that reduced the expected strength of the correlation.

The significance of this study resides in its improvement upon traditional methods of both LID and watershed-scale design employing LID principles. OBIA and *LIDSS* improve the ability of users to assess variability of local inputs and constraints, which are pertinent to LID planning and design. This project establishes the necessary baseline for incorporating additional datasets that influence both current and future mitigation plans. For instance, the ability to incorporate future urban build-out scenarios, from agent-based modeling, and greenway development improves the targeting of suitable sites throughout dynamic urban watersheds. Combining suitability results and methodologies with hydrologic models allows users to simulate and analyze the hydrologic responses of various scenarios relative to local thresholds and objectives. More importantly, the inclusion of monetary costs and benefits improves the ability of municipalities to establish tiered implementation plans as a function of budget and future projections of growth and build-out.

The topic of repurposing existing green space within the built environment to satisfy multiple objectives, including environmental, ecological, and social improvements, stands to benefit from such research (James et al., 2009). The ability to accurately classify existing and historical land use and land cover conditions with freely available public data extends to all of these realms, as indicated in past OBIA research on the complex urban-natural transition

(Tuominen & Pekkarinen, 2005), the range of land uses (Platt & Rapoza, 2008), urban area parcel-level classification (Zhou & Troy, 2008), and urban tree cover monitoring (Moskal et al., 2011). However, extension to watershed LID planning and design remains an under-researched area in literature. As such, this research provides a basis for future research requiring assessment of current watershed conditions to site and design LID practices that are representative of user requirements and physical constraints.

Building upon this work, the researchers are in the process of developing a prioritization protocol that combines the suitability analysis toolsets with hydrologic and cost analysis models. This work will further the ability and efficiency of users to refine targeting methods by focusing on stormwater hotspots and budgetary constraints. Future research will provide a hierarchy of potential applications and implementation plans for users, ranging from urban planners to municipal engineers. The Chollas Creek Watershed will, again, be used as the case study location.

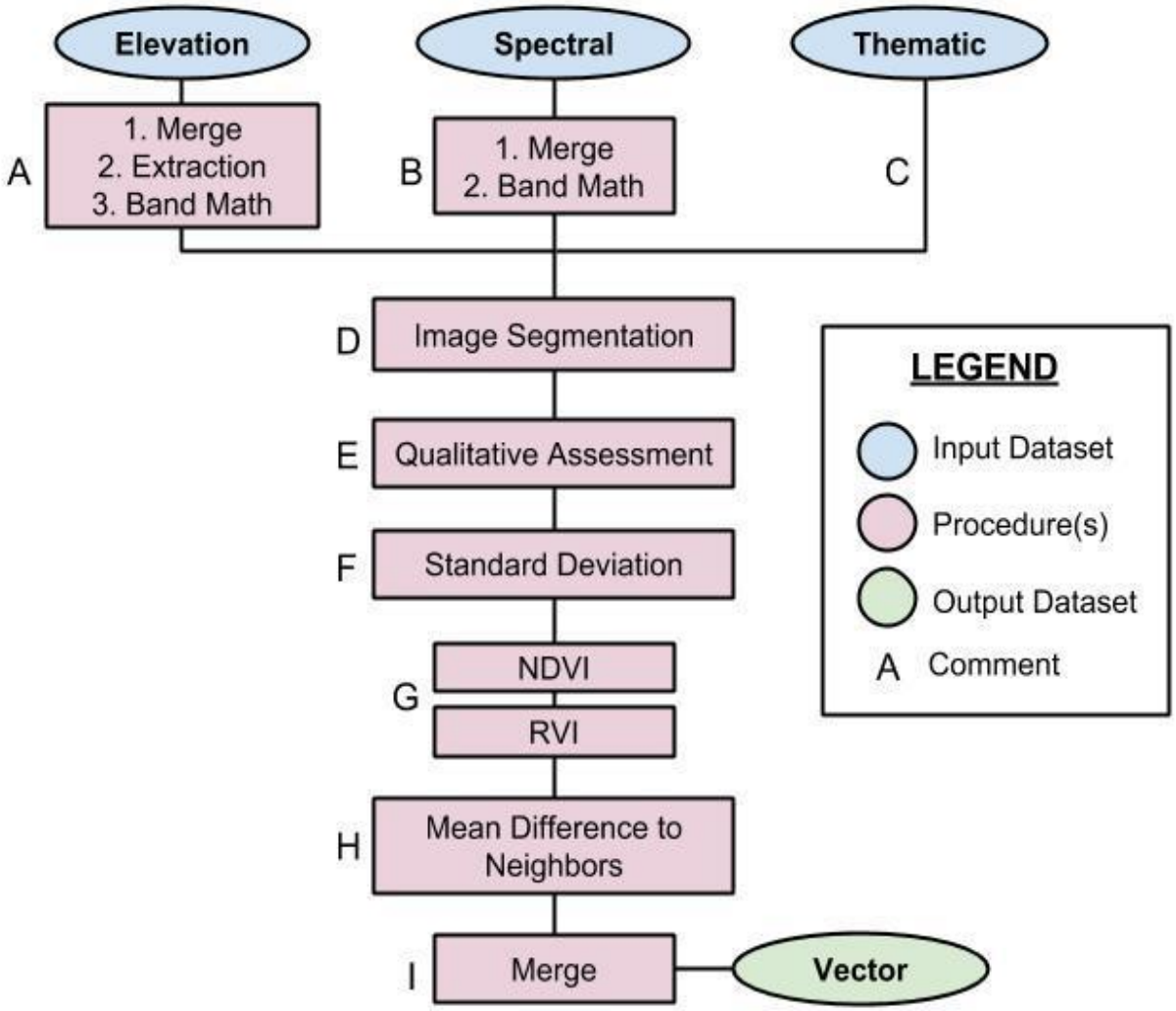

Figure 3.1: OBIA classification workflow. Comments are linked to the in-text methodology section.

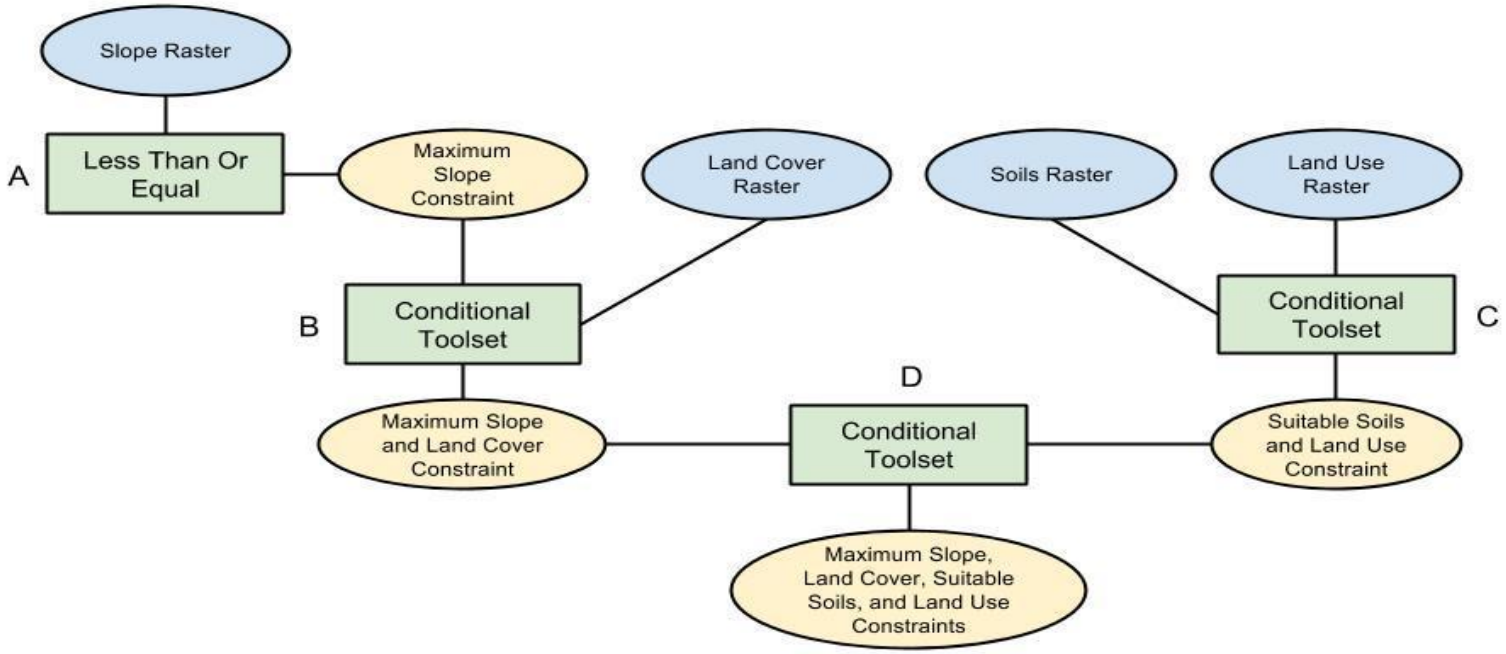

Figure 3.2: *LIDSS* workflow for filtering datasets: A. User defines the maximum slope allowed in the resulting *Maximum Slope Constraint*, B. User establishes the land cover type to extract as a function of the area satisfying slope criteria, C. User determines the soil type for conditional extraction of the land use dataset, and D. User extracts the land use areas that satisfy the previous steps' (A-C) results. The output, *Maximum Slope, Land Cover, Suitable Soils, and Land Use Constraints*, presents the suitable areas filtered according to user criteria guided by Table 3.1.

Figure 3.3: Sample area results presenting rooftop classification and validation polygons. Qualitative analysis of results indicates minor confusion between rooftops with reflectance values similar to paved objects, despite inclusion of lidar.

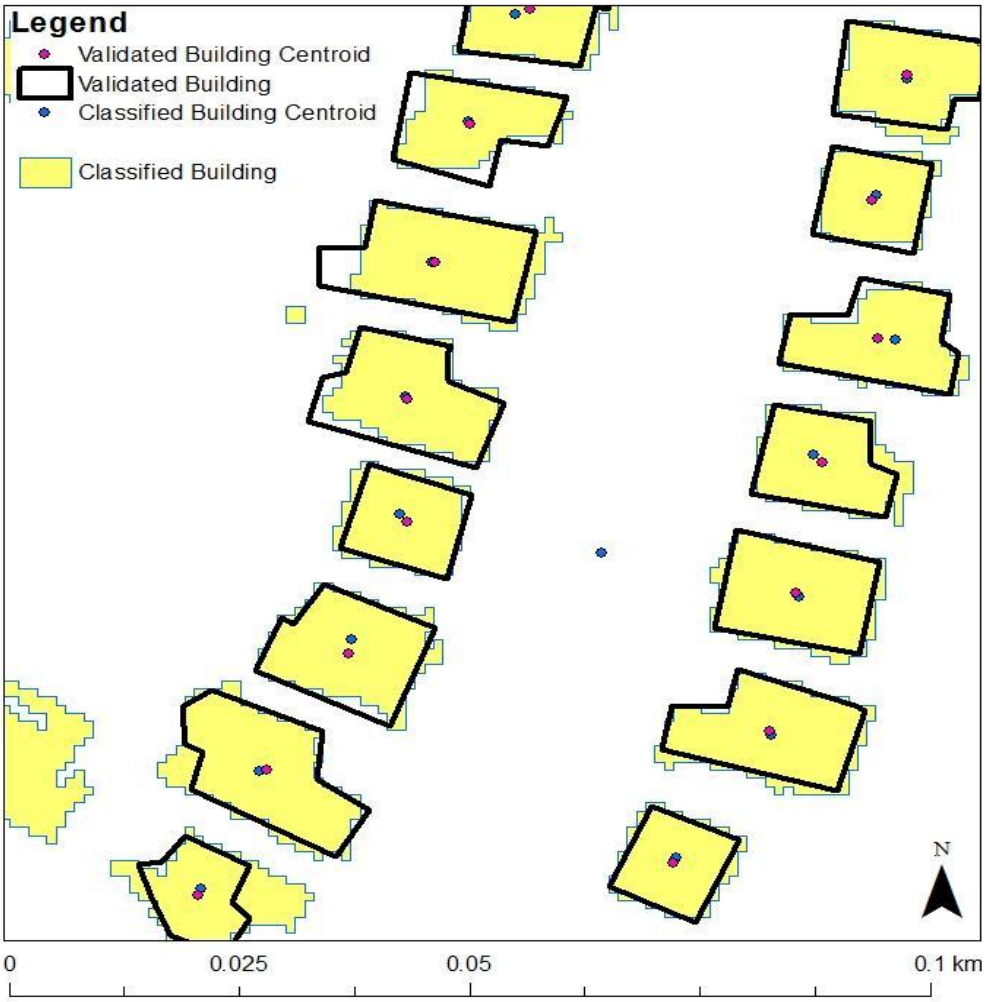

Figure 3.4: *QA* visualization for both area- and location-based RMSE for classified and validated buildings throughout sample sites.

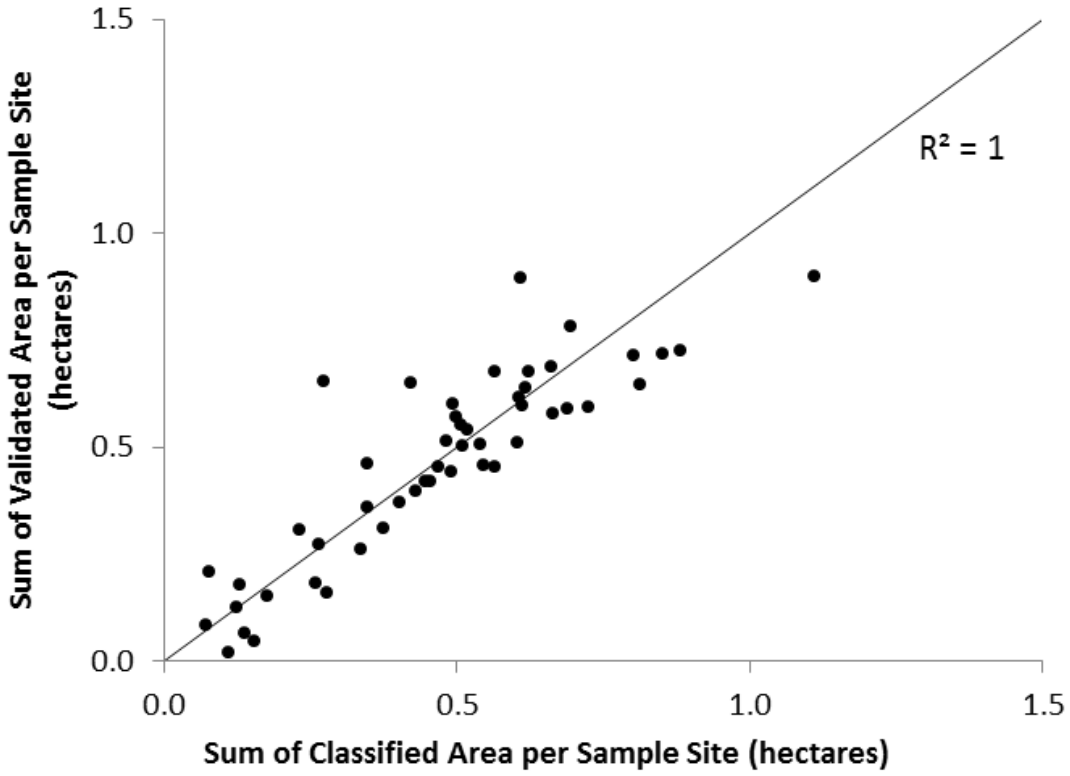

Figure 3.5: Comparison of classification accuracy assessment employing randomized sampling sites (n = 50, 3.14 hectares). Axes provide sample summation of classified and validated building areas (hectares).

Table 3.1: LID design constraints, adapted from Prince George's County (1999).

LID Practice	Dimensions	In-Situ Soils	Slope	Depths	Proximity	Maintenance
Bio-retention	**Min**.: 4.6-19 m^2 (area), 1.5-3 m (width), 3-6 m (length)	Permeable; Infiltration > 6.9 mm/hr; Underdrain	Design consideration; locate down gradient	**Min**.: 0.6-1.2 m (depth); 0.6-1.2 m separation with water table	**Min**.: 3 m; locate down gradient	Low; normal site landscape
RWH	Capacity=f(catchment area)	N/A	Design consideration for captured outflow location	N/A	N/A	Winterization; Vector control; Clean gutters
Rain Barrels	N/A	N/A	N/A	N/A	N/A	Low
Cisterns	N/A	N/A	N/A	N/A	N/A	Low
Swales (Grass, Infiltration, Wet)	**Min**.: 0.6 m (width); **Max**.: 1.8 m (width)	Not a limitation, can improve performance	Sides - 3:1 (H:V) - **Max**.; longitudinal of 1% - **Min**., Max.=f(allowable velocity)	0.6-1.2 m separation with water table; **Max**.: 1.8-3 m; =f(soil type)	No hotspot runoff; **Min**.: 3 m; locate down gradient	Low; routine landscape
Infiltration Trench	**Min**.: 0.7-2 m^2 (area), 0.6-1.2 m (width), 1.2-2.4 m (length)	Permeable; Infiltration > 13.2 mm/hr; A and B soils preferred	Design consideration; locate down gradient	0.6-1.2 m separation with water table; **Max**.: 1.8-3 m; =f(soil type)	No hotspot runoff; **Min**.: 3 m; locate down gradient	Moderate to High
Porous Pavement	**Min**.: 20% of drainage area; 50% recommended	Sandy or Silty; Infiltration - **Min**.: 1.27 mm/hr, underdrain required for <12.7 mm/hr; **Max**.: >762 mm/hr; D soils not recommended	**Max.**: 5%	**Min**.: 0.6 m with water table and bottom of unit	No hotspot runoff; **23-93 m^2**: 1.5 m down gradient, 7.6 m up; **93-929 m^2**: 3 m down, 15 m up; **>929 m^2**: 7.6 m down, 30.5 m up	Moderate to High; Vacuuming

Table 3.2: Confusion matrix for validated (column) and classified (row) feature area for all accuracy assessment sample sites.

Feature	Building	Unclassified	Total Classified Area (m^2)
Building	170,947	61,192	232,138
Unclassified	67,136	1,332,638	1,399,775
Total Validated Area (m^2)	238,083	1,393,830	1,631,913

Table 3.3: Watershed-scale hydrologic impacts for *UNI227* and *LID227*.

Hydrologic Response	Temporal Resolution	*UNI227*	*LID227*	*LID227* v. *UNI227*
Outflow Volume	Long-Term (1948-2012)	10%	16%	44%
Outflow Volume	Annual	7%-14%	10%-24%	+44% (34%-51%)
Outflow Rate (Peak)	Annual	0%-29%	0%-46%	+51% (22%-122%)

Table 3.4: Subcatchment-scale hydrologic impacts for *UNI227* and *LID227*.

Hydrologic Response	Temporal Resolution	*UNI227*	*LID227*	*LID227* v. *UNI227*
Outflow Volume	Long-Term (1948-2012)	14% (3%-73%)	22% (3%-44%)	+46% (*LID227*)
Outflow Volume	Annual	12%	20%	+50% (*LID227*)
Outflow Rate (Peak)	Annual	24%	40%	+52% (*LID227*)

3.8 References

Aguilar, M. A., Vicente R., Aguilar F. J., Fernandez A., & Saldana, M. M. (2012). Optimizing object-based classification in urban environments using very high resolution geoeye-1 imagery. Proceedings from: *ISPRS Annals of the Photogrammetry, Remote Sensing and Spatial Information Sciences, Volume 1-7. XXII ISPRS Congress.* Melbourne, AU: ISPRS.

Amatya, D., Trettin C., Panda S., & Ssegane, H. (2013). Application of lidar data for hydrologic assessments of low-gradient coastal watershed drainage characteristics. *Journal of Geographic Information System*, *5*, 175-191.

Anderson, T. K. (2009). Kernel density estimation and k-means clustering to profile road accident hot spots. *Accident Analysis & Prevention*, *41*(3), 359-364.

Bates, B. C., Kundzewicz Z. W., Wu, S., & Palutikof, J. P. (Eds.). (2008). *Climate change and water: Technical paper of the intergovernmental panel on climate change.* Geneva: IPCC Secretariat.

Bedan, E. S., & Clausen, J. C. (2009). Stormwater runoff quality and quantity from traditional and low impact development watersheds. *Journal of the American Water Resources Association*, *45*(4), 998-1008.

Blaschke, T. (2010). Object based image analysis for remote sensing. *ISPRS Journal of Photogrammetry and Remote Sensing*, *58*, 239-258.

Braden, J. B., & Johnston, D. M. (2004). Downstream economic benefits from storm-water management. *Journal of Water Resources Planning and Management*, *130*(6), 498-505.

Brown, K., Claytor, R., Holland, H., Kwon, H. Y., Winer, R., & Zielinski, J. (2007). *Better site design: An assessment of the better site design principles for communities implementing Virginia's Chesapeake Bay Preservation Act.* Ellicott City, MD: Center for Watershed Protection.

Burian, S. J., & Pomeroy, C. A. (2010). Urban impacts on the water cycle and potential green infrastructure implications. In J. Aitkenhead-Peterson & A. Volder (Eds.), *Urban ecosystem ecology* (pp. 277-296). Madison, WI: American Society of Agronomy, Crop Science Society of America, Soil Science Society of America.

Burns, M. J., Fletcher, T. D., Walsh, C. J., Ladson, A. R., & Hatt, B. E. (2012). Hydrologic shortcomings of conventional urban stormwater management and opportunities for reform. *Landscape and Urban Planning*, *105*(3), 230-240.

Burns, M. J., Fletcher, T. D., Duncan, H. P., Hatt, B. E., Ladson, A. R., & Walsh, C. J. (2014). The performance of rainwater tanks for stormwater retention and water supply at the household scale: An empirical study. *Hydrological Processes*, in press. doi 10.1002/hyp.10142.

Cao, Y., Wei, H., Zhao, H., & Li, N. (2012). An effective approach for land-cover classification from airborne lidar data fused with co-registered data. *International Journal of Remote Sensing*, *33*(18), 5927-5953.

Chocat, B., Ashley, R., Marsalek, J., Matos, M. R., Rauch, W., Schilling, W., & Urbonas, B. (2007). Toward the sustainable management of urban storm-water. *Indoor and Built Environment, 16*(3), 273-285.

City Data. (2011). Chollas Creek neighborhood in San Diego, California (CA), 92105 detailed profile. Retrieved from http://www.city-data.com/neighborhood/Chollas-Creek-San-Diego-CA.html

Congalton, R. G., & Green, K. (2009). Assessing the accuracy of remotely sensed data: Principles and practices (2nd ed.). Boca Raton, FL: CRC Press.

Debo, T. N., & Reese, A. (2010). *Municipal stormwater management* (2nd ed.). Boca Raton, FL: CRC Press.

Denault, C., Miller, R. G., & Lence, B. J. (2006). Assessment of possible impacts of climate change in an urban catchment. *Journal of the American Water Resources Association*, *45*(2), 512-533.

Dietz, M. E. (2007). Low impact development practices: A review of current research and recommendations for future directions. *Water, Air & Soil Pollution*, *186*, 351-363.

Dorfman, M., & Mehta, M. (2011). *Thirsty for answers: Preparing for the water-related impacts of climate change in American cities*. New York, NY: Natural Resources Defense Council.

ESRI (Environmental Systems Resource Institute). (2013). ESRI ArcMap Software (Version 10.1) [ArcMap 10.1]. Redlands, California.

Foody, G. M. (2002). Status of land cover classification accuracy assessment. *Remote Sensing of Environment*, *80*, 185-201

Frazier, P. S., & Page, K. J. (2000). Water body detection and delineation with landsat TM data. *Photogrammetric Engineering and Remote Sensing*, *66*(12), 1461-1467.

Han, M. Y., Mun, J. S., & Kim, H. J. (2008). An example of climate change

adaptation by rainwater management at the Star City rainwater project. Proceedings from: *3rd Rainwater Harvesting and Management Workshop*. Sydney, AU: IWA.

Hsieh, P. F., Lee, L. C., & Chen, N. Y. (2001). Effect of spatial resolution in classification errors of pure and mixed pixels in remote sensing. *IEEE Transactions on Geoscience and Remote Sensing*, *39*, 2657-2663.

Hu, X., & Weng, Q. (2011). Impervious surface area extraction from IKONOS imagery using an object-based fuzzy method. *Geocarto International*, *26*(1), 3-20.

Im, J., Jensen, J. R., & Hodgson, M. E. (2008). Object-based land cover classification using high-posting-density LiDAR data. *GIScience & Remote Sensing*, *45*(2), 209-228.

Isenburg, M. (2013). LAStools – efficient tools for lidar processing. Retrieved from http://lastools.org

Jacquez, G. M. (2008). Spatial cluster analysis. In J. P. Wilson & A. S. Fotheringham (Eds.), *The handbook of geographic information science* (1st ed., pp. 395-416). Victoria, AU: Blackwell Publishing.

James, L. A., Watson, D. G., & Hansen, W. F. (2007). Using lidar data to map gullies and headwater streams under forest canopy: South Carolina, USA. *CATENA*, *71*(1), 132-144.

James, P., Tzoulas, K., Adams, M. D., Barber, A., Box, J., Breuste, J., Elmqvist, T., Frith, M., Gordon, C., Greening, K. L., Handley, J., Haworth, S., Kazmierczak, A. E., Johnston, M., Korpela, K., Moretti, M., Niemela, J., Pauleit, S., Roe, M. H., Sadler, J. P., & Thompson, C. W. (2009). Towards an integrated understanding of green space in the European built environment. *Urban Forestry & Urban Greening*, *8*(2), 65-75.

Jensen, C. A., Quinn, R. J., & Davis, T. H. (2010). Urban watershed management: Using remote sensing to implement low impact development. Proceedings from: *2010 Third International Conference on Infrastructure Systems and Services: Next Generation Infrastructure Systems for Eco-Cities.* Shenzhen, China: IEEE.

Jia, H., Lu, Y., Yu, S. L., & Chen, Y. (2012). Planning of LID-BMPs for urban runoff control: The case of Beijing Olympic Village. *Separation and Purification Technology*, *84*, 112-119.

Kousky, C., Olmstead, S. M., Walls, M. A., & Macauley, M. (2013). Strategically placing green infrastructure: Cost-effective land conservation in the

floodplain. *Environmental Science & Technology*, *43*, 3563-3570.

Kunapo, J., Chandra, S., & Peterson, J. (2009). Drainage network modelling for water-sensitive urban design. *Transactions in GIS*, *13*(2), 167-178.

Lee, J. G., & Heaney, J. P. (2003). Estimation of urban imperviousness and its impacts on storm water systems. *Journal of Water Resources Planning and Management*, *129*, 419-426.

Lee, J. G., Selvakumar, A., Alvi, K., Riverson, J., Zhen, J. X., Shoemaker, L., & Lai, F. (2012). A watershed-scale design optimization model for stormwater best management practices. *Environmental Modelling and Software*, *37*, 6-18.

Lim, S-R, Suh, S., Kim, J-H, & Park, H. S. (2010). Urban water infrastructure optimization to reduce environmental impacts and costs. *Journal of Environmental Management*, *91*, 630-637.

Luzio, M. D., Arnold, J. G., & Srinivasan, R. (2005). Effect of GIS data quality on small watershed stream flow and sediment simulations. *Hydrological Processes*, *19*, 629-650.

Malczewski, J. (2004). GIS-based land-use suitability analysis: A critical overview. *Progress in Planning*, *62*(1), 3-65.

Marsalek, J., & Chocat, B. (2002). International report: Stormwater management. 2nd World Water Congress: Integrated water resources management. *Water Science and Technology, 46*(6-7), 1-17.

Mentens, J., Raes, D., & Hermy, M. (2006). Green roofs as a tool for solving the rainwater runoff problem in the urbanized 21st century? *Landscape and Urban Planning, 77*(3), 217-226.

Moskal, L. M., Styers, D. M., & Halabisky, M. (2011). Monitoring urban tree cover using object-based image analysis and public domain remotely sensed data. *Remote Sensing*, *3*, 2243-2262.

Myint, S. W., Gober, P., Brazel, A., Grossman-Clarke, S., & Weng, Q. (2011). Per-pixel vs. object-based classification of urban land cover extraction using high spatial resolution imagery. *Remote Sensing of Environment*, *115*(5), 1145-1161.

National Research Council of the National Academies (NRC). (2008). *Urban stormwater management in the United States.* Washington, DC: The National Academies Press.

NOAA (National Oceanic and Atmospheric Administration). (2012). NOAA atlas 14 point precipitation frequency estimates: ca. Retrieved from http://hdsc.nws.noaa.gov/hdsc/pfds/pfds_map_cont.html?bkmrk=pa

Pataki, D. E., Carreiro, M. M., Cherrier, J., Grulke, N. A., Jennings, V., Pincetl, S., Pouyat, R. V., Whitlow, T. H., & Zipperer, W. C. (2011). Coupling biogeochemical cycles in urban environments: Ecosystem services, green solutions, and misconceptions. *Frontiers in Ecology and the Environment, 9*(1), 27-36.

Prince George's County, Maryland. (June 1999). Low-impact development design strategies: An integrated design approach. Retrieved from http://water.epa.gov/polwaste/green/upload/lidnatl.pdf.

Roy, A. H., Wenger, S. J., Fletcher, T. D., Walsh, C. J., Ladson, A. R., Shuster, W. D., Thurston, H. W., & Brown, R. R. (2008). Impediments and solutions to sustainable, watershed-scale urban stormwater management: Lessons from Australia and the United States. *Environmental Management*, *42*, 344-359.

Rumman, N., Lin, G., & Li, J. (2005). Investigation of GIS-based surface hydrological modelling for identifying infiltration zones in an urban watershed. *Environmental Informatics Archives*, *3*, 315-322.

SanGIS. (2012). *GIS data warehouse.* Retrieved from http://www.sangis.org/download/index.html

Schopfer, E., Lang, S., & Albrecht, F. (2008). Object-fate analysis: Spatial relationships for the assessment of object transition and correspondence. In T. Blaschke, S. Lang, & G. J. Hay (Eds.), *Object-based image analysis: spatial concepts for knowledge-driven remote sensing applications* (pp. 785-801). Berlin, Germany: Springer.

Schueler, T. (1994). The importance of imperviousness. *Watershed Protection Techniques*, *1*(3), 100-111.

Shiravi, S., Zhong, M., & Beykaei, S. A. (2012). Accuracy assessment of building extraction using lidar data for urban planning/transportation application. Proceedings from: *2012 Conference of the Transportation Association of Canada.* Fredericton, New Brunswick.

Spatari, S., Zu, Y, & Montalto, F. A. (2011). Life cycle implications of urban green infrastructure. *Environmental Pollution*, *159*, 2174-2179.

Sterr, N., & Yui Lau, M. (2012). Impervious surfaces in WRIA 9-Green-Duwamish watershed. Report created for King County Department of Natural Resources and Parks Water and Land Resources Division as part of the course

requirements for Geography 469, Spring 2012.

Thomas, N., Hendrix, C., & Congalton, R. G. (2003). A comparison of urban mapping methods using high-resolution digital imagery. *Photogrammetric Engineering & Remote Sensing, 69*(9), 963-972.

Tuominen, S., & Pekkarinen, A. (2005). Performance of different spectral and textural aerial photograph features in multi-source forest inventory. *Remote Sensing of the Environment*, *94*, 256-268.

USEPA. (December, 2007). Reducing stormwater costs through low impact development (LID) strategies and practices. EPA 841-F-07-006. Retrieved from http://water.epa.gov/polwaste/green/costs07_index.cfm

Walsh, T. C., Pomeroy, C. A., & Burian, S. J. (2014). Hydrologic modeling analysis of a passive, residential rainwater harvesting program in an urbanized, semi-arid watershed. *Journal of Hydrology*, *508*, 240-253.

Wechsler, S. P. (2007). Uncertainties associated with digital elevation models for hydrologic applications: A review. *Hydrology and Earth System Sciences, 11*, 1481-1500.

Whiteside, T. G., Maier, S. W., & Boggs, G. S. (2014). Area-based and location-based validation of classified image objects. *International Journal of Applied Earth Observation and Geoinformation, 28*, 117-130.

Wu, C., & Yuan, F. (2011). Remote sensing of high resolution urban impervious surfaces. In X. Yang (Ed.), *Urban remote sensing: Monitoring, synthesis and modeling in the urban environment* (1st ed., pp. 239-252). Oxford, UK: John Wiley & Sons.

Yang, B., & Li, S. (2013). Green infrastructure design for stormwater runoff and water quality: Empirical evidence from large watershed-scale community developments. *Water*, *5*, 2038-2057.

Yang, H., Ma, B., Du, Q., & Yang, C. (2010a). Improving urban land use and land cover classification from high-spatial-resolution hyperspectral imagery using contextual information. *Journal of Applied Remote Sensing 4*, 041890, 1-13.

Yang, Y., Zhou, Q., Gong, J., & YingYing, W. (2010b). Gradient analysis of landscape spatial and temporal pattern changes in Beijing metropolitan area. *Science China, Technological Sciences*, *53*(1), 91-98.

Zhan, Q., Molenaar, M., Tempfli, K., & Shi, W. (2005). Quality assessment for geo-spatial objects derived from remotely sensed data. *International Journal of Remote Sensing, 26*, 2953-2974.

Zhou, W., & Troy, A. (2008). An object-oriented approach for analyzing and characterizing urban landscape at the parcel level. *International Journal of Remote Sensing*, *32*, 3119-3135.

Zhu, G., & Blumberg, D. G. (2002). Classification using ASTER data and SVM algorithms; the case study of Beer Sheva, Israel. *Remote Sensing of Environment*, *80*(2), 233-240.

Zhu, L., Shortridge, A. M., & Lusch, D. (2012). Conflating lidar data and multispectral imagery for efficient building detection. *Journal of Applied Remote Sensing*, *6*, 1-17.

CHAPTER 4

GREEN INFRASTRUCTURE PRIORITIZATION PROTOCOL

The proposed journal article, entitled Prioritization of Site-Suitable Green Infrastructure Practices, will be submitted to the *Journal of Urban Planning and Development* Summer 2014 with my co-author, Dr. Christine Pomeroy. This journal provides the best venue for the research goals of Chapter 4, targeting civil engineering aspects of urban planning, such as the coordination of planning and programming of public works and utilities, and the development and redevelopment of urban areas (ASCE 2014). While this journal currently only has an impact factor of 0.95, it is just over a decade old and increasing with time (e.g., 5-year impact factor of 1.17).

4.1 Abstract

This paper presents the development and application of a watershed-scale rainwater harvesting (RWH) prioritization study, based on cost and hydrologic reductions (i.e., cost-effectiveness). Uncertainty analysis with Monte Carlo Methods (MCM) was used to evaluate the impact of subcatchment percent imperviousness on watershed hydrologic response and subcatchment-scale LID

effectiveness. Regional precipitation datasets for the Mountain West, Southwest, Southeast, East Coast, Midwest, West Coast, and Pacific Northwest were used to drive continuous hourly rainfall-runoff simulations (1960-1991). This provided an analysis of regional climatic impacts on hydrologic response and RWH effectiveness.

The authors present a Prioritization Protocol, with related toolsets, that design, alter the hydrologic model input file, and target household RWH as a function of user-defined constraints and thresholds. Geospatial distribution and analysis of long-term hydrologic simulations and life-cycle costs (including capital, operation and maintenance, and replacement) for the Chollas Creek watershed, San Diego, California, USA provided cost-effectiveness estimates (liters of stormwater reduction per equivalent annual cost, L/$). Geospatial prioritization resulted in priority zones for initial targeting, which can be refined with finer-scale (e.g., household) hydrologic and suitability data. Prioritized results highlight the linear tradeoff between user-defined cost and watershed reductions (e.g., $1.0MIL for a 6.3% reduction). Uncertainty analysis indicated negligible impact from variations in subcatchment percent imperviousness on both watershed outlet volume and peak flow rate. Extended to RWH effectiveness, uncertainty analysis found RWH capable of buffering the impact of increasing subcatchment imperviousness on runoff (i.e., increasing runoff with increasing impervious area) by approximately 18%. For the Chollas Creek watershed, the cost-effectiveness methods were applicable for subcatchments with impervious areas less than 40 hectares. Application of the protocols found

that targeting watershed-scale reductions with RWH does not benefit from spatial prioritization for Chollas Creek. Analysis of regional climatic data indicated greater watershed hydrologic reductions for the Mountain West and West Coast regions. Overall reductions were found to be inversely proportional to individual event depths for all climates.

4.2 Introduction

Just as watershed-scale LID suitability analyses must account for site-specific conditions (i.e., physical constraints), the prioritization of LID must be capable of targeting user-defined objectives, including stormwater management benefits and costs. This paper addresses the ability to successfully prioritize the allocation of suitably-located LID practices, using rainwater harvesting (RWH) as the focus. The implementation is a function of a larger stormwater management framework using RWH to mitigate stormwater runoff quantity. An uncertainty analysis assessing the impact of variations in subcatchment percent imperviousness on watershed response and LID performance was also completed. This research applies a customized Prioritization Protocol, building on previous work by Walsh et al. (2014; in review), and investigates the impacts of uncertainty in subcatchment percent imperviousness on both overall watershed and LID reduction responses.

4.3 Background

4.3.1 Hydrologic Impacts of Urbanization

Urbanized areas are complex, heterogeneous, and dynamic landscapes upon which planning, design and management must adapt to provide sustainable solutions to resource management (Foresman et al., 1997; Cadenasso et al., 2007). Urbanization has resulted in the intensification of negative hydrologic impacts on stormwater runoff quantity, rates, and quality (Alley & Veenhuis, 1983; Schueler, 1994; Lee & Heaney, 2003; EPA, 2007b). Stormwater runoff is any source of water that is intercepted by a catchment and not lost to abstractions as it travels through a watershed. The relationship between rainfall and runoff is complex and dependent upon antecedent soil moisture conditions, evaporation, infiltration, land cover characteristics and the distribution or duration of the precipitation (Isik et al., 2013).

As changes in urban land use, land cover, and climate continue, increased stormwater runoff volumes, rates, and pollution concentrations can be expected, with synergistic amplification of impacts when alterations occur in tandem (Kirshen et al., 2008; Tong et al., 2012). In particular, Denault et al. (2007) indicate that efforts to mitigate small future increases in imperviousness (e.g., 5-10%) are likely to be overwhelmed by climate change related increases in runoff. As such, adaptive measures must be expanded to include multiple constraining parameters.

4.3.2 Urban Watershed Stormwater Management Plans

Traditional urban watershed drainage design, which relied on centralized stormwater controls, has been found to be increasingly inadequate (NRC, 2008). Centralized controls have resulted in greater durations of outflow rates and a lack of peak flow control for more frequent, smaller events that disturb downstream environments (Shaver et al., 2007; NRC, 2008). The paradigm shift that followed in response included the implementation of Best Management Practices (BMPs), which range from policy- to physically-based control measures. A BMP subgroup that follows this new paradigm includes low impact development (LID) practices.

LID practices are source controls designed to recreate the pre-development hydrologic conditions of the site. Specifically, the implementation of storage-based LID practices and pervious area routing of runoff (e.g., downspout disconnection) has been linked to improved stormwater runoff reductions (Brander et al., 2004; de Graaf & der Brugge, 2010; Spatari et al., 2011; Jia et al., 2012). One such application, rainwater harvesting (RWH), is unique in its ability to serve both runoff reduction and demand supplementation objectives. These targets, however, have been shown to exhibit tradeoffs with one another (Sample et al., 2012).

The benefits of RWH over other LID practices include the feasibility of implementation as part of larger, integrated management frameworks, low maintenance requirements, greater independence from soil infiltration rate constraints, and greater potential for retrofitting of existing impervious, or developed, areas (Prince George's County, 1999). With respect to the

homeowner, implementation of RWH can reduce water bills (Woods-Ballard et al., 2007; Foraste & Hirschmann, 2010) and supplement potable water demands, such as toilet flushing and outdoor irrigation (Mitchell et al., 2005a; 2005b; Rosemarin, 2005; Fletcher et al., 2007; Mitchell et al., 2007; Foraste & Hirschman, 2010). Potential limitations of RWH include storage capacity, reliance upon homeowner operation and maintenance, lack of direct water quality treatment, increased vector (e.g., mosquito) potential, restrictive local permitting and regulations, and additional infrastructure requirements (e.g., pumps, valves) to enable more complex end uses (Prince George's County, 1999; Roy et al., 2008; USEPA, 2013). Regarding sustainable watershed-scale management plans, Roy et al. (2008) highlighted the following seven impediments:

1. Uncertainties in LID performance and cost,
2. Insufficient engineering standards and guidelines,
3. Fragmentation of responsibilities,
4. Lack of institutional capacity,
5. Lack of legislative mandates for sustainable management,
6. Lack of funding and effective market incentives, and
7. Resistance to change on the part of the public and government.

Future interdisciplinary research that addresses these impediments must, therefore, consider the processes, interactions, and governing policies of the underlying heterogeneous, complex, and dynamic landscape (Brown et al., 2005). Distributing LID throughout a watershed has the potential to reconnect the hydrologic cycle, supplement existing system storage, and provide additional

treatment (Huber et al., 2006; Guo, 2008). However, prior to implementation, urban water management practices (e.g., LID) must be assessed for their collective ability to respond to future uncertainties at the scale of analysis, such as the watershed outlet (Benedict & McMahon, 2002; Maher & Lustig, 2003; USEPA, 2007a; Guo, 2008; Shuster et al., 2008; Endreny & Collins, 2009; NRC, 2009; USEPA, 2011b). Research by Gilroy & McCuen (2009) reinforced the importance of microscale (e.g., parcel) location and volumetric capacity when maximizing overall benefits. Often, location is overlooked with respect to stormwater management policies, which necessitates improvements in LID design procedures and cost benefit analysis to scale up and expand the foci of stormwater control systems (Schneider & McCuen, 2006; USEPA, 2007a; Pitt & Clark 2008; Roy et al., 2008; Gilroy & McCuen, 2009; Ahiablame et al., 2012). Prioritization is a method that incorporates site search components to distribute resources based on suitably-informed frameworks, hydrologic results, and cost estimations.

4.3.3 Prioritization of LID Implementation and Design Considerations

Proper LID implementation and design requires in-depth understanding and expertise on the part of the designer (Dietz, 2007; Han et al., 2008; Pitt & Clark, 2008; Spatari et al., 2011; Vermonden et al., 2011). Deviation from a case-by-case LID application requires greater time and resources as the scale increases (NRC, 2008). For instance, comprehensive plans, such as the US EPA's Smart Growth program, assess multidimensional parameters, including

ecological, economic, social, and planning, that aim to maximize benefits without creating redundancies (Hurd et al., 1999; Baycan-Levent et al., 2009; USEPA, 2013). With respect to economics, both policy- and physically-based options must be assessed to ensure cost-effectiveness is maximized for large areas. For instance, no-cost municipal zoning and subdivision regulations can improve cost-effectiveness by requiring neither size nor albedo modifications to the existing built infrastructure (Stone & Norman, 2006). Similarly, variations in climatic conditions should be investigated for their impact on costs and benefits of LID frameworks. This is especially pertinent for municipalities with limited budgets. As such, the ability to capture the spatial and temporal dynamics of the underlying landscape can improve the prioritization of suitable networks for the target watershed (Akbari et al., 2003; Akbari, 2008).

As economic thresholds are often the limiting factor in hydrologic mitigation plans, the ability to target resources to achieve the best result is preferred. Targeting is accomplished with increasing accuracy through remote sensing analysis (i.e., classification) of landscape data, hydrologic analysis, geospatial analysis, and geostatistical analysis of influencing datasets. For instance, conditional filtering based on user-defined values (Malczewski, 2004), spatial clustering (Jacquez, 2008), and hotspot analysis (Anderson, 2009) were shown to improve the identification of locations, magnitudes, and shapes of statistically-significant clusters. Clusters, for instance, can represent the simulated benefits (e.g., hydrologic reductions) and costs related to RWH distributed throughout the watershed. Despite the increasing prevalence of

considering multiple criteria for suitable spatial placement of LID with GIS resources and tools (e.g., multicriteria decision analysis, or MCDA), there remains a significant investment of time, resources, background expertise and technical knowledge on the part of designers and planners (Malczewski, 2004; Pitt & Clark, 2008; Burian & Pomeroy, 2010). When extensive, empirical data are available for expanded scales of LID analysis, as in research by Yang and Li (2013), the depth and complexity required to prioritize suitability results remains a limiting factor (Thomas et al., 2003; Jensen et al., 2010).

GIS-based postprocessing (i.e., site search analysis) can improve the ability to weigh and filter multiple datasets when assessing locations' ability to meet user-defined constraints (Malczewski, 2004). Specific search methods include MCDA and spatial clustering analysis, which weigh complex factors and present recommendations based upon input criteria (Malczewski, 2004). Jacquez (2008) used spatial clustering to recognize patterns with visualization, spatial statistics, and geostatistics such that locations, magnitudes, and shapes of statistically significant pattern descriptors were identified. Hotspot identification has also been applied for targeting resources and minimizing risk within a larger system (Anderson, 2009).

Site search analysis identifies the most critical problem areas to be targeted with available resources first. Site search examples are common in greenway and conservation planning and management studies, such as the Maryland Green Infrastructure Assessment (Weber, 2006) and the *New York Green Infrastructure Planning for Improved Stormwater Management in Central*

New York (Central New York Regional Planning & Review Board, 2012). Similarly, spatial decision support systems (SDSS), such as the Watershed Management Priority Indices (WMPI) framework by Zhang et al. (2011), prioritize based on weighting of multiple parameters based on the relative importance to the index considered. While these studies provide overall recommendations, final data resolution remains a function of user choice (i.e., weight). Improvement upon these methods, by allowing users to define constraints and thresholds rather than weights, can contribute to and improve future stormwater permitting, management needs, and modeling paradigms (NRC, 2008). For urban stormwater management research (e.g., flood risk mitigation), the targeting of long-term hydrologic benefits and economic valuations of distributed LID practices is a growing field of research (Kousky et al., 2013). This approach of targeting site-specific stormwater management with decentralized source controls in pursuit of wider goals (e.g., watershed health) has been termed 'flow-regime management' by Burns et al. (2012) and remains in its infancy.

This study synthesizes a Prioritization Protocol that builds on previous suitability analysis methods, toolsets, and results (Walsh et al., in review). The objective of Walsh et al. (in review) was to improve the ability of users to assess detailed watershed-scale parameter datasets to site LID as a function of local constraints. The methods listed and applied in this paper provide users with a framework for designing, implementing, and planning a basin-wide LID stormwater management plan based upon cost and hydrologic thresholds. Specifically, the application of RWH is targeted for analysis within the Chollas

Creek watershed, San Diego, CA, USA. The authors then address the uncertainty associated with the independent variable, subcatchment percent imperviousness, and how this impacts hydrologic runoff response(s) and LID benefit(s). The objective of this research is to improve users' abilities to prioritize the implementation of suitably-designed LID practices with geospatial analysis techniques such that targeting of resources (e.g., cost) yields the greatest benefits (e.g., hydrologic reductions). Application of uncertainty analysis allows for further basin-specific analysis relating the variation in subcatchment percent imperviousness and watershed outflow response.

4.4 Materials and Methods

This section provides an overview of the case study location, the materials and methods required for development and testing of the prioritization protocol and its toolsets, assessment of seven climatic regions' impact on watershed hydrologic response, and an uncertainty analysis for the impact(s) of subcatchment percent imperviousness on overall watershed hydrologic response.

4.4.1 Case Study Location

The area studied was located in the Chollas Creek watershed, San Diego, CA, USA (Fig. 4.1). This 3,110-hectare basin provided the basis for development, implementation, and analysis of a passive watershed RWH plan using traditional design methods (Walsh et al., 2014) and a proposed suitability protocol employing remote sensing and geospatial analysis to improve the targeting of

RWH at the watershed scale (Walsh et al., in review).

The watershed consists of 53% impervious cover, 44% pervious cover (e.g., grass, tree canopy), and 3% water surface. Walsh et al. (in review) quantified an average suitable rooftop area of 227 m^2 (102 – 517 m^2) per subcatchment. Total rooftop area per subcatchment averaged 4.0 hectares (0.3 – 22.5 hectares). Based on the Suitability Protocol, the total number of households was 13,566 (Walsh et al., in review). In total, approximately 310 hectares (10%) of the overall watershed were attributed to rooftops.

4.4.2 LID Prioritization Protocol

The goal of the LID Prioritization Protocol was to achieve the greatest overall stormwater management benefits, as defined by user thresholds, for the watershed as a function of the simulated hydrologic and economic results. Geospatial analysis of datasets provided visualization and analysis for the ultimate prioritization of individual and collective placements of RWH in the Chollas Creek watershed. Fig. 4.2 provides a workflow for the steps associated with the Prioritization Protocol.

4.4.2.1 Hydrologic Model Development and Simulation

To assess the impact of LID on watershed-scale hydrologic response, the validated case study watershed hydrologic model, created through work by Walsh et al. (2014), was employed. Details of the datasets and work required to complete this portion are presented in the hydrologic analysis completed by Walsh et al. (2014). The hydrologic model representing base conditions (*BASE*),

prior to LID implementation, was used to simulate the long-term rainfall-runoff response with continuous, hourly precipitation data (1948-2012). Time series results were collected at the watershed outlet, with long-term results collected for each subcatchment. This model served as the foundation upon which suitability studies for variations in the implementation and design of a RWH management plan were based. Suitability scenarios were driven by the results (*.dbf* file) from the Suitability Protocol and LID Site Suitability (*LIDSS*) toolset, created and tested by Walsh et al. (in review). This output *.dbf* file contained the household-specific values (e.g., rooftop area) and identifiers required to size and distribute individual RWH units throughout the watershed.

4.4.2.2 Establishment of Thresholds

To introduce benchmarks upon which to assess the protocol, hydrologic and cost thresholds were established. For this analysis, economic thresholds were instituted at the overall watershed scale and based on the maximum cost for RWH implementation. Economic prioritization of the subcatchments was established by the minimization of cost relative to the hydrologic benefits. The range of hydrologic thresholds was established before application of the Prioritization Protocol and assumed the user would account for and not exceed the maximum possible benefit. The maximum was established by implementing all suitable households with RWH (*LID227*). Hydrologic prioritization of subcatchments was assigned based on maximizing the individual volumetric reduction, or benefit, per equivalent annual cost (EAC).

4.4.2.3 LID Sizing, Modeling, and Simulation

LID sizing and modeling were completed with results from previous suitability research (Walsh et al., in review) and the creation of the Rainwater Harvesting Analyzer, or *RWHA* (Fig. 4.3). The *RWHA* guided users, step-by-step, to create an amended SWMM *.inp* file, referred to as *LID227*, that accounted for RWH. The graphical user interface (GUI) for the *RWHA* allows users to define specific rain barrel characteristics.

The *RWHA* facilitates the analysis and design of a watershed stormwater management network consisting of suitably located RWH units. To begin, users open the Microsoft Excel (*.xlsm*) file, which brings up the GUI. The GUI contains a list of directions for proper application of RWHA, including:

1. Click Here to Upload Your ARCGIS.DBF File. This button allows the user to upload the ArcGIS *.dbf* file, which identifies the unique parcels and subcatchments deemed suitable for RWH implementation. Specifically, this file contains drainage areas and parcel areas. *RWHA* uses these areas (m^2), to find the total required volume to be captured by the units.
2. Click Here to Upload Your Existing SWMM.inp File. This button allows the user to upload the existing SWMM *.inp* file, which contains the parameters for the validated hydrologic model representing *BASE* conditions. Model parameters representing RWH will be added to this file with RWHA.
3. Perform Volume Captured/# Barrels Employed Calcs. This button

creates a new worksheet within the tool that combines the parameters from the previously uploaded datasets (steps 1 and 2) and performs the following calculations.

a. Summation of the total drainage area per subcatchment. This value represents the total area that will be managed, or directed, by the LID. The pivotal value is the percent of impervious area managed by the LID, which is obtained by dividing this summed value by the subcatchment impervious area.
b. With the user-defined WQCV Depth (in), the total volume of runoff is calculated for each individual drainage area. This represents the total volume that must be managed, per household, by the LID. The total volume is then divided by the user-specified Size (gal), which results in a rounded-up value for the total number of units required to completely capture the targeted event. Users are provided with nominal sizes to choose from, which are linked to nominal parameters required by SWMM (Table 4.1).
c. The total number of rounded up units, along with Rain Barrel Characteristics, are then collated to the subcatchment scale.

4. Enter your WQCV Depth (in). This box allows users to type in a numeric value for the depth of analysis used to determine the total number of RWH units per household (step 3b).
    a. The water quality control volume (WQCV) is a function of the retention fraction of annual runoff to be retained on site, varying

as a function of climatic and catchment conditions (Chin 2012). For numerous states, this capture represents 80% to 95% of a site's runoff; however, the targeted sizing parameter can also be established as a set percentage, or percentile, of annual precipitation events (Clar et al., 2004). For instance, the 85th percentile correlates to the depth for which 85% of cumulative annual events will be exceeded.

5. The remaining fields, following the Rain Barrel Characteristics, are required to model and simulate the RWH units within SWMM. They include a unique identifier, the volumetric capacity of the units (step 3b), the drain coefficient for the individual units, the drain exponent, the drain offset height, and the drain delay time. These values are user-dependent, and caution should be exercised when choosing the best values for each scenario.
6. Construct SWMM Input Modifier, can then be selected, which automatically creates a new, modified SWMM *.inp* file for the RWH scenario chosen by the user (*LID*).

For this study, the 227-liter RWH barrel was chosen for analysis. The design WQCV depth for the study region was 16.5 mm, which is equivalent to the 85th Percentile event. A drain duration of 24 hours was established with a drain coefficient value of 0.5. The drain exponent was set to 0.5 (i.e., orifice), the drain offset height was set to 0, and a 24-hour drain delay was entered. With these rain barrel characteristics and suitability results, the *BASE* SWMM model was

amended (*LID227*) with the *RWHA*. *LID227 .inp* was then used to perform hydrologic simulations with the long-term precipitation data for comparison with the *BASE* scenario. This provided a range of hydrologic responses relative to variations in user-defined constraints. The use of batch processing facilitated the collation of hydrologic simulation results, which targeted both the overall watershed (long-term, annual, daily, and hourly) and the subcatchment (long-term) scales. Results for the hydrologic simulations were saved as *.csv* files at the subcatchment scale of analysis for relation to the geospatial framework.

4.4.2.4 Cost Estimation and Analysis

Linked with the *RWHA* is the ability for users to estimate the costs for the individual RWH units designed and implemented throughout the watershed. Cost estimation targeted both the parcel-specific units and the cumulative number of units at the subcatchment scale. Cost analysis was informed by the WERF BMP and LID Whole Life Cost Tools, Cistern toolset (Houdeshel et al., 2011) and implemented a low operation and maintenance (O&M) rate. This assumed homeowners would cover the majority of the annual costs for cleaning, emptying, and clearing drain lines for the units. A maximum annual O&M cost of $10 per unit was instituted, with full replacement of all units at 50 years. Replacement costs were accounted for as a net present value (NPV) per subcatchment, with a 3.5% interest rate (*i*) over 50 years. With capital costs of purchasing, the NPV for replacement at 50 years, and annual O&M costs, the EAC (Eq. 1) was calculated for each subcatchment for the entire 62-year study.

$$EAC = P\left[i(1+i)^{N} / (1+i)^{N-1}\right] \quad \text{.....(1)}$$

The total annual costs per year were represented by P while the total number of interest periods (N) was set 62. The EAC provided a comparison of results at the subcatchment scale for prioritized scenarios, with extension to annual hydrologic reductions (i.e., cost-effectiveness). The goal of this was to analyze each prioritized scenario as a function of the probability of annualized cost and hydrologic reduction. An interest rate, *i*, of 3.5% was applied. Results from the cost estimation were saved as *.csv* files at the subcatchment scale of analysis for relation to the geospatial framework.

4.4.2.5 Geospatial Distribution and Analysis of Results

With the results from the hydrologic and economic assessments, a geospatial framework was created for each subcatchment within the watershed. Geospatial analysis was accomplished by, first, joining the hydrologic and cost results and, then, applying a toolset that interpolated and iterated the classification of surfaces representing the input datasets. This toolset assessed the priority of locations based on the cost-effectiveness of each location within the greater watershed.

4.4.2.5.1 Surface Interpolation and Analysis

A surface, or grid, represents a functional surface that contains a single Z value for any (X,Y) location. Functional surfaces are different from three-dimensional surfaces in that they can also represent mathematical expressions

and statistical surfaces. Interpolation resulting in grids provides cells of equal size, contained in rows and columns, associated with attribute values that have been predicted between sampled data points. Interpolation is based on spatial autocorrelation, which determines the degree of dependence between objects both near and far.

The development of the prioritization toolset, *PriorLID*, allowed users to select the datasets to be interpolated and processed for any number of iterations to yield *.dbf* files indicating the total cost, total volumetric reduction, and average percent reductions for peak rates and outflow volumes relative to similarly grouped classes. *PriorLID* began with surface interpolation, using the Inverse Distance Weighted (IDW) method. Targeted datasets for interpolation included the long-term and annual volumetric reductions (as a fraction), long-term and annual peak rate reductions (as a fraction), and total costs. The IDW Method was chosen due to the density of point spacing with parcels, thereby capturing the local surface variations. With these surfaces, the cost-effectiveness raster was created with the math tool, Divide, and applying the volumetric reduction (denominator) and cost (numerator) raster datasets. This resulted in a cost per volume reduced by RWH ($/liter) surface.

Unsupervised classification, with the ISODATA classification algorithm, was then applied to the processed cost-effectiveness raster surface. The model builder iteration tool, For, enabled multiple class choices to be assessed. This choice ranged from one to a user-defined maximum and provided various grouping scenarios of similar cost-effectiveness values throughout the

watershed. Values driving classification were a function of the interpolated cost-effectiveness surface provided by dividing cost by the targeted hydrologic benefit.

Results from the classification were established on a per class basis, with the following datasets extracted: mean volumetric reduction, mean peak flow rate dampening, total runoff volume reduction, and total cost of implementation. The summary statistics function was used to export individual tables containing these class-specific datasets after each successful iteration. The toolset then exported the results as database (*.dbf*) files for collation and further analysis with Microsoft Excel. *A posteriori* knowledge was required on the part of the analyst in determination of the best classification options. This was facilitated by ranking the results relative to the classes. Since hydrologic simulations were limited to the subcatchment scale, parcel level cost-effectiveness was not possible for this study. Thus, the subcatchment served as the finest scale for cost-effectiveness prioritization. Parcel-scale costs were visualized and assessed for priority purely as a function of costs.

Users were then able to upload and assess the iterated classification results and choose the best options, via ranking of exported statistics, for targeting RWH. Once the best options were determined by the user, the *LID227 .inp* model could be amended to represent the targeted scenarios. This model was renamed *LID227p* to represent the analysis of the prioritized subcatchments based on the cost threshold. Hydrologic simulations for *LID227p* were then carried out with the long-term precipitation data. Results were collated for analysis with respect to the hydrologic threshold. This provided users with

greater insight to the potential benefits based on targeted prioritization.

4.4.3 Climatic Region Analysis

Building on previous research by Steffen et al. (2013), the long-term precipitation datasets of seven climatic regions were used to drive the Chollas Creek hydrologic model. Regions included the Mountain West (Denver, CO or *DEN*), Southwest (Phoenix, AZ or *PHX*), Southeast (Atlanta, GA or *ATL*), East Coast (Baltimore, MD or *BAL*), Midwest (Columbus, Ohio or *COL*), West Coast (Los Angeles, CA or *LA*) for replication, and Pacific Northwest (Portland, WA or *POR*). Long-term simulations (1960-1991) targeted the impact of precipitation pattern variations on watershed-scale hydrologic reductions (e.g., outflow volumes and peak flow rates) via the suitably implemented RWH scenarios. The number of units remained constant for all model simulation permutations.

The 85th percentile event depths for each region for the time period of analysis were estimated to be 25.4-mm (*ATL*), 22.1-mm (*BAL*), 14.7-mm (*COL*), 8.9-mm (*DEN*), 20.6-mm (*LA*), 21.7-mm (*PHX*), 12.4-mm (*POR*), and 13.7-mm (*SD*). Average annual precipitation depths for each region were 1,286-mm (*ATL*), 1,040-mm (*BAL*), 961-mm (*COL*), 391-mm (*DEN*), 304-mm (*LA*), 1,052-mm (*PHX*), 922-mm (*POR*), and 249-mm (*SD*).

4.4.4 Uncertainty Estimation and Analysis

As uncertainty is present in both parameters and model processes, it must be assessed to qualify recommendations. This was completed by, first, quantifying the basic statistics for the independent and dependent datasets. This

included the input parameters, subcatchment percent imperviousness and precipitation, and the results, watershed outflow volumes and peak rates. Frequency analysis was then applied to results. Finally, Monte Carlo Methods (MCM) of uncertainty estimation were used to assess the impact of variation in the subcatchment percent imperviousness values on the overall watershed hydrologic response (e.g., volume, peak flow rate). Fig. 4.4 provides an overview of the steps applied to perform uncertainty estimation and analysis for the research components.

4.4.4.1 Statistical Analysis of Dependent and Independent Data

In assessing sample datasets such as runoff volumes, flow rates (e.g., flood and low flows), and precipitation, statistical frequency analysis is commonly applied in hydrologic sciences. The goal of frequency analysis is to make predictions of either probabilities or magnitudes for random variables from a population (McCuen, 2005). For frequency analysis, the following steps were required to derive the frequency curve to represent the population (McCuen, 2005),

1. Hypothesize the underlying density function
2. Obtain a sample and compute the sample moments
3. Equate the sample moments and parameters of the proposed density function
4. Construct a frequency curve that represents the underlying population

The first step in this effort was to hypothesize the underlying density function. A log-transformed fit was hypothesized. Next, the computation of the

sample characteristics was completed, such that population characteristics could be estimated. This employed the method of moments, yielding quantification of the mean, standard deviation, and skew values for each sample dataset. From the long-term simulated results (i.e., dependent data), the annual peak outflow rate (CMS) and annual outflow volume (ML) were assessed. Independent data analyzed included the annual precipitation depth (mm) and subcatchment percent of imperviousness parameters. Since a logarithmic function was hypothesized as the underlying density for hydrologic datasets, the samples were transformed, creating new random variables. The method of moments was reapplied for transformed datasets.

To ensure the plots provided acceptable representation of the data, the fit was assessed with plotting positions. Plotting positions determine how well measured data agrees with the fitted curve of the assumed population. To assess this, the Cunnane (1978) method was applied (Eq. 2).

$$P_{Exceedence} = (i - 0.4)/(n + 0.2) \quad \text{.....(2)}$$

Samples were ranked in descending order, with the highest value receiving a rank of one. Eq. (2) incorporates the rank (*i*) and total sample dataset (*n*) to estimate the probability of exceedance. Exceedance probability is defined as the probability a given random variable will be equaled or exceeded in one time period. The data were then plotted, with the exceedance probability on the abscissa (or horizontal axis) and the ranked and ordered sample values on the ordinate (or vertical axis). These plots were assessed for which probability

distribution best fit the data.

Population fit was assessed for each logarithmic-based distribution with the Log-Pearson Type III (LP3) method. The LP3 distribution, which is recommended in Bulletin 17B (IACWD 1982), provides a good fit to measured annual peak flow rate data. The LP3 requires a logarithmic transformation of the sample data, with a standardized variate, *K*, which is a function of the dataset skew and selected values of exceedance probability. In plotting the population line of fit, LP3 calculates the population values with the sample set's average, μ, and one standard deviation, σ, from the mean multiplied by the standardized variate, *K* (Eq. 3).

$$Y = \mu + (K + \sigma) \quad \text{.....} \quad (3)$$

When extracting discharge values from these population lines, the antilogarithm of the transformed random variable, Y, must be applied. These data were used to construct histograms, probability mass functions (PMFs), cumulative distribution functions (CDFs), and probability density functions (PDFs). Histograms indicate the number of samples contained within a sample interval. The sample interval sizes were based on recommendations by Panofsky and Brier.

With histograms, the PMFs were constructed, which described the distribution of the discrete random variables. The height of the individual bars is equal to the number of occurrences divided by the total number of samples and represents the probability of occurrence for a given class interval. In conjunction

with frequency analysis, these plots were qualitatively analyzed to determine the distribution fit of the datasets. Determination of the probabilities associated with uncertainty around the datasets allows for a measurement of the likelihood an event will occur.

4.4.4.2 MCM Uncertainty Estimation

Since uncertainty is inherent in both modeling processes and datasets, its assessment becomes pivotal in qualifying the associated results and recommendations. One such method of uncertainty estimation is the Monte Carlo Method, or MCM. MCM simulations account for risk in quantitative analysis and decision making by providing a range of possible outcomes, or distributions, and the probabilities that will occur for any choice of action. These probability distributions provide a more realistic way of describing uncertainty in variables of a risk analysis. MCM indicates the potential for what could happen and how likely it is to occur. As such, MCM simulations can provide probabilistic results, graphical results, sensitivity analysis, scenario analysis, and correlation of inputs.

For this study, MCM uncertainty analysis targeted the subcatchment percent of imperviousness, since this parameter was expected to influence the generation of runoff. First, the subcatchment percent imperviousness PDF was used to randomly sample values that were then implemented into random models (Fig. 4.5).

A total of 100 randomized models were created and used to simulate the hydrologic response for a total of 8 years (1999-2007). This temporal period was chosen due to its inclusion of both the driest and wettest years of precipitation on

record. Long-term, annual, and daily results were collected for each random scenario simulation and compared with those of the original *BASE* model. Targeted metrics for comparison included both the monthly peak outflow rate and monthly total outflow volume results. These were collated, ranked from greatest to least, and plotted versus the exceedance probability (e.g., inverse time step in months) for the period of analysis. The Cunnane Method (Eq. 2) was used for ascertaining plotting positions. Next, the results' 97.5^{th} and 2.5^{th} percentiles, bounding the average for the 100 simulations, were plotted to assess the subcatchment percent of imperviousness' impact on overall watershed response.

The randomized models were then used to assess the impact of subcatchment imperviousness on the simulated LID benefits. This was facilitated by applying the suitably extracted subcatchment area managed by the LID to the randomized subcatchment impervious percentage. It is important to note that the LID-managed area remained constant for each subcatchment, since housing stock was not assumed to change over time. By keeping the household area to be managed by RWH constant, the impact of variations in overall impervious area was assessed. For scenarios in which the LID area exceeded the subcatchment impervious area, a value of 100% was assumed. The results of this analysis were presented as the percent change in subcatchment imperviousness versus the percent change in subcatchment runoff coefficients. Runoff coefficients are a metric relating the watershed outflow to inflow. Thus, a value closer to the maximum of 1.0 indicates that all inflow is converted to outflow (i.e., little reduction). For the percent change in outflow, a value closer to

100% indicated maximum reduction of outflow.

4.4.5 Annualization of Benefits

Annualized risk (Eq. 4) is often applied in the analysis of flood event risk relative to the annual costs of damages (Tsakiris, 2010).

$$Risk_{annualized} = P_{exceedence} \times Damage \quad \text{.....(4)}$$

This methodology has been applied to target the best flood control for various recurrence interval events (Kalyanapu et al., 2014). Similar to the annualized risk, the annualized benefit (Eq. 5) was calculated with the watershed-scale reductions per EAC.

$$Benefit_{annualized} = P_{exceedence} \times Benefit \quad \text{.....(5)}$$

The extraction of the annualized benefit followed a similar methodology, in which the annual watershed cost-effectiveness values (*Benefit*) were ranked in decreasing order following the Cunnane Method and multiplied by the *Exceedance Probability*. This methodology improves the ability to assess the probabilistic cost-effectiveness of a watershed-scale management plan. This goes beyond simple payback periods and event-specific reductions, visualizing the underlying driving characteristics as probabilistic long-term trends.

4.5 Results and Discussion

This section presents the results of applying the Prioritization Protocol for watershed stormwater management with RWH in meeting hydrologic and economic thresholds. The hydrologic thresholds were a function of the percent reduction in the watershed outlet outflow volume (e.g., 2.5%, 5.0%, 10.0%, 15.0%, and maximum). The economic thresholds were a function of the overall EAC for the scenario implemented, with budgets of $0.25MIL, $0.5MIL, $1.0MIL, $2.0MIL, and a maximum budget. Prioritized locations, via the *PriorLID* toolset, are visualized and presented. Following this, the uncertainty analysis results are presented, with respect to the overall watershed and LID-specific impacts.

4.5.1 Prioritization Protocol

The Prioritization Protocol was capable of sizing, modeling, costing, and assessing the hydrologic impacts of various RWH scenarios. These scenarios, a function of the iterated classification groups, improved the ability of users to spatially target RWH practices, via economic thresholds, such that hydrologic thresholds could be obtained. The maximum suitable scenario (*LID227*) provided the greatest potential watershed reductions and costs for the study area. For cost-effectiveness, a total of four classes were identified, represented by HIGH, MID, LOW, and NULL, and used to assess the prioritization based on economic and hydrologic thresholds.

4.5.1.1 RWH Design and Implementation

The *RWHA* toolset was capable of processing the suitability dataset for the WQCV event depth (16.5 mm). The number of households targeted per subcatchment ranged from 11 to 868 (watershed total 13,566). Total subcatchment rooftop area ranged from 0.28 hectares to 22 hectares (watershed total 310 hectares), with a 227-m^2 watershed average. Based on a nominal RWH capacity of 227 liters and a 16.5 mm design event, subcatchment units ranged from 210 to 16,688 (watershed total of 232,015). This represented a total watershed volumetric storage capacity of 52.7 million liters (ML).

Application of *PriorLID* with the *LID227* scenario's subcatchment hydrologic and economic results yielded locations throughout the watershed with similar cost-effectiveness values. A total of 25 iterations were established, resulting in unique classes of increasing resolution of priority. A subset, including iterations 3, 5, 10, 15, and 25, are presented (Fig. 4.6). These results highlight the presence of priority zones, which increase in resolution with each successive iteration.

4.5.1.2 Economic Implications

Economic valuations were a function of the sizing parameters established with *RWHA*, including the precipitation design depth and the nominal unit size. For 227-liter units and a design depth of 16.5 mm, the subcatchment EAC values for all prioritized scenario were calculated (Table 4.2). The original *LID227* scenario established the maximum cost for the user-defined conditions.

4.5.1.3 Hydrologic Implications

The watershed conditions for the fully-implemented RWH scenario were assessed with the results from *LIDSS* and the *RWHA* toolsets. This included the design, location, and collation of individual parcel-specific RWH practices to the subcatchment scale. Long-term hydrologic simulations yielded linearly increasing trends between RWH capacity and subcatchment reductions in both outflow rates and volumes. Frequency analysis of peak annual outflow rate (Fig. 4.7) and reductions in annual outflow volumes (Fig. 4.8) indicate greater reductions have a higher probability of exceedance. Simulation of the 85th percentile precipitation event (16.5 mm) with *LID227* yielded a maximum watershed reduction of 22 and 27% for outflow volume and peak flow rate, respectively.

At the watershed scale, reductions followed a similar linearly increasing trend with RWH capacity. Compared with the *BASE* scenario, *LID227* yielded average annual reductions of 10% and 24% for outflow volumes and peak outflow rates, respectively. Watershed hydrologic reductions for all scenarios are provided in Table 4.3.

4.5.1.4 Cost-Effectiveness Implications

Normalization of the annual volumetric reduction to the total EAC provided an estimate of the spatial and temporal distribution of cost-effectiveness (L/$) for the study area. For maximum RWH implementation (*LID227*), average annual cost-effectiveness ranged from 1.0 L/$ to 6.3 L/$ (average 3.1 L/$). Results from the prioritization scenarios targeting subcatchments designated based on homogeneous cost-effectiveness (e.g., HIGH, MID, LOW, NULL, and HIGH-MID)

are presented in Table 4.4. User thresholds were based on addressing these results with respect to the total watershed reductions and costs. The minimum and maximum annual cost-effectiveness establish the expected bounds for the watershed. This means that full implementation of 227-liter barrels throughout the study watershed targeting the capture of the WQCV event produce a minimum annual average of 0.95 L/$.

Annual cost-effectiveness results were ranked and plotted against the probability of exceedance (Fig. 4.9). Analysis of prioritized scenarios found the highest cost-effectiveness with the HIGH scenario, while the least cost-effective was NULL. Increasing annual cost-effectiveness resulted from years with higher precipitation amounts.

4.5.1.5 Annualized Benefits for Priority Scenarios

Annualization of scenario benefits (i.e., watershed volumetric reductions) with the scenario-specific EAC (Fig. 4.10) indicated a return of maximum annualized benefits (0.52-0.59 L/$) between 1.28-1.33 years for all priority scenarios except the Null. The Null returned a maximum benefit (0.36 L/$) every 2 years. The greatest annualized benefit was with the High priority scenario.

The analysis of annualized benefits for priority scenarios improves the ability to compare distributed measures' impacts on watershed-scale systems. Annualizing the benefits provides insight to the return, or probability, of achieving maximum reductions within the watershed for each proposed priority scenario. For instance, with a 99% probability of exceedance (i.e., 1 year recurrence), RWH can be expected to provide watershed benefits between 0.17 – 0.35 L/$

(average of 0.31 L/$). Prioritization can improve cost-effectiveness, though scenario annualized benefit results remain similar (neglecting the Null scenario).

4.5.2 Climatic Region Implications

4.5.2.1 Hydrologic Implications for Climatic Regions

For the regional 85th percentile events, the range of reductions in watershed outflow volume and peak flow rate was 9%-12% and 11%-18%, respectively. For the entire range of events, average reductions are provided (Fig. 4.11 and Fig. 4.12). These plots indicate the range of regional event-specific reductions. Long-term averages were similar throughout regions despite variations in extreme event reductions. Cities with tighter ranges include *ATL*, *BAL*, *COL*, *PHX*, and *POR*, which were also cities with annual average precipitation exceeding 350-mm. Greater ranges of reduction extremes were experienced in *DEN*, *LA*, and *SD* (average annual precipitation less than 400-mm).

Analysis of the reduction potential for events (Fig. 4.13 and Fig. 4.14), binned by depth, indicated exponentially decreasing reductions for greater depths. Outliers are due to undersized sample populations (n<10) and represent the uncertainty of reduction potential for individual events greater than 88.9-mm. The addition of *SD* results with the trend for all climatic regions analyzed indicates that RWH can reliably provide watershed-scale reductions for similar precipitation depths. For instance, despite regional variations in event intensities and timing (e.g., event duration, interevent time), the simulated reductions are comparable for each region's long-term analysis. For all precipitation datasets

analyzed, event bin reductions ranged from 17%-28% and 14%-24% for average peak flow rate and outflow volumes, respectively.

Targeting the change in average annual event depth (mm/event) versus the *SD* dataset (Y-axis), annual watershed volumetric reductions (X-axis) were shown to increase with greater average depths (Fig. 4.15). Thus, regions with smaller individual events and greater small events produced less reduction potential with the Chollas Creek model. With increasing event depths, or greater rainfall, long-term reductions are expected to increase.

While these results are different from those for the individual event analysis by bins, they indicate the long-term temporal benefits of RWH resulting from both immediate reduction and prolonged storage. While RWH may not be capable of providing volumetric and peak flow rate reductions for individual extreme events, such as the infamous chubascos, or Mexican storms (Tubbs, 1972), they can address more frequent individual events (i.e., 85th percentile) for a variety of regional climates.

4.5.2.2 Annualized Benefits for Climatic Regions

For climatic regions, annualized benefits distinguish two groups (Fig. 4.16), i. *ATL*, *BAL*, *COL*, *PHX*, and *POR*, and ii. *DEN*, *LA*, and *SD*. These groups yield the highest and lowest long-term annualized benefits (L/$). This shows that maximized watershed cost-effectiveness may not be as viable an option in climates such as the Mountain West and West Coast, where the annual precipitation averages less than 400 mm. This is further enforced by the cost-effectiveness plot for individual years as a function of the total annual

precipitation (Fig. 4.17).

4.5.3 Uncertainty Estimation and Analysis

4.5.3.1 Subcatchment Percent Impervious

The impact of variations in the subcatchment percent imperviousness on the overall watershed hydrologic response was found to be negligible for both outflow rate (Fig. 4.18) and outflow volumes (Fig. 4.19). Analysis focused on both monthly peak rates (CMS) and monthly total outflow volumes (ML) for the uncertainty years of analysis (1999-2007). The exceedance plots indicated that extreme events cause greater variation in the relationship between the dependent and independent variables being assessed. The effect, however, is predictable in that a greater event will cause greater differences for the range of imperviousness values considered.

4.5.3.2 RWH Effectiveness

Extension of randomized uncertainty models to the implementation of RWH found that the subcatchment influence of imperviousness is reduced when RWH is implemented throughout the study area. This indicates that the impact of alterations to an urban impervious area can be dampened with the addition of decentralized storage units. Fig. 4.20 presents the subcatchment-scale impacts of variations in imperviousness' impact on outflow for *BASE* and *LID227*.

The slope for *LID227* (0.9782) was steeper than that of *BASE* (0.7968), implying that the *BASE* scenario yields greater outflow for smaller changes in imperviousness, relative to when RWH is implemented. This shows that RWH

has the potential to buffer the impacts of future changes in imperviousness. Simulated long-term results for all scenarios found approximately 18% dampening of imperviousness' impact on outflow reductions with maximum RWH. Subcatchment outflow for *LID227* begins to exceed original *BASE* conditions when imperviousness increases by approximately eighteen percent (Fig. 4.21). These results indicate that while the overall watershed reductions with RWH may be small, the retrofit-ability of RWH may provide a more cost-effective option for further mitigating the impacts of altered land cover.

Validation of the results was completed by randomly implementing RWH for a total monetary input of $1.53 MIL. Locations were chosen regardless of priority class. The long-term simulation yielded a 10% reduction at the watershed outlet (Fig. 4.22).

4.6 Conclusions

The development and application of the Prioritization Protocol, based on prior suitability research (Walsh et al., in review), was assessed with the goal of targeting distributed RWH practices as a function of cost-effectiveness while meeting user-defined hydrologic and economic thresholds. The impact of parameter uncertainty on watershed hydrologic response was addressed using MCM for a randomized population (n=100). These were based on the PDF representing validated subcatchment percent imperviousness values. Uncertainty was extended to RWH effectiveness, focused on subcatchment-scale impacts.

Spatial targeting of resources found that central locations of priority (i.e., cost-effectiveness) exist across resolutions. When users minimize the number of

classes used to drive classification (i.e., homogeneous grouping) of cost-effectiveness values, coarse locations of priority are identified. As the number of classes increases, the resolution of spatial priority is refined, though still contained within coarse zones. These results reinforce findings by Perez-Pedini et al. (2005) and Haith (2003), who recommended a systems-based approach to watershed quantity and quality management via targeting.

Hydrologic modeling of prioritized scenarios reinforced a strong linear relationship between EAC and reductions; however, for the case study location, the subcatchment impervious area impacted the accuracy of this trend. For the subcatchments studied, a maximum impervious area of 40 hectares was established as the upper limit for reliable cost-benefit estimations. Beyond 40 hectares, costs and reductions were variable and less predictable for the Chollas Creek watershed. At the watershed-scale, plotting the maximized LID scenario's annual cost-effectiveness ($/L) against the probability of exceedance established the potential bounds for the watershed-scale RWH framework. Maximum reductions and costs should be used as guidance for users when using *PriorLID* to assess and target classes of similar cost-effectiveness within the watershed. For the Chollas Creek watershed, a linear relationship between cost and reduction can be expected, regardless of spatial location of RWH (Fig. 4.23).

Fig. 4.23 enables users to forecast the watershed volumetric reductions as a function of a total EAC. The total cost estimations, based on the simulated hydrologic reductions, are presented in Table 4.5. This indicates the trade-off that exists at watershed-scale, despite the ability to target individual subcatchments

based on cost-effectiveness.

MCM uncertainty analysis found that changing the subcatchment imperviousness had negligible impacts on the watershed outflow volumes and rates. This was based on 100 models created by randomly sampling the subcatchment imperviousness PDF. These results indicate the reliability of model simulations at the watershed outlet with respect to variations in subcatchment imperviousness. Further, uncertainty analysis infers that, regardless of the spatial variation, the change in watershed outflow response will remain relatively constant. Extended to analysis of the impacts on RWH effectiveness, maintaining the same impervious area managed by LID (i.e., rooftop disconnection) resulted in a dampened subcatchment response. This linear relationship, between changes in imperviousness and reductions in outflow, reinforces the subcatchment-scale benefits of distributed volumetric storage despite smaller impacts on the overall watershed response. Together, uncertainty and prioritization results at the watershed-scale highlight that negligible impacts exist with respect to subcatchment targeting, for subcatchments with impervious areas less than 40 hectares. On the other hand, if subcatchment benefits are required, finer-scale prioritization with the proposed protocols can be used to distribute RWH based on cost-effectiveness.

The ease of implementation and O&M of RWH, coupled with the ability to dampen the negative stormwater impacts of future land cover and potential climatic changes highlight passive watershed-scale RWH as a low-cost option for long-term management. This is especially important for urban planning and

management as urban areas expand and densify. The inclusion of seven regions' long-term precipitation in this hydrologic analysis found reliable reductions for more frequent events within the Chollas Creek watershed model. For instance, peak flow rate and volumetric outflow reductions ranged from 25%-28% (26% average) and 22%-24% (23% average), respectively, for events less than 25.4-mm in depth (e.g., 91% of all events). Extreme events, such as the chubascos, were more prevalent in the Mountain West and West Coast regions and were negligibly reduced with the implementation of passive RWH.

Annualization of benefits for priority scenarios found similar probabilities of maximum benefits for all scenarios except the Null. This translated to a return period ranging from 1.28-1.33 years (Null return was 2.0 years). Annualization of benefits for climatic regions yielded a regional distinction, resulting in two separate groupings. The first, including the Mountain West and West Coast cities (*DEN*, *LA*, and *SD*), which provided the least cost-effectiveness and annualized benefit for the long-term simulation. The maximized annualized benefits ranged between 1.53-2.60 L/$, with return periods spanning 1.14-1.60 years. These regions' annual average rainfall was less than 400 mm. The other group consisted of the remaining regions: Southwest (PHX), Southeast (ATL), East Coast (BAL), Midwest (COL), and Pacific Northwest (POR). This group had maximum annualized benefits ranging from 7.70-8.76 L/$, with return periods of 1.03-1.14 years. Annualization of the climatic region benefits highlighted the applicability of RWH for other regions over those with less annual precipitation. Similarly, this implied that prioritization may have a greater influence in other

regions, beyond the Mountain West and West Coast.

Areas for potential future research include the expansion of the protocols to include additional realms related to sustainability. These areas include ecological, social, and urban structure and function. The incorporation of these datasets would improve the targeting of resources. Beyond additions to the protocols, expansion of the Monte Carlo Method uncertainty estimation would further improve the insight of the results. Parameters informing the distribution and cost-effectiveness of RWH include the data-driven probability distribution functions (PDFs) for subcatchment percent imperviousness, precipitation characteristics, evaporation rates, and rooftop area as a percent of the impervious area. Finally, expanding the protocols' applications to include other LID practices, such as bioretention, green rooftops, and permeable pavement, will contribute to a greater base of recommended practices targeting sustainable stormwater management. Eventually, the incorporation of a cost valuation of services will be incorporated, such that an informed payback period or economic incentive can be provided. This will include a tax structure similar to that passed by the State of Maryland (HB987) in 2012 (MDE, 2014), in which parcel area imperviousness elicits a taxed rate for stormwater management.

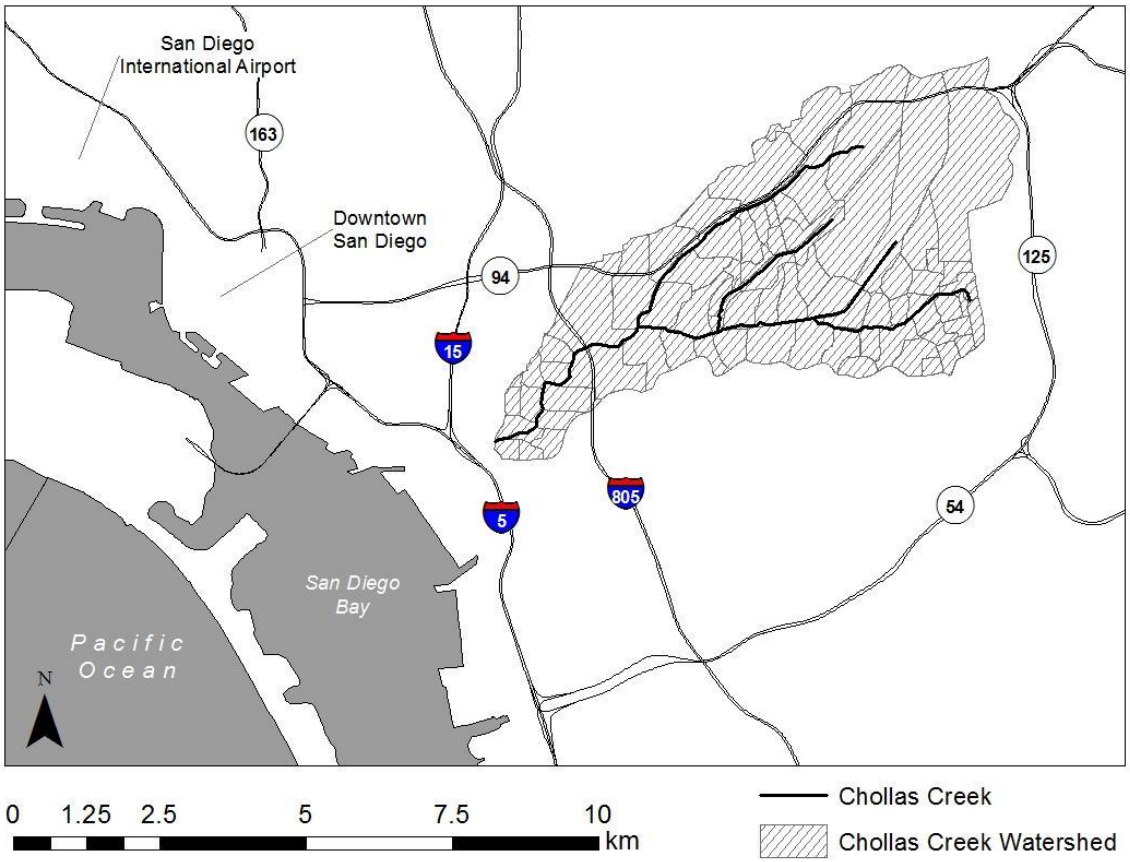

Figure 4.1: Study location, Chollas Creek watershed, San Diego, CA, USA.

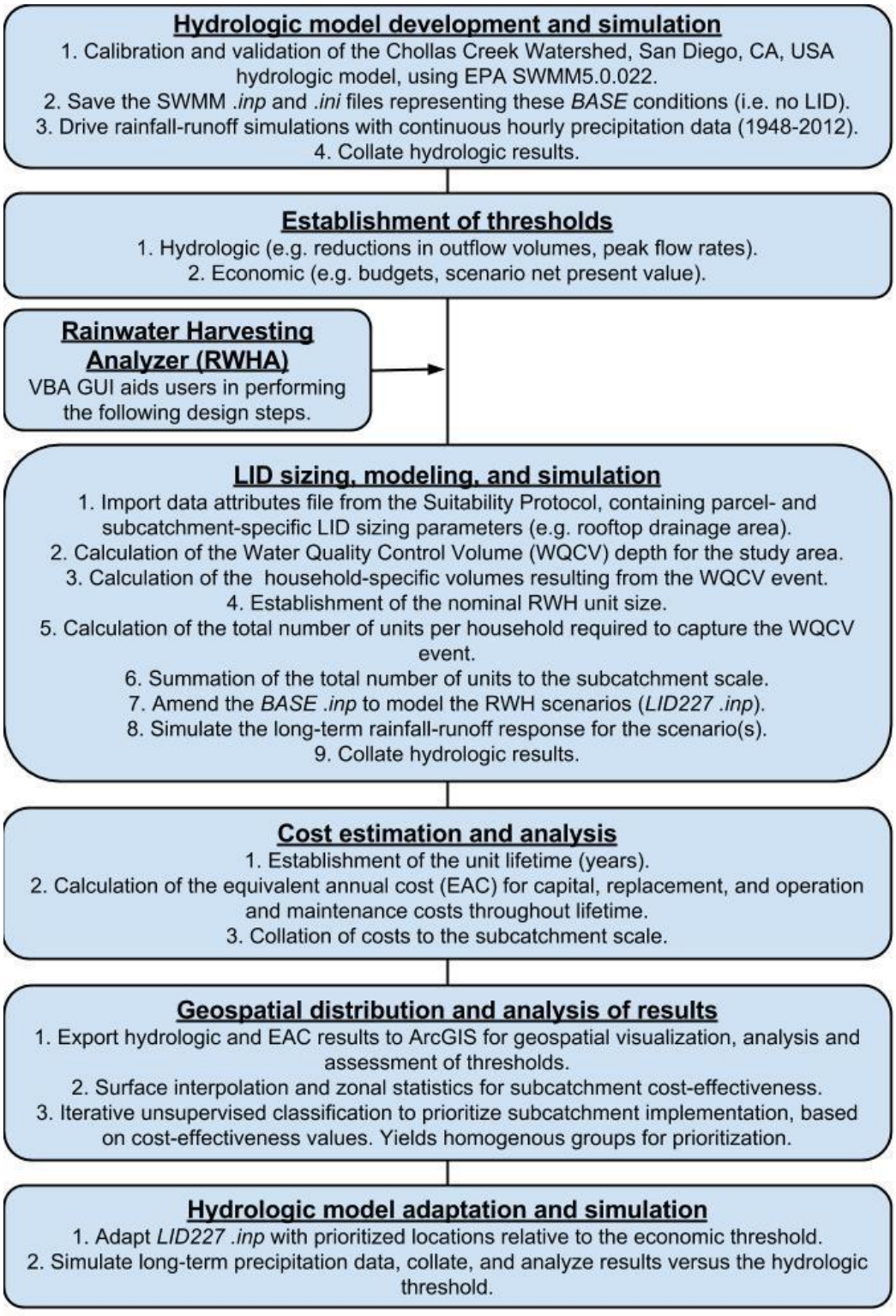

Figure 4.2: The Prioritization Protocol workflow, including the inputs, generalized steps, and outputs related to successful implementation.

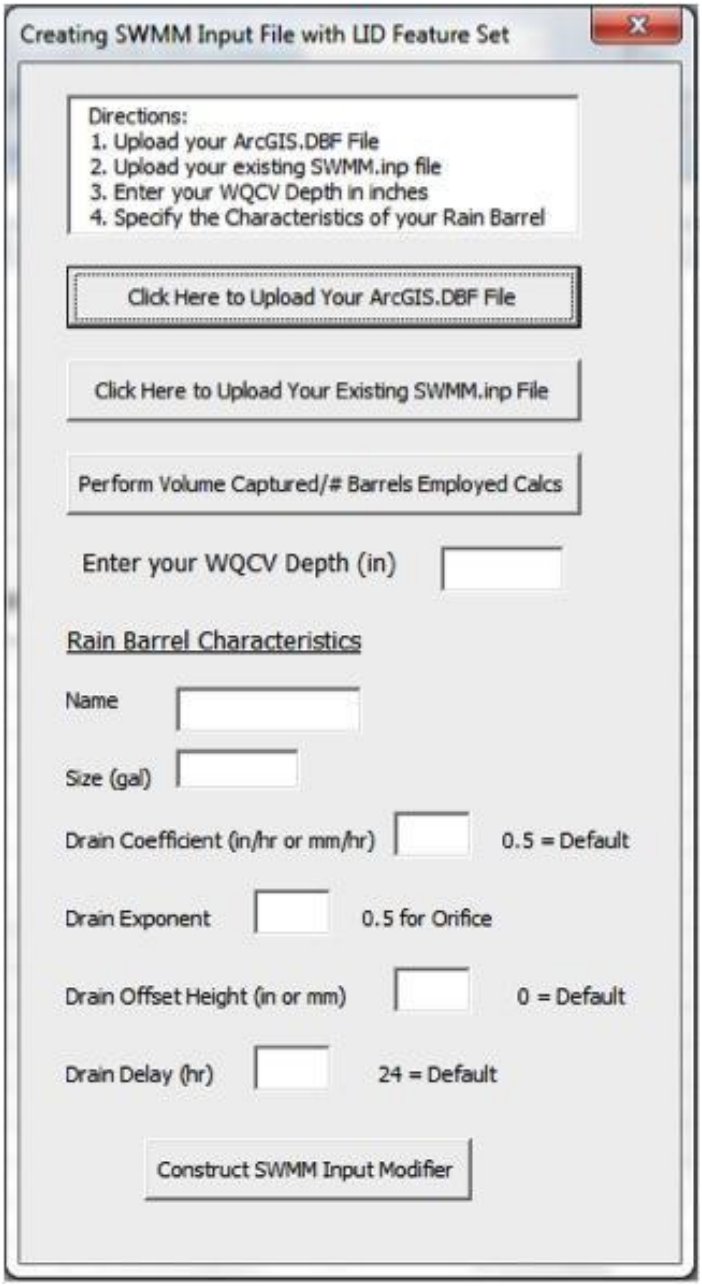

Figure 4.3: *RWHA* GUI. Users are prompted to upload suitability results and existing SWMM .inp datasets for use in the sizing and allocation of RWH units throughout the watershed.

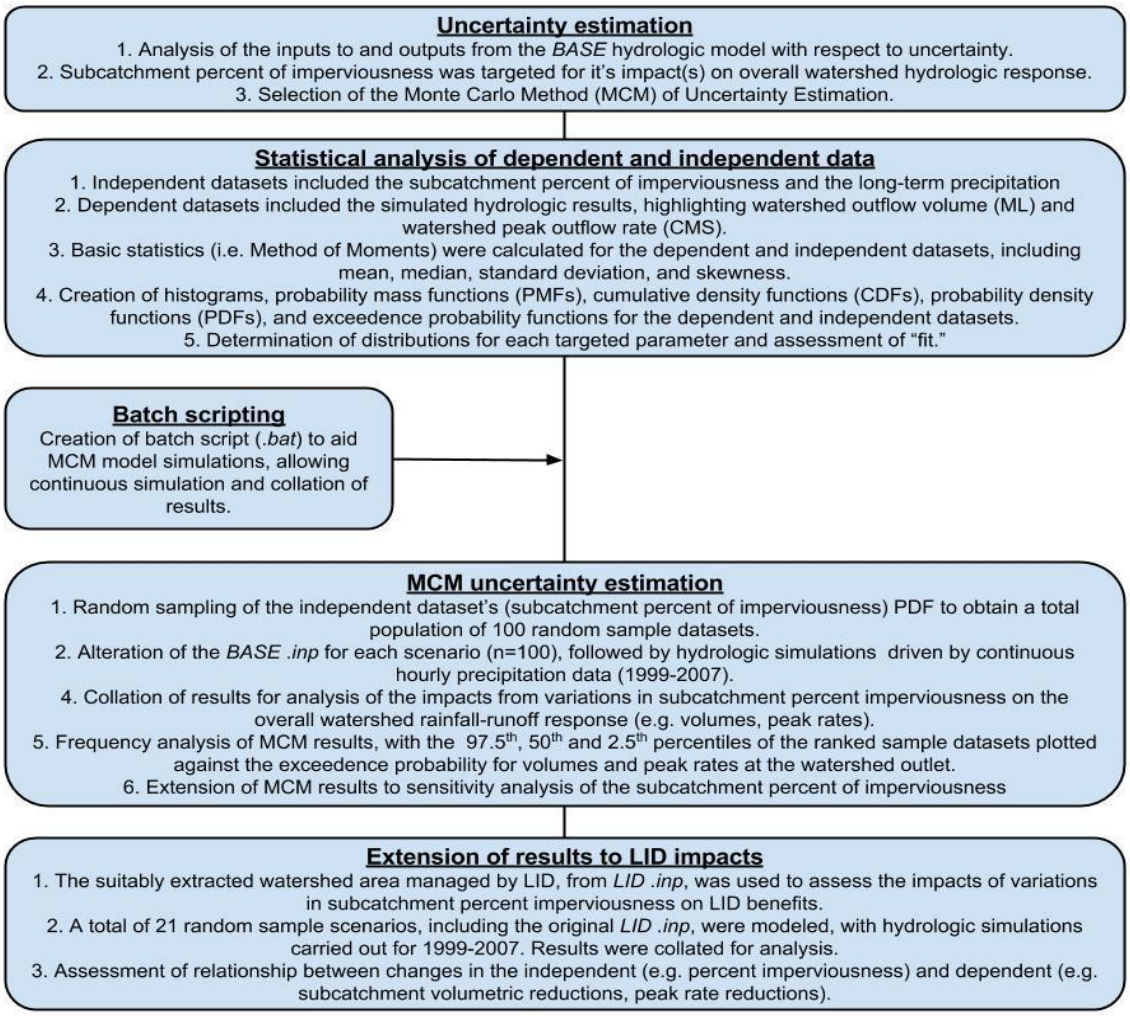

Figure 4.4: Steps required for MCM uncertainty estimation and analysis for the independent variable, subcatchment percent imperviousness.

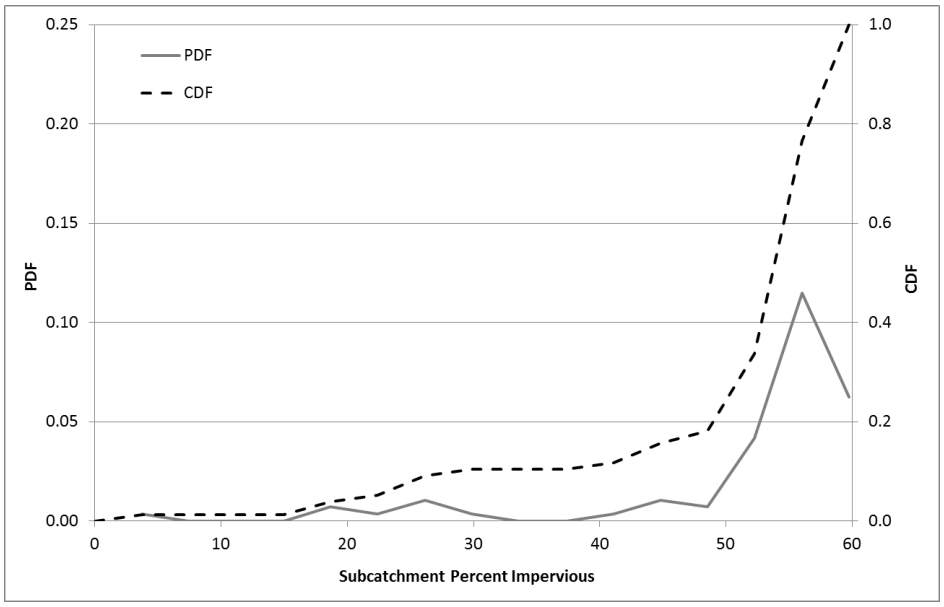

Figure 4.5: PDF and CDF plots for the subcatchment percent of imperviousness sample dataset. The PDF was used to randomly sample values as inputs for the randomized SWMM simulations (n=100).

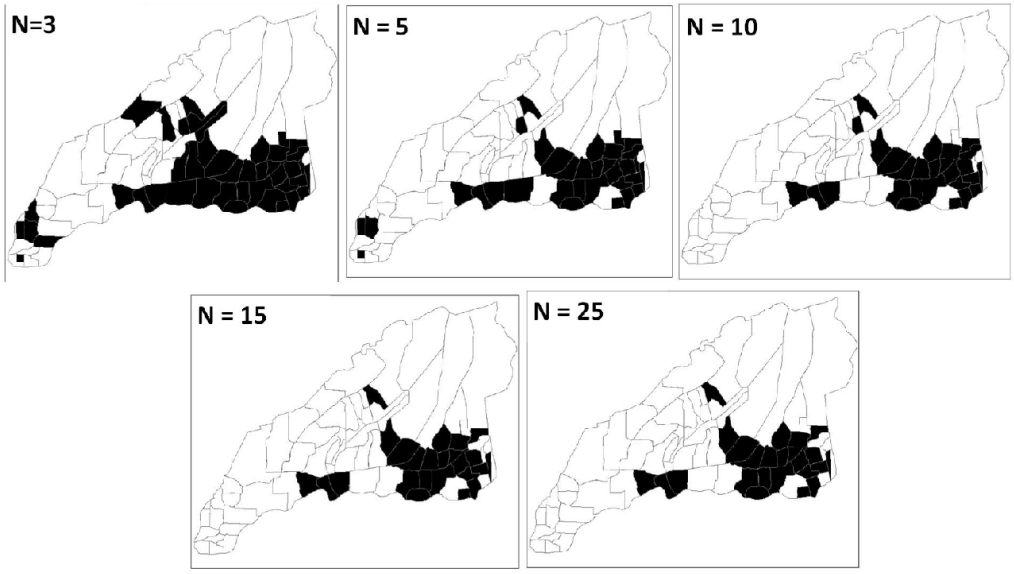

Figure 4.6: Prioritization Protocol results with *PriorLID* toolset for n=3, 5, 10, 15, and 25 classes. Comparison indicates the refinement in classifications when iterations increase the number of classes. Central locations to target remain.

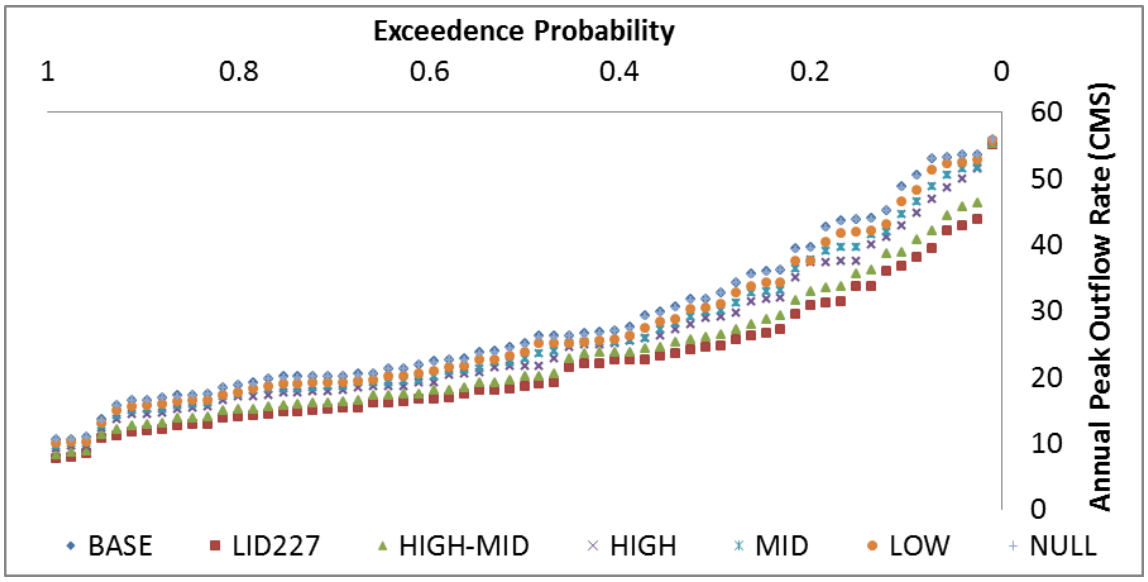

Figure 4.7: Exceedance probabilities for annual peak flow rate (CMS) sample populations for all scenarios assessed.

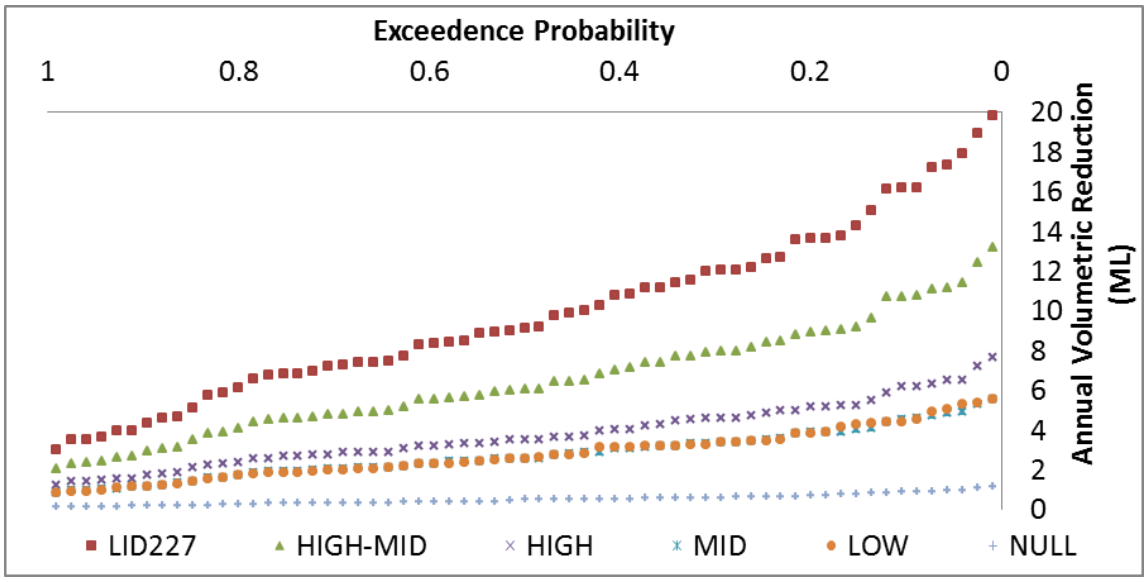

Figure 4.8: Exceedance probabilities for annual volumetric reductions (ML) in watershed outflow for all scenarios assessed.

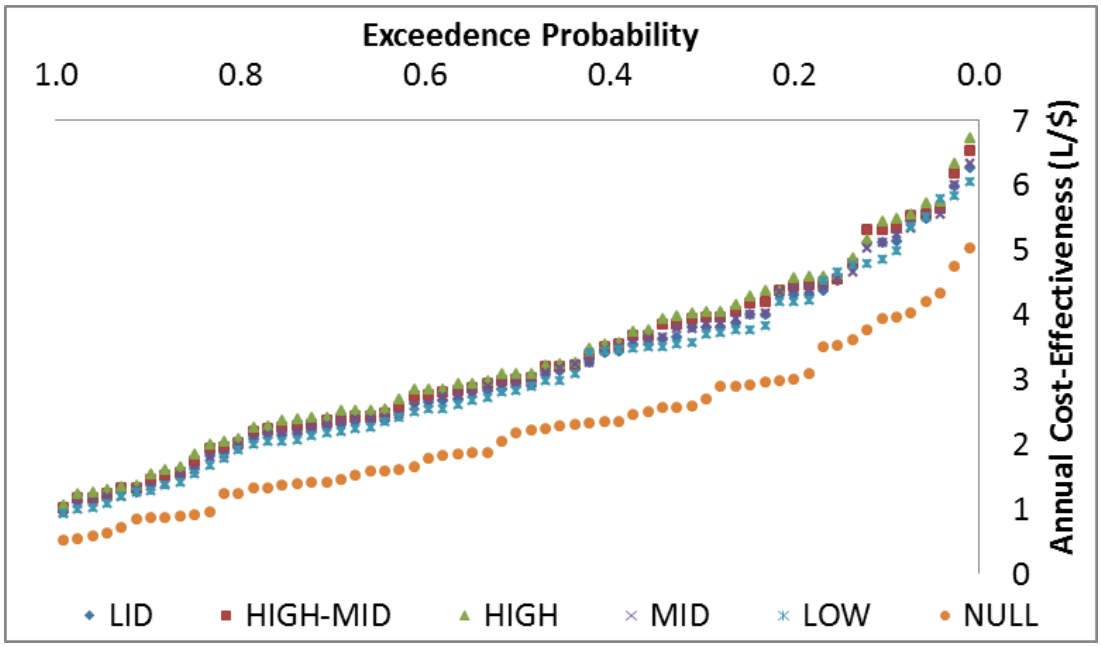

Figure 4.9: Exceedance probabilities for annual average cost-effectiveness results at the overall watershed-scale, for all scenarios targeting the WQCV event depth with 227-liter barrels. Increasing effectiveness is observed for less probable events, which indicates the importance of downspout disconnection.

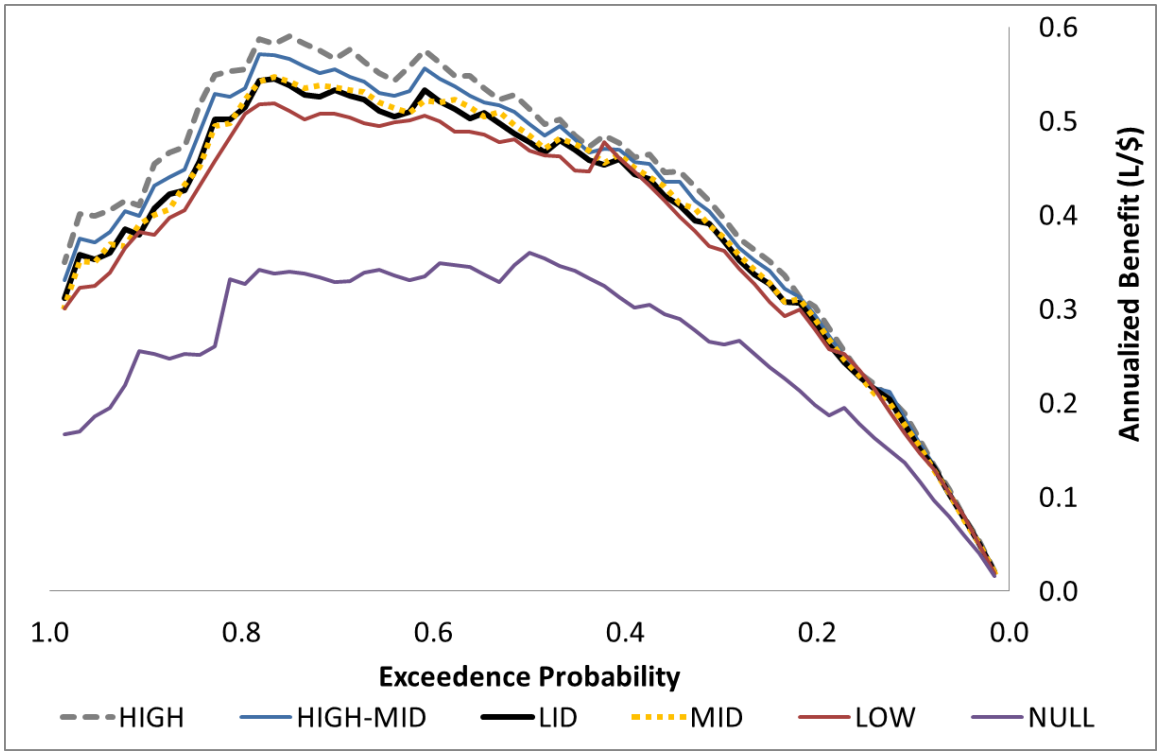

Figure 4.10: Annualized benefits (annual volumetric reduction, in liters, per equivalent annual dollar invested) for priority scenarios assessed.

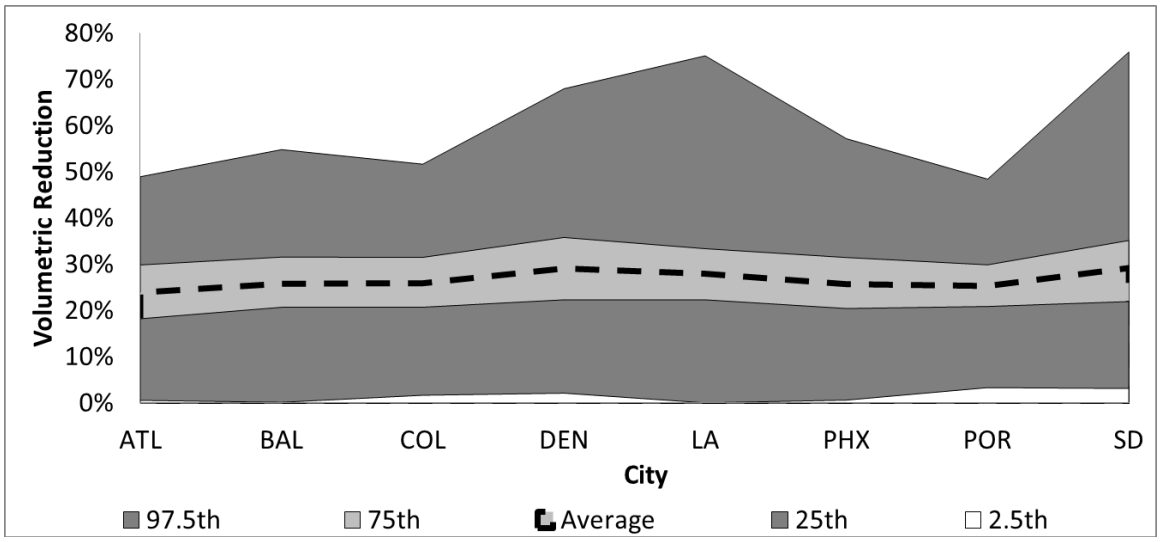

Figure 4.11: Regional volumetric outflow reductions for percentile events.

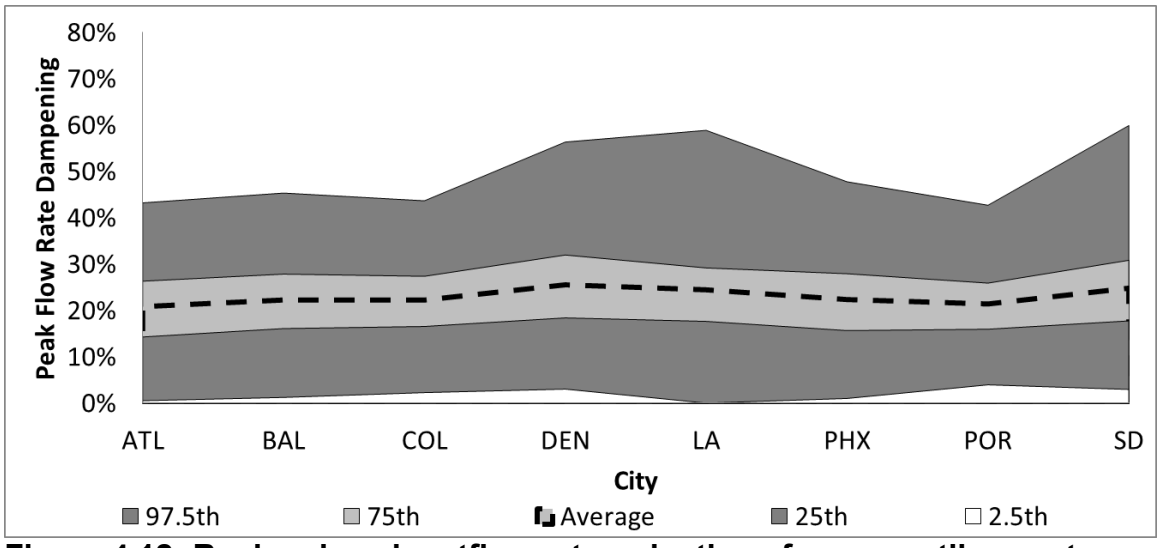

Figure 4.12: Regional peak outflow rate reductions for percentile events.

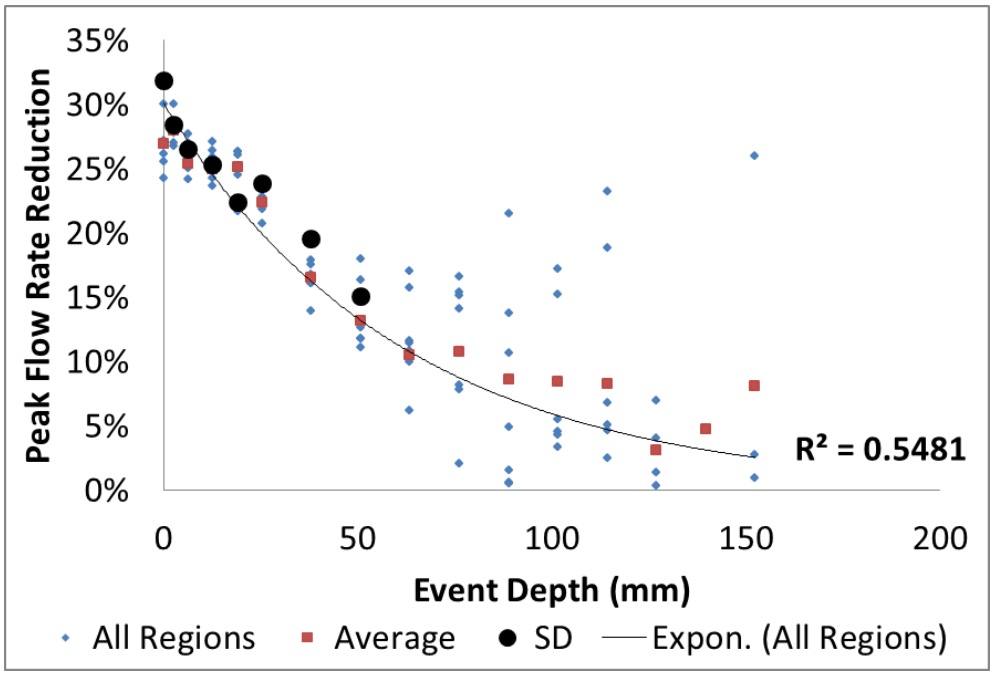

Figure 4.13: Averaged watershed peak outflow rate reductions for individual events, binned by depth (mm).

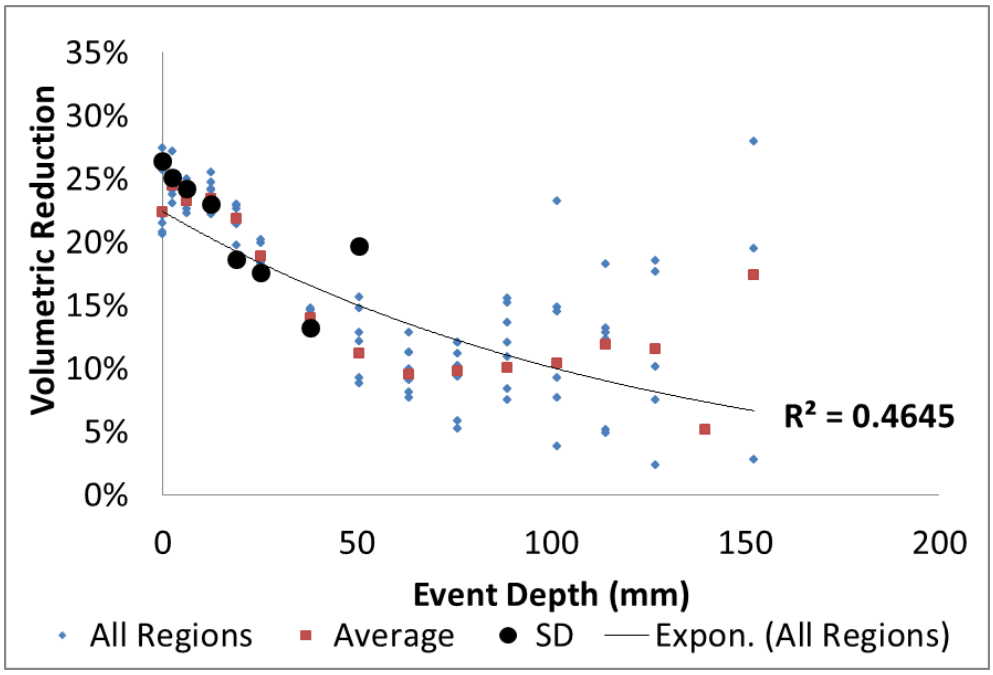

Figure 4.14: Averaged watershed outflow volume reductions for individual events, binned by depth (mm).

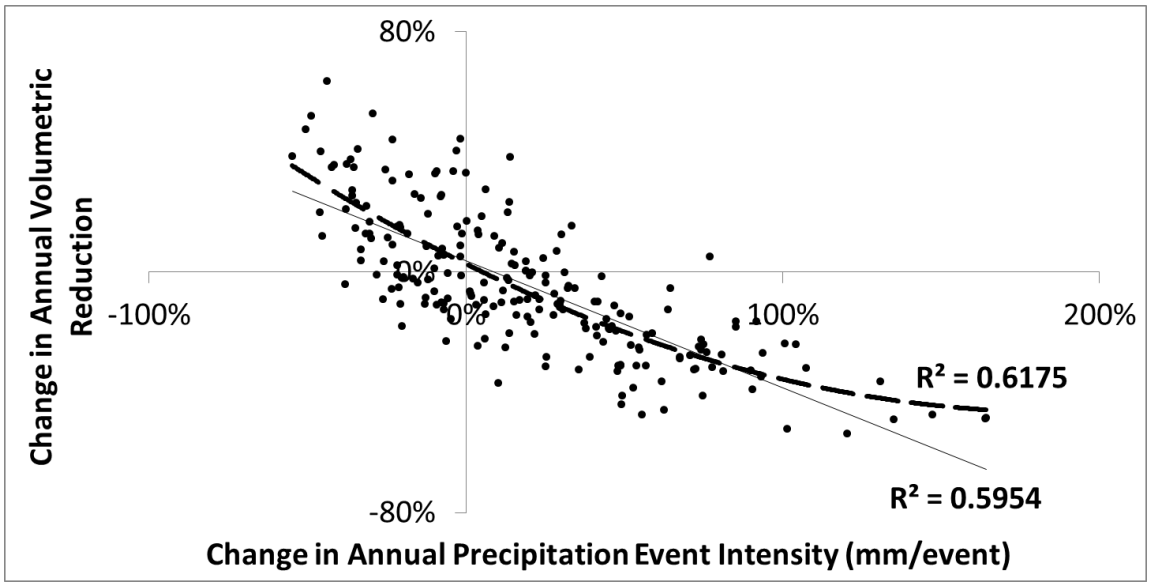

Figure 4.15: Change (versus SD data) in annual precipitation event depth (X-axis) versus the average annual watershed volumetric reduction (Y-axis).

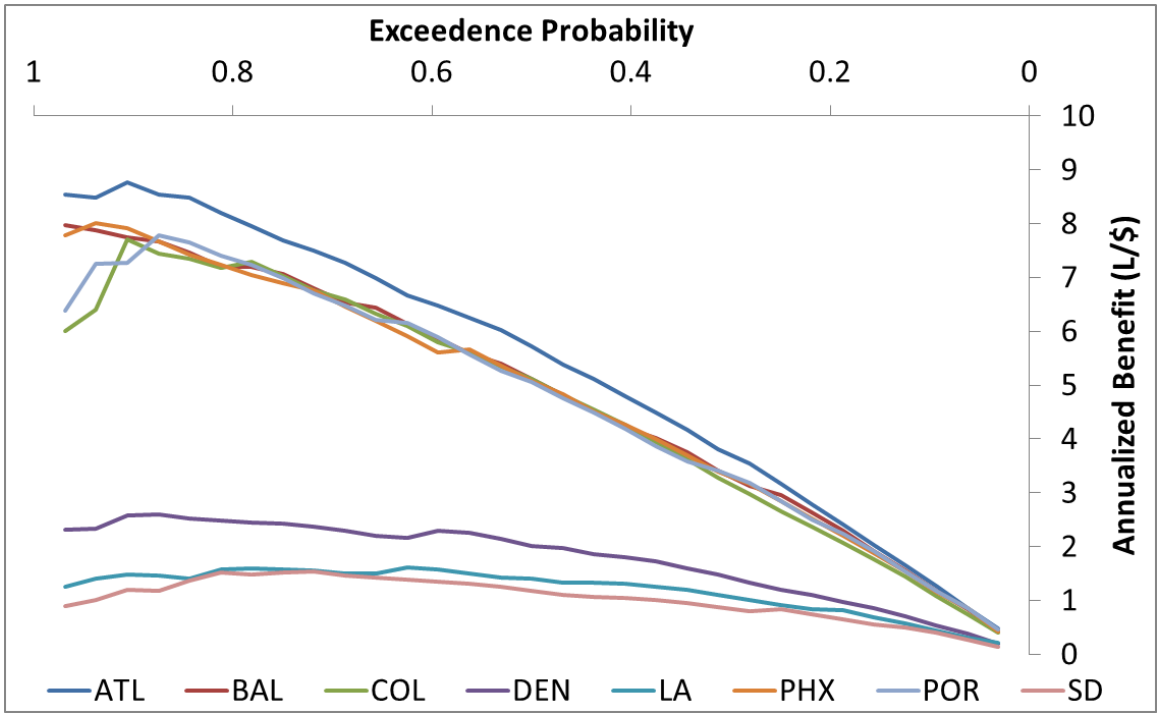

Figure 4.16:Annualized benefits for the regions assessed. Two groups are distinctly visualized, with *DEN*, *LA*, and *SD* providing the least cost-effectiveness and annualized benefit.

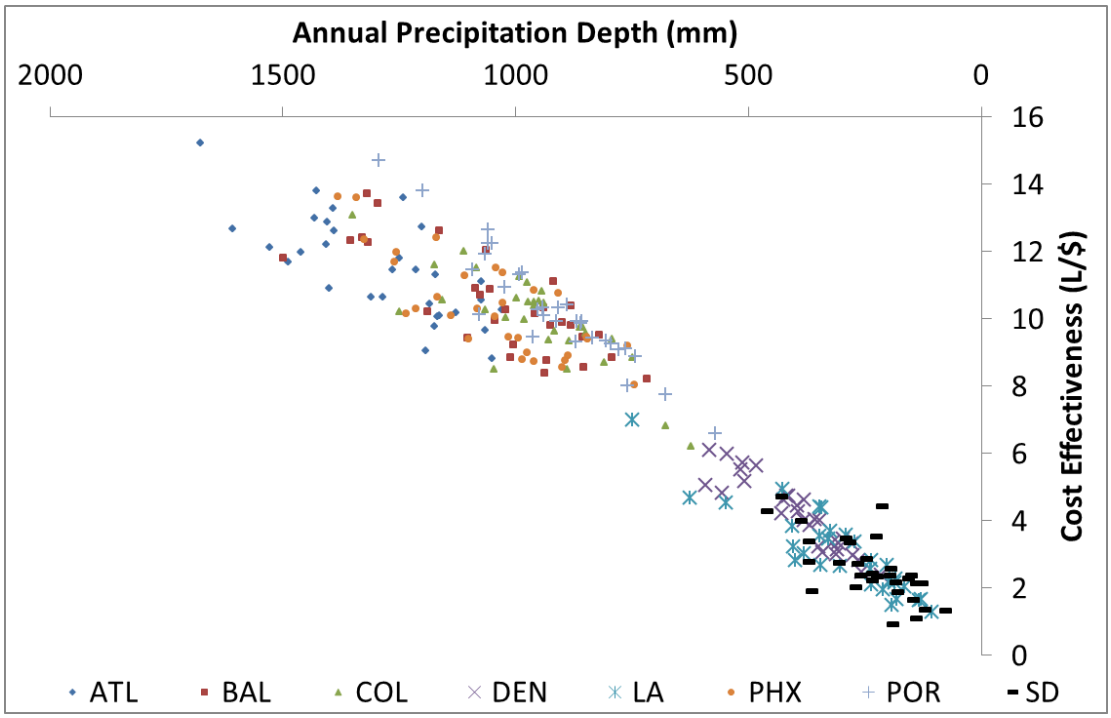

Figure 4.17: Annual precipitation depth (mm) versus the annual cost-effectiveness (L/$) for each climatic region. A linearly increasing trend exists.

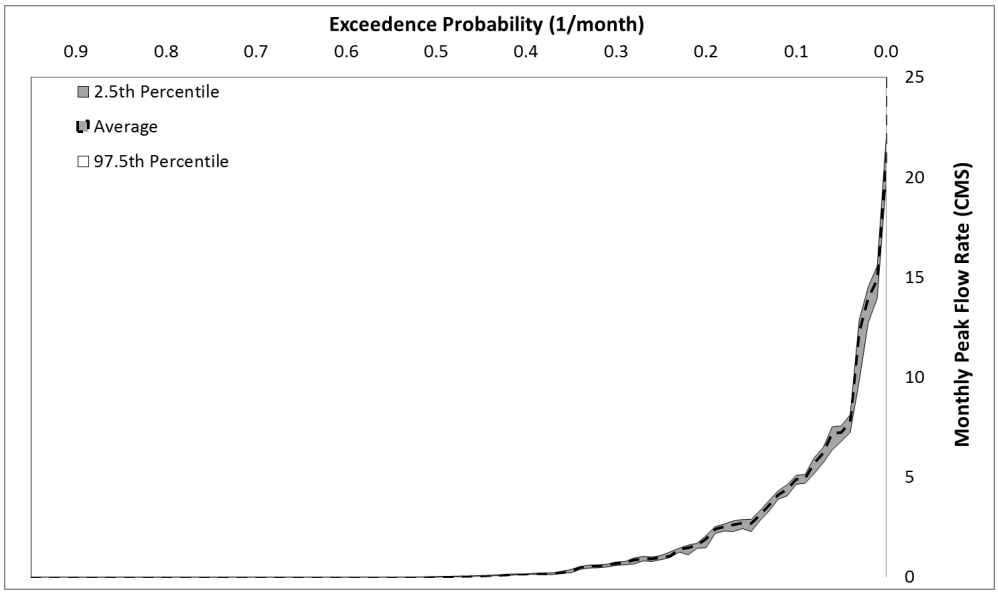

Figure 4.18: Exceedance probability versus the monthly peak flow rate (CMS) for random simulations (n=100) assessing the uncertainty of the hydrologic model, with respect to subcatchment percent imperviousness.

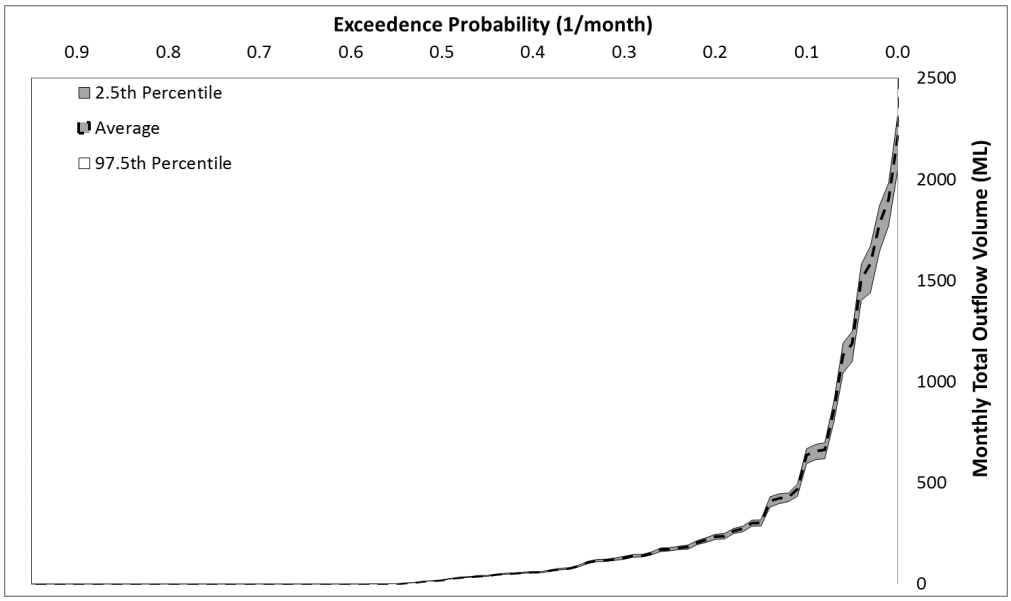

Figure 4.19: Exceedance probability versus the monthly total outflow volume (ML) for random simulations (n=100) assessing the uncertainty of the hydrologic model, with respect to subcatchment percent imperviousness.

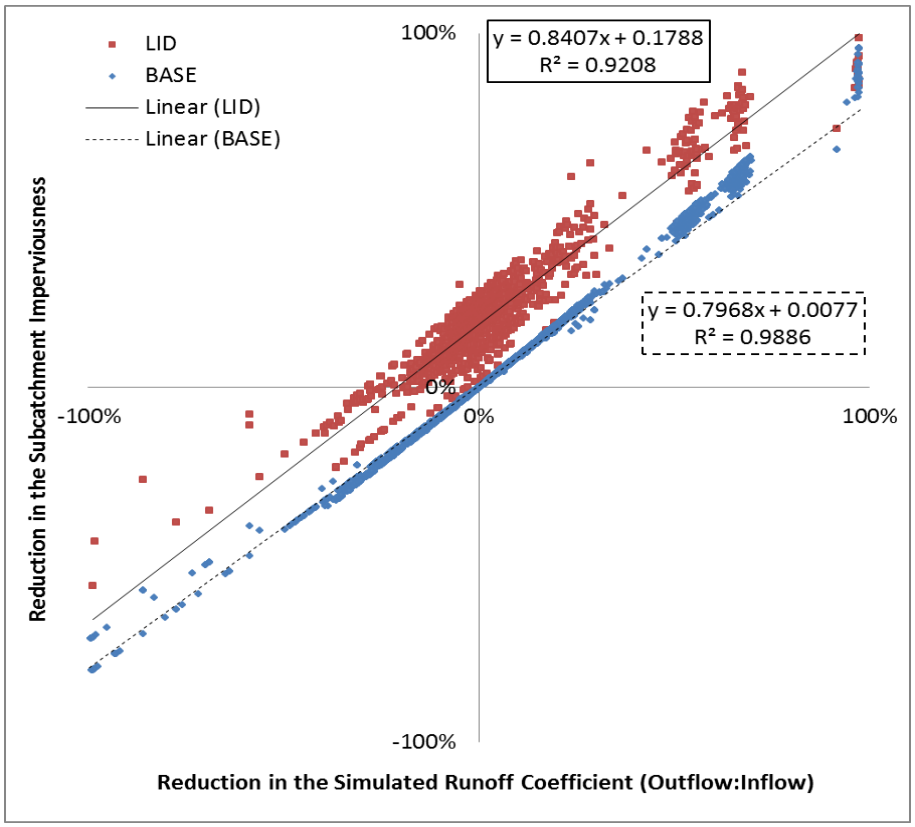

Figure 4.20: Uncertainty analysis results representing the change in subcatchment percent imperviousness (X-axis) versus the change in the subcatchment outflow reductions (Y-axis). The relationships between imperviousness and outflow reduction for *LID227* and *BASE* indicate the ability of RWH to dampen the impact of land cover change.

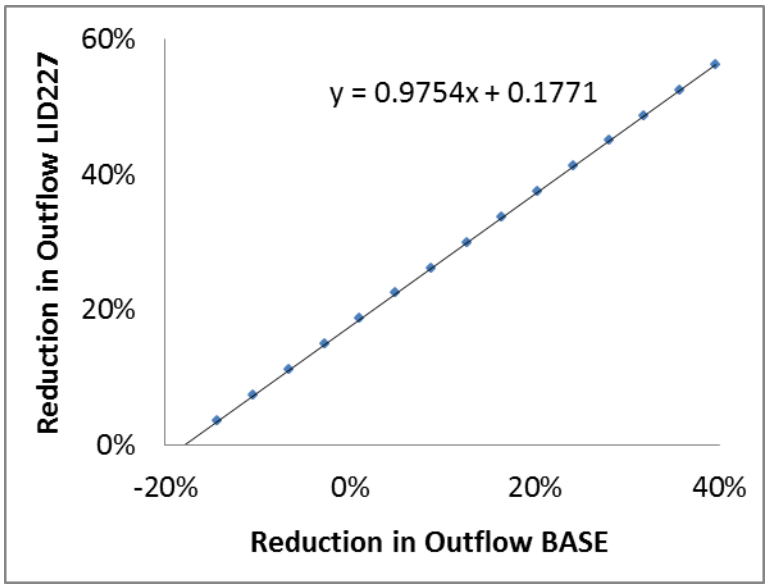

Figure 4.21: Graphical relationship between the reduction of outflow for *BASE* and *LID227* scenarios for the same change in subcatchment percent imperviousness. Relationship implies that RWH is capable of dampening the negative hydrologic impacts of development (i.e., alterations in imperviousness).

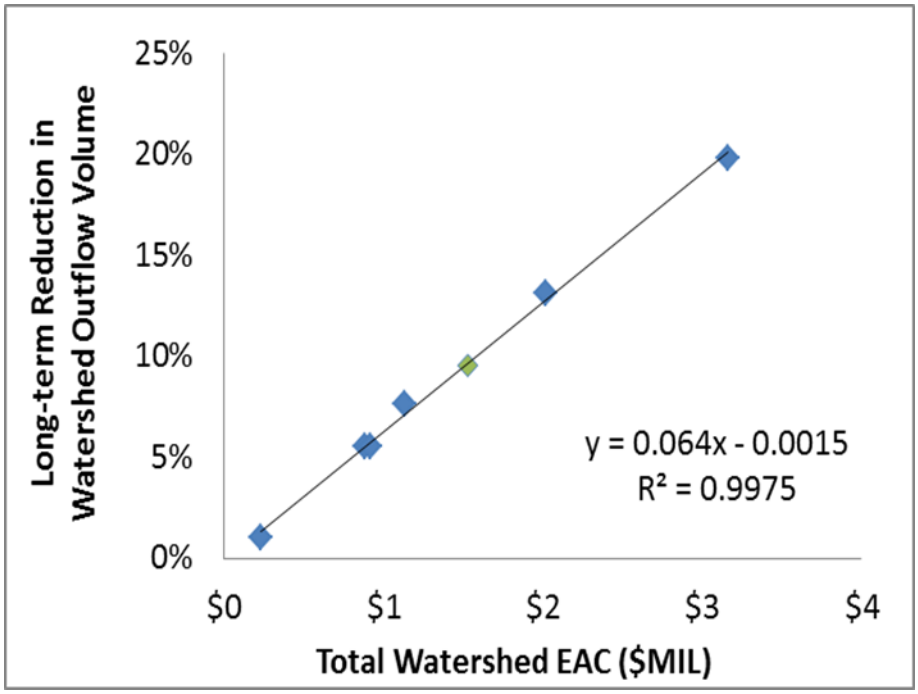

Figure 4.22: Validation of linear cost-effectiveness relation for watershed-scale RWH in the Chollas Creek watershed. Green dot represents the randomly applied RWH scenario for a total of $1.53 MIL.

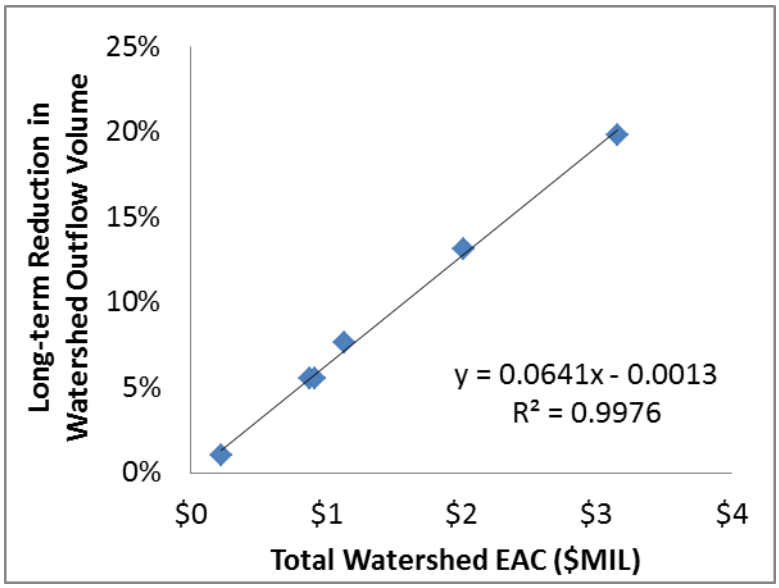

Figure 4.23: Total cost ($MIL) versus the total volumetric reduction for all scenarios assessed.

Table 4.1: Nominal RWH unit parameters for use with the *RWHA* toolset. As a note, all barrel geometries were circular whereas cisterns could be either circular or rectangular (differentiated under Dimensions). D represents the diameter, W represents the width, and L represents the length.

Nominal Designation	Dimensions	Unit Area (m^2)	Height (mm)	Volume (L)
RWH Barrel	(D) 564 mm	0.25	914	227
RWH Barrel	(D) 629 mm	0.31	1,219	379
RWH Barrel	(D) 889 mm	0.62	1,219	757
RWH Cistern	(D) 1,257 mm	1.24	1,524	1,893
RWH Cistern	(W) 1219 mm, (L) 2,348 mm	3	1,273	3,785

Table 4.2: Economic estimation, as EAC, for overall (maximum implementation) and prioritized RWH scenarios.

Scenario	Total EAC	Average Subcatchment EAC
LID227	$3,163,002	$41,078
HIGH-MID	$2,018,914	$69,250
HIGH	$1,135,621	$32,446
MID	$883,293	$36,804
LOW	$915,834	$83,258
NULL	$228,253	$32,608

Table 4.3: Average annual hydrologic results for overall (maximum implementation) and prioritized RWH scenarios.

Scenario	Average Annual Volumetric Reduction	Average Annual Peak Flow Rate Reduction
LID227	20%	24%
HIGH-MID	13%	19%
HIGH	8%	11%
MID	5%	8%
LOW	6%	5%
NULL	1%	0.40%

Table 4.4: Average annual cost-effectiveness for overall (maximum implementation) and prioritized RWH scenarios. Range of values are presented in parentheses.

Scenario	Average Annual Cost-Effectiveness (L/$)	Average Annual Cost-Effectiveness ($/L)
LID227	3.11 (0.95-6.27)	$0.40 ($0.16-$1.05)
HIGH-MID	3.22 (1.01-6.53)	$0.38 ($0.15-$0.99)
HIGH	3.3 (1.06-6.73)	$0.37 ($0.15-$0.94)
MID	3.13 (0.92-6.32)	$0.40 ($0.16-$1.09)
LOW	3.02 (0.91-6.05)	$0.42 ($0.17-$1.10)
NULL	2.19 (0.51-5.01)	$0.63 ($0.20-$1.96)

Table 4.5: Assessment of user-defined thresholds based on hydrologic simulations and cost estimations.

Watershed Reduction	Estimated Cost ($MIL)	User-Defined Cost Thresholds ($MIL)	Projected Cost Difference
2.50%	$0.41	$0.25	49%
5%	$0.80	$0.50	46%
10%	$1.58	$1.00	45%
15%	$2.36	$2.00	17%
20%	$3.14	$3.16	-1%

4.7 References

Ahiablame, L. M., Engel, B. E., & Chaubey, I. (2012). Effectiveness of low impact development practices: Literature review and suggestions for future research. *Water, Air, & Soil Pollution*, *223*, 4253-4273.

Akbari, H., Rose, L. S., & Taha, H. (2003). Analyzing the land cover of an urban environment using high-resolution orthophotos. *Landscape and Urban Planning*, *63*, 1-14.

Alley, W. M., & Veenhuis, J. E. (1983). Effective impervious area in urban runoff modeling. *Journal of Hydraulic Engineering, 109*(2), 313-319.

Anderson, T. K. (2009). Kernel density estimation and k-means clustering to profile road accident hot spots. *Accident Analysis & Prevention*, *41*(3), 359-364.

Baycan-Levent, T., Vreeker, R., & Nijkamp, P. (2009). A multi-criteria evaluation of green spaces in European cities. *European Urban and Regional Studies, 16*(2), 193-213.

Benedict, M. A., & McMahon, E. T. (2002). Green infrastructure: Smart conservation for the 21st century. *Renewable Resources Journal, 20*(3), 12-17.

Brander, K., Owen, K., & Potter, K. (2004). Modeled impacts of development type on runoff volume and infiltration performance. *Journal of the American Water Resources Association*, *40*(4), 961-969.

Brown, D. G., Johnson, K. M., Loveland, T. R., & Theobald, D. M. (2005). Rural land-use trends in the coterminous United States, 1950-2000. *Ecological Applications*, *15*, 1851-1863.

Burian, S. J., & Pomeroy, C. A. (2010). Urban impacts on the water cycle and potential green infrastructure implications. In J. Aitkenhead-Peterson & A. Volder (Eds.), *Urban ecosystem ecology* (pp. 277-296). Madison, WI: American Society of Agronomy, Crop Science Society of America, Soil Science Society of America.

Burns, M. J., Fletcher, T. D., Walsh, C. J., Ladson, A. R., & Hatt, B. E. (2012). Hydrologic shortcomings of conventional urban stormwater management and opportunities for reform. *Landscape and Urban Planning*, *105*(3), 230-240.

Cadenasso, M. L., Pickett, S. T. A., & Schwarz, S. (2007). Spatial heterogeneity in urban ecosystems: Reconceptualizing land cover and a framework for classification. *Frontiers in Ecology and Environment*, *5*, 80-88.

Central New York Regional Planning & Development Board. (2012). Green infrastructure planning for improved stormwater management in central New York. Retrieved from http://www.dec.ny.gov/docs/water_pdf/arrafnlrptcny265.pdf

Cunnane, C. (1978). Unbiased plotting positions – A review. *Journal of Hydrology*, *37*, 205-222.

De Graaf, R., & Der Brugge, R. (2010). Transforming water infrastructure by linking water management and urban renewal in Rotterdam. *Technological Forecasting and Social Change, 77*, 1282-1291.

Denault, C., Miller, R. G., & Lence, B. J. (2006). Assessment of possible impacts of climate change in an urban catchment. *Journal of the American Water Resources Association*, *45*(2), 512-533.

Dietz, M. E. (2007). Low impact development practices: A review of current research and recommendations for future directions. *Water, Air & Soil Pollution*, *186*, 351-363.

Endreny, T., & Collins, V. (2009). Implications of bioretention basin spatial arrangements on stormwater recharge and groundwater mounding. *Ecological Engineering*, *35*, 670-677.

Fletcher, T. D., Andrieu, H., & Hamel, P. (2013). Understanding, management and modelling of urban hydrology and its consequences for receiving waters: A state of the art. *Advances in Water Resources*, *51*(0), 261-279.

Foraste, J. A., & Hirschman, D. (2010). A methodology for using rainwater harvesting as a stormwater management bmp. Proceedings from: *ASCE International Low Impact Development Conference, Redefining Water in the City*. San Francisco, CA: ASCE.

Foresman, T. W., Pickett S. T. A., & Zipperer, W. C. (1997). Methods for spatial and temporal land use and land cover assessment for urban ecosystems and application in the greater Baltimore-Chesapeake region. *Urban Ecosys*tems, *1*, 201–216.

Gilroy, K. L., & McCuen, R. H. (2009). Spatio-temporal effects of low impact development practices. *Journal of Hydrology, 367*, 228-236.

Guo, J. C. Y. (2008). Volume-based imperviousness for storm water design. *Journal of Irrigation and Drainage Engineering*, *134*(2), 193-196.

Haith, D. A. (2003). Systems analysis, TMDLs and watershed approach. *Journal of Water Resources Planning and Management*, *129*(4), 257-260.

Han, M. Y., Mun, J. S., & Kim, H. J. (2008). An example of climate change adaptation by rainwater management at the Star City rainwater project. Proceedings from: *3rd Rainwater Harvesting and Management Workshop*. Sydney, AU: IWA.

Houdeshel, C. D., Pomeroy, C. A., Hair, L., & Moeller, J. (2011). Cost estimating tools for low-impact development best management practices: Challenges, limitations and implications. *Journal of Irrigation and Drainage*, *137*(3), 183-189.

Huber, W., Clannon, L., & Stouder, M. (2006). *BMP modeling concepts and simulation*. Cincinnati, OH: EPA.

Hurd, B., Leary, N., Jones, R., & Smith, J. (1999). Relative regional vulnerability of water resources to climate change. *Journal of the American Water Resources Association, 35*(6), 1399-1409.

Interagency Committee on Water Data (IACWD). (1982). Guidelines for determining flood frequency: Bulletin 17b (revised and corrected). Washington, DC: EPA.

Isik, S., Kalin, L., Schoonover, J. E., Srivastava, P., & Lockaby, B. G. (2013). Modeling effects of changing land use/cover on daily streamflow: An artificial neural network and curve number based hybrid approach. *Journal of Hydrology, 485*(2), 103-112.

Jacquez, G. M. (2008). Spatial cluster analysis. In J. P. Wilson & A. S. Fotheringham (Eds.), *The handbook of geographic information science* (1st ed., pp. 395-416). Victoria, AU: Blackwell Publishing

Jensen, C. A., Quinn, R. J., & Davis, T. H. (2010). Urban watershed management: Using remote sensing to implement low impact development. Proceedings from: *2010 Third International Conference on Infrastructure Systems and Services: Next Generation Infrastructure Systems for Eco-Cities.* Shenzhen, China: IEEE.

Jia, H., Lu, Y., Yu, S. L., & Chen, Y. (2012). Planning of LID-BMPs for urban runoff control: The case of Beijing Olympic Village. *Separation and Purification Technology*, *84*, 112-119.

Kalyanapu, A. J., Judi, D. R., McPherson, T. N., & Burian, S. J. (2014). Annualized risk analysis approach to recommend appropriate level of flood control: Application to Swannanoa River watershed. *Journal of Flood Risk Management,* doi: 10.1111/jfr3.12108.

Kirshen, P., Ruth, M., & Anderson, W. (2008). Interdependencies of urban

climate change impacts and adaptation strategies: A case study of metropolitan Boston USA. *Climatic Change, 86*, 105-122.

Kousky, C., Olmstead, S. M., Walls, M. A., & Macauley, M. (2013). Strategically placing green infrastructure: Cost-effective land conservation in the floodplain. *Environmental Science & Technology*, *43*, 3563-3570.

Lee, J. G., & Heaney, J. P. (2003). Estimation of urban imperviousness and its impacts on storm water systems. *Journal of Water Resources Planning and Management*, *129*, 419-426.

Maher, M., & Lustig, T. (2003). Sustainable water cycle design for urban areas. *Water Science and Technology, 47*(7-8), 25-31.

Malczewski, J. (2004). GIS-Based land-use suitability analysis: A critical overview. *Progress in Planning*, *62*(1), 3-65.

McCuen, R. H. (2005). *Hydrologic analysis and design* (3rd ed.). Upper Saddle River, NJ: Pearson-Prentice Hall.

Maryland Department of the Environment (MDE). (2014). Stormwater fee FAQ. Retrieved from http://www.mde.state.md.us/programs/Marylander/Pages/StormwaterFeeFAQ.aspx

Mitchell, V. G., McCarthy, D. T., Deletic, A., & Fletcher, T. D. (2005a). Development of novel integrated stormwater treatment and reuse systems: Assessing storage capacity requirements. Melbourne, AU: Institute for Sustainable Resources, Monash University.

Mitchell, V. G., McCarthy, D. T., Deletic, A., & Fletcher, T. D. (2005b). Optimising storage capacity for stormwater utilisation. Proceedings from: *10th International Conference on Urban Drainage*. Copenhagen, DK.

Mitchell, V. G., Deletic, A., Fletcher, T. D., Hatt, B. E., & McCarthy, D. T. (2007). Achieving multiple benefits from stormwater harvesting. *Water Science and Technology, 55*(4), 135-144.

National Research Council of the National Academies (NRC). (2008). *Urban stormwater management in the United States.* Washington, DC: The National Academies Press.

Perez-Pedini, C., Limbrunner, J. F., & Vogel, R. M. (2005). Optimal location of infiltration-based best management practices for storm water management. *Journal of Water Resources Planning and Management*, *131*(6), 441-448.

Pitt, R., & Clark, S. E. (2008). Integrated storm-water management for watershed sustainability. *Journal of Irrigation Drainage Engineering*, *134*, Special Issue: Urban Storm-Water Management: 548-555.

Prince George's County, Maryland. (June 1999). Low-impact development design strategies: An integrated design approach. Retrieved from http://water.epa.gov/polwaste/green/upload/lidnatl.pdf.

Rosemarin, A. (2005). Sustainable sanitation and water in small urban centres. *Water Science and Technology, 51*(8), 108-118.

Roy, A. H., Wenger, S. J., Fletcher, T. D., Walsh, C. J., Ladson, A. R., Shuster, W. D., Thurston, H. W., & Brown, R. R. (2008). Impediments and solutions to sustainable, watershed-scale urban stormwater management: Lessons from Australia and the United States. *Environmental Management, 42*, 344-359.

Sample, D., Liu, J., & Wang, S. (2013). Evaluating the dual benefits of rainwater harvesting systems using reliability analysis. *Journal of Hydrologic Engineering*, *18*(10), 1310-1321.

Scheuler, T. (1994). The importance of imperviousness. *Watershed Protection Techniques,* 1(3), 100-111.

Schneider, L., & McCuen, R. (2006). Assessing the hydrologic performance of best management practices. *Journal of Hydrologic Engineering, 11*(3), 278-281.

Shaver, E., Horner, R., Skupien, J., May, C., & Ridley, G. (2007). *Fundamentals of urban runoff management: Technical and institutional issues* (2nd ed.). Madison, WI: North American Lake Management Society.

Shuster, W. D., Morrison, M. A., & Webb, R. (2008). Front-loading urban stormwater management for success – a perspective incorporating current studies on the implementation of retrofit low-impact development. *Cities and the Environment (CATE), 1*(2), Art. 8.

Spatari, S., Yu, Z., & Montalto, F. A. (2011). Life cycle implications of urban green infrastructure. *Environmental Pollution, 159*, 2174-2179.

Stone, B., & Norman, J. M. (2006). Land use planning and surface heat island formation: A parcel-based radiation flux approach. *Atmospheric Environment, 40*, 3561-3573.

Thomas, N., Hendrix, C., & Congalton, R. G. (2003). A comparison of urban mapping methods using high-resolution digital imagery. *Photogrammetric Engineering & Remote Sensing, 69*(9), 963-972.

Tong, S. T. Y., Sun, Y., Ranatunga, T., He, J., & Yang, J. (2012). Predicting plausible impacts of sets of climate and land use change scenarios on water resources. *Applied Geography*, *32*(2), 477-489.

Tsakiris, P. (2010). Annualized risk: The key for rational flood protection design. *European Water*, *30*, 25-30.

USEPA. (December, 2007a). Reducing stormwater costs through low impact development (LID) strategies and practices, EPA 841-F-07-006. Retrieved from http://water.epa.gov/polwaste/green/costs07_index.cfm

USEPA. (2007b). Menu of BMP background. Retrieved from http://cfpub.epa.gov/npdes/stormwater/menuofbmps/bmp_background.cfm

USEPA. (2011). Managing wet weather with green infrastructure. Retrieved from http://cfpub.epa.gov/npdes/home.cfm?program_id=298

USEPA. (2013). Smart growth. Retrieved from http://www.epa.gov/dced/index.htm

Vermonden, K., Leuvan, R. S. E. W., van der Velde, G., van Katwijk, M. M., Roelofs, J. G. M., & Hendriks, A. J. (2009). Urban drainage systems: An undervalued habitat for aquatic macroinvertebrates. *Biological Conservation*, *142*, 1105-1115.

Walsh, T. C., Pomeroy, C. A., & Burian, S. J. (2014). Hydrologic modeling analysis of a passive, residential rainwater harvesting program in an urbanized, semi-arid watershed. *Journal of Hydrology*, *508*, 240-253.

Walsh, T. C., Pomeroy, C. A., & Dennison, P. (in review). Application of object-based image analysis with geospatial analysis to quantify suitable sites for watershed-scale low impact development.

Weber, T., Sloan, A., & Wolf, J. (2006). Maryland's green infrastructure assessment: Development of a comprehensive approach to land conservation. *Landscape and Urban Planning*, *77*, 94-110.

Woods-Ballard, B., Kellagher, R., Martin, P., Jefferies, C., Bray, R., & Shaffer, P. (2007). *The SUDS manual*. London, UK: CIRIA, Classic House.

Yang, B., & Li, S. (2013). Green infrastructure design for stormwater runoff and water quality: Empirical evidence from large watershed-scale community developments. *Water*, 5, 2038-2057.

Zhang, Y., Sugumaran, R., McBroom, M., DeGroote, J., Kauten, R., & Barten, P. K. (2011). Web-based spatial decision support system and watershed

management with a case study. *International Journal of Geosciences, 2*(3), 195-203.

CHAPTER 5

CONCLUSIONS

The objectives of this dissertation research are to improve the prioritized implementation of LID, targeting RWH, by enhancing the ability to assess local design constraints and long-term hydrologic conditions. This is accomplished by the following steps: (1) establishing the need for improvement with a traditional hydrologic analysis of a passive, watershed-scale RWH framework, (2) developing and testing a Suitability Protocol (with related toolsets, *LIDSS* and *QA*) that identifies suitable RWH locations with geospatial analysis of OBIA classifications and LID design constraints, and (3) developing and applying a Prioritization Protocol (with related toolsets, *RWHA* and *PriorLID*) to target cost-effective locations based on hydrologic and economic analyses of user-defined thresholds.

The first step resulted in a validated hydrologic model, using EPA SWMM5.0.022, for the Chollas Creek watershed. This model, built following a uniform application methodology, established the baseline for future assessments of suitability and prioritization of RWH scenarios. The focus of this research was on the impacts of variations in RWH capacity, watershed implementation rates, and unit-specific controls (e.g., drain delay, drain duration).

Results reinforced increasing benefits with increasing capacity and greater cost-effectiveness for smaller barrels (e.g., 227-liters) versus larger cisterns (e.g., 7,571-liters). However, both the drainage area and local precipitation characteristics were found to influence benefits. These findings support similar work, by Steffen et al. (2013), who determined the effectiveness of RWH throughout the US at a regional scale.

Analysis of variations in RWH outflow duration and drain delay found negligible impact on overall watershed reductions; however, as drain delay time approached, or exceeded, the local dry duration (i.e., consecutive time period in which precipitation does not occur), the unit's effectiveness was found to decrease. Effectiveness, in this case, was a function of the ability of the unit to properly empty prior to future precipitation events and, therefore, maximize long-term storage versus overflow. Thus, it is suggested that municipalities analyze the long-term precipitation when providing RWH management guidance for both sizing and regulating temporal storage and outflow. This is especially pertinent when systems are designated as passive, meaning that users are not actively draining or using the stored water.

This study and its results are presented in Chapter 2. The time required and uniformity assumptions of this research established the need for improved protocols and methodologies that classify existing land cover/use and provide assessment of pivotal constraints with publicly-available data. The ability to assess unique, distributed locations' conditions, such as slopes, soils, and floodway and floodplain zones, improves watershed-scale suitability analysis.

Further, such methodologies would contribute to watershed-scale management plans and frameworks targeting the implementation, design, and analysis of site-specific LID controls.

Based on the findings of the first step, the objective of the Suitability Protocol was to provide an improved method for watershed-scale implementation and design of LID practices. This study, presented in Chapter 3, targeted the improved, suitable implementation of RWH for the Chollas Creek watershed. The Suitability Protocol was based on the combination of OBIA with geospatial analysis of constraining datasets and driven by user-defined values. These values represented the targeted LID practice, which was RWH for this study. As such, research focused on the needs for both accurate OBIA and spatial filtering of LID constraints based on user goals. The results of this study found that OBIA can provide accurate classification (e.g., identification and quantification) of buildings throughout a dense (5,400 persons per square kilometer) and heterogeneous (52.7% impervious, approximately 10% rooftops) urban watershed. An overall accuracy of 92% was achieved for buildings, though some misclassification remained due to spatial registration issues and the surface interpolation algorithm choice.

Compared with the results from the traditional, uniform design method (Chapter 2), the Suitability Protocol estimated fewer rooftops (11% reduction), but a 51% greater impervious area targeted by RWH. This difference may result from clumping of households, which is a function of the spatial resolution of the classified datasets and the OBIA rule set parameters. Hydrologic analysis of

uniformly- and suitably-informed RWH scenarios (single 227-liter units at each household) found *LIDSS* increased the reduction of annual outflow volume and peak flow rate by 44% and 51%, respectively, compared with the single 227-liter model (*UNI227*) results from Chapter 2. For instance, the influence of disconnecting impervious areas over storage capacity was highlighted, since a 51% increase in targeted rooftop area (*LID227*) simulated similar differences in watershed-scale reductions (*UNI227* versus *LID227*).

Assessment of the Suitability Protocol for the Chollas Creek watershed indicated that OBIA can improve the ability of users to accurately identify and quantify site-specific rooftops using publicly-available spectral, elevation, and parcel datasets. The accuracy of quantifications and spatial locations impact not only the cumulative influence on watershed hydrologic response but also the costs of RWH systems at the parcel and subcatchment scales. These findings improve the design of watershed-scale LID measures that must account for local, site-specific constraints. However, suitability is not the only constraint in developing watershed water management plans. The ability to account for life-cycle costs and overall, long-term benefits must also be provided.

Based on the results of the suitability study in Chapter 3, the objective of the Prioritization Protocol (Chapter 4) focused on the improvement of distributing, or targeting, RWH practices as a function of both cost-effectiveness and user-defined thresholds. These thresholds included watershed hydrologic reductions, or benefits, and economic constraints (e.g., budgets). The goals of this step in the dissertation included (1) adapting the *BASE* hydrologic model to

accommodate *LIDSS* results from Chapter 3 and provide a baseline for improvement, (2) analyzing the long-term hydrologic impacts and life cycle costs, as EAC, for watershed-scale suitable RWH practices, (3) prioritization of subcatchments as a function of rasterized cost-effectiveness surfaces, resulting in homogenous priority classes, and (4) hydrologic analysis of priority scenarios to determine the extent to which thresholds could be met. Additionally, MCM uncertainty analysis was completed for the subcatchment percent imperviousness parameter to determine the impact of variations on the watershed hydrologic response. In addition, the long-term precipitation for seven climatic regions was used to assess the impact of variations in precipitation on RWH effectiveness at the watershed-scale.

The results of this research determined the Prioritization Protocol and toolsets were capable of providing prioritized recommendations of subcatchments based on cost-effectiveness. The protocol also improved the ability of users to target locations within a watershed, such that the spatial distribution of RWH maximized the hydrologic benefits relative to the cost. This targeting, combined with the hydrologic modeling and simulation of long-term precipitation, determined the economically-driven prioritized scenarios' impacts on the hydrologic thresholds. Visualization of the prioritization results from *PriorLID* indicated that core zones of prioritization exist for all iterative classifications based on cost-effectiveness. For fewer targeted classes (n=3), coarseness of resulting prioritization zones is anticipated, whereas increasing classes (n=25) refines the spatial targeting. These spatial distributions can be

further refined as scale is reduced (e.g., from subcatchment to parcel) for intra-subcatchment targeting; however, this requires finer-scale hydrologic models be developed and validated. The priority zones, via the Prioritization Protocol, offer an initial estimate for targeting locations and guiding analysts to these areas, since finer scale models may not be feasible for larger catchments.

Climatic regions indicated reliable reductions in both peak outflow rates and volumes for smaller, more frequent events (up to the 25.4-mm depth), which represented over 91% of all events simulated for all regions. Greater event-specific reductions were achieved for smaller depths, exponentially decreasing with depth. Overall, long-term reductions were increased for regions with greater precipitation, regardless of event duration and interevent time. This analysis indicated that RWH was incapable of providing reductions for more extreme events, such as the chubascos or Mexican storms, in the Chollas Creek watershed. That being said, these events make up a small component of the long-term record.

Uncertainty analysis of the subcatchment percent imperviousness indicated that random variations at the subcatchment-scale produced negligible watershed-scale impacts for volumes and peak flow rates. Extension of uncertainty results to RWH effectiveness found that RWH provided a buffer to the negative impacts stemming from land cover change (e.g., natural, or pervious, to impervious). Negative impacts included increases in the annual volumetric outflow for the watershed, as well as the annual peak flow rates. This buffer indicated that an 18% increase in imperviousness was required before

subcatchment volumetric outflow reductions would be reduced to the *BASE* model levels (i.e., no RWH). Thus, while the maximized LID implementation results highlight only 20% reductions in long-term watershed outflow volumes, the benefits related to the buffering capacity of RWH should also be considered at the subcatchment scale.

Analysis of cost-effectiveness for the prioritized homogeneous classes produced a positive linear trend (R^2 = 0.998) between total watershed EAC and watershed volumetric reductions for all scenarios. The relationship with annual peak flow rate had a similar, though weaker, linear trend (R^2 = 0.947). Hydrologic simulations of priority scenarios yielded a similar linear relationship between impervious area disconnection and effectiveness (L/$), further highlighting the importance of drainage area for simulated hydrologic results. However, the applicability of the protocol was restricted to a maximum subcatchment impervious area of 40 hectares, since volumetric reductions varied beyond this maximum. An R^2 of 0.67 was established for the long-term volumetric reductions in subcatchments with impervious areas less than 40 hectares. This indicates the areal limitations of not only the Prioritization Protocol, but also the hydrologic model. For watershed-scale analyses of RWH benefits, users should consider delineations of subcatchments such that impervious areas do not exceed 40 hectares.

Similarly, subcatchment EAC was more strongly related to long-term volumetric reductions when the maximum impervious area (40 hectares) was obeyed (R^2 = 0.94). Outliers in this relationship indicate the subcatchments

where added costs result in diminishing reductions. For targeting overall watershed reductions, prioritization highlighted the linear trade-off that exists between costs and hydrologic benefits. For the Chollas Creek watershed, a 6.3% reduction in long-term watershed outflow volume could be expected with $1.0MIL EAC invested, regardless of the location. This finding, in tandem with the uncertainty analysis, suggests that robust prioritization of subcatchments may not be pertinent when overall watershed reductions are targeted. However, the Prioritization Protocol was shown to improve subcatchment-scale targeting, which could be extended to finer scale prioritization.

The outcomes of the research presented in Chapters 2, 3, and 4 highlight (1) improved watershed-scale assessment of stormwater reduction benefits with RWH and (2) greater ability of users, through protocols and toolsets, to (i) identify suitable RWH locations, (ii) design individual RWH practices, and (iii) refine targeted implementation scenarios within a watershed based on cost-effectiveness. This work improves the methods of designing and assessing watershed-scale RWH frameworks by combining geospatial analysis, remote sensing analysis, hydrologic modeling and simulations, cost analysis, and uncertainty analysis. The protocols and toolsets employ publicly-available datasets and either industry standard or publicly-available software programs. Since only hydrologic and economic characteristics are targeted with this dissertation, future works can build upon it by incorporating the following:

1. Expanding Suitability Protocol metrics to include additional constraints, such as ecological, social (i.e., human health and well-being),

demographics, and urban planning and management datasets. This would improve the impact and extension of these protocols by targeting, for instance, improved urban conservation management and planning with decentralized LID.

2. Expanding the application of the protocols to more regions to assess the impact of land use and land cover variability on classification and targeting, or prioritization, accuracy.
3. Extending the MCM uncertainty analysis to other independent datasets, such as precipitation, to assess the impacts of future variability in climate on both the watershed response and the benefits, or disservices, of distributed RWH and other LID practices.
4. Expanding the applications of the Suitability and Prioritization Protocols to determine the accuracy and reliability of these proposed methodologies for other LID practices, including cisterns, green rooftops, bioretention, and permeable pavement.

5.1 References

Steffen, J., Jensen, M., Pomeroy, C. A., & Burian, S. J. (2013). Water supply and stormwater management benefits of residential rainwater harvesting in U.S. cities. *Journal of the American Water Resources Association*, *49*(4), 810-849.

APPENDIX A

SOFTWARE AND DATA SOURCES

This appendix lists the software programs and programming languages used to accomplish the work in this dissertation. It also provides an overview of the data sources for important input parameters.

A.1 Software

This section presents the software used in this dissertation. A discussion of the general purpose, available methodologies, and sources is provided for each.

ArcGIS is a geographic information system (GIS) software program that allows for map creation, compiling, visualizing, and analyzing geographic data, and managing this information as a database. Applications include spatial and temporal research. Data can be used with external software, such as MS Excel and ENVI, as well. The ArcGIS Model Builder tool offers the ability to create, edit, and manage models, or workflows, that string together sequences of geoprocessing tools (ESRI, 2011).

Website: www.esri.com/software/arcgis

BCAL Lidar Tools are a suite of open-source tools for the processing,

analysis, and visualization of lidar datasets. They are developed and maintained by Idaho State University, Boise Center Aerospace Laboratory (BCAL). They are written using IDL programming language and serve as an add-on to ENVI. Within ENVI, lidar data (as .las files) can be processed to create various outputs, including tiling of datasets, data exploration, data buffering, data filtering, and data rasterization.

Website: www.idaholdar.org/tools/bcal-lidar-tools

Building Life-Cycle Cost (BLCC), version 5.3, is software that provides economic analyses (e.g., cost-effectiveness) of buildings and building-related systems or components. It has the ability to consider numerous alternative designs with one another to rank and order the long-term benefits and costs. It calculates net savings, savings-to-investment ratios, adjusted internal rate of return, and payback period. While buildings are the primary focus of the software, it is applicable to nearly any design project that must balance higher capital investment costs with lower future operation-related costs.

Website: http://www.wbdg.org/tools/blcc.php

ENVI is an image-processing system designed to provide comprehensive data visualization and analysis for images of variable scale and type. ENVI combines file- and band-based techniques, such that processing, classification, and analysis can be carried out for both features. Inputs include large multiband data, screen-sized images, spectral plots and libraries, and image regions-of-interest. Functions include, but are not limited to, X, Y, Z profiling, image transects, linear and nonlinear histogramming and contrast stretching, color

tables, density slicing, and classification color mapping, quick filter preview, and region of interest definition and processing. Other functions include three-dimensional viewing, surface shading, image draping and animation, and geometric rectification and mosaicking. Image data can then be transferred to a final map via image-to-image and image-to-map registration, basic orthorectification, image mosaicking, and map composition. Exporting to shapefiles (e.g., ArcGIS) is facilitated.

Website: www.exelisvis.xom/ProductsServices/ENVI/ENVI.aspx

eCognition is an image-processing system designed to provide data visualization and analysis for images of variable scale and type. It differs from ENVI in that it allows for object-based classification with rule sets. Classification rule sets are a function of numerous processing options, including image segmentation and classification based on geometric, textural, spectral, height, and other characteristics. Rule sets are run as process trees, with resulting classifications exported as either raster or vector layers. Website: http://www.ecognition.com/products.

LAStools are a suite of open-source MS-DOS command line and ArcGIS plug-in available tools for the processing, analysis, and visualization of lidar datasets. They are developed and maintained by Martin Isenburg. The tools classify, tile, convert, filter, rasterize, triangulate, contour, clip, and polygonize lidar data.

Websites: www.rapidlasso.com/lastools/ and www.cs.unc.edu/~isenburg/lastools/

MS Excel is a software program within the Microsoft Office umbrella that

allows for collation, coordination, and analysis of data from multiple sources. Pivot tables are useful in coordination, filtering, and visualizing large amounts of data. For instance, extracting temporal and seasonal variations in hourly outflow data can be achieved with the use of pivot tables. MS Excel can be used with other software, including R, SWMM, ArcGIS, and the BMP and LID Whole Life Cost Models.

SWMM is a dynamic rainfall-runoff simulation model, specifically for urban areas, driven by either single event or long-term, continuous precipitation data. Runoff is generated from input precipitation applied to the subcatchments via a nonlinear reservoir method, which included overland flow routing. Subcatchments are represented as rectangular planes and characterized by area, width, slope, and imperviousness. Inputs are based on a priori knowledge of the user. Routing is achieved for both pervious and impervious subplanes, with outflow created and routed according to model development. SWMM couples the spatially lumped continuity equation with hydraulic flow equations (e.g., Manning's equation) to produce a nonlinear differential equation for the water depth. Results are simulated both as cumulative and as a time series, with recording time step determined by the user. The current version includes LID modeling components, though input is subcatchment-specific and simulated results are presented on a per unit basis in the SWMM output.

Website: www.epa.gov/nrmrl/wswrd/wq/models/swmm/

VBA, known as Visual Basic for Applications, is a programming language that enables user-defined functions, automation of processes, and other low-level

functions. VBA is built in and used with most Microsoft Office applications, including Excel and ArcGIS.

The **Water Quality Capture Optimization Statistical Model (WQ-COSM)**, version 2.0, is a Windows-based computer program that processes long-term precipitation data with catchment hydrologic parameters to determine the water quality capture volume (WQCV) for any stormwater treatment facility. The tool was developed by the Urban Watersheds Research Institute (UWRI) and Urban Drainage and Flood Control District (UDFCD). Users can specify the Rational, Horton, or Green-Ampt methods. The software provides percent and total runoff volume, percent of all runoff captured, and percent of individual storms captured in total by various WQCV basin sizes.

Website: http://www.uwtrshd.com/software/software.html

The **WERF BMP and LID Whole Life Cost Models**, Version 2.0, is a program developed to function within MS Excel. Spreadsheets allow user identification and quantification of one-time, construction, and long-term maintenance costs associated with different stormwater management options. The list of models is extensive, including retention ponds, extended detention basins, swales, permeable pavement, green rooftops, large commercial cisterns, residential rain gardens, curb-contained bioretention, and in-curb planter vaults. This software allows for the cost analysis of the different LID network options, for comparison against each other and with traditional stormwater management practices.

Website: www.werf.org/i/a/Ka/Search/ResearchProfile.aspx?ReportId=SW2R08

A.2 Data Sources

This section discusses the inputs required for successful image-based classification(s), development and validation of the hydrologic model(s), geospatial analysis of inputs for design and implementation of LID, cost estimation of LID, and geospatial analysis for prioritization of options. Table A.1 provides the pertinent details, source, and primary scale of analysis for each dataset.

Lidar point cloud data were obtained through the National Science Foundation (NSF) OpenTopography portal. Due to download size restrictions, a total of five point cloud datasets, in *.las* format, were downloaded. All returns (e.g., maximum, minimum, and intensity) were included in the returned datasets.

Orthoimagery was obtained from the National Agriculture Imagery Program (NAIP). NAIP image data were obtained through the USGS National Map Seamless Server. They can also be obtained through the USDA Geospatial Data Gateway.

Geospatial, or GIS, data were obtained from both the San Diego Geographic Information Source (SanGIS) and the San Diego Association of Governments (SANDAG) distributors. Both SanGIS and SANDAG provide users with a range of geospatial data through the Regional Data Warehouse. Datasets included land use, slopes, soil types, roads/transportation networks, storm sewer networks, stream and river networks, vegetation, flood zones, and estimations for groundwater depths.

Hydrologic data were obtained through the National Oceanic and

Atmospheric Administration (NOAA) Atlas 14 and the National Climatic Data Center (NCDC), with the Climate Data Online interactive map application. The following bullets discuss, specifically, the data sources for both design storm and long-term, continuous precipitation:

- Precipitation frequency data were obtained from NOAA Atlas 14 in 2011 and applied to create design storms. The Station Name for these data is Chollas Reservoir. The Site ID is 92-0510, at latitude (32.7333) and longitude (-117.0667) and an elevation of 131 meters. Design storm depths were obtained for the 24-hour duration storms at recurrence intervals of 1, 2, 5, 10, and 25 years. The depths were then processed into cumulative design storm events for modeling in SWMM. These events are presented in Appendix B.
- NCDC provided long-term, continuous historical precipitation data (e.g., hourly intervals) from 07/01/1948 to 07/13/2012. The Station Name for these data is San Diego Lindbergh Field, CA US. The Site ID is COOP:047740, at latitude (32.7336) and longitude (-117.1831) and an elevation of 4.6 meters. The station is approximately 7 km from the watershed outlet, though variation in climate was not expected to impact the resultant hydrologic simulations.

Table A.1: Dataset metadata and scale of analysis for the study.

Dataset	Details	Source	Primary Scale of Analysis
NAIP Aerial Imagery	1-meter resolution, 4-band (Red, Green, Blue, NIR); April 24-September 30, 2010; UTM, NAD83, Zone 11, California State Quarter Quadrangle.	NAIP	Watershed
			Subcatchment
			Parcel
Lidar	1.83-meter resolution (i.e., point spacing). Filtered layers include: bare earth, last (minimum), and first (maximum) returns.	Open Topography	Watershed
			Subcatchment
			Parcel
Land Use	Vector	SANGIS	Parcel
Slopes	Raster	SANGIS	Watershed
			Subcatchment
			Parcel
Soil Types	Vector (polygon)	SANGIS	Watershed
			Subcatchment
Roads/ Transportation	Vector (polygon)	SANGIS	Watershed
Storm Sewer Network	Vector (polyline)	SANGIS	Watershed
Stream and River Network	Vector (polyline)	SANGIS	Watershed
Vegetation	Vector (polygon); Raster	SANGIS; PBIA and OBIA Classification	Watershed
			Subcatchment
Flood Zones	Vector (polygon)	SANGIS	Watershed
			Subcatchment
Built Infrastructure	Vector (polygon); Raster	OBIA Classification	Parcel

APPENDIX B

HYDROLOGIC MODEL DEVELOPMENT, CALIBRATION, AND VALIDATION

This appendix provides the steps necessary to developing, calibrating, and validating the hydrologic model for the Chollas Creek watershed. Hydrologic modeling was accomplished with USEPA SWMM 5.0.022, a dynamic stormwater runoff and hydraulic routing software that simulates water quality, quantity, and LID controls (Rossman, 2010; USEPA, 2012). SWMM is a widely used framework suited to development of sizing guidelines for devices and programs across the catchment, subdivision, and site scales (Elliott & Trowsdale, 2007). Multiple sources of data were used to build the Chollas Creek model. To successfully calibrate and validate the model, the following bulleted steps were required for the Chollas Creek watershed:

- Delineation of the subcatchments was completed by former graduate students Pascaline Loricourt and Jennifer Steffen, and was determined through conversations with San Diego Coastkeeper and San Diego County officials. Validation of the subcatchments was provided by digital elevation model (DEM) and land use datasets, resulting in 78 subcatchments ranging in size from 0.02 – 3.06 km^2. Land surface

slopes were estimated using 0.61-m contours acquired from SanGIS (2012), ranging between 0.5% - 10.9%. Manning's roughness values of 0.20 (e.g., dense grass) and 0.009 were assigned to pervious and impervious surfaces, respectively. Pervious depression storage was representative of lawns (e.g., 0.381 cm) and impervious depression storage was set as 0.0635 cm (ASCE 1992). Finalized values for subcatchment areas can be found in Table B.1.

- Land use datasets were obtained through the Regional Data Warehouse for the 2008 temporal period. These datasets were cross-referenced with that available through the US Census Bureau, known as the Topologically Integrated Geographic Encoding and Referencing (TIGER).
- Impervious area was a user-defined parameter and was one of the parameters varied in the process of calibration and validation; however, it should be noted that the overall values were not qualitatively misrepresentative of actual conditions. Reports for the San Diego watershed stated the overall impervious area to be approximately 50%. This was confirmed by PBIA analysis, finding a 51% overall imperviousness. Final values for the subcatchment impervious areas can be found in Table B.1.
- Infiltration parameters were estimated using the soils data layer (provided by SanGIS Regional Data Warehouse). The majority of the watershed's soils were representative of Hydrologic Soils Group D.

This class of soil is associated with the following infiltration parameters for application of the Green-Ampt Equation, which was used in SWMM to drive infiltration (Rossman, 2010; County of San Diego, 2012),

  - Suction Head – 239 mm (i.e., sandy clay)
  - Conductivity – 1.27 mm per hour
  - Initial Deficit – 0.25

- Subcatchment overland flow path widths were estimated within ArcGIS by former graduate students Pascaline Loricourt and Jennifer Steffen. Final input values are provided in Table B.1.
- Subcatchment average surface slopes were estimated within ArcGIS by former graduate students Pascaline Loricourt and Jennifer Steffen. Final input values are provided in Table B.1.
- Flow routing was governed by the existing storm sewer network in the watershed. Conduit parameters (e.g., geometry, length) were extracted from Storm Sewer System GIS data provided by the SanGIS Regional Data Warehouse (2012). Conduit slopes were determined via the node elevations extracted from the storm drain network dataset (SanGIS, 2012). The storm drainage network was comprised of 151 open (e.g., natural channel) and closed (e.g., drain pipe) segments. GIS and aerial imagery datasets were used to characterize the channel geometry and lengths throughout the watershed. Confirmation was provided qualitatively with aerial imagery and topographic maps (SanGIS, 2012). Conduit roughness was set as 0.013 for circular, concrete pipes

and 0.02 for trapezoidal concrete-lined channels (USDOT, 1986; ASCE, 1992). Final values are provided in Table B.1.

- Junction invert elevations were determined with ArcGIS elevation contours and node inlet datasets provided by the SanGIS Regional Data Warehouse. Aerial imagery overlaid with the sewer network polyline and inlet node point features provided these estimates.
- Depression storage was a user-defined estimate for both the impervious and pervious land surfaces. These parameters were changed as part of the calibration and validation of the hydrologic model. Guidance for values was provided by ASCE (1992). Final values are provided in Table B.1.
- Surface roughness of subcatchments was a user-defined estimate for both the impervious and pervious land surfaces. These parameters were used in the calibration and validation of the hydrologic model. Guidance for values was provided by ASCE (1992). The resulting, final value can be found in Table B.1.
- Surface runoff routing was set to the outlet for all subcatchments, with 100% routed. This was assumed since the watershed is densely urbanized, with a large amount of directly connected impervious areas. The ability to route a percentage of impervious area to the LID within the model provided an additional level of disaggregation, which was representative of the actual conditions. To minimize flooding and system losses, surcharge and ponding depths were established at the

nodes of the largest subcatchments. This ensured that all input precipitation could be accounted for through the length of the simulation.

As continuous streamflow data were unavailable, model calibration was performed using an iterative method of extracting individual storm event results from the long-term simulations and comparing them against measured values for these events. Comparison event data were provided by annual water quality and urban runoff monitoring reports (Weston Solutions, Inc., 2007; 2010a; 2010b). Simulated peak flow rates matched the seven monitored events to within an average of 3.1%. Validation was accomplished by the same method but for a different set of measured events. These events were provided by Schiff & Carter (2007). Differences in volume and outflow rate ranged from 5% to 20% for the seven monitored events from 2006 (Schiff & Carter, 2007). These storms represented a range of event sizes and durations. A final check involved the simulation of the 100-year, 24-hour event used by the Federal Emergency Management Act (FEMA) for floodplain mapping. This simulation yielded a 5.8% difference in the peak flow rate measured upstream of the confluence of the two reaches, known as the Encanto Branch (City of San Diego, n.d.).

Discrepancies between the modeled and measured values were attributed to differences in contributing watershed area and variation in the temporal pattern of rainfall associated with each runoff producing event. Since continuously monitored streamflow data do not exist for the watershed, the resulting calibration and validation were deemed acceptable in meeting the quantification

and scenario comparison goals of the researchers. Subcatchment parameters are provided below (Table B.1.), which were used as input for the SWMM model *.inp* file.

Table B.1: Final SWMM subcatchment input parameters.

Basin	Rain Gage	Outlet	Total Area (acres)	Imperviousness (%)	Width (m)	Slope (%)	Basin	Rain Gage	Outlet	Total Area (acres)	Imperviousness (%)	Width (m)	Slope (%)
D1	1	I1	31.9	59.76	300	5	**D40**	1	I40	102	52	250	7.3
D2	1	I2	26.7	57.68	300	5.4	**D42**	1	I42	68	50.51	300	7.8
D4	1	I4	21.2	19.08	300	3	**D43**	1	I43	82	50.51	300	7
D3	1	I3	46.2	49.58	300	0.5	**D44**	1	I44	120	55.12	100	7.1
D5	1	i73	48.9	55.58	300	2.4	**D45**	1	I45	115	42.92	300	10.4
D6	1	I6	98.4	59.37	300	3.5	**D46**	1	I46	101	26.19	300	6.9
D7	1	I7	215	50.6	300	5	**D47**	1	I47	66.6	56.25	300	6.3
D8	1	I8	122	55.05	300	4	**D48**	1	I48	41.1	55.26	300	7
D9	1	I9	73.9	54.28	300	7	**D49**	1	I49	5	25	300	5
D10	1	I10	48.2	52.59	300	7.6	**D50**	1	I50	97.3	25	300	5.8
D11	1	I11	75.7	50.6	300	8.1	**D51**	1	I51	378	58.82	100	2.3
D12	1	I12	113	47.22	300	5.5	**D52**	1	I52	115	52.08	300	8.6
D13	1	I13	125	52.6	300	8.2	**D53**	1	I53	127	58.63	300	5.5
D14	1	I14	119	44	150	9.6	**D54**	1	I54	210	55.15	300	3
D15	1	I15	76.9	52.01	300	10.7	**D55**	1	I55	330	56.47	300	3.8
D16	1	I16	48.3	52.92	300	5.6	**D56**	1	I56	39.9	56.91	300	2.6
D17	1	I17	45.2	52.9	300	10.9	**D57**	1	I57	36.8	56.76	300	5
D18	1	I18	84.2	56.17	300	8.9	**D58**	1	I58	7.22	53.04	300	5.6
D19	1	I19	78.2	52.22	100	7.6	**D59**	1	I59	49.2	53.72	300	3.3
D20	1	I20	24	55.16	300	6.3	**D60**	1	I60	30.3	57.39	300	3.2
D21	1	I21	36.8	55.01	100	8.3	**D61**	1	I61	41.3	55.48	100	4.7
D22	1	I22	31.1	53.71	300	9.8	**D62**	1	I62	427	54.72	50	1
D23	1	I23	47.1	52.94	300	9.3	**D63**	1	I63	436	58.28	250	1
D24	1	I24	23.5	53.6	300	7.3	**D64**	1	I64	556	56.72	50	10
D25	1	I25	29.9	55.16	300	4.2	**D65**	1	I65	124	53.13	100	3
D26	1	I26	42.8	55.32	300	6.5	**D66**	1	I66	33.6	52.65	300	9
D27	1	I27	38.9	55.6	300	2.2	**D67**	1	I67	89.1	51.72	150	7
D28	1	I28	11.1	53.89	300	4.9	**D68**	1	I68	279	18.6	300	3
D29	1	I124	15.3	46.48	300	8.7	**D69**	1	I69	51.8	1.47	300	4.7
D30	1	I30	32.9	50.27	300	4.2	**D70**	1	I142	15.2	56.83	300	7
D31	1	I31	34.7	53.45	300	5.5	**D71**	1	I134	32.9	39.65	300	5.5
D32	1	I32	755	53.2	50	0.7	**D72**	1	I135	5	25.39	100	5
D33	1	I33	24.6	54.11	300	6.3	**D73**	1	I136	17.3	17.83	100	10.4
D34	1	I34	49.9	52.14	300	7	**D74**	1	I137	30	55.09	300	7.8
D35	1	I35	26	58.07	300	7.5	**D75**	1	I138	67.7	43.16	100	7
D36	1	I36	67.3	53.23	300	4.8	**D76**	1	I139	68.5	56.43	250	2.3
D37	1	I37	57	53.73	300	8.9	**D77**	1	I140	52.3	56.28	250	2.3
D38	1	I38	65.7	53.73	300	8.4	**D78**	1	I141	30.3	58.88	300	6.3
D39	1	i107	103	52.55	250	6.6							

B.1 References

ASCE (American Society of Civil Engineers). (1992). *Design and construction of urban stormwater management systems*. New York, NY: ASCE.

City of San Diego. (n.d.). Chollas Creek south branch implementation program. Retrieved from http://www.sandiego.gov/planning/community/pdf/chollassouthmaster.pdf

County of San Diego. (2012). Standard urban stormwater mitigation plan for land development and public improvement projects. Retrieved from http://www.sdcounty.ca.gov/dpw/watersheds/susmp/susmppdf/susmp_manual_2012.pdf

Elliott, A. H., & Trowsdale, S. (2007). A review of models for low impact urban stormwater drainage. *Environmental Modelling & Software,* 22(3), 394-405.

Rossman, L. A. (2010). Storm water management model user's manual, version 5.0. Washington, DC: EPA.

SanGIS. (2012). GIS data warehouse. Retrieved from http://www.sangis.org/download/index.html

Schiff, K., & Carter, S. (2007). Monitoring and modeling of Chollas, Paleta, and Switzer creeks, technical report 513. Retrieved from http://www.waterboards.ca.gov/rwqcb9/water_issues/programs/tmdls/docs/sediment_toxicity/SCCWRP_Final_C_P_S_Monitoring_ModelingReport.pdf

USDOT (United States Department of Transportation). (1986). *Design of roadside channels with flexible linings, hydraulic engineering circular #15*. Washington, DC: USDOT.

USEPA. (2012). Storm water management model (SWMM), version 5.0.022 with low impact development (LID) controls. Retrieved from http://www.epa.gov/nrmrl/wswrd/wq/models/swmm/

Weston Solutions, Inc. (2007). San Diego County municipal committees 2005-2006 urban runoff monitoring: Volume i – final report. Final Report prepared for County of San Diego.

Weston Solutions, Inc. (2010a). Chollas Creek total maximum daily load (TMDL) 2009-2010 water quality compliance monitoring. Final Report submitted to San Diego Regional Water Quality Control Board.

Weston Solutions, Inc. (2010b). Rain barrel/downspout disconnect best management practice effectiveness monitoring and operations program.

Final Report submitted to City of San Diego, Storm Water Department, Pollution Prevention Division.

APPENDIX C

LID DESIGN GUIDANCE AND RESOURCES

This appendix provides an overview of the methods and models used to simulate the rainfall-runoff response of catchments with RWH applied. It specifically discusses the EPA SWMM5.0.022 software and provides an example of a neighborhood-scale RWH scenario.

C.1 Introduction

Since LID practices are limited by the constraints of the site they are meant to manage, there are steps that must be considered. In developing a site or, moreover, a watershed for the application of LID either individually or as part of a larger framework, the following steps should be considered by the designer (Prince George's County, 1999),

1. Define the hydrologic control required or warranted for both the site and the overall watershed. Hydrologic controls include:
    a. Infiltration, discharge frequency, volume of discharges, groundwater recharge
2. Evaluate the site constraints, including:
    a. Available space, soil infiltration characteristics, water table,

slopes, drainage patterns

3. Screen the candidate practices available that meet the suitability criteria and determine the following:
    a. Site opportunities, site constraints, functions and limitations of integrated management practices
4. Evaluate the hydrologic performance of candidate integrated management practices in various configurations
    a. Develop a list for potential implementation, including number, size, volume, etc.
5. Select the preferred configuration and design, with the goal of:
    a. Choosing the configurations that best meet the goals of the watershed
6. Supplement with conventional controls, if necessary, such as:
    a. Determination of whether additional stormwater control is needed, identification of siting operations, consideration and design end of pipe controls

It is important to note that each LID practice has different design guideline specifics, despite the aforementioned universal recommendations for overall site development (Prince George's County, 1999).

C.2 RWH Modeling

The following sections provide brief descriptions of RWH as a stormwater management practice. Discussions of available software for modeling RWH are provided, with a primary focus on the EPA SWMM5.0.022 program. A full

presentation of modeling components for SWMM5.0.022 is provided, with a case study example of potential results for a residential neighborhood. This document was developed as a chapter in the upcoming EWRI LID Computations Task Committee's Stormwater Control Measures (SCMs) technical guidance document.

C.2.1 Description

Harvesting rainwater runoff can be divided into two categories, passive and active systems. The former include no moving parts and focus on capture via land surface modification (e.g., curb cuts, rain gardens, rainscapes, and permeable pavement). Active systems provide containment structures with the goal of extending temporal use. For this report, active rainwater harvesting techniques are highlighted. Rainwater harvesting (RWH) intercepts stormwater runoff generated by impervious surfaces, such as household rooftops, to meet end goals. These include reductions in runoff volumes, time to peak flow rates, water quality improvement, and supplementation of water demands. End uses determine system complexity, ranging from simple to intricate, and thereby the cost of the system.

C.2.2 System Components

The primary components of RWH include the catchment surface, a conveyance network, the storage unit, the outflow distribution network, and storage unit stabilization considerations. Catchment surfaces include rooftops, parking lots, and any impervious surface intercepting rainfall. Conveyance

components include gutters, downspouts, and piping for movement of runoff to the collection unit(s). Storage units are available in a range of capacities. Rain barrels are smaller (e.g., 50-100 gallons, or 189-379 liters) and typically placed aboveground, whereas cisterns have greater capacities (e.g., greater than 100 gallons, or 379 liters) and can be placed either above or below ground. Outflow considerations include discharge orifice(s), overflow piping, discharge piping (e.g., underdrain-mediated outflow), and the location of discharge. Discharge locations should direct flow away from building foundations and prevent nuisance flows to adjacent properties. Unit stabilization must be provided to address the added weight of stored water, which is more important for cisterns.

Additional components are directly a function of system complexity, including prestorage bypass and treatment, pump(s), and dual piping network(s). When reuse of stored rainfall is an end goal, owners must consider the quality and distribution of the water. Prestorage considerations target water quality with pretreatment measures. This includes the diversion, or removal, of the first flush volume. Conventional guidance suggests a 50% reduction in contamination with every mm of rainfall depth flushed (Martinson & Thomas, 2005) and flushing one to two gallons per 100 square feet of catchment area (e.g., 0.41-0.81 mm). Additionally, filtration via screening removes particulates and prevents future clogging. Pumps must be considered when movement of water is required. Local plumbing codes provide accurate guidance on piping requirements regarding both potable and nonpotable applications.

C.2.3 Benefits and Limitations

Research indicates increasing stormwater runoff volumetric reductions with increasing unit capacity and runoff routing to pervious areas (e.g., downspout disconnection) (Brander et al., 2004; de Graaf & der Brugge, 2010; Spatari et al., 2011; Jia et al., 2012). Water quality improvements have also been noted for individual applications. In general, advantages of RWH include (Prince George's County, 1999),

- Source control capture of runoff,
- Feasible implementation as part of a larger BMP treatment train,
- Low maintenance requirements,
- Less reliance on soil infiltration rates,
- Reductions in homeowner water bills (Woods-Ballard et al., 2007; Foraste & Hirschmann, 2010)
- Supplementation of potable water demands, such as irrigation and toilet flushing (Mitchell et al., 2005a; 2005b; Rosemarin, 2005; Fletcher et al., 2007; Mitchell et al., 2007; Foraste & Hirschman, 2010), and
- Greater ability to retrofit existing, space-limited areas.

Limitations of RWH include storage capacity restrictions (e.g., rain barrels provide less storage), a lack of direct water quality treatment, infrastructure requirements (e.g., pumps, valves) for complex end uses, an increased vector potential when maintenance is neglected, and implementation and design may require building permits, fulfillment of government code, or geotechnical considerations.

C.2.4 Design and Implementation

Numerous sources of design guidance exist and vary by region for green infrastructure practices. Increasingly, states and municipalities consider RWH for its potential to meet stormwater reduction and demand supplementation goals. For instance, the Texas Development Water Board (2010), Virginia Department of Health (2011), and Minnesota Pollution Control Agency (2008; 2013) provide comprehensive documents regarding the applicability, technical constraints, and considerations related to RWH. Another work, the *Low-Impact Development Design Strategies: An Integrated Design Approach* by Prince George's County (1999), was one of the first to address LID in detail. Additional resources are provided in the section Resources.

C.2.5 Maintenance

While RWH has low maintenance requirements, such activities ensure long-term reliability and vary with climatic regime. These include twice annual inspection for adequate operation (e.g., no leaking or broken parts); annual and seasonal cleaning of gutters, conveyance systems, screens, and internal tank to prevent clogging and control vectors; regular drainage of captured water to increase capacity for future storm events, and; annual system winterization to prevent freeze damage (if applicable).

C.3 Computational Methods for RWH Modeling and Simulation

This section provides an overview of the computational methods available for modeling, simulating, and/or analyzing the implementation of RWH as a stormwater control measure. The individual and watershed scales serve as separate foci.

C.3.1 Individual Scale

Numerous methods exist to assess RWH performance at individual scales (Ward et al., 2010). In general, designs balance regional climatic variables and household demands with water supply. Variables include the catchment area, storage size, and end uses. The following are four examples of various models available for site-scale design and analysis of RWH:

- The Rainwater Harvester (RH), version 2.0, released by researchers at North Carolina State University assists in sizing RWH as a function of rainfall data and demand, or usage. Outputs include cost summary and use statistics. Available at: http://www.bae.ncsu.edu/topic/waterharvesting/model.html.
- The RainCycle (RC) is a Microsoft Excel spreadsheet-based simulation program that provides whole-life costing analysis with hydraulic simulations of water fluxes (e.g., supply and demand). A freeware is available. Available at: http://sudsolutions.co.uk/raincycle.htm.
- The Storm Water Calculator is another Microsoft Excel spreadsheet-based program used to determine the quantity of stormwater that will

need to be managed to meet permit requirements for the City of Santa Rosa, California. This software accompanies the City of Santa Rosa and County of Sonoma *Storm Water Low Impact Development Technical Design Manual* (2011). Available at: http://ci.santa-rosa.ca.us/departments/utilities/stormwatercreeks/swpermit/Pages/swLIDtechManual.aspx.

- The Rainwater Analysis and Simulation Program (RASP) is a MATLAB-based program developed to assess single-scenario operation of RWH, with reliability metrics relating water supply and runoff capture. This aids in sizing RWH units to achieve runoff reduction and demand supplementation goals (Sample et al., 2013).

C.3.2 Watershed Scale

The application of source controls, such as RWH, within the greater watershed is an area of increasing interest. Improvements in software to assess the hydrologic impacts of distributed LID are increasing. The following are two examples of models used in the design and testing of catchment-scale RWH applications:

- The EPA Storm Water Management Model (SWMM), version 5.0.022, a widely used dynamic rainfall-runoff model, now includes explicit modeling of LID controls. These include porous pavement, rain gardens, green roofs, street planters, rainwater harvesting, infiltration trenches, and vegetative swales. LID controls are represented at the subcatchment scale. SWMM requires users to calibrate and validate

watershed parameters such that simulations are reliable and accurate. The model is capable of processing both individual events and long-term continuous precipitation. Available at: http://www.epa.gov/nrmrl/wswrd/wq/models/swmm/.

- The EPA National Stormwater Calculator (SWC), which uses SWMM as its computational engine, offers a simple calculation of LID hydrologic impacts for uniform, small sites (e.g., recommended up to several dozens of acres) within the United States. Simulations of hydrologic reductions from LID are based on user-defined soil type, landscape, land use, and historical precipitation datasets. As of October 2013, the ability to link the SWC with future climate scenarios had not been released. Available at: http://epa.gov/nrmrl/wswrd/wq/models/swc/.

C.4 SWMM5.0.022 LID Editor

In SWMM, RWH is represented using the LID Control Editor, located under the Hydrology tab. Within the LID Control Editor, the user defines the type of LID, which is Rain Barrel in this case. The process layers for RWH encompass both storage and underdrain, representative of the capacity and the drainage components. For the Storage layer, the only input is the height of the unit (*D*), in inches (in) or millimeters (mm). A typical height for a 227-liter rain barrel is 914 mm. Cistern heights will vary, as a function of the capacity. The Underdrain layer governs the temporal outflow parameters, with the drain coefficient (*C*), drain exponent (*n*), drain offset height (H_d), and drain delay.

The drain delay is determined by users and establishes the consecutive dry conditions time (hours) that must elapse before the RWH unit is allowed to discharge. This establishes the opening of units after a storm event as a simple temporal constraint related to the interevent precipitation characteristics. All other underdrain parameters simulate the outflow (*q*) through a simplified submerged orifice (Eq. 1), in unit depth per hour (in/hr or mm/hr). This outflow is normalized to the areal footprint of the unit. If no underdrain exists (i.e., units capture water and overflow but have no underdrain-mediated flow), then *C* is set to zero.

$$q = C\left(h - H_d\right)^n \quad \text{.....(1)}$$

To understand and quantify the parameters influencing unit outflow, users should first establish the required time to drain the unit (*T*), in hours. This temporal variable is different from the drain delay period. The *T* establishes how quickly the unit will drain once allowed to open. This value is used with Eq. (2) to estimate the *C* value for Eq. (1). It is important to note that Eq. (2), as presented, is specific to a circular orifice (i.e., $n = 0.5$). The parameter H_d represents the height of the outflow drain from the bottom of the unit (in or mm). Last, *h* is a dynamic parameter, changing with the volume of water stored over time (in or mm) and never exceeding the maximum depth, which is the height of the unit.

$$C = \left(2\sqrt{D}\right)\Big/T \quad \text{.....(2)}$$

Using C, h, H_d, and n, SWMM simulates the outflow through the underdrain (in/hr, mm/hr) once the unit is allowed to open, as dictated by the drain delay time. Users can enter the information for the LID Control Editor, located in the Hydrology tab.

LID Controls are manually added by users for each subcatchment desired. This entails opening the subcatchment editor and selecting the LID Controls drop-down. This opens a pop-up where users must Add the desired control(s). After clicking Add, users are prompted with the LID Usage Editor. This is specific to each subcatchment and allows users to determine the extent of LID control. Extent is a function of the number of replicate units, the area of each unit, the percent of impervious area treated, and the outflow discharge location (e.g., return to pervious or directly to the outlet). This establishes the desired drain time for units. A screenshot of the model interface (Fig. C.1) illustrates where users will find and apply LID parameters.

As a note, the percent of impervious area treated is dependent on the subcatchment characteristics and must account for the ratio of rooftop area to impervious area per subcatchment. In general, the cumulative percent of impervious area treated per subcatchment may not exceed 100%. The Usage Editor allows users to establish the flow routing location via the Send Outflow to Pervious Area button. Checking this sends LID mediated flow back to the pervious area of the subcatchment while not checking routes it directly to the subcatchment outlet node. Pervious routing allows for further losses (e.g., evaporation, infiltration). This is represented in the *.inp* file as either a 0 or a 1. If

RWH-routed water is assumed to supplement irrigation uses, it is justifiable to route it back to the subcatchment pervious area. The other parameters, LID occupies full subcatchment, top width of overland flow surface of each unit, and percent initially saturated, do not apply to RWH and, therefore, should remain as the default values.

Last, users have the option to create a detailed report file for each subcatchment LID control. This report (as a tab-delimited *.txt* file) provides the individual temporal LID unit flow routing results. These are recorded at the same rate as the reporting time step. Results include total inflow (in/hr), total evaporation (in/hr), surface infiltration (in/hr), soil percolation (in/hr), bottom infiltration (in/hr), surface runoff (in/hr), drain outflow (in/hr), surface depth (in), soil/pave moisture, and storage depth (in). The contents of the detailed report are more detailed than those presented in the Status Report, which provide a per unit summary of the LID water balance at the subcatchment level. The Status Report's LID Results section presents the total inflow, evaporative losses, infiltration losses, surface outflow, drain outflow, initial storage, and final storage results as depths per the LID footprint area. To obtain the total volume of runoff reduced, in gallons, at the subcatchment level (i.e., cumulative removal), the user should apply Eq. (3).

$$V_{subcstchment} = 7.481 \times n_{LID} \times \left(depth / footpr\,\text{int}\right) \times Area_{unit} \quad \text{.....(3)}$$

Eq. (3) consists of the total number of LID implemented within the subcatchment (n_{LID}), the simulated result of depth per areal footprint (in) (found in

the Summary Report), the area of the unit (ft^2), and a conversion from cubic feet to gallons. This results in the $V_{subcatchment}$, which is the cumulative volume (gallons) mediated by the LID control implemented. In the case of RWH, the surface outflow column represents all flow that passes through the unit as overflow, while the drain outflow column represents all flow that passes through the underdrain (i.e., captured). The underdrain flow is subject to the drain delay and Eq. (1), while overflow is not. See the simplified schematic (Fig. C.2) for flow routing using RWH in SWMM.

C.4.1 Model Simulations

To assess the impacts of the passive RWH programs on the local hydrology, SWMM models should be driven by long-term, continuous precipitation data. Users establish the climatic conditions in the Options and Rain Gage layers. For this application, an 8.45-hectare residential watershed was chosen in Murray, Utah, USA. A total of three SWMM models were created to provide an analysis of the impacts of RWH, implemented as either rain barrels (227-liter) or cisterns (6,375-liter), on the stormwater runoff for the residential catchment. Manual delineation and subsequent quantification of impervious surfaces, including household footprints, were completed for each parcel. These values represented current conditions within the watershed at the parcel level. Subcatchment percent imperviousness ranged from 16% to 65% (average 36%) and was representative of all impervious surfaces on the property (e.g., rooftops, driveways, and sidewalks). Rooftop area, as a percent of the subcatchment impervious area, was then calculated with household footprints to determine the

percent of subcatchment area directed to, or managed by, the LID practice. In this application, rooftops accounted for 60% of the cumulative impervious area and 21.4% of the total watershed area. In essence, 60% of the impervious area was disconnected from the impervious area. For RWH, this is referred to as downspout disconnection.

A model representing the existing conditions (*BASE)*, in which no RWH was implemented, provided the basis for comparison with RWH scenarios. The Salt Lake City International Airport (COOP: 427598) historical precipitation dataset was used for long-term, continuous simulations (1950-2010). These datasets can be acquired from the National Oceanic and Atmospheric Administration's (NOAA) National Climatic Data Center (NCDC) portal (NCDC, 2013). Necessary corrections to precipitation data file format should be made to ensure the model runs correctly. Research suggests subdaily (i.e., hourly or finer) precipitation time steps for hydrologic simulations used to estimate RWH performance (Coombes & Barry, 2007; Mitchell et al., 2007; Burian & Jones, 2010).

C.4.2 Results

For the residential, case study watershed, the following results were obtained by modeling the 227-liter rain barrels (*227Liter)* and 6,735-liter cisterns (*6375Liter)* at each household (n=100). Simulations driven by continuous, long-term (e.g., hourly) precipitation (1950-2010) indicate 58% reductions in long-term runoff volumes for both *227Liter* and *6375Liter* scenarios (Table C.1). Average annual reductions follow a similar trend for the case study watershed, with an

equivalent average reduction of 58% (range 46% to 59%).

When the RWH discharge location is changed from pervious (i.e., checked) to the subcatchment outlet (i.e., unchecked), the overall simulations indicate negligible volumetric reductions with both RWH scenarios versus the base case. This is a function of not allowing disconnected rooftop runoff to infiltrate, reinforcing that this disconnection to pervious area provides the actual volumetric reductions. Flow rate timing changes are more pronounced when routing to impervious, especially for larger RWH volumes, since all RWH-mediated runoff will exit the system as surface flow and not as infiltrated, subsurface loss. The flow frequency at the outlet for the *BASE* model is 7.3%, whereas the *227Liter* models simulate 6.4% and 18.3% for pervious and impervious routing scenarios and the *6375Liter* models simulate 6.4% and 42.6% for pervious and impervious routing scenarios. Percent differences with the *BASE* are minor for pervious area routing while routing to the outlet results in flow frequency differences of 43% and 71% for the *227Liter* and *6375Liter* model simulations, respectively. Greater flow losses occur when routing to impervious areas, hence the discrepancy in runoff and outflow volumes for the LID scenarios (Table C.2).

Design storm simulations provide an instantaneous estimate of potential reductions stemming from RWH. This differs from long-term, continuous analyses in that antecedent conditions are not considered. Additionally, subsequent precipitation events do not occur outside of that included in the design event. The former implication influences the amount of potential infiltration

while the latter results in consistent opening of the RWH units, based on the drain delay time. Therefore, to quantify the long-term impacts of RWH, users should choose long-term, continuous precipitation.

In terms of average annual runoff time (days), both scenarios simulate a long-term reduction of 17%. This correlates to runoff conditions for an average of 14 days per year (range 9 to 26 days), compared with a pre-LID annual average of 17 days (range 11 to 30 days). For monthly analysis, runoff-producing events are reduced with RWH by an average of 14% (range 2% to 23%). This is a function of the season, with the least reductions occurring in the following two groups: a. April and May (4%, 3%), and b. August and September (2%, 3%). Remaining months provide an average of 20% fewer runoff-producing events.

C.5 Conclusions

A one-way between subjects analysis of variance (ANOVA) was conducted to compare the effects RWH unit volume had on annual runoff volumes for the three scenarios tested, including the base. ANOVA assumes independent, normally distributed datasets, with equal variances among the populations. The null hypothesis states there is no difference between the dataset means. The Tukey HSD post hoc test was applied to the ANOVA results in which the null hypothesis was rejected. This determined which groups differed significantly. There was a significant effect of RWH storage capacity on annual average runoff volumes (MGAL) at the $p<0.05$ level for the three model conditions [$F(3,177)=247.6$, $p=5.2E-52$]. Post hoc comparisons using the Tukey HSD test indicated that the mean score for the base model ($M=2.55$, $SD=0.62$)

was significantly different than both RWH conditions, *227Liter* (M=1.06, SD=0.26) and *6375Liter* (M=1.08, SD=0.07). There was no difference between means of the RWH scenarios for the conditions tested.

Reductions in the peak annual outflow rates match those for runoff volumes, with long-term averages of 52% and 56% for the *227Liter* and *6375Liter* scenarios, respectively. It should be noted that these pre-LID peak flow rates range from 0.034 CMS to 0.58 CMS. Thus, the results for this catchment (at 8.45 hectares and primarily residential) should not be extended to other watersheds with differing land use and land cover compositions. Simulation fluctuations can be expected from variations in other parameters governing the operation of RWH units. These include the drain delay time, the drain coefficient, the LID-mediated catchment area, and the precipitation regime (i.e., climate).

C.5.1 Model Improvements

As SWMM, version 5.0.022, currently exists, the application of passive RWH system is limited in its ability to model variable demands placed on individual RWH units. The addition of a demand driven option to the RWH LID Control, representative of a diurnal demand pattern, would add benefit to the SWMM model. Opposite of head-driven discharge, RWH outflow would be governed by a time series, representative of variable uses. These include indoor nonpotable functions, such as flushing toilets and washing laundry. Research indicates a conservative estimate of household demand supplementation is achievable by applying the Yield After Spillage (YAS) algorithm (Fewkes, 2000). This would open up the possibility for SWMM to produce a postanalysis water

savings estimate, or efficiency, for RWH at the various levels of analysis.

C.6 Resources

This section provides resources that present, in detail, the applicability, site and design considerations, limitations, operation and maintenance considerations, effectiveness, and cost considerations for RWH practices in regions throughout the United States.

- Prince George's County (1999), pp 4-18 – 4-19.
- CASQA (2003), Website: http://www.cabmphandbooks.com/Documents/Development/SD-11.pdf
- Southern California Stormwater Monitoring Coalition (2010), pp 114-124.
- County of San Diego (2007i, 2007ii), pp 64-65; Appendix 4, pp 84-86.
- US EPA (2013). *Rainwater Harvesting: Conservation, Codes, and Cost Literature Review and Case Studies*. EPA-841-R-13-002.

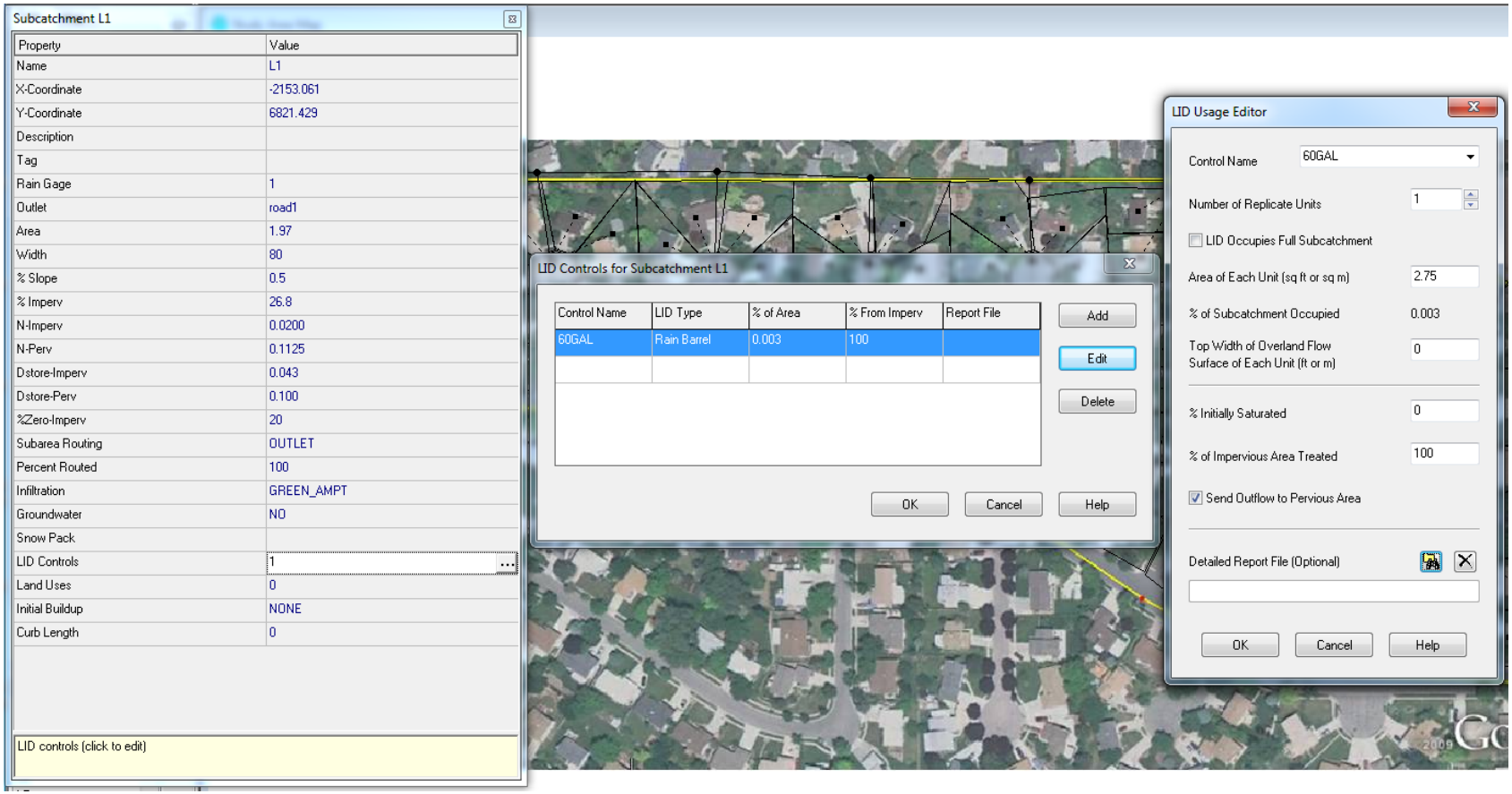

Figure C.1: SWMM screenshot, with arrows indicating the process by which users enter LID Usage data at the subcatchment level.

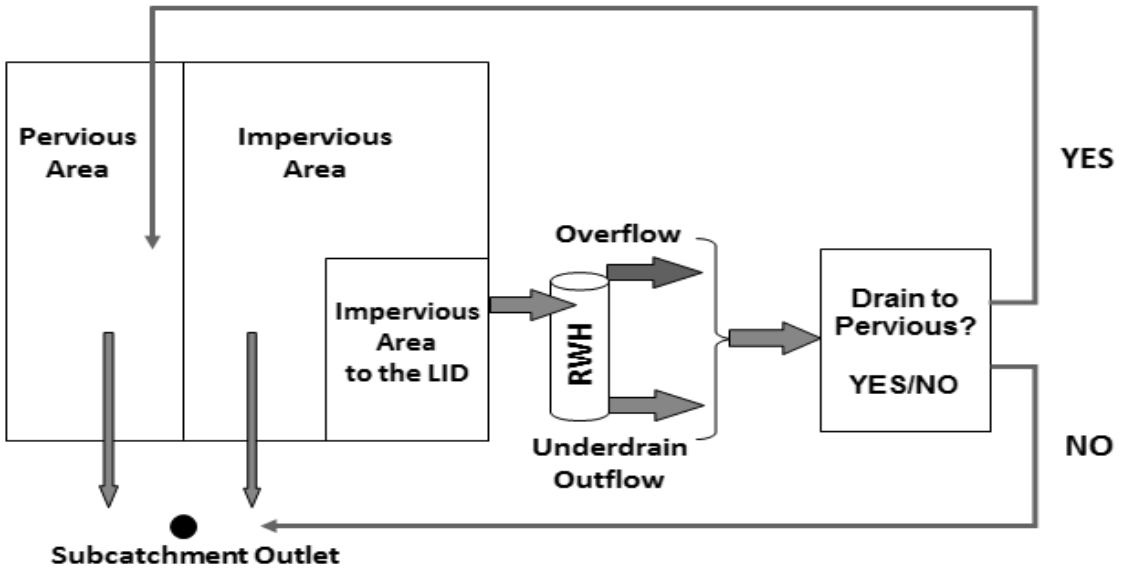

Figure C.2: SWMM5.0.022 flow routing for RWH, with underdrain outflow established via the drain delay and Eq. (1) functions and drain outflow driven by head (Walsh et al., 2014).

Table C.1: Overall, long-term simulation results for Murray, UT. LID-mediated flow is directed to subcatchment pervious areas for further infiltration (i.e., downspout disconnection).

Scenario	Precipitation	Evaporation	Infiltration	Runoff	Outflow Volume	Peak Outflow Rate	Average Outflow Rate
	1,000 mm	1,000 mm	1,000 mm	1,000 mm	ML	CMS	CMS
BASE	23.3	1.94	15	6.4	544.7	0.58	0.0051
227Liter	23.3	1.93	18.7	2.7	228.1	0.57	0.002
6375Liter	23.3	1.94	18.7	2.7	230.2	0.58	0.0022

Table C.2: Overall, long-term simulation results for Murray, UT. LID-mediated flow is directed to the subcatchment outlet, without further potential for infiltration (i.e., directly connected impervious areas).

Scenario	Precipitation	Evaporation	Infiltration	Runoff	Outflow Volume	Peak Outflow Rate	Average Outflow Rate
	1,000 mm	1,000 mm	1,000 mm	1,000 mm	ML	CMS	CMS
BASE	23.3	1.94	15	6.44	544.3	0.578	0.0051
227Liter	23.3	1.94	15	6.45	545.1	0.58	0.002
6375Liter	23.3	1.93	14.9	6.26	551.2	0.577	0.0008

C.7 References

Brander, K., Owen, K., & Potter, K. (2004). Modeled impacts of development type on runoff volume and infiltration performance. *Journal of the American Water Resources Association*, *40*(4), 961-969.

Burian, S., & Jones, D. (2010). National assessment of rainwater harvesting as a stormwater practice: Challenges, needs, and recommendations. Proceedings from: *Low Impact Development Conference 2010*. San Francisco, CA: AWRA.

Coombes, P. J., & Barry, M. E. (2008). The relative efficiency of water supply catchments and rainwater tanks in cities subject to variable climate and the potential for climate change. *Australian Journal of Water Resources*, *12*(2), 85-100.

De Graaf, R., & Der Brugge, R. (2010). Transforming water infrastructure by linking water management and urban renewal in Rotterdam. *Technological Forecasting and Social Change, 77*, 1282-1291.

Fewkes, A. (2000). Modelling the performance of rainwater collection systems: Towards a generalized approach. *Urban Water*, *1*(4), 323-333.

Fletcher, T. D., Andrieu, H., & Hamel, P. (2013). Understanding, management and modelling of urban hydrology and its consequences for receiving waters: A state of the art. *Advances in Water Resources*, *51*(0), 261-279.

Foraste, J. A., & Hirschman, D. (2010). A methodology for using rainwater harvesting as a stormwater management BMP. Proceedings from: *ASCE International Low Impact Development Conference, Redefining Water in the City*. San Francisco, CA: ASCE.

Jia, H., Lu, Y., Yu, S. L., & Chen, Y. (2012). Planning of LID-BMPs for urban runoff control: The case of Beijing Olympic Village. *Separation and Purification Technology, 84*, 112-119.

Martinson, D., & Thomas, T. (2005). Quantifying the first-flush phenomenon. Proceedings from: *12th International Rainwater Catchment Systems Association Conference*. New Delhi, India: Conventry.

Mitchell, V. G., McCarthy, D. T., Deletic, A., & Fletcher, T. D. (2005a). Development of novel integrated stormwater treatment and reuse systems: Assessing storage capacity requirements. Institute for Sustainable Resources Report 05/01, Monash University.

Mitchell, V. G., McCarthy, D. T., Deletic, A., & Fletcher, T. D. (2005b). Optimising

storage capacity for stormwater utilisation. Proceedings from: *10th International Conference on Urban Drainage*. Copenhagen, DK.

Mitchell, V. G., Deletic, A., Fletcher, T. D., Hatt, B. E., & McCarthy, D. T. (2007). Achieving multiple benefits from stormwater harvesting. *Water Science and Technology, 55*(4), 135-144.

Prince George's County, Maryland. (June 1999). Low-impact development design strategies: An integrated design approach. Retrieved from http://water.epa.gov/polwaste/green/upload/lidnatl.pdf.

Rosemarin, A. (2005). Sustainable sanitation and water in small urban centres. *Water Science and Technology, 51*(8), 108-118.

Sample, D., Liu, J., & Wang, S. (2013). Evaluating the dual benefits of rainwater harvesting systems using reliability analysis. *Journal of Hydrologic Engineering*, *18*(10), 1310-1321.

Spatari, S., Yu, Z., & Montalto, F. A. (2011). Life cycle implications of urban green infrastructure. *Environmental Pollution, 159*, 2174-2179.

Ward, S., Memon, F. A., & Butler, D. (2010). Rainwater harvesting: Model-based design evaluation. *Water Science & Technology*, *61*(1), 85-96.

Woods-Ballard, B., Kellagher, R., Martin, P., Jefferies, C., Bray, R., & Shaffer, P. (2007). *The SUDS manual*. London, UK: CIRIA, Classic House.

APPENDIX D

PROTOCOL APPLICATION GUIDELINES

This appendix provides guidelines for the application of both the Suitability and Prioritization Protocols, including the toolsets: *LIDSS*, *QA*, *RWHA*, and *PriorLID*. The following sections provide a summarized list of steps required to successfully apply the Suitability and Prioritization protocols. In addition, the steps for assessing the uncertainty and accuracy of the individual components are discussed.

D.1 Suitability Protocol

The Suitability Protocol follows a workflow (Fig. D.1) requiring users to process both lidar and spectral datasets prior to the application of classification methodologies and geospatial analysis of results. Using Fig. D.1 as a reference, the following steps are required to successfully apply the Suitability Protocol, beginning with a general overview:

1. Suitability Protocol Overview: The protocol incorporates the classification of watershed conditions using publicly-available datasets and, combined with the toolsets created (*LIDSS*, *QA*), improves the ability and accuracy of targeting of site-suitable LID practices based on

user-defined constraints. These constraints include slopes, land use, land cover, soils, and floodplain zones. The potential for expansion of layers to include more constraints is also possible. The creation of a *.dbf* file contains the locations and areas specific to the LID constraints chosen, which can be assessed using the Prioritization Protocol's *RWHA* toolset. Based upon the user's choice of LID and the imported *.dbf* file from the *LIDSS* toolset, users can size individual LID units as a function of any precipitation depth (e.g., WQCV event depth). The result is a subcatchment-by-subcatchment summation of the total number of units and related characteristics (e.g., areal footprint, height, drainage coefficient, drainage delay time, underdrain height, and discharge location). These data are then imported into the user-uploaded base SWMM *.inp* file to model the LID practices for the scale chosen (e.g., subcatchment).

2. Process lidar datasets: Since a high-resolution image (e.g., 1-meter) is necessary for delineating specific classes present within the heterogeneous urban region, the need to address within-class confusion can be met with the inclusion of lidar data. Lidar data improve the extraction of elevation and attribute height information to discriminate man-made structures from natural objects (Hartfield et al., 2011). Lidar point cloud datasets (*.las* files) can obtained from the Open Topography, or any state or federal data repository, and merged using BCAL Tools and LAStools. For this research, a methodology

similar to Shiravi et al. (2012) was applied to process lidar datasets, which contained multiple returns. Lidar datasets should processed to separate the minimum (i.e., last), maximum (i.e., first), and bare earth returns. These points are then used to extract a raster surface for use within ENVI and eCognition. If the bare earth raster contains too many No Data and erroneous points, the elevation contours polyline (e.g., 0.5-meter resolution) can also be used to generate a bare earth raster with ArcGIS. To ensure raster datasets are aligned properly, image-to-image orthorecitification can be applied using ENVI.

3. ENVI processing of datasets: Using methods similar to Zhu et al. (2012), perform band math on the processed lidar rasters, DTM and DSM, to obtain the nDSM. Height filtering can also be carried out to remove low ground objects such as cars, leaving only objects of targeted heights (e.g., houses and trees). The height chosen is a function of both the data and the user's choice of threshold. Differentiation of vegetation from buildings can be improved with band indices, such as the NDVI. This is calculated on the spectral dataset (e.g., NAIP orthoimagery) using the NIR and Red bands (Rottensteiner et al., 2003). Next, the processed NDVI and lidar datasets can be used to differentiate natural from manmade structures with greater height and NDVI values for trees (Zhu et al., 2012). To improve the inclusion of texture in the data (i.e., smoothness or roughness of a surface), the Co-occurrence methods of Variance and Entropy can be included.

Once preprocessing has been completed, a layer-stacked image band can be created for all previously mentioned datasets.

4. Pixel-Based Image Analysis: First, users are required to delineate regions of interest (ROIs) that represent both training and reference (i.e., accuracy assessment) goals. For training, a minimum of 20 to 30 ROIs per class should be delineated, following recommendations by Van Genderen & Lock (1977). This is done to ensure between 85% and 90% classification accuracy with a 0.05 confidence. For reference ROIs, a minimum of 50 sites per class is recommended to provide sound statistical analysis (Congalton & Green, 1999). Users can then apply the classification algorithm of choice. This choice is a function of the datasets and needs of the analyst. Classification is then carried out on the layer stacked image with the training ROIs for the user-defined classes. Anderson et al. (1976) should be used as guidance in choosing classes.
5. Object-Based Image Analysis: With spectral, height-filtered, and parcel thematic layers, eCognition can be used to perform OBIA. Users are required to create a customized process rule set for their respective datasets. This is accomplished through the process of trial-and-error such that targeted features are accurately classified. With RWH, the targeted features are households and, specifically, rooftops. For heterogeneous, complex areas (i.e., urban centers), a wide range of rooftops, represented by the dataset values, should be accounted for.

6. Export Classifications to ArcGIS: Classified thematic map components can be sent to ArcGIS for visualization and geospatial assessment either as vector or raster datasets. In ENVI, the Classification to Vector and Vector to Shapefile tools can be used. In eCognition, results can be exported as both data types. Users should indicate whether to export one class per layer or multiple classes per layer. This is important for large datasets, since exporting to ArcGIS can be time intensive. Classification layers can then be imported into ArcGIS and assessed against the background imagery for qualitative analysis of the classification(s).
7. *LIDSS* Tool: In ArcGIS, users are prompted to upload classification layers and constraining datasets. These include soils, slopes, land use, floodplain and flood zones, and land cover. These watershed parameters (i.e., constraints to suitability of LID implementation) can then be applied to the *LIDSS* toolset. *LIDSS* then allows users to establish constraint values, including the maximum allowable slope (entered as a degree), the targeted land use type (e.g., Residential, Commercial/Industrial, etc.), the maximum allowable flood risk (e.g., 100-year Floodplain, 100-year Floodway), and the targeted soils (e.g., Hydrologic Soils Types A, B, C, or D). Running *LIDSS* results in a quantifiable framework of suitable locations specific to the user-defined constraints (e.g., soils, slopes, land use, land cover). Specific parameters include drainage areas, parameters, unique location

identifiers, and subcatchment identifiers. After having successfully run for the user's constraints and datasets, output database files (*.dbf*) are exported to the user-defined folder with the area, perimeter, unique identifier (e.g., building centroid location, parcel identifier, building identifier), and subcatchment identifier. These are representative of each extracted framework and are specific to the constraints identified. Further analysis of the *.dbf* is possible in Microsoft Excel.

8. Quality Assessment: The first step in assessing the accuracy of the Suitability Protocol is with the classification results. PBIA classifications are assessed with confusion matrices while OBIA results must be assessed with areal-based methods. PBIA accuracy is assessed with the previously delineated reference ROIs (different from the training ROIs). Within ENVI, users can quickly assess the accuracy by building a confusion matrix that is a function of the reference ROIs and the classified image. Overall, user's, and producer's accuracies are provided with this matrix, indicating the accuracy of the results. For OBIA results, quality assessment can be carried out using the *QA* toolset developed with this dissertation. Prior to its application, the user must perform the following tasks: (1) randomly distribute sample points throughout the area of analysis for a total of 50 sites (n=50), (2) buffer the random points with a justifiable distance (e.g., 100 meters), (3) qualitatively assess the buffered sites to ensure overall watershed conditions are represented, and (4) manually delineate targeted

feature areas using the spectral imagery dataset. Manually delineated objects represent the validated classes within each random sample site for the entire classification area. *QA* requires users to upload the classification dataset (as vector), the validated dataset, and the sample site dataset. With this completed, *QA* quantified the true positive, false negative, and false positive areas. Results are then presented as a confusion matrix, which is similar to PBIA except as a function of the area-specific objects rather than pixels. A minimum 85% accuracy is targeted with the Suitability Protocol for the overall watershed.

D.2 Prioritization Protocol

The workflow for the Prioritization Protocol is provided in Fig. D.2. This includes (1) the development, calibration, and validation of a hydrologic model that represents the targeted watershed area, (2) the establishment of economic and hydrologic thresholds, (3) the sizing, modeling, and simulation of LID practices based on Suitability Protocol results, (4) cost estimation and analysis, and (5) geospatial distribution and analysis of previous results (e.g., hydrologic, economic). The following steps were required to successfully apply the Prioritization Protocol:

1. Development, calibration, and validation of the base hydrologic model:

   A hydrologic model representing the targeted study area should be created using the pertinent resources (see Appendix A for an example workflow required to develop, calibrate, and validate a hydrologic model). This hydrologic model serves as the basis upon which both

uncertainty analysis and LID scenarios will be implemented, as per the results of the Suitability Protocol and the Prioritization Protocol. As such, no LID practices should be implemented if the impact of LID is targeted.

2. Hydrologic simulations: Hydrologic simulations should be completed for the base model previously developed and validated. These results serve as the framework for comparison with future scenarios that are adapted based on extracted suitable LID results. All hydrologic model permutations should be driven by continuous, long-term precipitation to assess the impacts of the LID on the watershed hydrologic response. All hydrologic model files (*.inp* and *.ini* for SWMM) should be saved to a unique folder for future batch simulation and analysis. For reference, the base model should be named *BASE*, or similar, to differentiate from LID-adapted permutations.
3. Establishment of thresholds: To frame prioritization, thresholds should be developed for both hydrologic and economic aspects of the analysis. These are based on the maximum reduction and maximum cost for the watershed, based on the Suitability Protocol and *RWHA* results. Hydrologic thresholds, which focus on the subcatchment and overall watershed scales, can be assessed as a function of any of the following:
    a. Reductions in the stormwater runoff volumes for long-term and annual time frames

b. Dampening of the peak flow rates for annual time frames, and/or

c. Capture of annual events

d. Stormwater runoff volumes and flow rates can be assessed for simulations driven by both long-term continuous and design storm precipitation events. The point of hydrologic analysis for this study is the watershed outlet, which is where the municipality would be focusing; however, this can vary based on the objective of the user. For instance, this study establishes the range of hydrologic thresholds as: A. 2.5%, B. 5%, C. 10%, D. 15%, and E. maximum reductions. Hydrologic priority is assigned on the basis that the greater the reduction or benefit, the higher the priority. For economic thresholds, the equivalent annual cost (EAC) is tabulated for each scale of analysis (e.g., parcel, subcatchment). The breakdown of budgets is based on the user's preference and should represent the maximum budget allowable, as determined by the Suitability Protocol. For this study, the following municipal budget ranges were applied: A. $0.25MIL, B. $0.5MIL, C. $1.0MIL, D. $2.0MIL, and E. maximum budget. For the economic prioritization, the focus can be on the overall watershed costs, individual households, and subcatchments.

4. Sizing, design, and implementation of LID practices: The sizing of units is provided using the extracted locations' data (as *.dbf* file from ArcGIS), including the contributing drainage area (e.g., rooftop), parcel

area, unique location identifier, and subcatchment identifier. Sizing is completed by the *RWHA* (see Chapter 4, section 4.4.2.3 for extensive application of this toolset in the sizing and design of LID practices). Implementation is provided by the *.dbf* file from the Suitability Protocol, with unique identifiers for the targeted scale of analysis (e.g., household, subcatchment).

5. Amend hydrologic model: The hydrologic model representing *BASE* conditions should be amended to represent the LID practices extracted and sized with the *RWHA*. This is done easily with the *RWHA* and instructions provided the user with unique resultant *.inp* files for simulation and analysis. For simplicity, a nominal range of RWH units can be selected for each individual scenario to be modeled. For example, this study chose the 227-liter nominal size for analysis, though others are available, including: 379- and 757-liter RWH barrels, and 1,893-, 3,785- and 7,571-liter cisterns. Amended hydrologic models should be stored in unique folders for future batch analysis.
6. Cost estimation and analysis: Cost analysis of each suitable LID framework can be completed with the aid of the WERF BMP and LID Whole List Cost Models. To account for long-term operation and maintenance costs, BLCC5.3 can also be used, which provides scenario life-cycle assessments. For this study, the EAC for each subcatchment-collated scenario was assessed, including the operation and maintenance, capital, and replacement costs (from the WERF

Cistern toolset). These values should be saved at the targeted scale of analysis and in-line with the unique identifier for future joining in ArcGIS.

7. Prioritization protocol: To improve the ability of users to collate, visualize, and assess the existing watershed and economic conditions, a prioritization toolset was created. Extensive protocol steps are specifically addressed in Chapter 4, section 4.4.2. The ArcGIS Model Builder tool was employed in facilitating the prioritization (*PriorLID*). The first step of the toolset includes importing, or joining, both the simulated hydrologic and cost estimate results for LIDs as point shapefiles. For hydrologic results, the level of projection was limited to subcatchment in this case. Cost estimates were capable of spanning the range of scales (parcel, subcatchment), though they were collated to the subcatchment-scale for cost-effectiveness estimation. Visualization of results was improved through surface interpolation. These surfaces represented the EAC, volumetric reductions (annual, long-term), and peak rate reductions (annual, long-term). The Inverse Distance Weighted (IDW) method was used for this study to extract surfaces based on the values. Using Raster Math, the cost surface can be divided by the hydrologic reduction surface, resulting in data values equivalent to the cost ($) per volume of runoff reduced (ML). To perform grouping of distributed locations with similar data values, the unsupervised classification algorithm, ISODATA, was employed. To

provide a range of priority alternatives, such that the top-down threshold of budget could be assessed, an iterative approach was implemented via the Model Builder (For tool). This improves the potential to, first, identify priority zones and, further, refine these zones to target variations in groups based on class iterations determined by the user. Further analysis of resultant classes is provided by importing the *.dbf* files containing the zonal statistics (at the subcatchment scale) for each classes in MS Excel. Zonal statistics included: average volumetric reductions (percent), total volumetric reductions (ML), and total costs ($) per class. Ranking and ordering these results allows users to select the groups, or classes, meeting the economic thresholds while attempting to provide a maximized hydrologic reduction. The hydrologic impact of the priority scenarios can then be used to amend the original LID *.inp* model and carry out long-term hydrologic simulations.

D.3 Uncertainty Estimation and Analysis

For this dissertation, the workflow provided in Fig. D.3 presents the steps necessary to carry out Monte Carlo Methods (MCM) of uncertainty estimation for the hydrologic components of the Suitability and Prioritization protocols. With Fig. D.3, the following tasks are required for users to assess the accuracy of the previously applied protocols:

1. Uncertainty analysis: Monte Carlo (MC) methods of uncertainty analysis can be applied to the calibrated and validated hydrologic

model representing the *BASE* conditions. The targeted independent variable for MC analysis, in this dissertation, was the subcatchment percent of imperviousness. The specific steps for accomplishing the MC analysis included:

a. Creation of a probability density function (PDF) for the sample dataset containing the subcatchment percent imperviousness values.
b. Random sampling of values from the PDF to create sample models (n=100), which were used to simulate long-term, continuous precipitation data for analysis of the independent variable's impacts on the overall watershed and subcatchment hydrologic regime(s).
c. Application of batch scripting to run and collate sample models for the user's determined period of hydrologic analysis. Of note, this should contain variation in the expected annual precipitation patterns to reliably assess the hydrologic conditions of the study watershed. Batch scripting steps include:
d. Creation of a unique folder for housing the batch script components
e. Importing the swmm.exe file for use with the batch script
f. Importing the unique SWMM *.inp* and *.ini* files for use with the batch script (n=100)
g. Creation of a batch (.bat) file, with the following example lines of

code, for n=100 randomized models:

```
swmm5.exe C:\Users\batch\chollas.inp
Z:\Students\Walsh\PhD\Uncertainty\chollas.rpt
swmm5.exe C:\Users\batch\chollas1.inp
Z:\Students\Walsh\PhD\Uncertainty\chollas1.rpt
swmm5.exe C:\Users\batch\chollas2.inp
Z:\Students\Walsh\PhD\Uncertainty\chollas2.rpt
swmm5.exe C:\Users\batch\chollas3.inp
Z:\Students\Walsh\PhD\Uncertainty\chollas3.rpt
swmm5.exe C:\Users\batch\chollas4.inp
Z:\Students\Walsh\PhD\Uncertainty\chollas4.rpt
swmm5.exe C:\Users\batch\chollas5.inp
Z:\Students\Walsh\PhD\Uncertainty\chollas5.rpt
swmm5.exe C:\Users\batch\chollas6.inp
Z:\Students\Walsh\PhD\Uncertainty\chollas6.rpt
swmm5.exe C:\Users\batch\chollas7.inp
Z:\Students\Walsh\PhD\Uncertainty\chollas7.rpt
swmm5.exe C:\Users\batch\chollas8.inp
Z:\Students\Walsh\PhD\Uncertainty\chollas8.rpt
swmm5.exe C:\Users\batch\chollas9.inp
Z:\Students\Walsh\PhD\Uncertainty\chollas9.rpt
swmm5.exe C:\Users\batch\chollas10.inp
Z:\Students\Walsh\PhD\Uncertainty\chollas10.rpt
swmm5.exe C:\Users\batch\chollas11.inp
Z:\Students\Walsh\PhD\Uncertainty\chollas11.rpt
swmm5.exe C:\Users\batch\chollas12.inp
Z:\Students\Walsh\PhD\Uncertainty\chollas12.rpt
swmm5.exe C:\Users\batch\chollas13.inp
Z:\Students\Walsh\PhD\Uncertainty\chollas13.rpt
swmm5.exe C:\Users\batch\chollas14.inp
Z:\Students\Walsh\PhD\Uncertainty\chollas14.rpt
swmm5.exe C:\Users\batch\chollas15.inp
Z:\Students\Walsh\PhD\Uncertainty\chollas15.rpt
swmm5.exe C:\Users\batch\chollas16.inp
Z:\Students\Walsh\PhD\Uncertainty\chollas16.rpt
swmm5.exe C:\Users\batch\chollas17.inp
Z:\Students\Walsh\PhD\Uncertainty\chollas17.rpt
swmm5.exe C:\Users\batch\chollas18.inp
Z:\Students\Walsh\PhD\Uncertainty\chollas18.rpt
swmm5.exe C:\Users\batch\chollas19.inp
Z:\Students\Walsh\PhD\Uncertainty\chollas19.rpt
swmm5.exe C:\Users\batch\chollas20.inp
Z:\Students\Walsh\PhD\Uncertainty\chollas20.rpt
swmm5.exe C:\Users\batch\chollas21.inp
Z:\Students\Walsh\PhD\Uncertainty\chollas21.rpt
```

swmm5.exe C:\Users\batch\chollas22.inp
Z:\Students\Walsh\PhD\Uncertainty\chollas22.rpt
swmm5.exe C:\Users\batch\chollas23.inp
Z:\Students\Walsh\PhD\Uncertainty\chollas23.rpt
swmm5.exe C:\Users\batch\chollas24.inp
Z:\Students\Walsh\PhD\Uncertainty\chollas24.rpt
swmm5.exe C:\Users\batch\chollas25.inp
Z:\Students\Walsh\PhD\Uncertainty\chollas25.rpt
swmm5.exe C:\Users\batch\chollas26.inp
Z:\Students\Walsh\PhD\Uncertainty\chollas26.rpt
swmm5.exe C:\Users\batch\chollas27.inp
Z:\Students\Walsh\PhD\Uncertainty\chollas27.rpt
swmm5.exe C:\Users\batch\chollas28.inp
Z:\Students\Walsh\PhD\Uncertainty\chollas28.rpt
swmm5.exe C:\Users\batch\chollas29.inp
Z:\Students\Walsh\PhD\Uncertainty\chollas29.rpt
swmm5.exe C:\Users\batch\chollas30.inp
Z:\Students\Walsh\PhD\Uncertainty\chollas30.rpt
swmm5.exe C:\Users\batch\chollas31.inp
Z:\Students\Walsh\PhD\Uncertainty\chollas31.rpt
swmm5.exe C:\Users\batch\chollas32.inp
Z:\Students\Walsh\PhD\Uncertainty\chollas32.rpt
swmm5.exe C:\Users\batch\chollas33.inp
Z:\Students\Walsh\PhD\Uncertainty\chollas33.rpt
swmm5.exe C:\Users\batch\chollas34.inp
Z:\Students\Walsh\PhD\Uncertainty\chollas34.rpt
swmm5.exe C:\Users\batch\chollas35.inp
Z:\Students\Walsh\PhD\Uncertainty\chollas35.rpt
swmm5.exe C:\Users\batch\chollas36.inp
Z:\Students\Walsh\PhD\Uncertainty\chollas36.rpt
swmm5.exe C:\Users\batch\chollas37.inp
Z:\Students\Walsh\PhD\Uncertainty\chollas37.rpt
swmm5.exe C:\Users\batch\chollas38.inp
Z:\Students\Walsh\PhD\Uncertainty\chollas38.rpt
swmm5.exe C:\Users\batch\chollas39.inp
Z:\Students\Walsh\PhD\Uncertainty\chollas39.rpt
swmm5.exe C:\Users\batch\chollas40.inp
Z:\Students\Walsh\PhD\Uncertainty\chollas40.rpt
swmm5.exe C:\Users\batch\chollas41.inp
Z:\Students\Walsh\PhD\Uncertainty\chollas41.rpt
swmm5.exe C:\Users\batch\chollas42.inp
Z:\Students\Walsh\PhD\Uncertainty\chollas42.rpt
swmm5.exe C:\Users\batch\chollas43.inp
Z:\Students\Walsh\PhD\Uncertainty\chollas43.rpt
swmm5.exe C:\Users\batch\chollas44.inp
Z:\Students\Walsh\PhD\Uncertainty\chollas44.rpt

swmm5.exe C:\Users\batch\chollas45.inp
Z:\Students\Walsh\PhD\Uncertainty\chollas45.rpt
swmm5.exe C:\Users\batch\chollas46.inp
Z:\Students\Walsh\PhD\Uncertainty\chollas46.rpt
swmm5.exe C:\Users\batch\chollas47.inp
Z:\Students\Walsh\PhD\Uncertainty\chollas47.rpt
swmm5.exe C:\Users\batch\chollas48.inp
Z:\Students\Walsh\PhD\Uncertainty\chollas48.rpt
swmm5.exe C:\Users\batch\chollas49.inp
Z:\Students\Walsh\PhD\Uncertainty\chollas49.rpt
swmm5.exe C:\Users\batch\chollas50.inp
Z:\Students\Walsh\PhD\Uncertainty\chollas50.rpt
swmm5.exe C:\Users\batch\chollas51.inp
Z:\Students\Walsh\PhD\Uncertainty\chollas51.rpt
swmm5.exe C:\Users\batch\chollas52.inp
Z:\Students\Walsh\PhD\Uncertainty\chollas52.rpt
swmm5.exe C:\Users\batch\chollas53.inp
Z:\Students\Walsh\PhD\Uncertainty\chollas53.rpt
swmm5.exe C:\Users\batch\chollas54.inp
Z:\Students\Walsh\PhD\Uncertainty\chollas54.rpt
swmm5.exe C:\Users\batch\chollas55.inp
Z:\Students\Walsh\PhD\Uncertainty\chollas55.rpt
swmm5.exe C:\Users\batch\chollas56.inp
Z:\Students\Walsh\PhD\Uncertainty\chollas56.rpt
swmm5.exe C:\Users\batch\chollas57.inp
Z:\Students\Walsh\PhD\Uncertainty\chollas57.rpt
swmm5.exe C:\Users\batch\chollas58.inp
Z:\Students\Walsh\PhD\Uncertainty\chollas58.rpt
swmm5.exe C:\Users\batch\chollas59.inp
Z:\Students\Walsh\PhD\Uncertainty\chollas59.rpt
swmm5.exe C:\Users\batch\chollas60.inp
Z:\Students\Walsh\PhD\Uncertainty\chollas60.rpt
swmm5.exe C:\Users\batch\chollas61.inp
Z:\Students\Walsh\PhD\Uncertainty\chollas61.rpt
swmm5.exe C:\Users\batch\chollas62.inp
Z:\Students\Walsh\PhD\Uncertainty\chollas62.rpt
swmm5.exe C:\Users\batch\chollas63.inp
Z:\Students\Walsh\PhD\Uncertainty\chollas63.rpt
swmm5.exe C:\Users\batch\chollas64.inp
Z:\Students\Walsh\PhD\Uncertainty\chollas64.rpt
swmm5.exe C:\Users\batch\chollas65.inp
Z:\Students\Walsh\PhD\Uncertainty\chollas65.rpt
swmm5.exe C:\Users\batch\chollas66.inp
Z:\Students\Walsh\PhD\Uncertainty\chollas66.rpt
swmm5.exe C:\Users\batch\chollas67.inp
Z:\Students\Walsh\PhD\Uncertainty\chollas67.rpt

swmm5.exe C:\Users\batch\chollas68.inp
Z:\Students\Walsh\PhD\Uncertainty\chollas68.rpt
swmm5.exe C:\Users\batch\chollas69.inp
Z:\Students\Walsh\PhD\Uncertainty\chollas69.rpt
swmm5.exe C:\Users\batch\chollas70.inp
Z:\Students\Walsh\PhD\Uncertainty\chollas70.rpt
swmm5.exe C:\Users\batch\chollas71.inp
Z:\Students\Walsh\PhD\Uncertainty\chollas71.rpt
swmm5.exe C:\Users\batch\chollas72.inp
Z:\Students\Walsh\PhD\Uncertainty\chollas72.rpt
swmm5.exe C:\Users\batch\chollas73.inp
Z:\Students\Walsh\PhD\Uncertainty\chollas73.rpt
swmm5.exe C:\Users\batch\chollas74.inp
Z:\Students\Walsh\PhD\Uncertainty\chollas74.rpt
swmm5.exe C:\Users\batch\chollas75.inp
Z:\Students\Walsh\PhD\Uncertainty\chollas75.rpt
swmm5.exe C:\Users\batch\chollas76.inp
Z:\Students\Walsh\PhD\Uncertainty\chollas76.rpt
swmm5.exe C:\Users\batch\chollas77.inp
Z:\Students\Walsh\PhD\Uncertainty\chollas77.rpt
swmm5.exe C:\Users\batch\chollas78.inp
Z:\Students\Walsh\PhD\Uncertainty\chollas78.rpt
swmm5.exe C:\Users\batch\chollas79.inp
Z:\Students\Walsh\PhD\Uncertainty\chollas79.rpt
swmm5.exe C:\Users\batch\chollas80.inp
Z:\Students\Walsh\PhD\Uncertainty\chollas80.rpt
swmm5.exe C:\Users\batch\chollas81.inp
Z:\Students\Walsh\PhD\Uncertainty\chollas81.rpt
swmm5.exe C:\Users\batch\chollas82.inp
Z:\Students\Walsh\PhD\Uncertainty\chollas82.rpt
swmm5.exe C:\Users\batch\chollas83.inp
Z:\Students\Walsh\PhD\Uncertainty\chollas83.rpt
swmm5.exe C:\Users\batch\chollas84.inp
Z:\Students\Walsh\PhD\Uncertainty\chollas84.rpt
swmm5.exe C:\Users\batch\chollas85.inp
Z:\Students\Walsh\PhD\Uncertainty\chollas85.rpt
swmm5.exe C:\Users\batch\chollas86.inp
Z:\Students\Walsh\PhD\Uncertainty\chollas86.rpt
swmm5.exe C:\Users\batch\chollas87.inp
Z:\Students\Walsh\PhD\Uncertainty\chollas87.rpt
swmm5.exe C:\Users\batch\chollas88.inp
Z:\Students\Walsh\PhD\Uncertainty\chollas88.rpt
swmm5.exe C:\Users\batch\chollas89.inp
Z:\Students\Walsh\PhD\Uncertainty\chollas89.rpt
swmm5.exe C:\Users\batch\chollas90.inp
Z:\Students\Walsh\PhD\Uncertainty\chollas90.rpt

```
swmm5.exe C:\Users\batch\chollas91.inp
Z:\Students\Walsh\PhD\Uncertainty\chollas91.rpt
swmm5.exe C:\Users\batch\chollas92.inp
Z:\Students\Walsh\PhD\Uncertainty\chollas92.rpt
swmm5.exe C:\Users\batch\chollas93.inp
Z:\Students\Walsh\PhD\Uncertainty\chollas93.rpt
swmm5.exe C:\Users\batch\chollas94.inp
Z:\Students\Walsh\PhD\Uncertainty\chollas94.rpt
swmm5.exe C:\Users\batch\chollas95.inp
Z:\Students\Walsh\PhD\Uncertainty\chollas95.rpt
swmm5.exe C:\Users\batch\chollas96.inp
Z:\Students\Walsh\PhD\Uncertainty\chollas96.rpt
swmm5.exe C:\Users\batch\chollas97.inp
Z:\Students\Walsh\PhD\Uncertainty\chollas97.rpt
swmm5.exe C:\Users\batch\chollas98.inp
Z:\Students\Walsh\PhD\Uncertainty\chollas98.rpt
swmm5.exe C:\Users\batch\chollas99.inp
Z:\Students\Walsh\PhD\Uncertainty\chollas99.rpt
swmm5.exe C:\Users\batch\chollas100.inp
Z:\Students\Walsh\PhD\Uncertainty\chollas100.rpt
pause
```

a. This code identifies the executable file (swmm5.exe) the location of the *.inp* file for simulation, and the location of the output location for the *.rpt* file

b. The batch file can either simply be double-clicked to commence simulations in the background of the computer or the user can access the command prompt (*.cmd*), navigate to the folder containing the batch script, call the script, and run it. Either method will run through the multiple models and collate the results as separate report files.

c. Analysis of collated results to determine the impacts of random variations in subcatchment percent imperviousness on the overall watershed hydrologic characteristics can be completed for the

exported *.rpt* files in MS Excel. Collation of results is improved by creating an import function based on the number of rows targeted for analysis within the desired file (e.g., *.rpt*). The following VBA script can perform this, specifically created for this dissertation's Chollas Creek watershed model

i. To import the long-term results' Status Report file:

```
Private Sub CommandButton2_Click()

Dim fPATH As String, fNAME As String, wbDATA As Workbook, wsMAIN As Worksheet

MsgBox Please select the folder containing the original files.
With Application.FileDialog(msoFileDialogFolderPicker)
'choose folder with files to import
.AllowMultiSelect = False
.InitialFileName = Z:\Students\Walsh\PhD\Uncertainty\
.Show
If .SelectedItems.Count = 0 Then Exit Sub Else fPATH = .SelectedItems(1) & \
End With

Set wsMAIN = ThisWorkbook.Sheets(Sheet1)          'sheet in thisworkbook to collect data into
fNAME = Dir(fPATH & *.rpt*)                       'get first filename from chosen path
Application.ScreenUpdating = False                'turn off screen flicker

Do While Len(fNAME) > 0                           'repeat actions until no more files found
Set wbDATA = Workbooks.Open(fPATH & fNAME)        'open current file
Range(A99:A189).Copy wsMAIN.Range(A & Rows.Count).End(xlUp).Offset(1)    'copy data
wbDATA.Close False                                'close opened file

fNAME = Dir                                       'get next filename
Loop

Application.ScreenUpdating = True                 'screen back to normal
```

```
End Sub
```

ii. To import the continuous, time series results for the watershed outlet:

```
Private Sub CommandButton3_Click()
Dim fPATH As String, fNAME As String, wbDATA As Workbook, wsMAIN As Worksheet

MsgBox Please select the folder containing the original files.
With Application.FileDialog(msoFileDialogFolderPicker)
'choose folder with files to import
   .AllowMultiSelect = False
   .InitialFileName = Z:\Students\Walsh\PhD\Uncertainty\
   .Show
   If .SelectedItems.Count = 0 Then Exit Sub Else fPATH = .SelectedItems(1) & \
End With

   Set wsMAIN = ThisWorkbook.Sheets(Sheet2)          'sheet in thisworkbook to collect data into
   fNAME = Dir(fPATH & *.rpt*)                       'get first filename from chosen path
   Application.ScreenUpdating = False                'turn off screen flicker

   Do While Len(fNAME) > 0                           'repeat actions until no more files found
      Set wbDATA = Workbooks.Open(fPATH & fNAME)     'open current file
      Range(A1020:A71190).Copy wsMAIN.Range(A & Rows.Count).End(xlUp).Offset(1)    'copy data
      wbDATA.Close False                             'close opened file

      fNAME = Dir                                    'get next filename
   Loop

   Application.ScreenUpdating = True                 'screen back to normal

End Sub
```

iii. To condense these results, use:

```
Private Sub CommandButton1_Click()
```

```
Dim vaCells As Variant
   Dim vOutput() As Variant
   Dim i As Long, j As Long
   Dim lRow As Long

   If TypeName(Selection) = Range Then
      If Selection.Count > 1 Then
         If Selection.Count <= Selection.Parent.Rows.Count
Then
            vaCells = Selection.Value

            ReDim vOutput(1 To UBound(vaCells, 1) *
UBound(vaCells, 2), 1 To 1)

            For j = LBound(vaCells, 2) To UBound(vaCells, 2)
               For i = LBound(vaCells, 1) To UBound(vaCells, 1)
                  If Len(vaCells(i, j)) > 0 Then
                     lRow = lRow + 1
                     vOutput(lRow, 1) = vaCells(i, j)
                  End If
               Next i
            Next j

            Selection.ClearContents
            Selection.Cells(1).Resize(lRow).Value = vOutput
         End If
      End If
   End If
End Sub
```

a. Calculation of the 97.5th and 2.5th percentiles is provided for the data, ranked and order, and plotted against the exceedance, or return, frequency using the Cunnane Plotting position (or whichever method is preferred by the user). This indicated the bounds of the simulated results and the impacts of the variations in the independent variable.

2. Prioritization protocol assessment: Since prioritization was based on both top-down and bottom-up thresholds determined by the user, accuracy assessment targeted the ability of the protocol to extract

unique scenarios within to reach the targeted threshold(s). Assessments can be based on:

a. Overall watershed hydrologic impacts (e.g., reduction in volumes, dampening of peak flow rates) and
b. Total costs of the LID scenario chosen at the overall watershed and subcatchment scales.

These results are analyzed based on comparing the anticipated hydrologic reduction versus the actual, simulated watershed response. Similarly, the costs are analyzed by quantifying the difference in total cost (i.e., budget) versus the actual cost required to provide the hydrologic benefit desired.

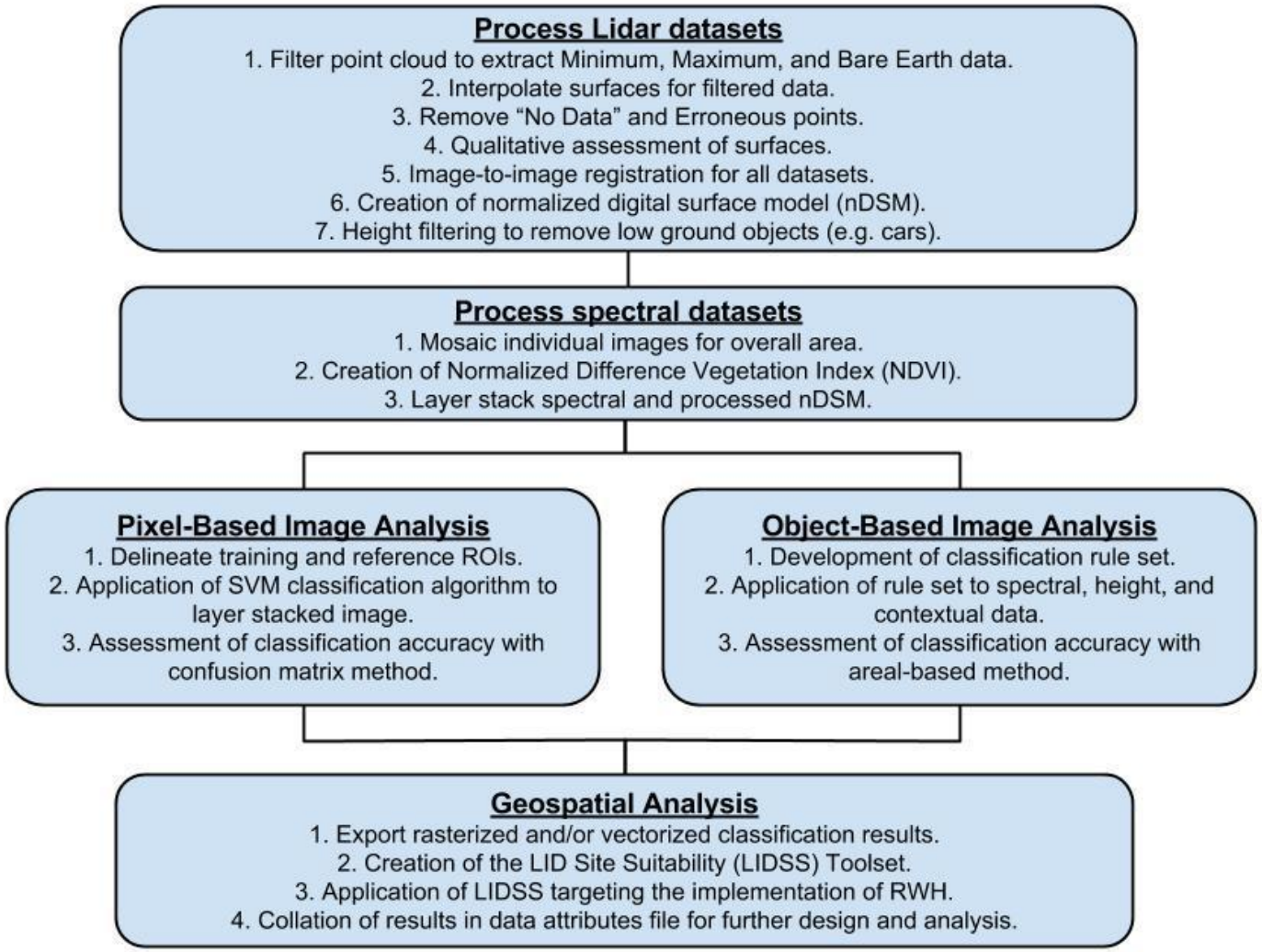

Figure D.1: Suitability protocol workflow

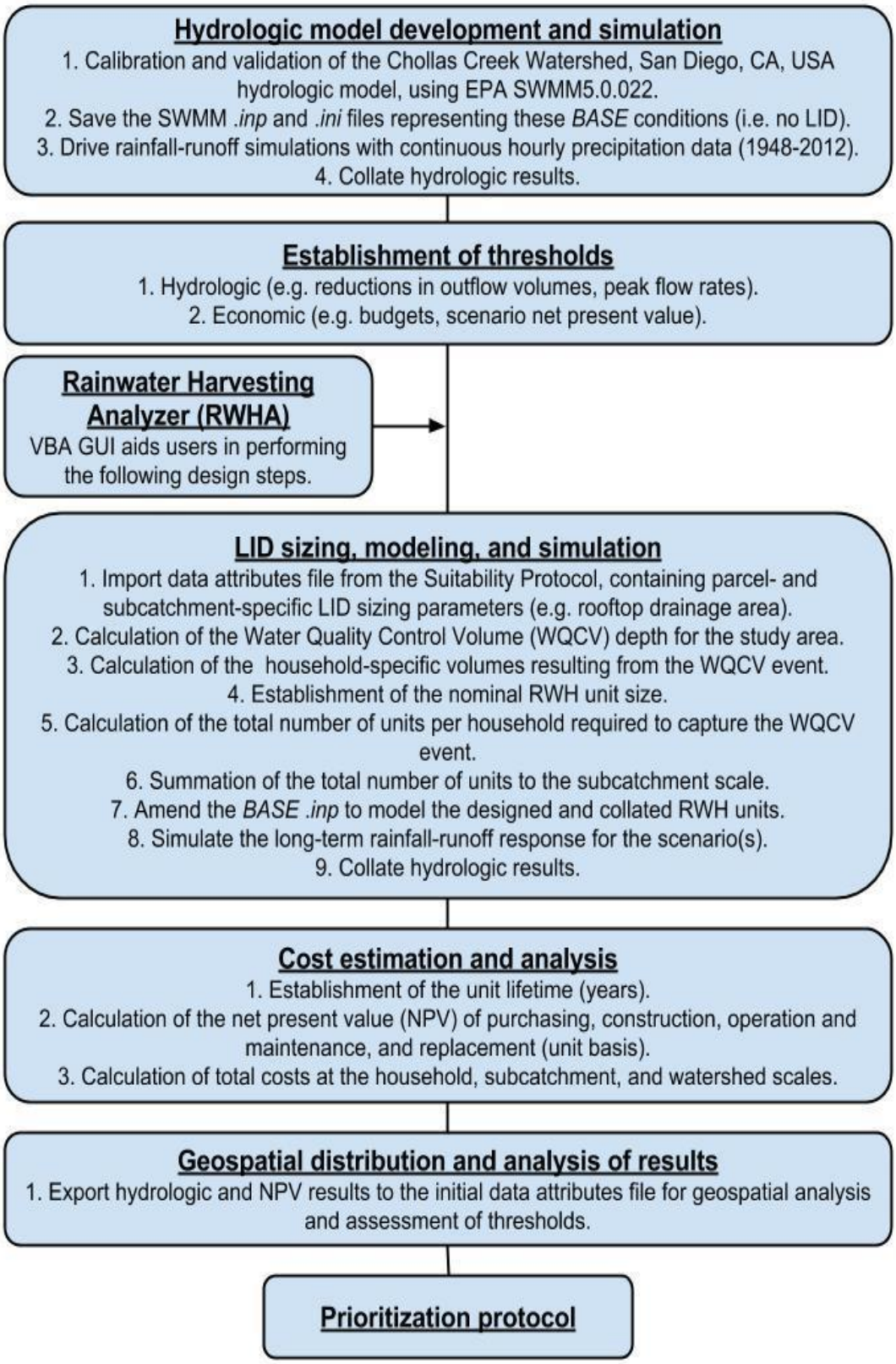

Figure D.2: Prioritization protocol workflow.

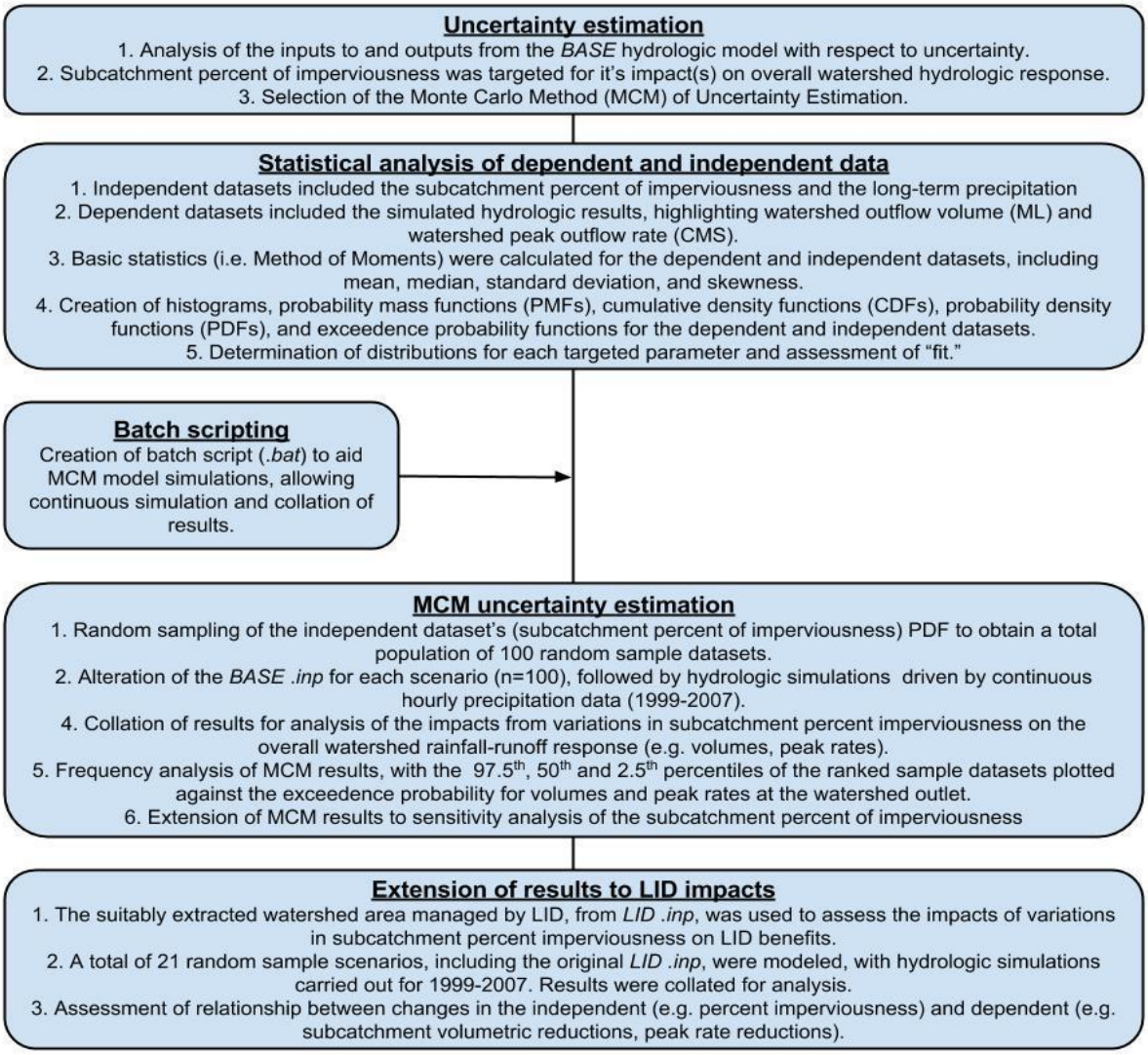

Figure D.3: MCM uncertainty estimation and analysis workflow.

D.4 References

Anderson, J. R., Hardy, E. E., Roach, J. T., & Witmer, R. E. (1976). *A land cover/land use classification system for use with remote sensor data.* Washington, DC: United States Government Printing Office.

Congalton, R. G., & Green, K. (2009). *Assessing the accuracy of remotely sensed data: Principles and practices* (2nd ed.). Boca Raton, FL: CRC Press.

Hartfield, K. A., Landau, K. I., & Van Leeuwen, J. D. (2011). Fusion of high resolution aerial multispectral and lidar data: Land cover in the context of urban mosquito habitat. *Remote Sensing in Public Health*, Special Issue, *3*(11), 2364-2383.

Rottensteiner, F., Trinder, J., Code, S., & Kubik, K. (2005). Automated delineation of roof planes from lidar data. Proceedings from: *International Archives of Photogrammetry and Remote Sensing, XXXVI, 3/W19*. Enschede, Netherlands: IAPRS.

Shiravi, S., Zhong, M., & Beykaei, S. A. (2012). Accuracy assessment of building extraction using lidar data for urban planning/transportation application. Proceedings from: *2012 Conference of the Transportation Association of Canada.* Fredericton, New Brunswick.

Van Genderen, J. L., & Lock, B. F. (1977). Testing land-use map accuracy. *Photogrammetric Engineering and Remote Sensing*, *43*(9), 1135-1139.

Zhu, L., Shortridge, A. M., & Lusch, D. (2012). Conflating lidar data and multispectral imagery for efficient building detection. *Journal of Applied Remote Sensing*, *6*, 1-17.